Synthesis of Luminescent Tellurophenes for Optoelectronic Applications

By

William Torres Delgado

A thesis submitted in partial fulfillment of the requirements for the degree of

Doctor of Philosophy

Department of Chemistry

University of Alberta

ABSTRACT

With the goal to form stable, solid state tunable emitters at room temperature, the work within this thesis describes the synthesis of both symmetric and unsymmetric tellurophenes along with the study of their optoelectronic properties in solution and in the solid state.

Chapter 2 describes the synthesis of a series of tetraborylated thiophenes, selenophenes and tellurophenes via transmetallation reactions. The optical properties of the series were studied by UV-vis spectroscopy, fluorescence spectroscopy and cyclic voltammetry, as well as using theoretical calculations (TD DFT). Luminescence from tetraborylated/diborylated tellurophenes was studied under argon and in aerated conditions, given O_2-dependent phosphorescence in solution and the solid state.

Chapter 3 reports the synthesis of new borylated and bromide-functionalized tellurophenes via selective protodeboronation reactions of tetraborylated tellurophenes under thermal and microwave conditions and via exchange reactions using copper dibromide. The protodeboronation of tetraborylated chalcogenophenes (thiophene, selenophene and tellurophene) is described and their respective 3,4-diborylated products featured non-emissive properties in the solid state and in solution. It is expected that both new borylated and brominated tellurophenes will serve as building blocks for the further preparation of conjugated polymers.

Chapter 4 features the synthesis of symmetric and unsymmetric aryl-tellurophenes through Suzuki-Miyaura and Sonogashira cross coupling reactions. The goal was to tune the phosphorescent properties *via* modification of the central tellurophene in the 2,5-positions with electron donating/withdrawing substituents. It was found that the electron withdrawing group, *m*-$(CF_3)_2C_6H_3$, attached to the tellurophene forms a couple acceptor-donor-acceptor with intense phosphorescent emission. This study showed the possibility of achieving phosphorescence using readily available di-arylated tellurophenes.

PREFACE

Parts of the thesis were completed in collaboration with other researchers within the Rivard group and the Chemistry Department, Department of Electrical & Computer Engineering and outside of the University of Alberta.

The X-ray crystallographic studies were entirely performed by Dr. Robert McDonald and Dr. Michael Ferguson, including the mounting of crystals, set-up and operation of the diffractometer, as well as refinement and preparation of all crystallographic tables.

Measurements of lifetime, absolute quantum yield and aggregation-induced measurements of the majority of the tellurophenes described in the thesis were performed by Prof. Gang He at Xi'an Jiaotong University, China.

Prof. Karthik Shankar and his collaborators from the Department of Electrical & Computer Engineering at the University of Alberta measured lifetime and quantum yields of **B-Te-6-B** and **T-H-T** and their results are partly described in Chapter 2.

Fluorescence studies in the solid state and in solution of **B-Te-6-B** and **4BTe** that allowed to measure fluorescence events with short lifetimes and study the quenching effects of oxygen described in Chapter 2 were performed in collaboration with Dr. Przemyslaw Data at Durham University, UK.

Theoretical calculations of the series of chalcogenophenes **4BE** and **B-E-6-B** (E = S, Se and Te) described in Chapter 2 were performed by Prof. Alexander Brown and his collaborators at the University of Alberta.

In Chapter 2: part of the work described in this Chapter can be found published in two papers as:

1. He, G.; Kang, L.; **Torres Delgado, W.**; Shynkaruk, O.; Ferguson, M. J.; McDonald, R.; Rivard, E. *J. Am. Chem. Soc.* **2013**, *135*, 5360–5363.

2. He, G.; **Torres Delgado, W.**; Schatz, D. J.; Merten, C.; Mohammadpour, A.; Mayr, L.; Ferguson, M. J.; McDonald, R.; Brown, A.; Shankar, K.; Rivard, E. *Angew. Chem. Int. Ed.* **2014**, *53*, 4587–4591.

In Chapter 3, the synthesis of **BTe** and its characterization and as well as assistance for the synthesis of precursors were performed by Mrs. Fatemeh Shahin as part of her 401/403 project as an undergraduate student from University of Alberta. The entire Chapter 3 was published as:

3. **Torres Delgado, W.**; Shahin, F.; Ferguson, M. J.; McDonald, R.; He, G.; Rivard, E. *Organometallics* **2016**, *35*, 2140–2148.

Publications not highlighted in this thesis are:

4. Mohammadpour, A.; Wiltshire, B. D.; Farsinezhad, S.; Zhang, Y.; Askar, A. M.; Kisslinger, R.; **Delgado, W. T.**; He, G.; Kar, P.; Rivard, E.; Shankar, K. *Org. Electron.* **2016**, *39*, 153–162.

   I was responsible for the synthesis of **B-Te-6-B** material used in this paper.

5. Shynkaruk, O.; Qi, Y.; Cottrell-Callbeck, A.; **Torres Delgado, W.**; McDonald, R.; Ferguson, M. J.; He, G.; Rivard, E. *Organometallics* **2016**, *35*, 2232–2241.

   I was responsible for the synthesis of **PinBC≡CBPin** used as a starting material in this paper.

6. Braun, C. A.; Zomerman, D.; De Aguiar, I.; Qi, Y.; **Delgado, W. T.**; Ferguson, M. J.; McDonald, R.; De Souza, G. L. C.; He, G.; Brown, A.; Rivard, E. *Faraday Discuss.* **2017**, *196*, 255–268.

I was responsible for supervising the experimental work done by Mr. Derek Zomerman as part of his 401/403 project as an undergraduate student from University of Alberta, that lead to part of his work to be published in the aforementioned paper.

Dedicated to my mother, Alicia, my sister, Angela María and grandparents Rosa Tulia and Ruperto.

ACKNOWLEDGEMENTS AND STATEMENT OF COLLABORATIONS

I would like to thank my advisor Professor Eric Rivard for allowing me to be part of his research group and for his support, teaching, help, guidance and patience to make the whole experience of my PhD invaluable. I recognize his hard work and prompt feedback when I needed most, I will be always thankful for that. I would also like to thank Prof. Jonathan Veinot, Prof. Jeff Stryker, Prof. Mariusz Klobukowski, Prof. Dennis Hall, Prof. Michael Serpe and Prof. Paul Ragogna for serving on my supervisory and examination committees and their thoughtful advice on my chemistry.

I want to express my respect for their knowledge and expertise to the technical staff at the University of Alberta. I would like to thank Dr. Robert McDonald and Dr. Michael Ferguson for their contribution with X-ray crystallography, Dr. Randy Whittal and Mrs. Jin Zheng for the Mass Spectrometry studies, Mr Wayne Moffat for his contribution, support and training in the analytical techniques, Mr. Ed Fu for his training in the use of microwave reactor. Dr. Ryan McKay and his staff, Mrs. Nupur Dabral and Mr. Mark Miskolzie, their hard work behind the NMR machines make those measurements an easy daily task.

I would like give special thanks to Dr. Jason Cooke and Dr. Norman Gee for their mentorship and guidance in the very difficult but grateful task of teaching Inorganic Chemistry and Introductory Chemistry Labs.

I would like also to express my gratitude to Anita Weiler for her invaluable help during my graduate school and in the application process to the University of Alberta as a support staff in the PhD graduate program in the Chemistry Department at U of A. Her knowledge and guidance were always well received.

I want to give thanks to all the group members that have gone through my stay in the Rivard group. Their contribution expressed in comments and discussions and as well as support in my presentations were invaluable to improve my overall teaching and

communication skills. Special thanks to Alyona Shynkaruk, Anindya Swarnakar and Prof. Gang He for their companionship during the long hours at work.

And finally, I would like to thank my family, without their support and unconditional love, nothing would have been possible. My goals became their goals too.

I also take the opportunity to give special thanks to our collaborators; with their expertise and knowledge was possible to characterize and understand the luminescence properties of tellurophenes. I want to give special thanks to Prof. Alex Brown and Dr. Karthik Shankar from University of Alberta, for their contribution in the theoretical calculations and luminescence characterization. Thanks again to Dr. Gang He from Xi'an Jiaotong University, People's Republic of China, for the luminescence measurements, quantum yield and lifetime determination, Dr. Przemyslaw Data from Durham University, United Kingdow, for the measurements of prompt and delayed fluorescence.

I would like to give special thanks to the agencies that support and fund my projects, NSERC CRSNG, Alberta Innovates Technology Futures, INNOVATION.CA Canada Foundation for Innovation, Suncor Energy and to the ATUMS program for its funding and dedication to the professional development of the graduate students.

TABLE OF CONTENTS

LIST OF TABLES

LIST OF SCHEMES

LIST OF FIGURES

LIST OF SYMBOLS AND ABBREVIATIONS

Ac	acetyl
ACQ	aggregation-caused quenching
AIE	aggregation-induced emission
aq.	aqueous
Ar	aromatic group
Ar^F	*m*-$(CF_3)_2C_6H_3$
Bipy	2,2′-bipyridine
BPin or PinB	pinacolborane
ca.	circa, approximately
cat.	catalyst
Cp	cyclopentadienyl ligand (η^5-C_5H_5)
CV	cyclic voltammetry
d	doublet
D-A	donor-acceptor
dba	dibenzylideneacetone
DCM	dychloromethane
dd	doublet of doublets
DET	Dexter electron transfer

DMAP	4-dimethylaminopyridine
DMEDA	N,N′-dimethylethane-1,2-diamine
DMF	N,N-dimethylformamide
DMSO	dimethyl sulfoxide
dt	doublet of triplets
EDGs	electron-donating groups
E_g	optical band gap of energy
$E_{ox/onset}$	potential at the onset of oxidation
equiv.	equivalent
$E_{red/onset}$	potential at the onset of reduction
Et	Ethyl (C_2H_5)
eV	electron volt
EWGs	electron-withdrawing groups
Fc/Fc^+	ferrocene/ferrocenium
Fl	fluorene
FRET	Förster resonance energy transfer
GRIM	Grignard metathesis
h	hour(s)
HOMO	highest occupied molecular orbital
I	nuclear spin angular momentum

^{i}Pr	iso-propyl (Me_2CH)
ISC	intersystem crossing
K	Kelvin
LUMO	lowest unoccupied molecular orbital
MeCN	acetonitrile
MHz	megahertz
min	minutes
mL	millilitre
mmol	millimole
Mp	melting point
Mw	weight average molecular weight
Naph	naphthalene
NBS	N-bromosuccinimide
^{n}Bu	n-butyl (C_4H_9)
NHC	*N*-heterocyclic carbene
$^{n}J_{AB}$	n-bond AB coupling constant
NMR	nuclear magnetic resonance
LED	light-emitting device
OFET	organic field effect transistor
OLED	organic light-emitting device

O.N.	overnight
OPV	organic photovoltaic
PCE	power conversion efficiency
$PC_{61}BM$	[6,6]-phenyl C61 butyric acid methyl ester
PDB	protodeboronation
PDI	polydispersity index
Ph	phenyl (C_6H_5)
PivOH	pivalic acid
PL	photoluminescent
py	pyridine
rt	room temperature
rxn.	reaction
s	singlet
S_0	ground singlet state
S cm^{-1}	Siemens per centimetre
S_n	excited singlet state (n > 0)
S_N2	substitution, nucleophilic, bimolecular reaction
t	triplet
T_n	excited triplet state
THF	tetrahydrofuran

TICT	twisted intramolecular charge transfer
TPA	triphenylamine
TPE	tetraphenylethylene
TD-DFT	time-dependent density functional theory
td	triplet of doublets
T_n	excited triplet state
TPA	triphenylamine
TTA	triplet-triplet annihilation
UV-vis	ultraviolet-visible spectroscopy
Xphos	2-dicyclohexylphosphino-2′,4′,6′-triisopropylbiphenyl
δ	partial charge or chemical shift in ppm
ε	absorption coefficient
λ	wavelength
λ_{ex}	excitation wavelength
λ_{em}	emission wavelength
λ_{max}	wavelength of maximum absorbance
η	number of atoms through which a ligand coordinates
υ	frequency of light
τ	luminescence lifetime
ϕ	luminescence quantum yield

μW	microwave conditions
4BE	tetraborylated chalcogenophene (E = S, Se or Te)

Chapter 1

Introduction

1.1. METALLACYCLE TRANSFER REACTIONS FOR THE SYNTHESIS OF MAIN GROUP ELEMENT-CONTAINING HETEROCYCLES

1.1.1. Introduction

Heterocycles containing main group elements from groups 13 to 16 have been widely used in the fields of material science, medicinal chemistry and biology.[1] Among heterocycles, the synthesis of metalloles, derivatives of cyclopentadienes in which the methylene unit is replaced by a heteroatom, is of paramount importance both for further understanding their properties and for unlocking potential applications, such as in OLEDs, OPVs and sensors. A general protocol for metalloles synthesis is the metallacycle transfer reaction in which a zirconacyclopentadiene complex, prepared from a low-valent zirconocene intermediate (e.g., $Cp_2Zr(II)$) that is generated in the presence of two alkynes, transfers the carbon-based butadiene fragment to the corresponding main group element halide (Scheme 1.1).[2,3] Using this protocol, a variety of heterocycles can be formed such as thiophenes, selenophenes, and tellurophenes (group 16 chalcogenophenes), pyrroles, phospholes and bismoles (group 15 heterocycles), or siloles and germoles (from group 14), among others.

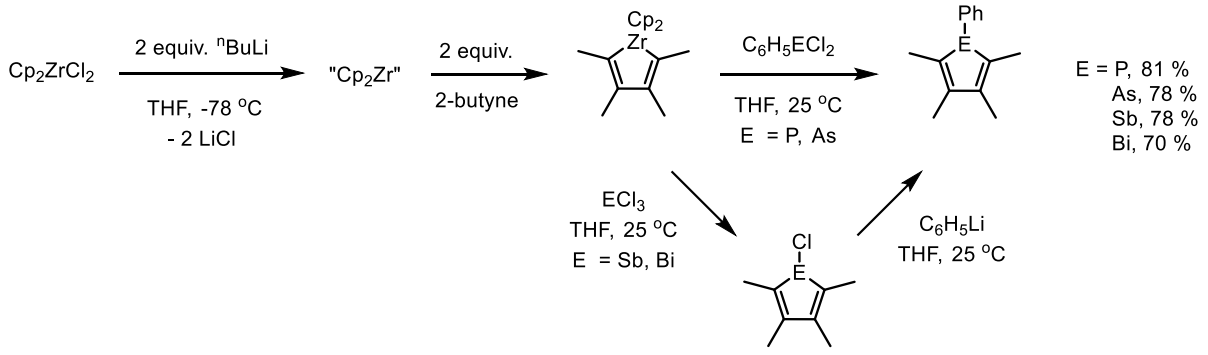

Scheme 1.1. Oxidative cyclization and metallacycle transfer reaction.[3]

The synthesis of zirconacyclopentadienes is very important not only for the formation of main group element-containing metalloles but as precursors for the synthesis of natural products and functional materials[4,5] (Figure 1.1) with benzene, pyridine, ketonic, cyclopentadiene and cyclooctatetraene cores.[6] Many natural compounds share the 1,3-butadiene motif, which can be formed by the hydrolysis of the respective metallocene complex.[4] The first example of the use of metallacycle-mediated oxidative cyclization reactions in the synthesis of a natural product, callystatin A, a cytotoxic natural product with potential as antitumor agent, was reported in 2008 by the Micalizio group.[7]

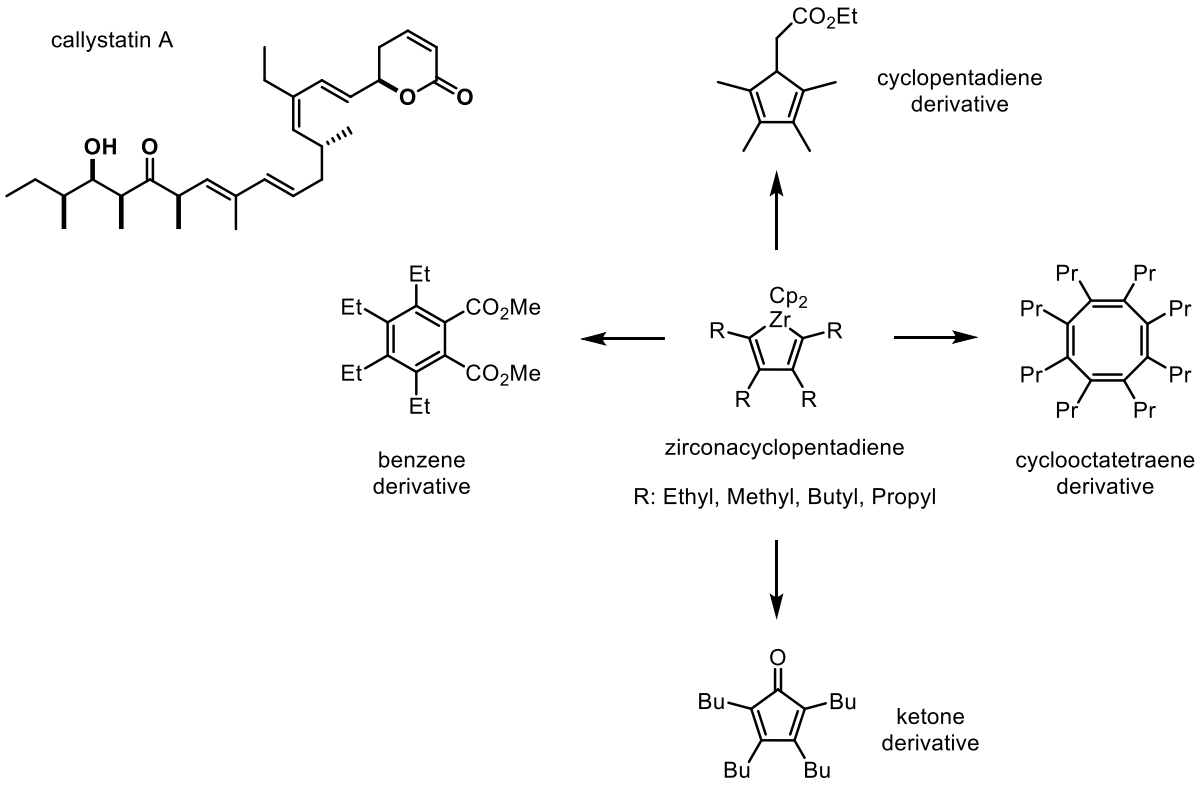

Figure 1.1. Some organic derivatives obtained from zirconacyclopentadiene precursors.

1.1.2. Formation of zirconacyclopentadienes

Many zirconacyclopentadienes have been made since the first report in 1961 by Caplier and coworkers[8] (Scheme 1.2). Of substantial relevance to this thesis, the reductive coupling of two equivalents of alkyne in the presence of a low-valent zirconocene species

"$Cp_2Zr(II)$" is an efficient way to construct zirconacycles. "$Cp_2Zr(II)$" can be generated by the reduction of the ready available Cp_2ZrCl_2 complex using different types of reducing agents, such as Na/Hg, Mg/Hg and ^{n}BuLi; "Cp_2Zr" units can also be stabilized in the presence of electron donating compounds, such as pyridine, and by π-complex formation with alkynes.

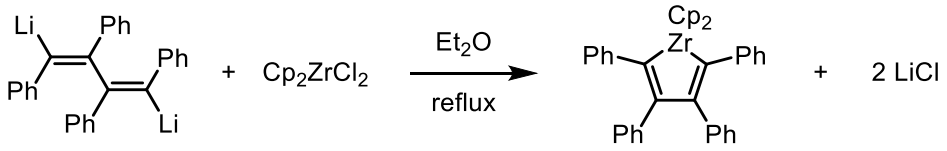

Scheme 1.2. The first synthesis of a zirconacyclopentadiene.

The treatment of Cp_2ZrCl_2 with 2 equivalents of ^{n}BuLi yields Cp_2ZrBu_2 (Negishi reagent), which exists as a mixture of many products that act as a source of "Cp_2Zr". The series of reactions to reach the low-valent zirconocene has been studied in detail by Harrod and coworkers[9] using electron paramagnetic resonance (EPR) and multinuclear NMR spectroscopy. They found that Cp_2ZrBu_2 suffers thermal decomposition starting with a γ-H elimination and liberation of butane to generate a 1,1-bis(cyclopentadienyl)-2-methyl-1-zirconacyclobutane (IV) (Scheme 1.3), which by a series of transformations occur to form paramagnetic and diamagnetic zirconocene complexes in equilibrium, one of them being Cp_2Zr(1-butene).

The Takahashi reagent $Cp_2Zr(C_2H_4)$ (Scheme 1.3) is formed by combining Cp_2ZrCl_2 with 2 equivalents of EtMgBr or EtLi at low temperature.[10] The related PMe_3, stabilized complex $Cp_2Zr(C_2H_4)(PMe_3)$, was reported by Alt and coworkers.[11]

In other work by Rosenthal and coworkers, they reduced the high-valent zirconocene Cp_2ZrCl_2 with Mg in the presence of $Me_3SiC{\equiv}CSiMe_3$ (Scheme 1.3) to form the isolable complex of $Cp_2Zr(THF)(Me_3SiCCSiMe_3)$. This complex in the presence of the weakly coordinated solvents benzene or pentane, or when heated under vacuum, decomposes to form a zirconocene dimer via loss of coordinated THF. X-ray measurements show the Zr-O bond

length in $Cp_2Zr(THF)(Me_3SiCCSiMe_3)$ to be relatively long (2.390(5) Å), suggesting that the lability of Zr-THF interaction might be the cause of complex decomposition. The zirconocene dimer (Scheme 1.4) is an air- and moisture-sensitive complex that decomposes at 142-143 °C. To circumvent the decomposition of $Cp_2Zr(THF)(Me_3SiCCSiMe_3)$ in hydrocarbon solvents, which prevented the reagent to be used in synthesis involving these solvents, the same group prepared $Cp_2Zr(NC_5H_5)(Me_3SiCCSiMe_3)$[12] by displacement of THF with pyridine; this new, formally Zr(II) complex, is still air- and moisture-sensitive, but now it can be used as a reagent in a wide range of weakly-coordinating solvents.

Negishi reagent:

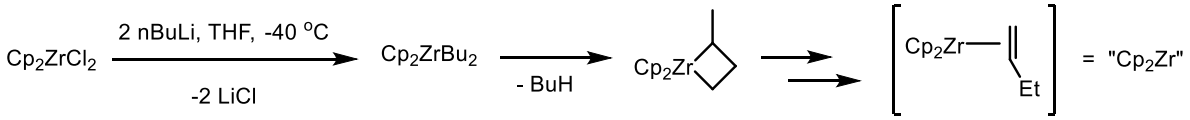

Takahashi reagent:

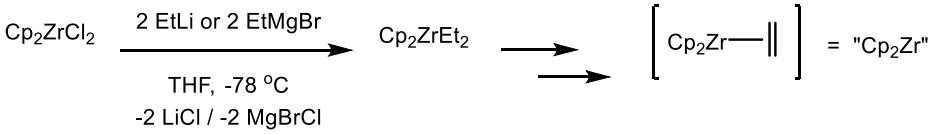

Rosenthal reagent:

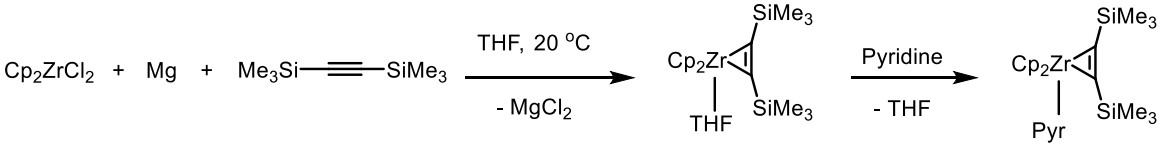

Namy-Szymoniak reagent:

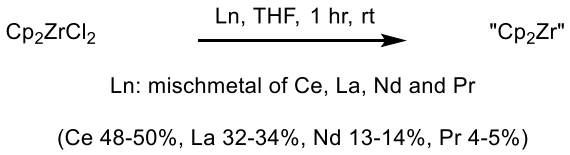

Scheme 1.3. Synthesis of the "Cp_2Zr"-sources. Negishi,[9,13] Takahashi,[10] Rosenthal[14] and Namy-Szymoniak[15] reagents.

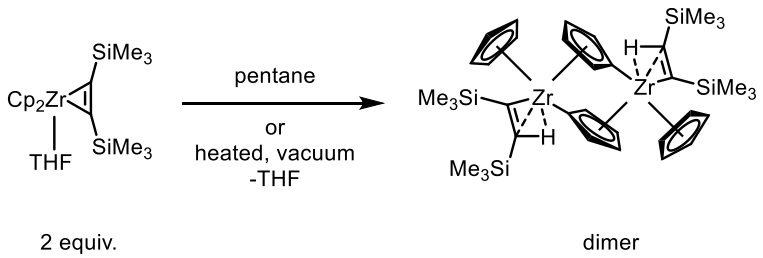

Scheme 1.4. Formation of zirconocene dimer via THF loss.

In 2006, Szymoniak and coworkers,[15] developed an efficient protocol to generate "Cp_2Zr" under mild conditions (1 h at room temperature, THF) (Scheme 1.3). In the presence of mischmetal, an easy available alloy composed of rare earths (Ce 48-50%, La 32-34%, Nd 13-14%, Pr 4-5%), Cp_2ZrCl_2 is reduced to Cp_2Zr(II); this reagent was then used in intermolecular couplings involving terminal alkynes.

One criteria for determining the "Cp_2Zr" source to be used (Scheme 1.3) is the final structure of zirconacyclopentadiene to be synthesized. The synthesis of zirconacycle-pentadienes depends on the supporting ligands at Zr, type of alkyne (terminal or internal) and the amount of alkyne added.[16] The Negishi reagent (Cp_2ZrBu_2) shows some limitations in that it cannot be used with terminal alkynes and it is very challenging to form regioselective unsymmetrical zirconacyclopentadienes due to a lack of regioselectivity. The Takahashi reagent proved to be useful in forming unsymmetrical zirconacyclopentadienes by the stepwise addition of two different alkynes as shown in Scheme 1.5.[10]

The coupling of symmetrical alkynes can be performed with almost all of the "Cp_2Zr(II)" species mentioned before, however, there are limitations in the use of most of the low-valent species to couple terminal alkynes;[15] for example, the intramolecular coupling of the symmetrical 1,7-octadiyne is not possible using the Negishi reagent and the result is an unidentified mixture of products with deprotonation of a terminal alkyne being a likely side reaction. The relatively high acidity of terminal alkynes leads to proton-transfer to the low-valent "Cp_2Zr(II)" species, as a result the formation of zirconacyclopentadienes from terminal alkynes is rare.[16]

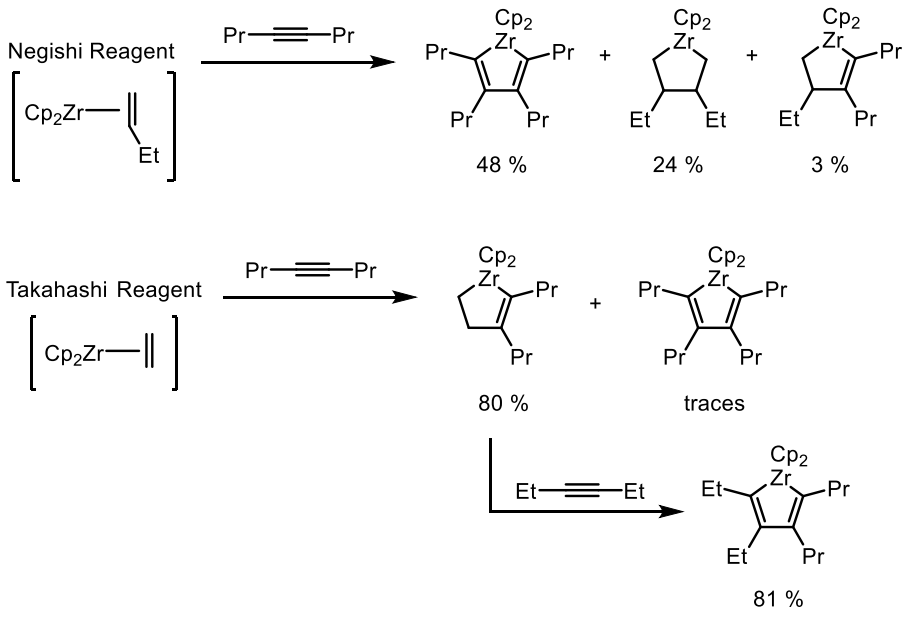

Scheme 1.5. Selectivity of Negishi and Takahashi reagents in the target synthesis of unsymmetrically-substituted zirconacyclopentadienes.

The Namy-Szymoniak reagent mentioned before can facilitate the intermolecular reductive coupling of terminal diynes,[15] as was evidenced by the reductive coupling of phenylacetylene to afford a mixture of 2,5- and 2,4-diphenylzirconacyclopentadienes in a ratio of 2.5 to 1 (Scheme 1.6, eq. 1). In another example, bulky tris(trimethylsilyl)silyl-acetylenes were coupled to form exclusively 2,5-disubstituted zirconacyclopentadienes after the reduction of Cp_2ZrCl_2 with Mg (Scheme 1.6, eq. 2).[17] High regioselectivity towards the coupling of aromatic-substituted terminal alkynes[18] was found using the isolable indenyl (Ind) zirconium complexes $(Ind)_3ZrH$ or $(Ind)_2Zr(CO)_2$ to form exclusively 2,5-disubstituted-diarylzirconacyclopentadienes (Scheme 1.6, eq. 3).

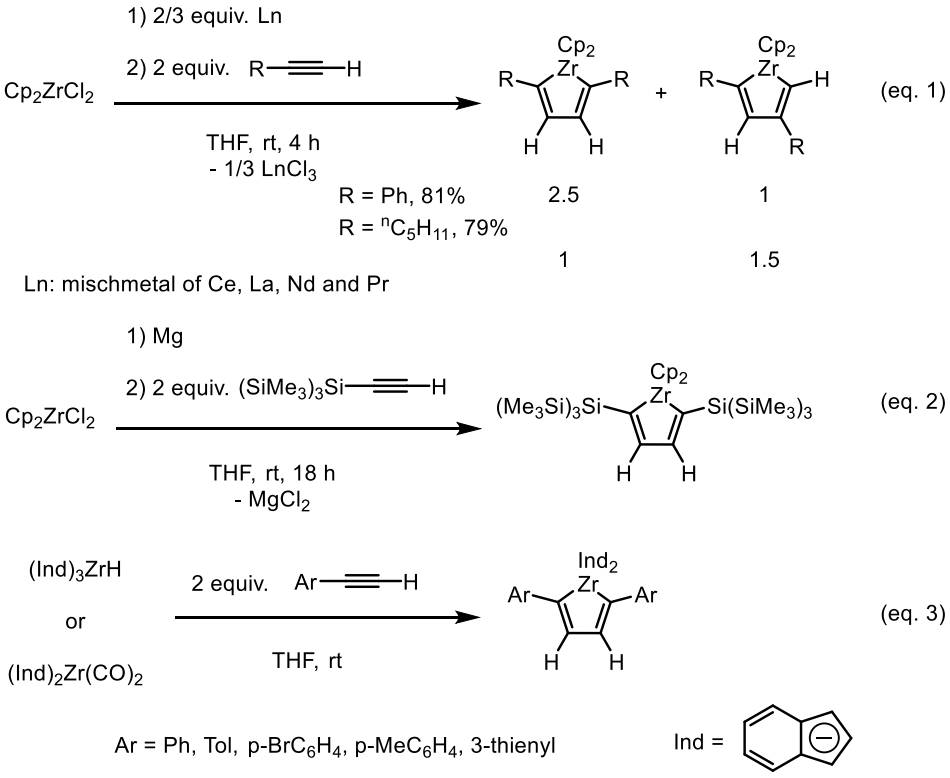

Scheme 1.6. Reductive coupling of terminal alkynes towards the formation of regioselective 2,5-disubstituted zirconacyclopentadienes.

The use of symmetric alkynes ($R^1C{\equiv}CR^1$) leads to the formation of zircona-cyclopentadienes through a stepwise mechanism described first by Negishi[20] in 1989 and then further studied by Tilley[19] (Scheme 1.7 - A). "$Cp_2Zr(II)$" is a 14-electron species, with a filled non-bonding orbital and two empty frontier molecular orbitals; in the first step, the "$Cp_2Zr(II)$" uses its filled non-bonding orbital and one of the empty orbitals to react with alkyne to form a zirconacyclopropene intermediate, which binds a second equivalent of alkyne to form a transient species that undergoes intramolecular carbometallation to afford the respective zirconacyclopentadiene.

Reductive coupling of symmetric or unsymmetric alkynes follow the same mechanism proposed by Negishi,[19] leading to a transition state where one alkyne is strongly

bound to Zr while the other alkyne interacts more weakly, proving a stepwise mechanism and strong electronic bias that can sometimes lead to regioselectivity in the coupling reaction.

Coupling two different symmetric alkynes ($R^1C{\equiv}CR^1$ and $R^2C{\equiv}CR^2$) can lead to the formation of unsymmetric zirconacycles (Scheme 1.6-C Path 3 and 4), with the reaction outcome dependent on the stability of the initially formed three-membered zirconacycle formed after addition of the first alkyne equivalent.

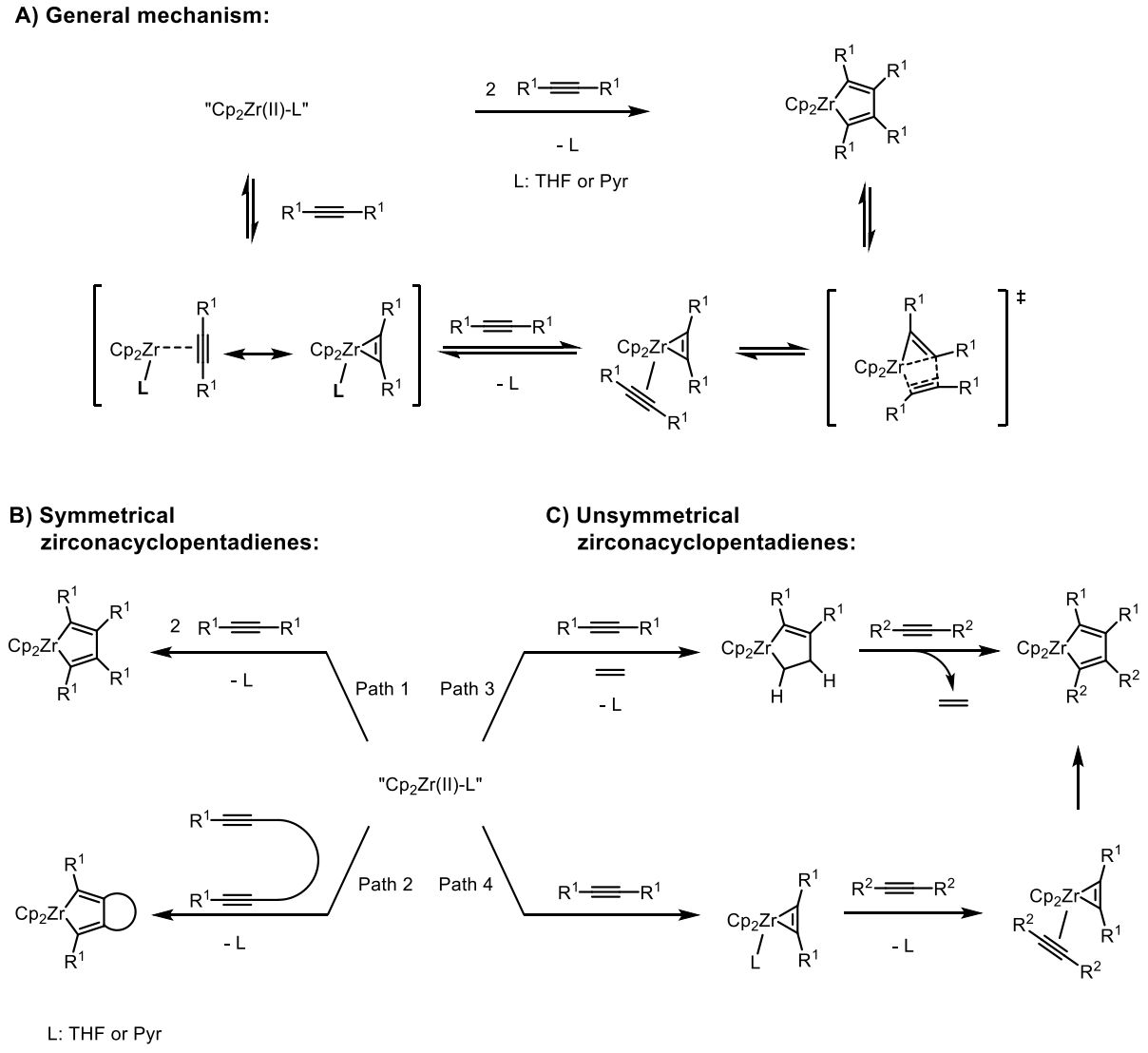

Scheme 1.7. Mechanism of five-membered zirconacycle formation[19,5] and general pathways of reductive coupling of alkynes in the synthesis of symmetric and unsymmetric zirconacyclopentadienes.

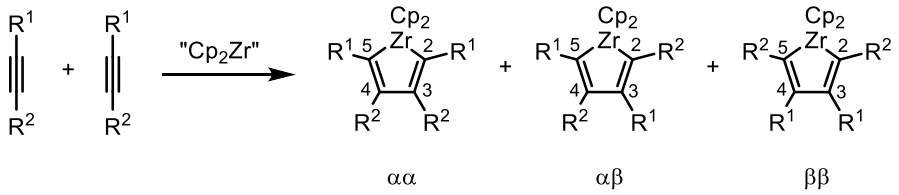

Scheme 1.8. Regioselective reductive coupling of two unsymmetric alkynes. Three isomers are possible: αα, αβ and ββ.

In the case of using unsymmetric alkynes ($R^1C{\equiv}CR^2$), three possible isomers can be formed (Scheme 1.8). In order to gain control over the regioselectivity of alkyne-alkyne reductive coupling, it is important to understand the role of substituents on the reaction outcome.[21,22] The regioselectivity can be controlled by both steric and electronic effects. Steric effects become significant when bulky substituents, such as mesityl (Mes), are present and often lead to placement of these groups in the β-position of the zirconacycle. Despite the challenges often encountered in achieving regioselectivity in the reductive coupling with Negishi's reagent, the selectivity of the reaction can still be influenced greatly by groups such as $SiMe_3$[23] (Scheme 1.9, eq. 1) and PPh_2 (Scheme 1.9, eq. 2) which each prefer α-substitution about a zirconacyclopentadiene.[24] Of note, there is no known zirconacycle containing a $SiMe_3$ group at the β-position (eq. 1). Zirconacycles containing two $SiMe_3$ groups at the β-position are unstable and tend to undergo alkyne exchange readily, to form unsymmetric zirconacycles.[23] The α-position is initially preferred by the $SiMe_3$ at room temperature, however, at higher temperature (eq. 1), the steric effects of $SiMe_3$ group become important and the final product of reductive coupling of alkynes happens with the less hindered groups attached to the alkyne. Electron-withdrawing fluoroaryl groups (C_6F_5 and C_6HF_4)[19] tend to adopt β-positions upon coupling (Scheme 1.9, eq. 3) over α-positions, due to increased steric repulsion between the cyclopentadienyl ligands and the fluorinated aryl groups at the α-positions in the respective transition state. Moreover, attractive π-π interactions between parallel fluoride-containing aryl groups in the transition state, would favour the formation of the β isomer. Overall, electronic, steric and attractive interactions,

would favour the formation of the ββ over the αβ zirconacyclopentadiene isomer, according to the authors.

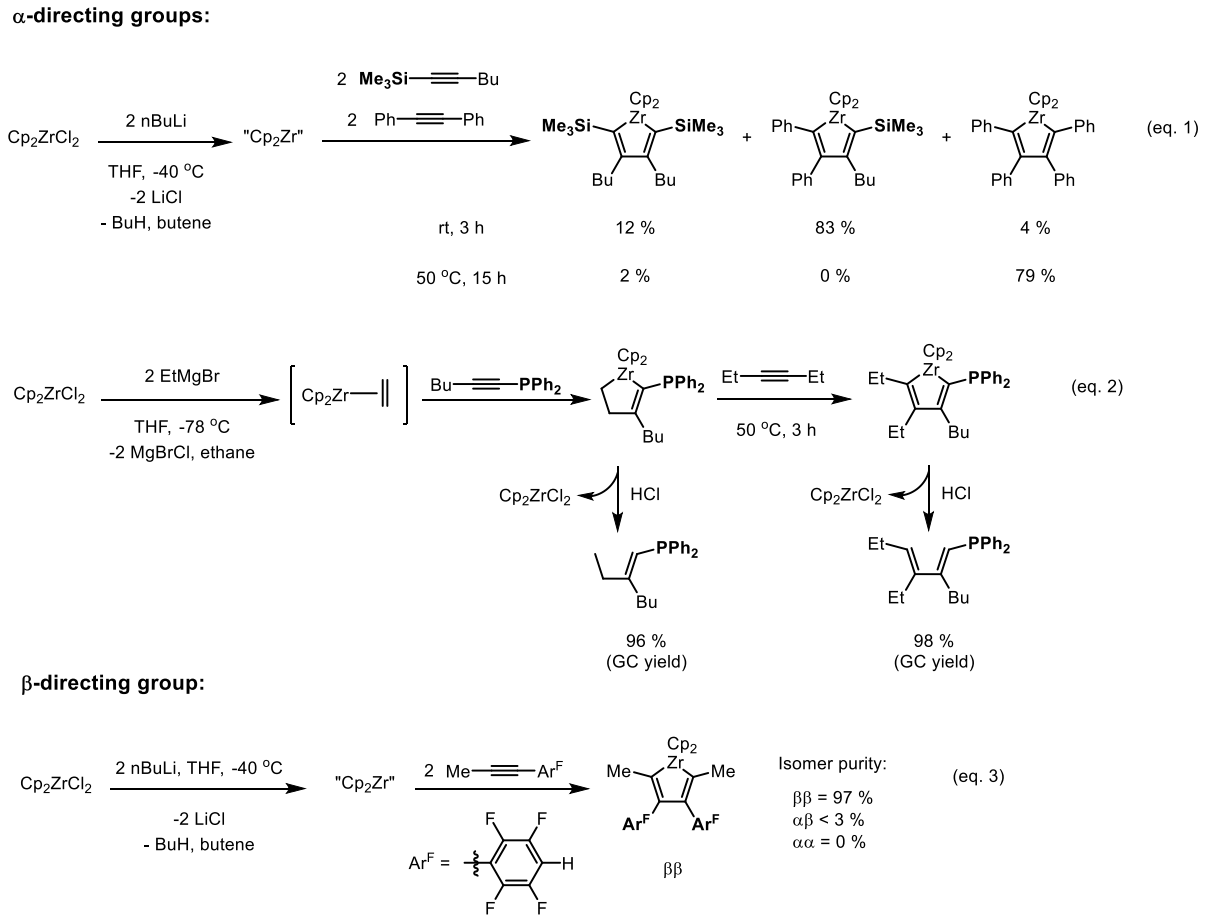

Scheme 1.9. Examples of α- and β-directing regioselective synthesis of zirconacyclopentadienes.

When (η^2-propene)Ti(O^iPr)$_2$ is used as an alkyne coupling reagent, the second terminal alkyne is coupled regioselective to the α-position by using hydroxyl and ketonic -COX (X = OR, NR_2; R = alkyl) groups (Scheme 1.10, top), leading to unsymmetrical titanacycles.[4,25] In the case of highly branched-substituted alkynes, having hydroxyl groups (Scheme 1.10, bottom) attached to the alkyl branch, the reaction is directed towards a

regioisomer (fused bicyclic titanacyclopentadiene) with a sterically demanding group attached at the 2-position of the metallocene.[4,26]

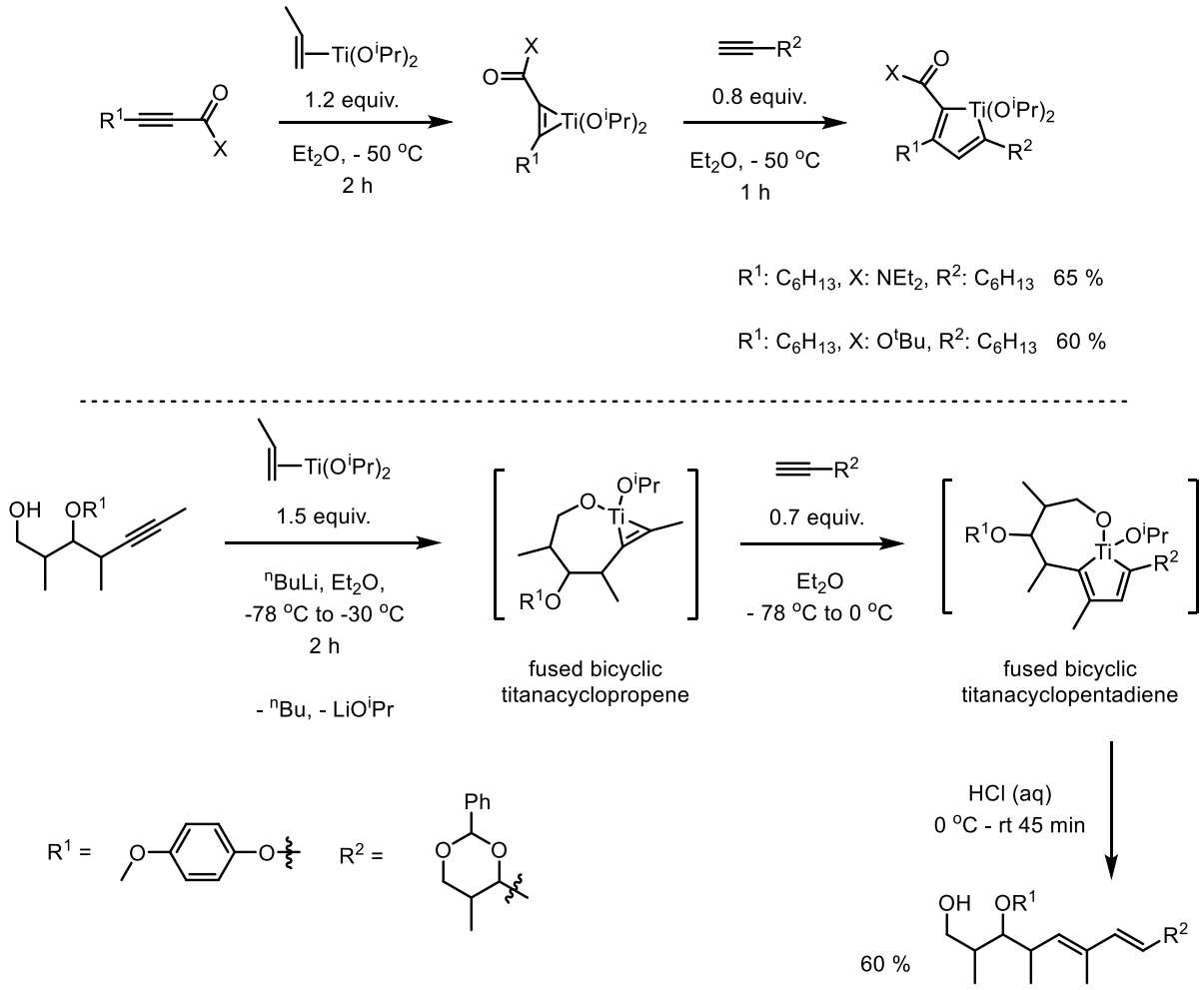

Scheme 1.10. Selective synthesis of titanacyclopentadienes by COX and OH α-directing groups.

1.1.3. Conversion of zirconacyclopentadienes into main group metalloles by transmetallation

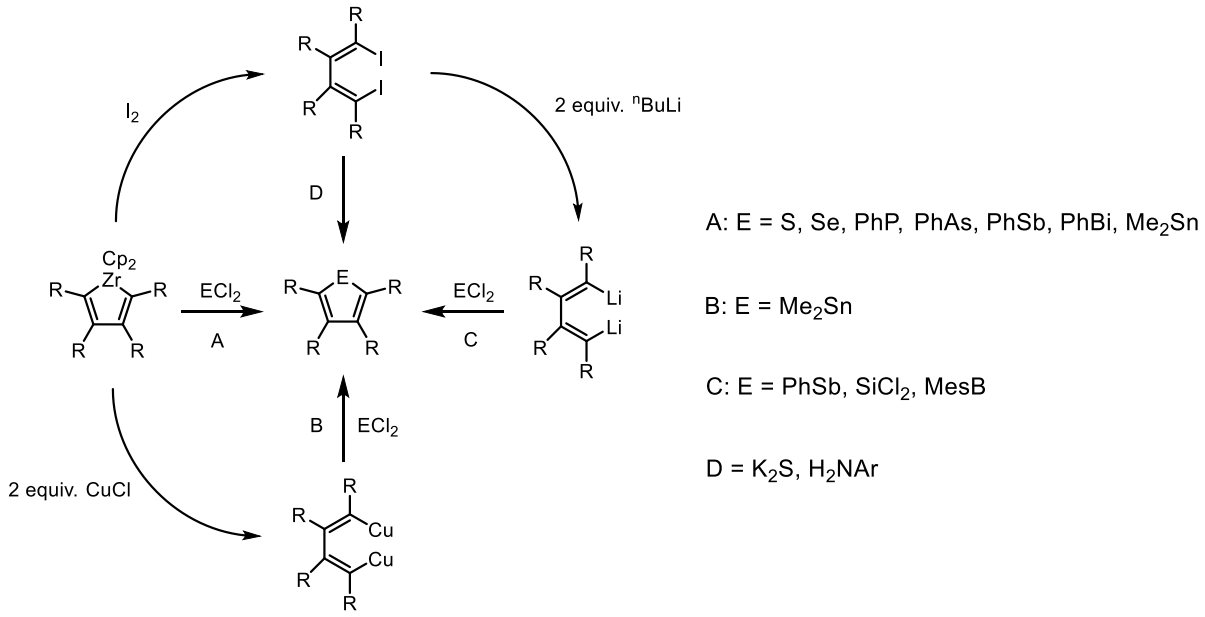

Scheme 1.11. Main group metalloles from zirconacyclopentadienes; E = main group element.

Since the first Zr/E transmetallation (E = main group element) reaction carried out by Fagan and Nugent in 1988,[2] a lot of progress have been made in the reaction of zirconacyclopentadienes with main group element halides. This transmetallation reaction involves the transfer of a 1,3-butadiene unit from a zirconacyclopentadiene to a main-group element center to form a new five-membered main group heterocycle. In general, there are four general modes of synthesis through transmetallation starting from zirconacyclo-pentadienes as summarized in Scheme 1.11. Direct transmetallation (Scheme 1.11, route A) is the reaction of zirconacyclopentadiene with the main group element halide. However, the lack of reactivity of zirconacyclopentadienes (due to a lower nucleophilicity relative to other sources of formally anionic carbon nucleophiles) in the presence of some main group halides makes the reaction slow and sometimes it does not proceed at all, e.g. in the attempted preparation of pyrroles and siloles. In these cases, in order to facilitate transmetallation, it is

necessary to have more reactive species, such as dicopper- or dilithiated-1,3-butadienes (Scheme 1.11, route B and C, respectively) to deliver the substituted 1,3-butadiene unit to a main group element.

In 1994 Fagan and Nugent[3] proposed that metallacycle transfer proceeds via a 4-membered transition state. Also, they found that the transfer of the metallacycle to the main group element is more readily when the main group element is able to expand its coordination number. A general proposed mechanism for metallacycle transfer is shown in Scheme 1.12.

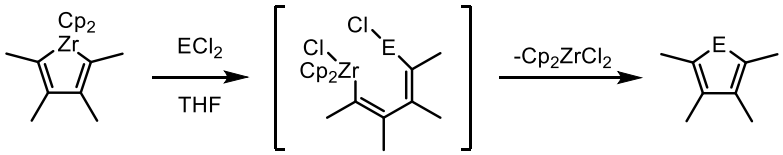

Scheme 1.12. Proposed mechanism for metallacycle transfer. E = main group element (e.g. S, Se).

An example of direct transmetallation is the one-pot synthesis of phospholes, arsoles, stiboles and bismoles in high yield (Scheme 1.13), using the corresponding main group halides $PhECl_2$ or ECl_3/PhLi.

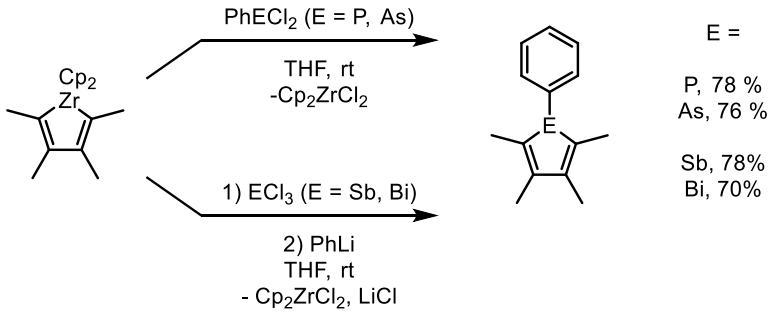

Scheme 1.13. Preparation of phospholes, arsoles, stiboles and bismoles through direct transmetallation.[2,3]

Direct transmetallation is not always adequate to form main group metalloles, as is the case for the attempted synthesis of furans, pyrroles and siloles. Instead an efficient protocol for the synthesis of pyrroles has been developed using zirconacyclopentadienes and azides as reactants in the presence of a copper (I) salt (Scheme 1.11, route B and Scheme 1.14).[27] The authors found that the reaction did not proceed in the absence of CuCl, and the proposed mechanism of the transformation is described in Scheme 1.14. In the first step, formation of a dicopper butadienide occurs through transmetallation of zirconacyclopentadiene with CuCl, then the azide coordinates to the two copper metals to give a copper-azide complex, which later releases N_2 upon nucleophilic attack of alkenylcopper on the azide. The pyrrole end-product is proposed to form by a ring-closure reaction.

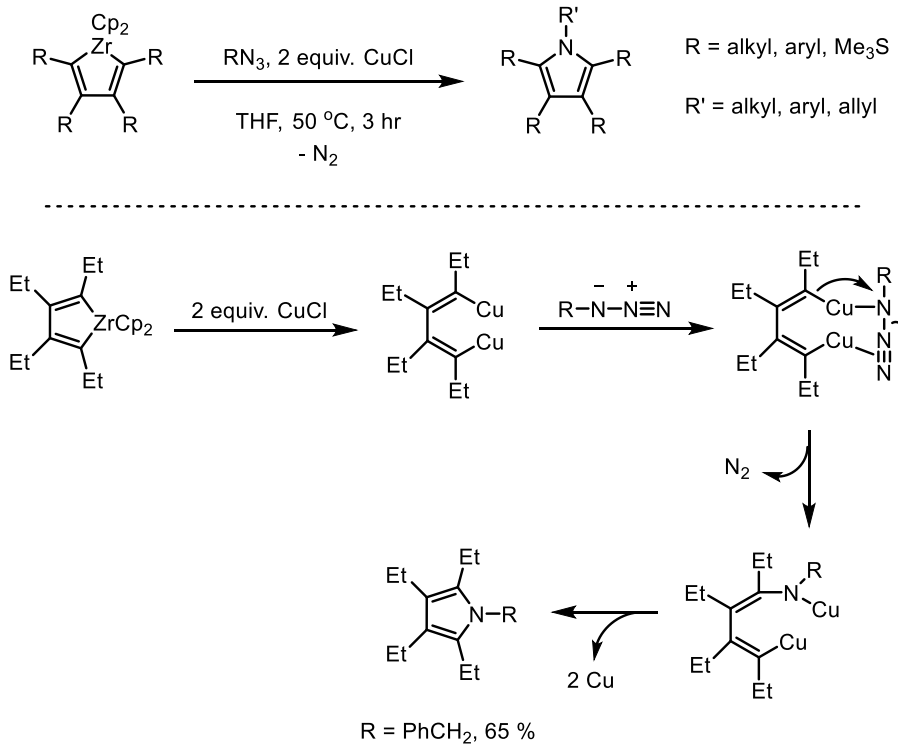

Scheme 1.14. Synthesis of pyrroles using azides and CuCl and proposed mechanism.[27]

The synthesis of siloles using $SiCl_4$ and R_2SiCl_2 does not proceed by direct transmetallation, even in the presence of CuCl as a catalyst/promoter. However, efficient synthetic procedures have been developed to form siloles by first forming dilithiated dienes;

these dilithiated dienes are available from the reaction of dihalobutadienes and two equivalents of ^{n}BuLi (Scheme 1.11, route C; Scheme 1.15).[28,29] In this reaction, the main issue is the formation of the requisite diiododienes. The reaction between the zirconacycle and I_2 needs longer reaction times and heating (50 °C) to form diiododienes. A great improvement was made by Takahashi in 1999[29] with the addition of CuCl to the reaction mixture, which affords the required diiododiene quantitatively (Scheme 1.15).

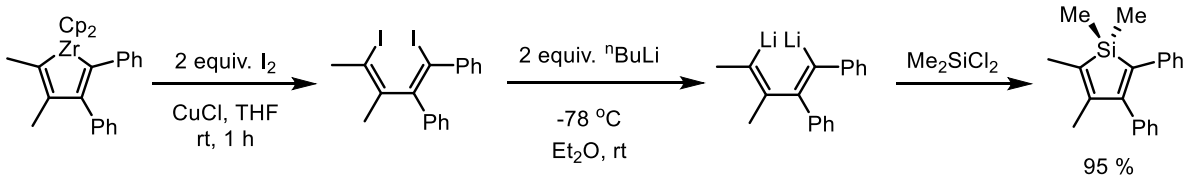

Scheme 1.15. Synthesis of siloles through an iodination/lithiation process.[29]

The last strategy to form five-membered metalloles of main group elements is through the route D (Scheme 1.11) in which a 1,4-dihalo-1,3-butadiene reacts with amines (as a source of N-R) or potassium sulfide (K_2S) or carbon disulfide (CS_2) (as a source of sulfur), to form the respective *N*-arylpyrroles[30] and tetra-substituted thiophenes[31] (Scheme 1.16).

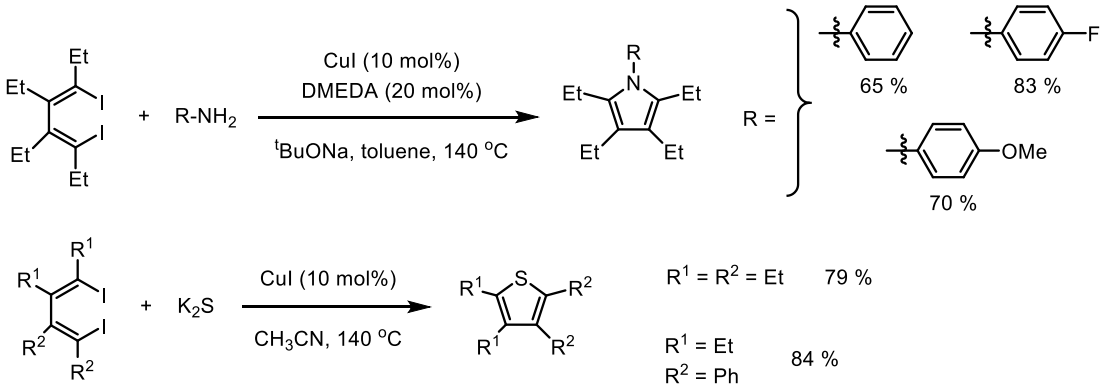

Scheme 1.16. Synthesis of pyrroles and thiophenes through copper-catalyzed transmetallation.

1.2. CHALCOGENOPHENES AND RELATED GROUP 16 ELEMENT-BASED HETEROCYCLES

1.2.1. Synthetic methods and existing challenges with accessing tellurophenes

Chalcogenophenes are five-membered heterocycles containing group 16 elements (e.g. O, S, Se and Te). Interest in chalcogenophene synthesis lies in the potential use in pharmacology[32,33] and in the search for new optoelectronic materials. Specifically, some chalcogenophenes have shown potent antitumor[34–36] and antiviral[37] activities. Chalcogenophenes also find possible applications in organic photovoltaics,[38,39] light-emitting devices,[40] bio-imaging dyes[41,42] and in high-performance air-stable thin-film transistors.[43–45]

Three general approaches can be found in the literature for the synthesis of chalcogenophenes: 1) ring-closing reactions involving 1,3-diynes, 2) transmetallation of suitable chalcogen-halides with zirconacyclopentadienes under mild conditions, 3) intramolecular cyclization of acyclic chalcogen precursors.

As shown in Scheme 1.17 (eq. 1) 2,5-disubstituted chalcogenophenes (including precursor small molecule chalcogenophenes that can later be functionalized at the 2- and 5-positions) can be prepared via ring-closing reactions between 1,3-diynes and Na_2S, H_2Se or Na_2Te, respectively. Both symmetric and unsymmetric 2,5-disubstituted thiophenes can be synthesized in excellent yields with this method under mild conditions.[46] Interestingly, Zhao and Tang noted that ring-closure with Na_2S or NaSH is a very solvent-dependent reaction with high yields obtained in DMF; however no reaction was observed in toluene, THF, CH_2Cl_2, Et_2O, MeOH, dioxane or CH_3CN.

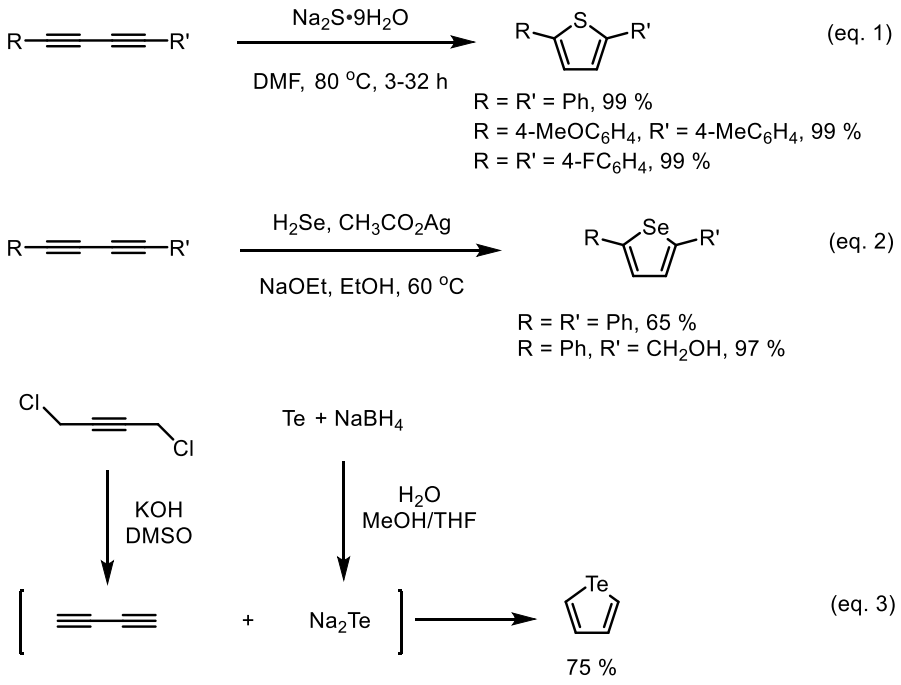

Scheme 1.17. Synthesis of chalcogenophenes via the ring-closing of 1,3-butadiynes.

2,5-Disubstituted selenophenes were formed in good yields using an excess hydrogen selenide, H_2Se, and a silver salt as a catalyst in EtOH (Scheme 1.17, eq. 2).[47] Fortunately, there are other methods to form disubstituted selenophenes that avoid the use of the very toxic gas H_2Se. For example, $SeCl_2$ can be stabilized in the form of the 2,2′-bipyridine (Bipy) adduct Bipy•$SeCl_2$[47] and transmetallation of this Se^{II} source with zirconacyclopentadienes yield selenophene heterocycles at room temperature.

2,5-Disubstituted tellurophenes were first synthesized in 1966 by Mack[48] via the reaction of 1,3-diynes with sodium telluride (Na_2Te); Na_2Te was formed *in situ* by the reduction of tellurium metal with sodium in liquid ammonia. Additional investigations were conducted by Fringuelli and Taticchi in order to obtain better yields of Te heterocycle,[49] such as the *in situ* generation of butadiyne, the exclusion of oxygen and moisture, the use of liquid ammonia free of iron. Later the improved synthesis of Na_2Te from the reduction of Te metal with $NaBH_4$ in water and the use of 1,4-dichloro-2-butyne as a source of diacetylene[50] afforded tellurophene in 32-48% yield. More recently the Seferos group used DMSO instead

of dioxane as a solvent in the above tellurophene synthesis, leading to an increase in the yield of tellurophene to 75 % (Scheme 1.17, eq. 3).[51]

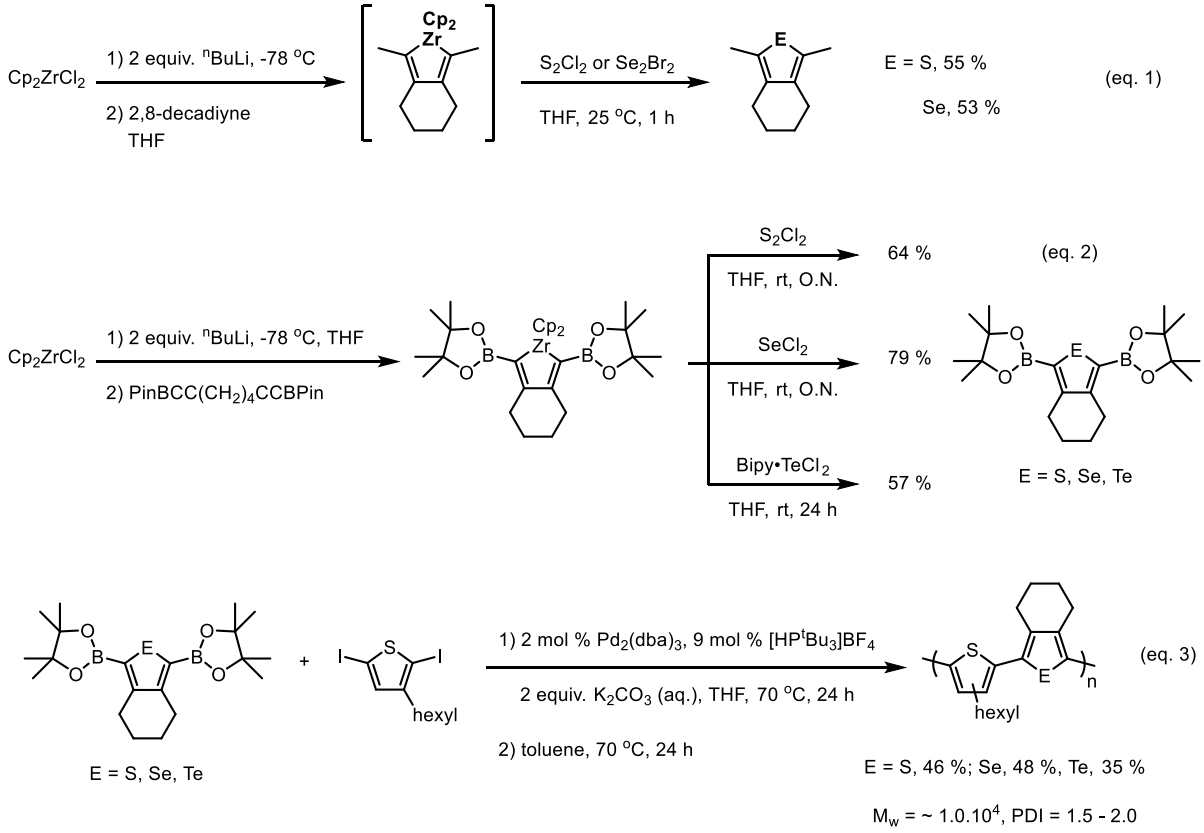

Scheme 1.18. Synthesis of chalcogenophenes through transmetallation reactions via zircona-cyclopentadiene intermediates.

Transmetallation is also an effective route to prepare chalcogenophenes in one-pot via the reaction of *in situ* generated zirconacycles with main group halides. Thiophenes and selenophenes were first synthesized in this way by Fagan and Nugent using sulfur monochloride (S_2Cl_2) and selenium dibromide (Se_2Br_2) as chalcogen sources (Scheme 1.18, eq. 1).[3] In 2013 the Rivard group synthesized a series of boryl-substituted tellurophenes from the Te^{II} source Bipy•$TeCl_2$ under mild conditions (Scheme 1.18 eq. 2); the resulting tellurophenes were then co-polymerized with conjugated monomers with Suzuki-Miyaura cross-coupling to form novel chalcogenophene-containing polymers (Scheme 1.18 eq. 3).[52]

The preparation of Bipy•$TeCl_2$ is possible by treating [Bipy•$TeCl_3$]Cl (made from $TeCl_4$ and bipy) with the reducing agent Ph_3Sb.[53]

Being able to functionalize chalcogenophenes with different molecular groups at different positions in the five-membered ring is very important due to the potential applications of these compounds in optoelectronics and as pharmaceuticals. In this regard, the synthesis of 3-halo-2,5-disubstituted chalcogenophenes (Scheme 1.19) is noteworthy as these products can be functionalized at the 3-position using palladium-catalyzed Suzuki-Miyaura, Sonogashira, and Stille cross-coupling reactions, leading to a large number of new substituted chalcogenophenes of tunable optoelectronic behavior.

One way to obtain 3-halo-2,5-disubstituted chalcogenophenes is via electrophilic cyclization of alkyl/aryl chalcogeno ether precursors (Scheme 1.19).[54] Electrophilic cyclization proceeds by the coordination of the electrophile to the triple bond, this activates the triple bond toward the nucleophilic attack by the chalcogen center on an alkyne, which forms a cationic intermediate. Then the leaving group (R: alkyl or aryl) on the chalcogenophene is displaced in an S_N2 process by a nucleophilic halide that is generated *in situ*, to eventually yield the final cyclized product. [54]

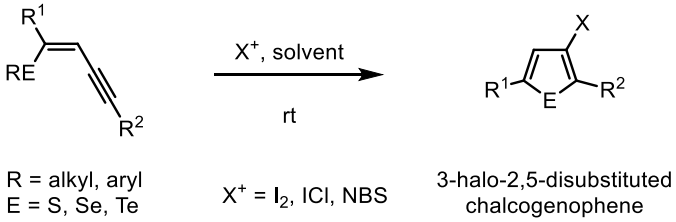

Scheme 1.19. Electrophilic cyclization of acyclic chalcogen precursors to form 3-halo-2,5-disubstituted chalcogenophenes.

2,3-Benzo[b]thiophenes have also been prepared under mild conditions by electrophilic cyclization using the halogens I_2 or Br_2 as reactants (Scheme 1.20, eq. 1).[55,56] This reaction proceeds under very mild reaction conditions and other electrophiles, such as NBS and PhSeCl can be used to give 2,3-benzo[b]chalcogenophenes in good yields. In

another work, the synthesis of 4-iodo-thiophenes/selenophenes via the cyclization of diynols promoted by dichalcogenides (MeSSMe or ^{n}BuSeSeBu^{n}) and a halogen source have also been reported (Scheme 1.20, eq. 2).[57] These reactions were showed to be selective by controlling the halogen source and the ratio of reagents. When other sources of halogen (in place of I_2) such as NBS or Br_2, were used, the formation of a by-product transpired wherein a thio- or seleno-ether unit was installed at the 3-position of the chalcogenophene. [57]

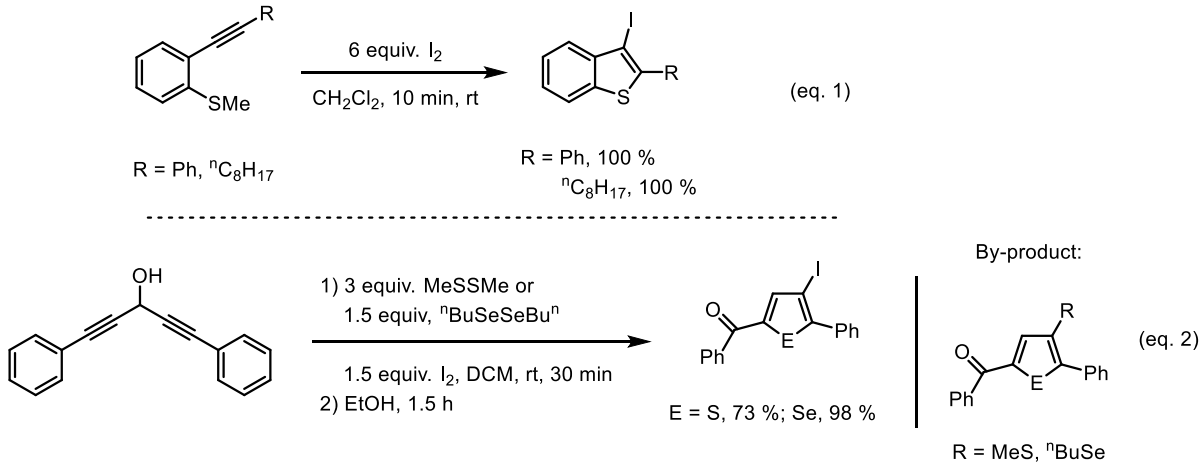

Scheme 1.20. Synthesis of 3-iodide-benzothiophenes and 4-iodide-thiophene/selenophene via electrophilic cyclization.

A very thorough study was done by Zeni on the synthesis of 3-halogen-2,3-disubstituted selenophenes. Using (Z)-selenoenynes as precursors, they managed to conduct the target selenophene cyclizations reaction under very mild conditions (Scheme 1.21).[58] This cyclization reaction is solvent-dependent and interestingly only proceeds when the leaving group has a Se-C(sp^3) bond. The resulting 3-iodoselenophenes are valuable precursors to 3-substituted selenophenes.

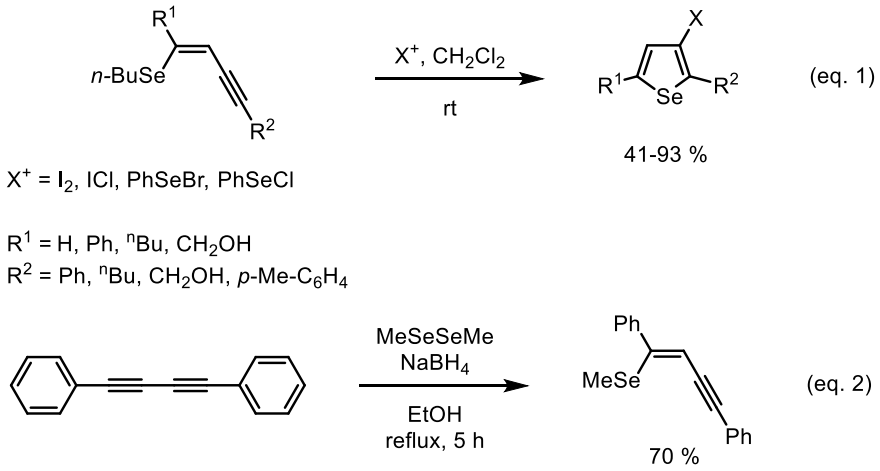

Scheme 1.21. Synthesis of 3-substituted selenophenes via electrophilic cyclization and synthesis of the acyclic ene-yne precursor.

3-Iodo-tellurophenes were prepared from tellurobutenynes by electrophilic cyclization using two equivalents of iodine in petroleum ether. $NaBH_4$ was used to reduce the likely diiodide tellurophene (Te^{IV}) intermediate to afford the final 3-iodo-2,5-disubstituted tellurophenes in moderate to good yields (Scheme 1.22).[59]

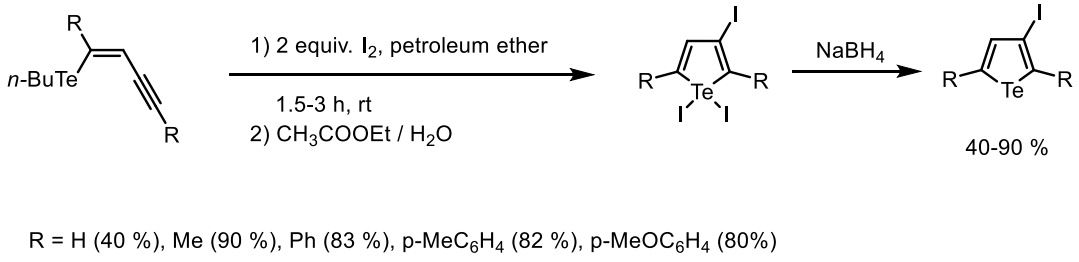

Scheme 1.22. Electrophilic cyclization of tellurobutenynes to form 3-iodo-2,5-disubstituted tellurophenes.

1.2.2. Optoelectronic properties of tellurophenes

To better understand the optoelectronic properties of tellurophenes and/or polytellurophenes it is important to first determine the intrinsic characteristics that the heavy Te atom brings to heterocycles in comparison with the lighter sulfur- and selenium-based analogues. Among the characteristics to have in mind is the low electronegativity of Te, its larger atomic size, and related factors such as polarizability, the aromaticity of the heterocycles, intermolecular interactions (via Te---Te contacts) and the heavy atom effect on luminescence. These intrinsic characteristics are interrelated and therefore sometimes a specific final property improves at the expense of another one, such as charge transport and luminescence properties: while charge transfer is favoured by close intermolecular packing, luminescence in the solid state might be quenched by the same close molecular packing.

Some optoelectronic properties being investigated with tellurophenes are enhanced light absorption for organic photovoltaic (OPV) applications and phosphorescence for LEDs; in relation to the development of efficient LEDs, aggregation induced emission (AIE) is now commonplace and leads to improved light emission efficiencies in the solid state. Improved charge transport properties are also of value in the development of next generation organic field effect transistors (OFETs).[59]

The presence of more polarizable (and larger) Te atoms in tellurophenes leads to stronger intermolecular Te--Te interactions when compared to Se--Se and S--S interactions in related thiophene and selenophene systems. These interactions promote close intermolecular packing that can enhance crystallinity, at the expense of lower solubility in organic solvents. Substantial aggregation in the solid state can also negatively impact the morphology within films of polytellurophenes/acceptor blends in OPV devices,[60] thus designing tellurophenes-based materials with improved solubility is a key point for tellurophene-containing solar cells.

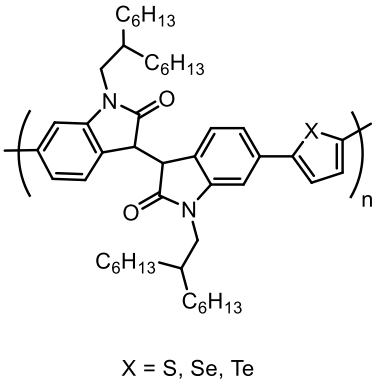

	E_g (eV)	HOMO (eV)	LUMO (eV)	PCE (%)
S:	1.81	-5.61	-3.70	3.94
Se:	1.72	-5.66	-3.68	5.69
Te:	1.64	-5.69	-3.74	1.07

Figure 1.2. Chalcogenophenes as co-monomers within isoindigo-based conjugated copolymers.

Tellurium is less electronegative and more polarizable than Se and S, respectively, which can lead to a lowering of the oxidation potential of the corresponding heterocycles via raising the energy of the HOMO. However, deep HOMO energy levels are often desired in OPVs to obtain high open-circuit voltages (V_{OC}). Conversely, raising the HOMO level, leads to a smaller HOMO-LUMO gap, leading to an increase in overall solar light absorption at longer wavelengths, affording possible improvement in power conversion efficiencies (PCEs). The effect of tellurophene in isoindigo-based conjugated copolymers on the photovoltaic properties has been reported (Figure 1.2).[60] As expected, the band gap is slightly reduced going from the polythiophene derivative to its polyselenophene and polytellurophene counterparts (E_g = 1.62, 1.58, 1.53 eV; as determined by optical spectroscopy and cyclic voltammetry). In this case a slight decrease in the HOMO energy was noted in the Te-containing polymer (-5.69 eV). As mentioned before, deep HOMO energy levels in tellurophenes-containing polymers are expected to afford high open-circuit voltage (V_{OC}), which was observed (0.92 V), however its short-circuit current density (J_{SC}) (which depends on the efficiency of light absorption, exciton diffusion to and dissociation at the donor-acceptor interface, and charge mobility)[61] was very low (2.51 %). An overall performance in the solar cell of power conversion efficiency (PCE) of only 1.07 % was obtained. Further studies showed a more crystalline structure in the Te-substituted polymers, which is in agreement with the highest hole mobility found in FETs among the chalcogenophene series

(0.072 $cm^2 V^{-1} s^{-1}$). Studies of the morphology of the polymer/$PC_{61}BM$ blends showed that in films containing Te, there was more phase separation, possibly due to the abovementioned strong Te--Te interactions, leading to localized aggregates and less miscibility of the polymer with $PC_{61}BM$, thus affecting the charge transport and lowering the J_{SC} value.[60]

In theory it should be easier to electropolymerize tellurophenes than selenophenes and thiophenes. Polyselenophenes have been obtained electrochemically with optical bandgaps as narrow as 1.4 eV and conductivity values approaching of 0.1 S cm^{-1}.[62] It is expected then, that the respective polytellurophenes analogues of polyselenophenes will have better properties in this regard, although polytellurophene synthesis is generally harder than the lighter element analogues. Because of the lower oxidation potentials of the tellurium-containing monomers, electropolymerization should occur at lower potentials and possibly yield better quality of polymer films since there is less material degradation at lower voltages; also the expected higher values of conductivity in polytellurophenes should assist in the electropolymerization process. Electropolymerization has been reported using as a monomers tellurophene, small tellurophenes oligomers (2 and 3 repeat units) and 3-hexyl-tellurophenes to form polytellurophenes and poly(3-hexyltellurophene), respectively.[63]

In terms of aromaticity, theoretical and experimental studies have shown tellurophenes to be less aromatic[38] than selenophenes and thiophenes, yet more than furans; therefore a more quinoidal/planar structure is expected in polytellurophenes, leading to more delocalization of charge and also lower optical bandgaps (E_g). However aromaticity is important since it helps to extend the delocalization along the polymer backbone, which is the reason the optical bandgap in polyfurans (2.35 eV) (the less aromatic congener) is larger than polythiophenes (2.0 eV). The more delocalized nature of the orbital manifold should also lead to a red-shift in the absorption and emission properties.

The reduced aromaticity in tellurophenes compared to selenophenes and thiophenes can be explained in terms of poor overlap between the p_z orbitals in the diene unit and one of the lone pairs on Te due to the differences in the atom size (bigger in Te) and the longer Te-C distances compared to C-Se and C-S. Overall, the reduced aromaticity would bring desta-bilization of the HOMO (upwards) and LUMO stabilization (downwards) which in turn

would help to decrease the bandgap leading to enhanced light absorption in the red to near IR spectral region. As an example of the effect of tellurium has in the absorption properties, a cyclopentadithiophene polymer with tellurophene as a co-monomer was studied and its properties compared to its lighter chalcogenophene analogues (Figure 1.3). A red-shift (reduced E_g) in the absorption properties occurred due to a lowering of the LUMO level when heavier atom Te is in place. A moderate rise in the HOMO level was also found, along with aggregate formation in the polymer film due to Te---Te interactions.[64]

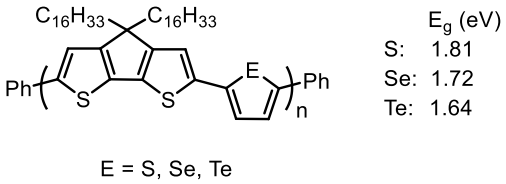

Figure 1.3. Chalcogenophene-containing cyclopentadithiophene polymers.

Tellurophene-based materials have the potential to exhibit phosphorescence due to the heavy atom effect (Figure 1.4). In these cases, excited triplet states (T_n) become accessible during either photo- or electroluminescence by intersystem crossing (ISC) from populated excited singlet states (S_n) in a process that is facilitated by enhanced spin-orbit coupling in the presence of heavy atoms. These excited triplet states are highly susceptible to be quenched by energy transfer to O_2 and via triplet-triplet annihilation (TTA) in the condensed phase. Due to these quenching mechanisms, emission from tellurophenes is usually not observed in the solid state or in air. However, if there is no O_2 present, the chances of getting tellurophenes-based phosphorescence materials increases, especially if the tellurophenes possess other molecular characteristics such as molecular rigidity in solution (or in the solid state) that limits intramolecular rotations and therefore loss of energy by non-radiative pathways.[63]

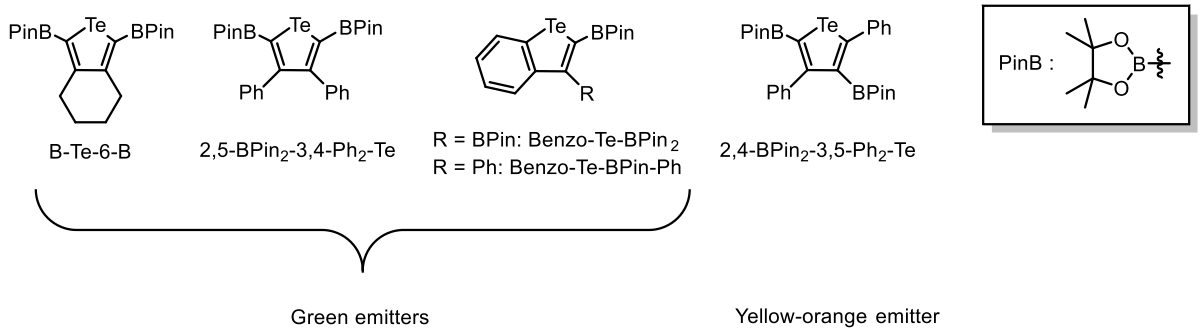

Figure 1.4. Room temperature phosphorescent tellurophenes reported by the Rivard group.[52,65,66]

1.3. LUMINESCENCE AND AGGREGATION-INDUCED EMISSION (AIE)

1.3.1. Overview and mechanism of fluorescence, phosphorescence and AIE

The emission of light by a sample is called luminescence, and depending on the spin state of the excited state and the lifetime of the emission process, one can classify the emission as either fluorescence or phosphorescence. Figure 1.5 outlines the basic pathways available in luminescence, with light absorption to give excited singlet states (10^{-15}) being favored by spin-selection rules. In fluorescence the lifetime of the excited state is about 10^{-8} to 10^{-9} s before direct electron relaxation from the S_1 state to the ground singlet state, S_0 with a release of a photon; if higher singlet states are occupied (S_n; $n > 1$), rapid internal conversion to the S_1 states occurs as stated in Kasha's rule.[67] The difference in the energy of light absorbed and the light emitted is called the Stokes shift and is never zero since some of the energy that is absorbed is lost by collisions with other molecules and by other non-radiative processes, which will be considered later. Each electronic state is associated with its own vibrational states, which are very close in energy, and the vibrational states have its own fine structure of rotational states. Therefore, partly the energy is lost when the electron from a high energy vibrational state reaches a lower vibrational state within a singlet excited state, S_n, which leads to the Stokes shift.

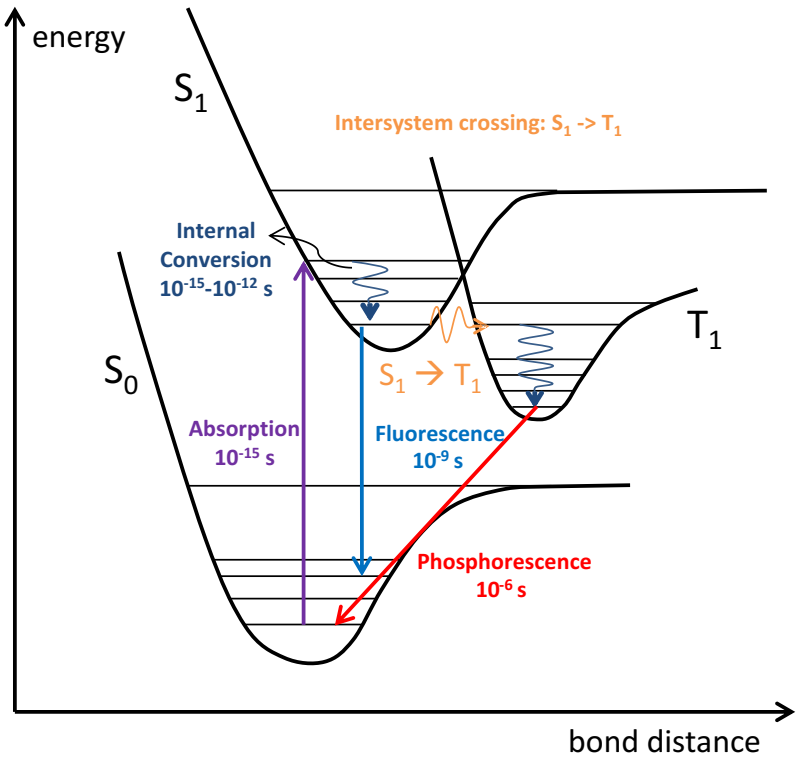

Figure 1.5. Jablonski diagram and possible photophysical processes upon absorption.

When the lifetime of the excited state is substantially longer than the nanosecond regime (e.g. microseconds or longer), the most likely mechanism for luminescence is phosphorescence whereby emission from an excited triplet state (T_1) occurs (Figure 1.5). As the direct population of triplet excited states (T_n) upon photoexcitation is not allowed by spin-selection rules, population of T_n states occurs by intersystem crossing (ISC) from excited singlet states (S_n). The lifetimes of triplet states are longer than excited singlet states and since the light emission (phosphorescence) would be from the lowest excited triplet state, T_1, to the ground singlet state, S_0, a transition that is formally spin forbidden and therefore of low probability. Since more energy is lost when intersystem crossing takes place, the energy of phosphorescence is generally smaller than fluorescence-based emission, leading to a red-shift in the emission and a correspondingly larger Stokes shift. It has been observed experimentally that low temperatures extend the lifetime and increase the intensity of

phosphorescence emission. Also, the fine structure of electronic states becomes more visible (for non-charge transfer-based processes), since large-scale molecular motion is halted at very low temperatures (e.g. 77 K). Less rotational and vibrational modes in a molecule provides less pathways for non-radiative energy loss and a concomitant increase in photoluminescent (PL) emission quantum yield.

In most cases, molecules that present luminescence in solution show decreased luminescence or full quenching of emission in the solid state. In these instances, intermolecular interactions such as close π-π contacts enables electron transfer between the excited species as surrounding molecules to transpire, providing a non-radiative route to relax to the ground state. In order to avoid this aggregation-caused quenching (ACQ), large flanking units can be placed in close proximity to the luminogenic core of the molecule to suppresses close intermolecular contacts and prevent quenching electron transfer processes from transpiring. In 2001, Prof. Ben Zhong Tang and his team noted that a series of aryl-functionalized siloles,[68,69] such as $Ph_2SiC_4Ph_4$ emit more strongly when in the aggregated state than in solution. He coined the term aggregation-induced emission (AIE) for this effect. The principle behind AIE is restriction of intramolecular motion (either rotation or vibrations) in the aggregate state while suppressing close intermolecular molecular contacts, which normally contributes to non-radiative decay/energy loss from the excited state (Figure 1.6).[68,69] Since this initial report, there are now many examples of AIE active luminogens and detailed mechanistic studies and applications in sensing have been reported.[70–74]

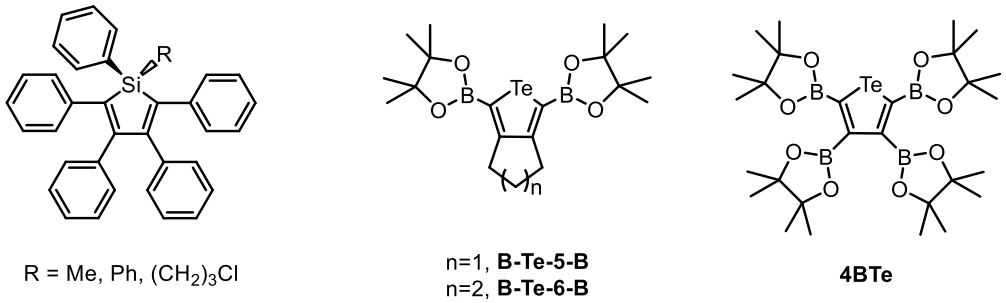

Figure 1.6. Examples of silole fluorogens[69] and phosphorescent tellurophenes presenting AIE.[65]

1.3.2. Luminescence quenching pathways

There are several mechanisms by which the luminescent intensity of a fluorophore diminishes (quenches). Among these mechanisms are static quenching and dynamic quenching (Figure 1.7). However, there are other processes by which the observed intensity of the emission can be decreased, e.g. inner filter effects. Because of the selectivity for binding found in some quenchers and fluorophores, quenching has important bioanalytical applications and also useful to elucidate structural information of fluorophores.[75,76]

Luminescence:

$$F \xrightarrow{h\nu_i} F^* \longrightarrow F + h\nu_f$$

Static quenching:

$$F \xrightarrow{Q} FQ \xrightarrow{h\nu_i} FQ^* \longrightarrow FQ + Heat + (h\nu_f)$$

Dynamic quenching:

$$F \xrightarrow{h\nu_i} F^* \xrightarrow{Q} FQ^* \longrightarrow F + Q + Heat + (h\nu_f)$$

Figure 1.7. Representation of normal luminescence, static and dynamic quenching. F: fluorophore, Q: quencher, F*: fluorophore in its excited state, FQ: ground state complex of fluorophore and quencher, FQ*: excited state complex of fluorophore and quencher, υ_i: frequency of light absorption, υ_f: frequency of light emission.[75]

Inner filter effects are those related to absorption or dispersion of light at the excitation or emission wavelength in fluorophore solutions.[77] Those are due to the presence of substances that can absorb light before or after initial beam light is in contact with the fluorophore. When light is absorbed before to reach the fluorophore, less light reaches the fluorophore and so less luminescence is emitted by the fluorophore. When absorption occurs at the emission wavelength, the emitted light that reaches the detector is reduced and so the

intensity measured by the fluorometer is also reduced; inner filter effects can also be caused by substances present in the solution that are able to scatter light. Inner filter effects can be minimized by reducing cuvette thickness, selecting excitation and emission wavelengths that reduce absorption by the quencher and reducing the concentration of the substances that might absorb or scatter the light.[77] Inner filter effects might not be considered as a true quenching mechanism; however, it should be regarded as a possible source of decreased luminescence, which in routine luminescent studies should be minimized.

Static quenching refers to any process that prevents the formation of the excited state of the fluorophore and therefore completely quenches its original luminescence,[77] such as complex formation between the quencher and the fluorophore in its ground state (Figure 1.7). Since the ground state complex in which the luminescence of the fluorophore is completely quenched does not affect the excited state of the few fluorophores remaining without complexation, the lifetime of the fluorophore is not affected.[77] However if the strong quencher is in excess, emission from the fluorophore is not observable or sometimes very little fluorescence emission from the fluorophore might be detected with very short lifetimes, depending on the sensitivity of the experimental instrumentation.[76]

On the contrary, dynamic quenching relates to any process involving the excited state of the fluorophore that leads to a reduction in the intensity of the emission. Among the dynamic quenching mechanisms are collisional quenching (such as in dioxygen and iodine quenching), processes that requires direct contact between the fluorophore in its excited state, and quenching pathways that do not require direct contact (~ 10 nm), such as Förster Resonance Energy Transfer (FRET).[77] In dynamic quenching, since the nature of the excited electronic state of the fluorophore changes, the overall fluorescence lifetime (τ) will decrease. In the case of collisional quenching, upon collision of the quencher and fluorophore, some energy is taken away from the excited fluorophore by the quencher and in consequence less energy is left to the fluorophore for emission.[76]

FRET is present when an excited fluorophore (donor) transfers its energy to the quencher acting as an acceptor through dipole-dipole interactions (no emission of photons) (Figure 1.8).[76] For FRET to occur, there must be an overlap between the emission spectrum

of the donor and the absorption of the acceptor, as well as close proximity and relative orientation of the dipole moments of the donor and acceptor.[78] Due to the energy loss of the fluorophore during the energy transfer, the fluorescence intensity, quantum yield and lifetime will also decrease.[76]

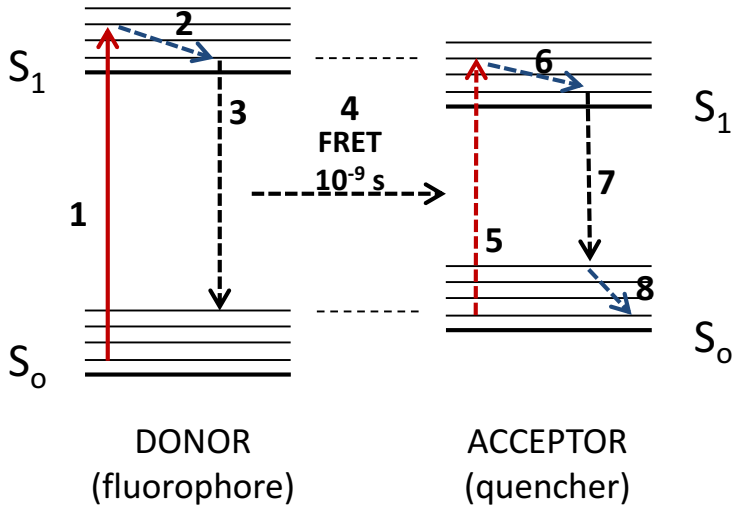

Figure 1.8. Jablonski diagram of FRET. 1: excitation of donor, 2: internal conversion, 3: relaxation via non-radiation process, 4: non-radiative energy transfer, 5: excitation of acceptor, 6: internal conversion, 7: relaxation via non-radiation process, 8: internal conversion.

Not only energy can be transferred, but charge can also be transferred as in Dexter Electron Transfer (DET) (Figure 1.9). DET is a transfer electron process between two molecules or two parts of the same molecule. Intermolecularly, one molecule is the fluorophore in its excited state (donor) and the other is the acceptor (quencher) and in order for a charge transfer happens, orbital overlap between donor and acceptor is required. This charge transfer process includes the formation of very short-lived entities, such as excimers (if the donor and acceptor, quencher, are the same molecule) or exciplexes (donor and acceptor are different), which occur via electrostatic attraction because of the partial charge transfer.[78] Now, emission from this dimer/complex can be possible or might not be observable as in complete quenching[67] because the final excited state of the acceptor relaxed

back through non-radiative processes. DET is very common in the solid state, since short distances have to be reached in order to orbitals overlap.[79]

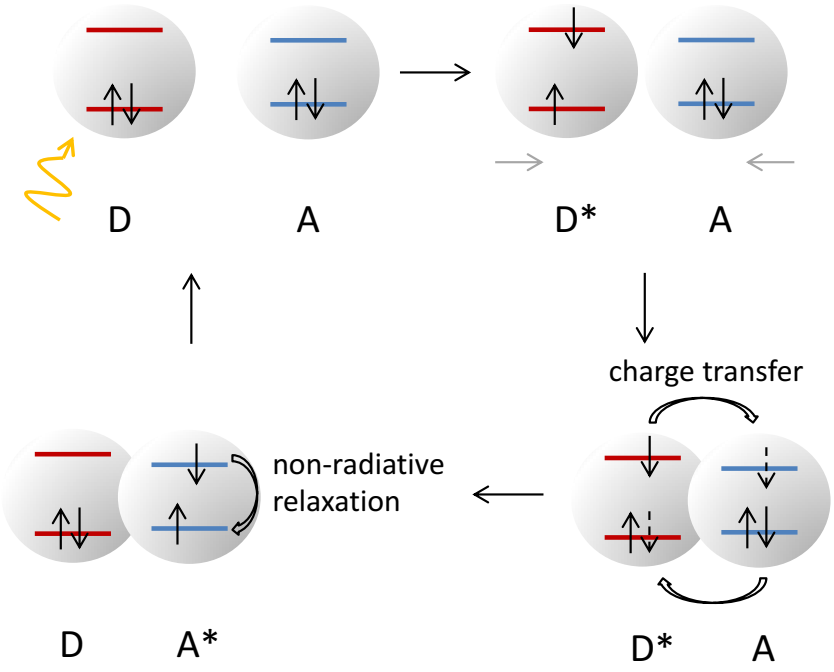

Figure 1.9. Representation of Dexter Electronic Transfer, DET.[79]

A special case of local charge transfer involving different conformations of the fluorophore in its excited state is Twisted Intramolecular Charge Transfer (TICT). Here, donor (electron donating) and acceptor (electron accepting) groups are linked by a single bond in the same fluorophore structure. Upon electron transfer from the donor to the acceptor, there is an intramolecular twisting around the single bond, which forms a more stable conformation (twisted) that can then be relaxed back to its initial conformation (ground state) via fluorescence emission or through non-radiative processes (quenching). Interestingly, TICT, usually is characterized by presenting dual fluorescence, one from the locally excited state (before twisting) and the other emission from the TICT state.[78]

Static and dynamic quenching can be differentiated by measuring fluorescence life times with and without quencher, as mentioned before. Another alternative is measuring the

change in UV-vis absorption of the fluorophore plus quencher versus the absorption of only the fluorophore, which it will not change in the case of dynamic quenching.[80] Temperature-dependent fluorescence studies are also useful to distinguish between dynamic and static quenching, if the quantum yield of the emission is independent of temperature. If this is the case, increasing the temperature, increases the diffusion of quencher in the media, which collisional quenching (dynamic) would increase, while binding-related quenching (ground state complex static quenching) would decrease.[67]

$$\frac{F_o}{F} = 1 + k_q \tau_o [Q] \qquad (1) \qquad\qquad \frac{F_o}{F} = 10^{-A} \qquad (2)$$

Figure 1.10. Stern-Volmer equations describing dynamic quenching (1) and linear filter effects (2). F and F_o are the fluorescence intensities of the fluorophore in the presence and absence of the quencher, k_q: bimolecular quenching constant, τ_o: lifetime of the fluorophore in the absence of the quencher and A: absorbance of the quencher.

Quenching studies can be represented mathematically with the Stern-Volmer equation by plotting the concentration of the quencher vs. the ratio F_o/F (F_o and F are the fluorescence intensities of the fluorophore without and with quencher) (Figure 1.10, equation 1). Dynamic quenching always gives a linear plot, however, the presence of static quenching introduces deviations to the linear behavior (curvatures).[76] Therefore, non-linear features in a Stern-Volmer graph could be interpreted as a result of both quenching mechanisms might be present, assuming homogeneous emission (the system has only one emitting center).[75] Now if the curvature is significant, then inner filter effects are should be considered and thus the equation Stern-Volmer becomes exponential (equation 2, Figure 1.10).[75]

Quenching mechanisms such as FRET and DET can be classified as external quenching mechanisms, since two molecules are involved in the process. On the other hand, intramolecular processes due to intrinsic characteristics of the fluorophore, such as intramolecular rotations and spin-orbit coupling to reach triplet states (T_n) can also lead to

quenching of the emission from the fluorophore (in the case of singlet based fluorescent emitters). Internal rotations of fluorogenic groups around single bonds is the most common process of non-radiative energy loss and usually happens in the excited state; notably, double bonds can also be converted into single bonds upon excitation and thereby facilitating internal quenching.[79] Internal rotations can be affected by temperature, viscosity and the overall rigidity of the fluorophore. Restriction of internal rotations by steric effects, decreasing viscosity and temperature can lead to enhanced the luminescence behaviour and thus increasing the lifetime of emission.[79] In the case of intersystem crossing (ISC), population of triplet states (T_n) by using heavy atoms (*vide infra*) makes the fluorophores more susceptible to be quenched, since first by promoting exited singlet states (S_n) to triplet states (T_n) the intensity of luminescence (and lifetime) coming from excited singlet states (S_1) to the ground singlet state (S_0) will be reduced, and secondly, the triplet states are highly sensitive to quenching by species such as molecular oxygen. Overall, the first event (fluorescence) might not be observable because the lifetime drops from nanoseconds to picoseconds and the second event (phosphorescence) might be quenched by available oxygen from air or being reduced because of the rate of intersystem crossing for S_1 to T_1 also increases by the same heavy atom effect.[79,81,82]

1.4. BORYLATION AND PROTODEBORONATION REACTIONS

1.4.1. Synthesis of boronate esters

Boronate esters can be synthesized by using stoichiometric amounts of a diol and a boronic acid ($RB(OH)_2$), typically in aprotic solvents such as benzene, toluene, CH_2Cl_2. The reaction can be driven towards the boronate ester when the water by-product is trapped /removed by using drying agents such as molecular sieves or $CaSO_4$.[83–86] Boronate esters are less polar and more stable (towards nucleophilic attack) than boronic acids, although boronate esters can be cleaved under mild conditions, such as washing an organic solution of the boronate ester with aqueous hydroxide (Scheme 1.23). Six-membered cyclic boronate esters are less strained than the five-membered ring analogues. These species usually have

three-coordinate boron centers, except under basic conditions when hydroxide complexation can occur to yield tetrahedral hydroxylated borates.[87]

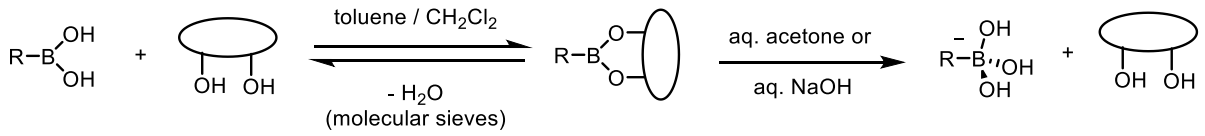

Scheme 1.23. Synthesis of boronate esters via condensation reactions and cleavage under mild conditions.

Synthetic methods have been developed to prepare both arylated and alkylated boronate esters (from the corresponding aromatic or alkyl halides) under mild conditions. The direct synthesis of boronate esters by C-H activation of aromatic substrates is also known, but requires the use of expensive Rh- and Ir-based catalysts and bis(pinacolato)-diboron (B_2Pin_2) under harsh reaction conditions.[88,89] Instead, the synthesis of boronic acids under mild conditions that *in situ* can be converted to boronate esters have been developed (Scheme 1.24, top). Worth nothing is the common and inexpensive aromatic chlorides used to form the boronic acid and tetrahydroxyboron, $B_2(OH)_4$, as the source of boron center via Pd-catalyzed cross-coupling. This procedure allows one to form the boronic esters entirely in one-pot in good to excellent yields using air stable reagents (albeit the Pd-catalysts do have some sensitivity to oxygen). [90]

The synthesis of alkyl boronate esters have been reported using Zn^{II}/NHC (NHC = *N*-heterocyclic carbene) as a catalyst precursor (Scheme 1.24, bottom). This protocol is very attractive since uses less toxic catalysts than the usual procedures (Pd, Ni or Cu), while zinc is inexpensive, abundant and environmentally less harmful. The reported syntheses were conducted at room temperature and were applicable to the coupling of primary, secondary and tertiary alkyl halides.[91]

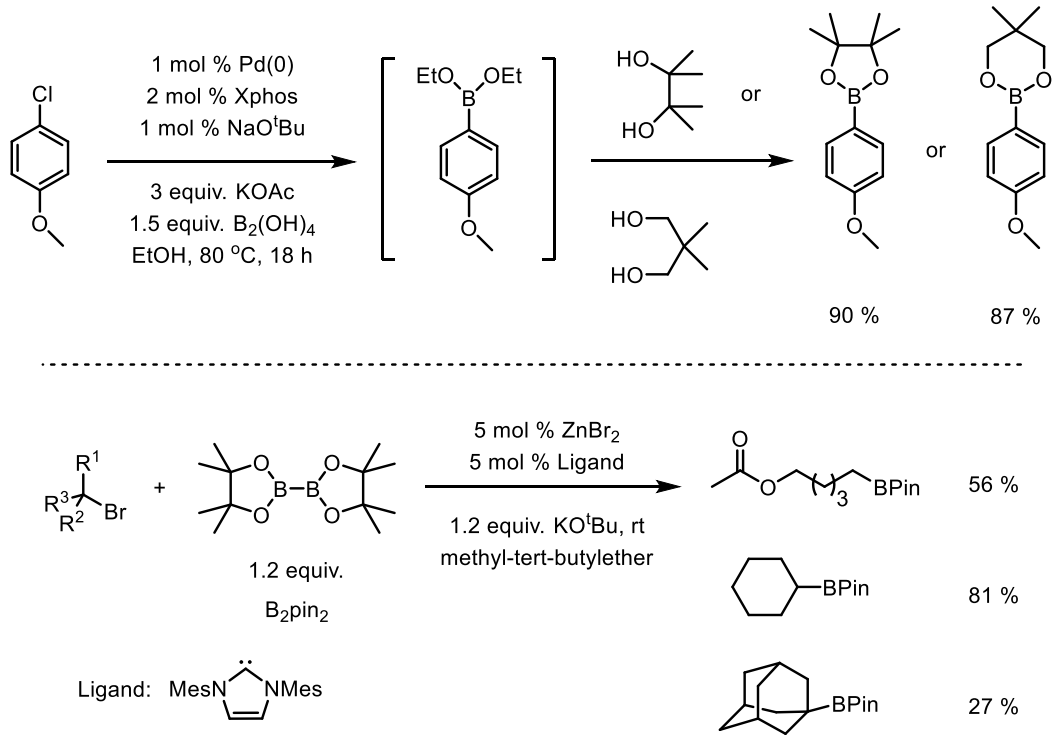

Scheme 1.24. Synthesis of boronate esters via palladium (top) and zinc (bottom) catalyzed reactions of aromatic chloride and alkyl halides and boron substrates.

Not only aromatic/alkyl halides can be converted into boronate esters, but esters can be used as reactants. Specifically, under more drastic conditions it is possible to cleave the ester group by C-O bond activation and functionalization via the nickel-catalyzed decarbonylative borylation of aromatic esters (Scheme 1.25, top).[92] The authors showed broad substrate scope and scalability of this borylation protocol, along with chemoselectivity, making the conversion of carboxylic esters into boronate esters a valuable tool in organic chemistry.

The generation of C(sp^2)-boronate esters often requires the use of transition metals (Pd, Ni, Zn), thus alternate protocols using metal-free C(sp^2)-B bond formation are highly desirable. In this context, borylative cyclization of alkynes can be used to form polycyclic boronate esters in the presence of a boron electrophile (BCl_3), which activates the alkyne for

intramolecular electrophilic cyclization under mild reaction conditions (Scheme 1.25, bottom).[93]

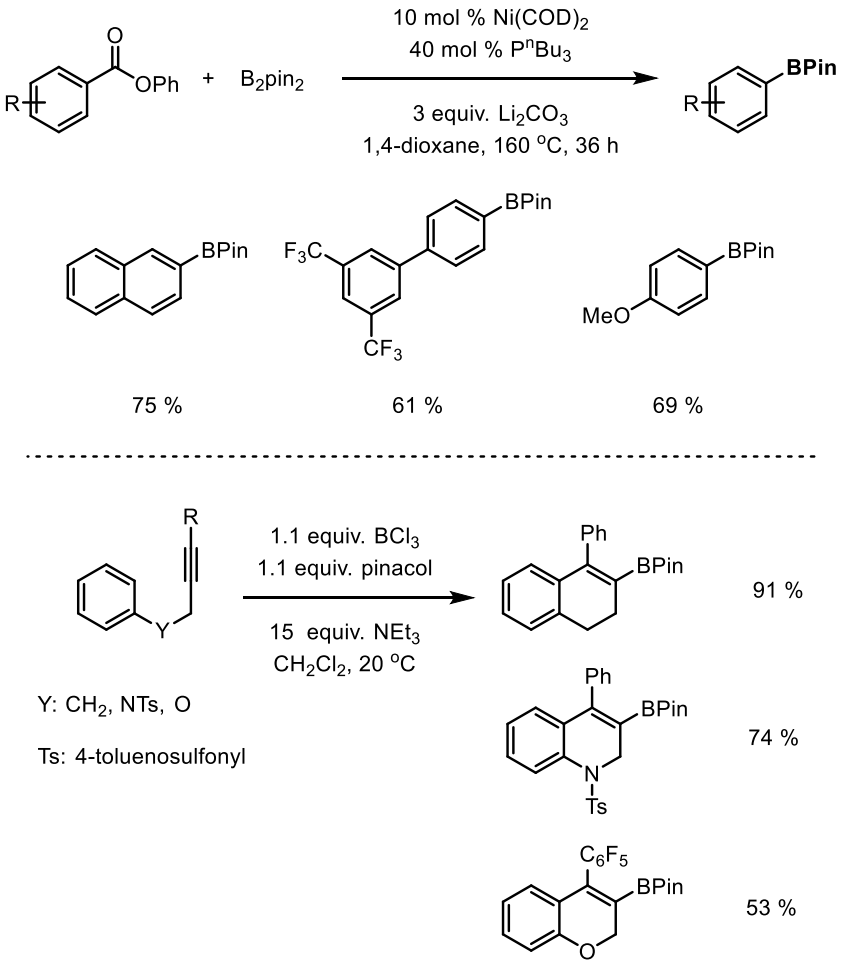

Scheme 1.25. Synthesis of boronate esters via decarbonylative borylation reaction of carboxylic esters (top) and borylative cyclization of alkynes (bottom).

1.4.2. Effect of reaction conditions in protodeboronation

Organoboron compounds are widely used in Suzuki-Miyaura cross-coupling reactions where different types of Pd catalysts, bases, ligands, solvent media and conditions have been tested to increase the efficiency of the reaction. However, a common side reaction during cross-coupling is protodeboronation (PDB) where the C-B bond is cleaved; basic, acidic,

metal-mediated (copper and silver salts) and thermal conditions can be used cleave C-B bonds.[94–98] While boronate esters are considered to be more stable than boronic acids, they can also protodeboronate under Suzuki-Miyaura conditions, albeit at a lower rate. PDB can also occur with MIDA (N-methyliminodiacetic acid)-stabilized boronates but only under more drastic conditions (Scheme 1.26).[99] In general, the more Lewis acidic the boron center is, the more prone the resulting boronic ester (or acid) is to protodeboronation under neutral conditions (DMSO at 120 °C) as it is shown in Scheme 1.26.[99]

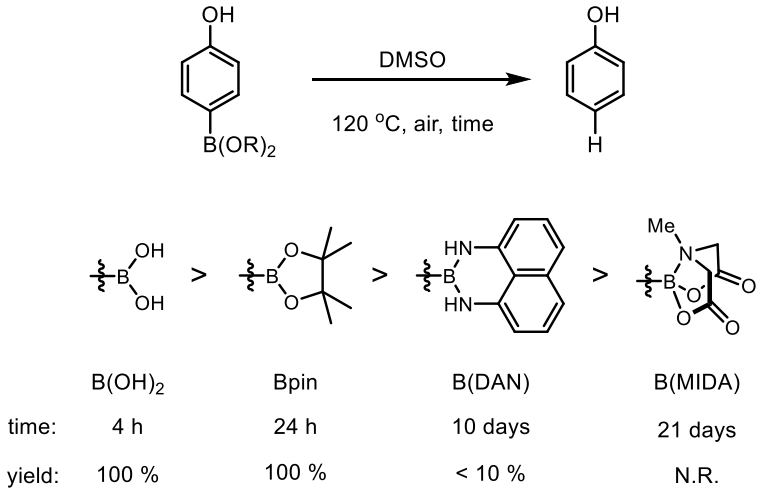

Scheme 1.26. Rate of protodeboronation according to different Lewis acidity on boron.[99]

In one study, the PDB of 4-(dimethylamino)phenylboronic acid was examined using wet DMSO as a proton source; it was found that the PDB reaction was slower in the presence of added phosphine.[94] The slow PDB in the case of added phosphine is due to the competing formation of an intermediate ate complex (Scheme 1.27). The aforementioned proves that PDB goes through a complexation between the boron source and the proton source before cleavage of the C-B bond by a σ-bond metathesis reaction.

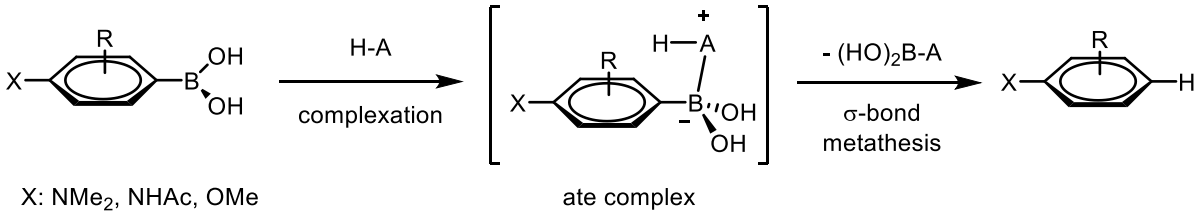

Scheme 1.27. Proposed mechanism for protodeboronation reaction.[94]

The electron density of the aromatic group along with the pH of the reaction medium also plays a role in PDB. It has been observed that more electron density in the aromatic ring under acidic conditions increases the reactivity of boronic acids/esters towards PDB, by facilitating the σ-bond metathesis step in the proposed mechanism of PDB (Scheme 1.27). On the contrary, electron-poor boronic acids protodeboronate faster at high pH, as it was shown in the PDB reaction of diortho-electron-withdrawing (CF_3,NO_2 and F) substituted phenylboronic acids under basic conditions.[95] Based on this, it is expected that electron rich boronic acids/esters would be more stable towards PDB reactions under basic Suzuki-Miyaura conditions.

There are different strategies reported in the literature to diminish PDB, especially when the organoboron species are going to be used in cross-coupling reactions.[100] One of the strategies is named “masking”, since it stabilizes the arylboronic acid by forming a more stable anionic tetrahedral ate complexes. Examples of these complexes are the cyclic triolborate[101] and the lithium triisopropyl arylborate[102] complexes shown in the Figure 1.11. Another strategy is to use the very air and stable potassium organotrifluoroborates[103,104] and N-methyliminodiacetic acid (MIDA) boronates[105] complexes (Figure 1.11), which under mild aqueous base conditions release slowly the respective boronic acid. The slow release of the boronic acid ensures that the transmetallation step is more efficient and less exposure of the boronic acid to the reaction conditions whereby protodeboronation can occur. Finally, by increasing the rate of transmetallation in Suzuki-Miyaura cross-coupling, it reduces the time that boronic acids are exposed to the basic conditions and so less chance of protodeboronation. Buchwald and coworkers[106–108] have developed dialkylbiaryl phosphine ligands (e.g.

Xphos) that increase the rate of transmetallation and reductive elimination; specifically, they have managed to form very active pre-catalysts using these ligands as will be described below.[109]

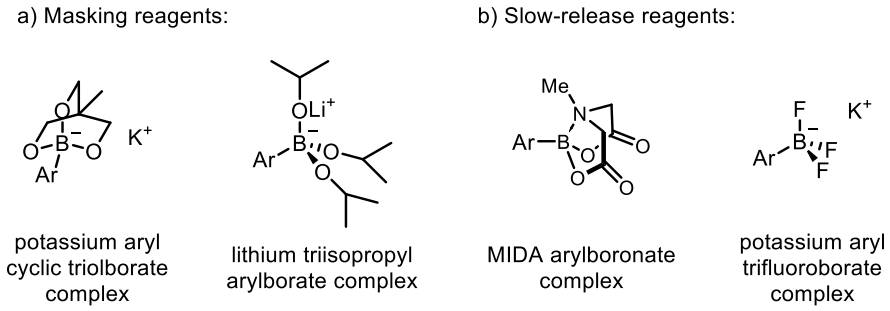

Figure 1.11. Examples of boron reagents that show slow PDB reactions under Suzuki-Miyaura coupling conditions.

As it was mentioned before, one of these strategies is to make the boron atom less Lewis acidic, more stable, as in the formation of lithium triisopropyl borates (Scheme 1.28, eq. 1).[102] This lithium salt is much more stable toward PDB and is easy to handle under benchtop conditions at room temperature. Buchwald and coworkers[102] could also generated Li[Ar-B(O^iPr)$_3$] species in one-pot via a series of lithiation, borylation and Suzuki-Miyaura cross-coupling reactions with good overall yields of coupled products (Scheme 1.28, eq. 2). Previous to this study, the same group developed an air- and moisture-stable Pd pre-catalyst (Scheme 1.28, bottom). This Pd pre-catalyst can easily be activated to the active catalyst form under mild reaction conditions (room temperature and short reaction times) where the PDB is slowed down. It was tested successfully in the Suzuki-Miyaura cross-coupling reaction using polyfluorophenyl and five-membered 2-heterocyclic boronic acids, which are well known to be very sensitive to protodeboronation.[109]

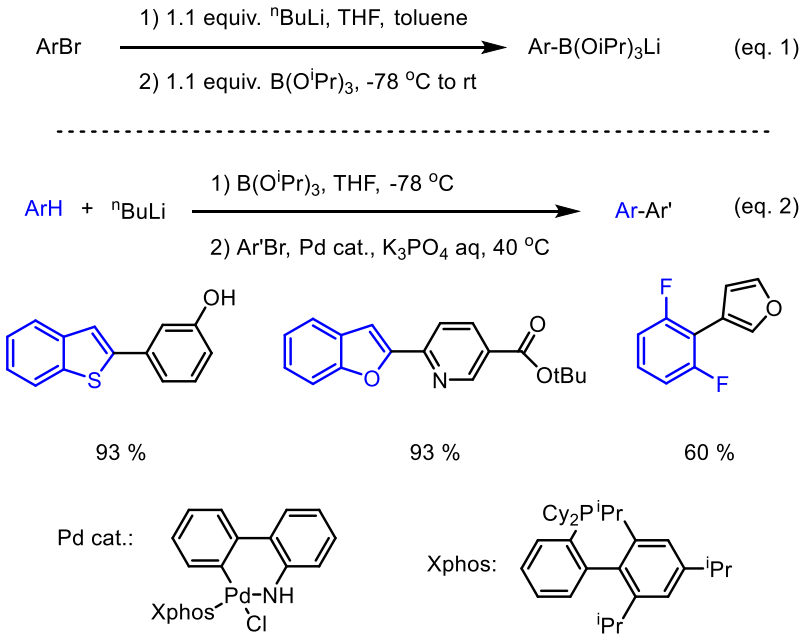

Scheme 1.28. Lithium triisopropyl borate formation (eq. 1) and one-pot borylation and Suzuki-Miyaura cross-coupling procedure (eq. 2).[102]

Despite the general consensus that tellurophenes-based materials could have improved optoelectronic properties in relation to well-known thiophene analogues,[63,110,111] there is not too much variety in efficient protocols[48,112–114] to form new tellurophene heterocycles. For the same reason, the study of the optical properties of tellurophenes in the context of light absorption and phosphorescence emission for optoelectronic applications is limited. In that sense, in this thesis, the functionalization of tellurophenes through different coupling techniques will be addressed to form new stable phosphorescent materials. While doing this, new tellurophene precursor materials have been synthesized through very simple techniques such as the selective promotion of protodeboronation reactions on tetraborylated-substituted tellurophenes. The optical properties of the new functionalized tellurophenes have been studied using UV-vis, fluorescence spectroscopy and cyclic voltammetry, and as well as calculations of the energy of the frontier orbitals in order to explain the optical properties.

1.5. REFERENCES

1. Zhao, X.; Chaudhry, S. T.; Mei, J. In *Advances in Heterocyclic Chemistry*; Scriven, E. F. V.; Ramsden, C. A., Eds.; Elsevier Inc., **2016**; Vol. 121, pp. 133–171.

2. Fagan, P. J.; Nugent, W. A. *J. Am. Chem. Soc.* **1988**, *110*, 2310–2312.

3. Fagan, P. J.; Nugent, W. A.; Calabrese, J. C. *J. Am. Chem. Soc.* **1994**, *116*, 1880–1889.

4. O'Rourke, N. F.; Kier, M. J.; Micalizio, G. C. *Tetrahedron* **2016**, *72*, 7093–7123.

5. Gessner, V. H.; Tannaci, J. F.; Miller, A. D.; Tilley, T. D. *Acc. Chem. Res.* **2011**, *44*, 435–446.

6. Marek, I. *Titanium and Zirconium in Organic Synthesis*; Wiley-VCH Verlag GmbH & Co. KGaA, **2002**.

7. Reichard, H. A.; Rieger, J. C.; Micalizio, G. C. *Angew. Chem. Int. Ed.* **2008**, *47*, 7837–7840.

8. Braye, E. H.; Hübel, W.; Caplier, I. *J. Am. Chem. Soc.* **1961**, *83*, 4406–4413.

9. Dioumaev, V. K.; Harrod, J. F. *Organometallics* **1997**, *16*, 1452–1464.

10. Takahashi, T.; Kageyama, M.; Denisov, V.; Hara, R.; Negishi, E. *Tetrahedron Lett.* **1993**, *34*, 687–690.

11. Alt, H. G.; Denner, C. E. *J. Organomet. Chem.* **1990**, *390*, 53–60.

12. Rosenthal, U.; Ohff, A.; Baumann, W.; Tillack, A.; Görls, H.; Burlakov, V. V.; Shur, V. B. *Z. Anorg. Allg. Chem.* **1995**, *621*, 77–83.

13. Negishi, E.-I.; Cederbaum, F. E.; Takahashi, T. *Tetrahedron Lett.* **1986**, *27*, 2829–2832.

14. Rosenthal, U.; Ohff, A.; Michalik, M.; Görls, H.; Burlakov, V. V.; Shur, V. B. *Angew. Chem. Int. Ed.* **1993**, *32*, 1193–1195.

15. Denhez, C.; Médégan, S.; Hélion, F.; Namy, J.-L.; Vasse, J.-L.; Szymoniak, J. *Org. Lett.* **2006**, *8*, 2945–2947.

16. Ma, W.; Yu, C.; Chen, T.; Xu, L.; Zhang, W.-X.; Xi, Z. *Chem. Soc. Rev.* **2017**, *46*, 1160–1192.

17. Zirngast, M.; Marschner, C.; Baumgartner, J. *Organometallics* **2008**, *27*, 2570–2583.

18. Ren, S.; Seki, T.; Necas, D.; Shimizu, H.; Nakajima, K.; Kanno, K.; Song, Z.; Takahashi, T. *Chem. Lett.* **2011**, *40*, 1443–1444.

19. Johnson, S. A.; Liu, F. Q.; Suh, M. C.; Zürcher, S.; Haufe, M.; Mao, S. S. H.; Tilley, T. D. *J. Am. Chem. Soc.* **2003**, *125*, 4199–4211.

20. Negishi, E.; Holmes, S.; Tour, J. *J. Am. Chem. Soc.* **1989**, *111*, 3336–3346.

21. Nugent, W. A.; Thorn, D. L.; Harlow, R. L. *J. Am. Chem. Soc.* **1987**, *109*, 2788–2796.

22. Buchwald, S. L.; Nielsen, R. B. *J. Am. Chem. Soc.* **1989**, *111*, 2870–2874.

23. Hara, R.; Xi, Z.; Kotora, M.; Xi, C.; Takahashi, T. *Chem. Lett.* **1996**, *25*, 1003–1004.

24. Xi, Z.; Zhang, W.; Takahashi, T. *Tetrahedron Lett.* **2004**, *45*, 2427–2429.

25. Hamada, T.; Suzuki, D.; Urabe, H.; Sato, F. *J. Am. Chem. Soc.* **1999**, *121*, 7342–7344.

26. Perez, L. J.; Shimp, H. L.; Micalizio, G. C. *J. Org. Chem.* **2009**, *74*, 7211–7219.

27. Zhou, Y.; Yan, X.; Chen, C.; Xi, C. *Organometallics* **2013**, *32*, 6182–6185.

28. Bankwitz, U.; Sohn, H.; Powell, D. R.; West, R. *J. Organomet. Chem.* **1995**, *499*, C7–C9.

29. Xi, C.; Hou, S.; Afifi, T. H.; Hara, R.; Takahashi, T. *Tetrahedron Lett.* **1997**, *38*, 4099–4102.

30. Liao, Q.; Zhang, L.; Wang, F.; Li, S.; Xi, C. *Eur. J. Org. Chem.* **2010**, 5426–5431.

31. You, W.; Yan, X.; Liao, Q.; Xi, C. *Org. Lett.* **2010**, *12*, 3930–3933.

32. Gonzalez, J. L.; Stephens, C. E.; Wenzler, T.; Brun, R.; Tanious, F. A.; Wilson, W. D.; Barszcz, T.; Werbovetz, K. A.; Boykin, D. W. *Eur. J. Med. Chem.* **2007**, *42*, 552–557.

33. Wilhelm, E. A.; Gai, B. M.; Souza, A. C. G.; Bortolatto, C. F.; Roehrs, J. A.; Nogueira, C. W. *Mol. Cell. Biochem.* **2012**, *365*, 175–180.

34. Fleming, J.; Ghose, A.; Harrison, P. R. *Nutr. Cancer* **2001**, *40*, 42–49.

35. Gasparian, A. V; Yao, Y. J.; Lu, J.; Yemelyanov, A. Y.; Lyakh, L. A.; Slaga, T. J.; Budunova, I. V *Mol. Cancer Ther.* **2002**, *1*, 1079–1087.

36. Srivastava, P. C.; Robins, R. K. *J. Med. Chem.* **1983**, *26*, 445–448.

37. Jayaram, H. N.; Dion, R. L.; Glazer, R. I.; Johns, D. G.; Robins, R. K.; Srivastava, P. C.; Cooney, D. A. *Biochem. Pharmacol.* **1982**, *31*, 2371–2380.

38. Je, M.; Kobilka, B. M.; Hale, B. J. *Macromolecules* **2014**, *47*, 7253–7271.

39. Park, Y. S.; Kale, T. S.; Nam, C.-Y.; Choi, D.; Grubbs, R. B. *Chem. Commun.* **2014**, *50*, 7964–7967.

40. Yamaguchi, S.; Xu, C. H.; Okamoto, T. *Pure Appl. Chem.* **2006**, *78*, 721–730.

41. Manjare, S. T.; Kim, Y.; Churchill, D. G. *Acc. Chem. Res.* **2014**, *47*, 2985–2998.

42. Kryman, M. W.; Schamerhorn, G. A.; Hill, J. E.; Calitree, B. D.; Davies, K. S.; Linder, M. K.; Ohulchanskyy, T. Y.; Detty, M. R. *Organometallics* **2014**, *33*, 2628–2640.

43. Yamamoto, T.; Takimiya, K. *J. Am. Chem. Soc.* **2007**, *129*, 2224–2225.

44. Shinamura, S.; Osaka, I.; Miyazaki, E.; Takimiya, K. *Heterocycles* **2011**, *83*, 1187–1204.

45. Choi, T. L.; Han, K. M.; Park, J. I.; Kim, D. H.; Park, J. M.; Lee, S. *Macromolecules* **2010**, *43*, 6045–6049.

46. Tang, J.; Zhao, X. *RSC Adv.* **2012**, *2*, 5488–5490.

47. Curtis, R. F.; Hasnain, S. N.; Taylor, J. A. *J. Chem. Soc. Chem. Commun.* **1968**, 365.

48. Mack, W. *Angew. Chem. Int. Ed.* **1966**, *5*, 896.

49. Fringuelli, F.; Taticchi, A. *J. Chem. Soc. Perkin Trans. 1* **1972**, 199–203.

50. Sweat, D. P.; Stephens, C. E. *J. Organomet. Chem.* **2008**, *693*, 2463–2464.

51. Li, P.-F.; Carrera, E. I.; Seferos, D. S. *Chem Plus Chem* **2016**, *81*, 917–921.

52. He, G.; Kang, L.; Torres Delgado, W.; Shynkaruk, O.; Ferguson, M. J.; McDonald, R.; Rivard, E. *J. Am. Chem. Soc.* **2013**, *135*, 5360–5363.

53. Dutton, J. L.; Farrar, G. J.; Sgro, M. J.; Battista, T. L.; Ragogna, P. J. *Chem. Eur. J.* **2009**, *15*, 10263–10271.

54. Godoi, B.; Schumacher, R. F.; Zeni, G. *Chem. Rev.* **2011**, *111*, 2937–2980.

55. Larock, R. C.; Yue, D. *Tetrahedron Lett.* **2001**, *42*, 6011–6013.

56. Yue, D.; Larock, R. C. *J. Org. Chem.* **2002**, *67*, 1905–1909.

57. Roehrs, J. A.; Pistoia, R. P.; Back, D. F.; Zeni, G. *J. Org. Chem.* **2015**, *80*, 12470–12481.

58. Alves, D.; Luchese, C.; Nogueira, C. W.; Zeni, G. *J. Org. Chem.* **2007**, *72*, 6726–6734.

59. Dabdoub, M. J.; Dabdoub, B.; Pereira, M. A.; Zukerman-Schpector, J. *J. Org. Chem.* **1996**, *61*, 9503–9511.

60. Jung, E. H.; Bae, S.; Yoo, T. W.; Jo, W. H. *Polym. Chem.* **2014**, *5*, 6545–6550.

61. Chen, L.; Shen, P.; Zhang, Z.-G.; Li, Y. *J. Mater. Chem. A* **2015**, *3*, 12005–12015.

62. Westgate, T. D.; Skabara, P. J.; Cortizo-Lacalle, D. In *Handbook of Chalcogen Chemistry: New Perspectives in Sulfur, Selenium and Tellurium*; Devillanova, F. A.; Du Mont, W. W., Eds.; Royal Society of Chemistry, **2013**; Vol. 2, pp. 99–126.

63. Rivard, E. *Chem. Lett.* **2015**, *44*, 730–736.

64. Planells, M.; Schroeder, B. C.; McCulloch, I. *Macromolecules* **2014**, *47*, 5889–5894.

65. He, G.; Torres Delgado, W.; Schatz, D. J.; Merten, C.; Mohammadpour, A.; Mayr, L.; Ferguson, M. J.; McDonald, R.; Brown, A.; Shankar, K.; Rivard, E. *Angew. Chem. Int. Ed.* **2014**, *53*, 4587–4591.

66. He, G.; Wiltshire, B. D.; Choi, P.; Savin, A.; Sun, S.; Mohammadpour, A.; Ferguson, M. J.; McDonald, R.; Farsinezhad, S.; Brown, A.; Shankar, K.; Rivard, E. *Chem. Commun.* **2015**, *51*, 5444–5447.

67. Callis, P. R. *J. Mol. Struct.* **2014**, *1077*, 14–21.

68. Luo, J.; Xie, Z.; Lam, J. W. Y.; Cheng, L.; Tang, B. Z.; Chen, H.; Qiu, C.; Kwok, H. S.; Zhan, X.; Liu, Y.; Zhu, D. *Chem. Commun.* **2001**, *381*, 1740–1741.

69. Tang, B.; Zhan, X.; Yu, G.; Lee, P. *J. Mater. Chem.* **2001**, *11*, 2974–2978.

70. Hong, Y.; Lam, J. W. Y.; Tang, B. Z. *Chem. Soc. Rev.* **2011**, *40*, 5361–5388.

71. Mei, J.; Leung, N. L. C.; Kwok, R. T. K.; Lam, J. W. Y.; Tang, B. Z. *Chem. Rev.* **2015**, *115*, 11718–11940.

72. Kwok, R. T. K.; Leung, C. W. T.; Lam, J. W. Y.; Tang, B. Z. *Chem. Soc. Rev.* **2015**, *44*, 4228–4238.

73. Hu, R.; Kang, Y.; Tang, B. Z. *Polym. J.* **2016**, *48*, 359–370.

74. Hong, Y.; Lam, J. W. Y.; Tang, B. Z. *Chem. Commun.* **2009**, 4332–4353.

75. Ho, C. N.; Patonay, G.; Warner, I. M. *Trends Anal. Chem.* **1986**, *5*, 37–43.

76. Mátyus, L.; Szöllosi, J.; Jenei, A. *J. Photochem. Photobiol. B Biol.* **2006**, *83*, 223–236.

77. Van De Weert, M.; Stella, L. *J. Mol. Struct.* **2011**, *998*, 145–150.

78. Sasaki, S.; Drummen, G. P. C.; Konishi, G. *J. Mater. Chem. C* **2016**, *4*, 2731–2743.

79. Berezin, M. Y.; Achilefu, S. *Chem. Rev.* **2010**, *110*, 2641–2684.

80. Chai, J.; Wang, J.; Xu, Q.; Hao, F.; Liu, R. *Mol. Biosyst.* **2012**, *8*, 1902–1907.

81. Solovyov, K. N.; Borisevich, E. A. *Usp. Fiz. Nauk* **2005**, *48*, 231–253.

82. Koziar, J. C.; Cowan, D. O. *Acc. Chem. Res.* **1978**, *11*, 334–341.

83. Kuivila, H. G.; Keough, A. H.; Soboczenski, E. J. *J. Org. Chem.* **1953**, *19*, 780–783.

84. Liljebris, C.; Nilsson, B. M.; Resul, B.; Hacksell, U. *J. Org. Chem.* **1996**, *61*, 4028–4034.

85. Oshima, K.; Aoyama, Y. *J. Am. Chem. Soc.* **1999**, *121*, 2315–2316.

86. Oshima, K.; Kitazono, E. I.; Aoyama, Y. *Tetrahedron Lett.* **1997**, *38*, 5001–5004.

87. Duggan, P. J.; Tyndall, E. M. *J. Chem. Soc. Perkin Trans. 1* **2002**, 1325–1339.

88. Cho, J. Y.; Iverson, C. N.; Smith, M. R. *J. Am. Chem. Soc.* **2000**, *122*, 12868–12869.

89. Shimada, S.; Batsanov, A. S.; Howard, J. A. K.; Marder, T. B. *Angew. Chem. Int. Ed.* **2001**, *40*, 2168–2171.

90. Molander, G. A.; Trice, S. L. J.; Dreher, S. D. *J. Am. Chem. Soc.* **2010**, *132*, 17701–17703.

91. Bose, S. K.; Fucke, K.; Liu, L.; Steel, P. G.; Marder, T. B. *Angew. Chem. Int. Ed.* **2014**, *53*, 1799–1803.

92. Guo, L.; Rueping, M. *Chem. - A Eur. J.* **2016**, *22*, 16787–16790.

93. Warner, A. J.; Lawson, J. R.; Fasano, V.; Ingleson, M. J. *Angew. Chem. Int. Ed.* **2015**, *54*, 11245–11249.

94. Ahn, S. J.; Lee, C. Y.; Kim, N. K.; Cheon, C. H. *J. Org. Chem.* **2014**, *79*, 7277–7285.

95. Lozada, J.; Liu, Z.; Perrin, D. M. *J. Org. Chem.* **2014**, *79*, 5365–5368.

96. Liu, C.; Li, X.; Wu, Y.; Qiu, J. *RSC Adv.* **2014**, *4*, 54307–54311.

97. Liu, C.; Li, X.; Wu, Y. *RSC Adv.* **2015**, *5*, 15354–15358.

98. Thakur, A.; Zhang, K.; Louie, J. *Chem. Commun.* **2012**, *48*, 203.

99. Lee, C. Y.; Ahn, S. J.; Cheon, C. H. *J. Org. Chem.* **2013**, *78*, 12154–12160.

100. Lennox, A. J. J.; Lloyd-Jones, G. C. *Isr. J. Chem.* **2010**, *50*, 664–674.

101. Yamamoto, Y.; Takizawa, M.; Yu, X. Q.; Miyaura, N. *Angew. Chem. Int. Ed.* **2008**, *47*, 928–931.

102. Oberli, M. A.; Buchwald, S. L. *Org. Lett.* **2012**, *14*, 4606–4609.

103. Molander, G. A.; Biolatto, B. *J. Org. Chem.* **2003**, *68*, 4302–4314.

104. Molander, G. A.; Canturk, B.; Kennedy, L. E. *J. Org. Chem.* **2009**, *74*, 973–980.

105. Carrillo, J. A.; Ingleson, M. J.; Turner, M. L. *Macromolecules* **2015**, *48*, 979–986.

106. Billingsley, K. L.; Anderson, K. W.; Buchwald, S. L. *Angew. Chem. Int. Ed.* **2006**, *45*, 3484–3488.

107. Billingsley, K.; Buchwald, S. L. *J. Am. Chem. Soc.* **2007**, *129*, 3358–3366.

108. Martin, R.; Buchwald, S. L. *Acc. Chem. Res.* **2008**, *41*, 1461–1473.

109. Kinzel, T.; Zhang, Y.; Buchwald, S. L. *J. Am. Chem. Soc.* **2010**, *132*, 14073–14075.

110. Chivers, Tristram; Laitinen, R. S. *Chem. Soc. Rev.* **2015**, *44*, 1725–1739.

111. Carrera, E. I.; Seferos, D. S. *Macromolecules* **2015**, *48*, 297–308.

112. Barton, T. J.; Roth, R. W. *J. Organomet. Chem.* **1972**, *39*, 66–68.

113. Sweat, D.; Stephens, C. *Synthesis (Stuttg).* **2009**, 3214–3218.

114. Rhoden, C. R. B.; Zeni, G. *Org. Biomol. Chem.* **2011**, *9*, 1301–1313.

Chapter 2

Synthesis of tetra-boryl substituted chalcogenophenes and aggregation-induced emission properties of tellurophenes

2.1. INTRODUCTION

Chalcogenophenes are five-membered heterocycles containing group 16 elements (e.g. S, Se and Te). Due to the useful optoelectronic properties of chalcogenophenes, including photoluminescence and their role in efficient solar cells, molecular and polymeric chalcogenophenes have been studied in detail.[1–5] Moreover, the presence of heavier chalcogen atoms with low electronegativity, larger atomic size and higher polarizability can lead to heterocycles with increased intermolecular interactions, smaller optical band gaps and favourable (enhanced) charge transport properties.[6,7] These properties, combined with the recent discovery of phosphorescence,[8] makes the heavier chalcogenophene analogues desirable for potential applications in organic photovoltaics, light-emitting devices, and as next generation bio-imaging dyes.[9–11]

Despite the emerging consensus that heavier chalcogenophene derivatives should have advantageous optoelectronic properties in relation to those exhibited by the widely studied thiophene analogues, there is still comparatively few selenium and tellurium-containing chalcogenophenes known, mainly due to a lack of suitable synthetic routes and precursors.[12–15]

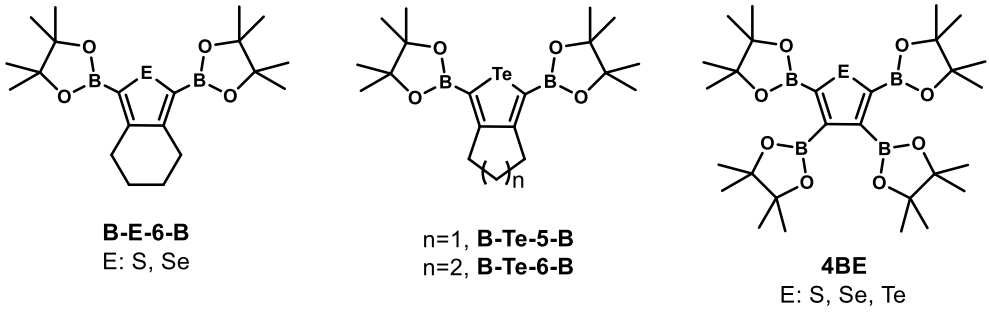

Figure 2.1. Di-substituted and tetra-substituted BPin-capped chalcogenophenes.

In this chapter, an efficient alkyne-coupling / transmetallation route[16,17] was used to gain access to a tetraborylated phosphorescent tellurophene (**4BTe**; Figure 2.1) and its sulfur and selenium analogues (**4BS** and **4BSe**, respectively). These species not only have interesting luminescence properties, they represent potentially useful building blocks for the construction of new π-conjugated arrays via Suzuki-Miyaura coupling. Specifically, the effect of heteroatom substitution on the absorption, emission and electrochemical properties of **4BS**, **4BSe** and **4BTe** has been studied and the results compared with previous chalcogenophenes synthesized by the Rivard group.[16] Cyclic voltammetry measurements were also used to evaluate the electrochemical stability of the newly reported chalcogenophenes and to determine the HOMO/LUMO energy levels. Initial experiments involving the coupling of 2-iodothiophene with **4BTe** were conducted under Suzuki-Miyaura cross-coupling conditions with the intended goal of forming star-shaped conjugated structures; this last study indicated that base-induced pinacolboronate (BPin) cleavage from heterocycle in **4BTe** readily occurred.

2.2. RESULTS AND DISCUSSION

The strategy used to form the chalcogenophenes **4BE** (E = S, Se, Te), listed in Schemes 2.1 and 2.2, started with the synthesis of the borylated zirconacyclopentadiene $Cp_2ZrC_4BPin_4$. The formation of 1,2,3,4-tetrasubstituted cyclopentadienes through intermolecular coupling of two equal or different alkynes has been reported.[18–20] The resulting zirconacycle is air- and moisture-sensitive, thus it must be handled under N_2. Once $Cp_2ZrC_4BPin_4$ was prepared, the synthesis of the various chalcogenophenes **4BE** was possible through a transmetallation reactions at room temperature using the heteroatom sources S_2Cl_2, Bipy•$SeCl_2$ or Bipy•$TeCl_2$ (Bipy = 2,2′-bipyridine).[21]

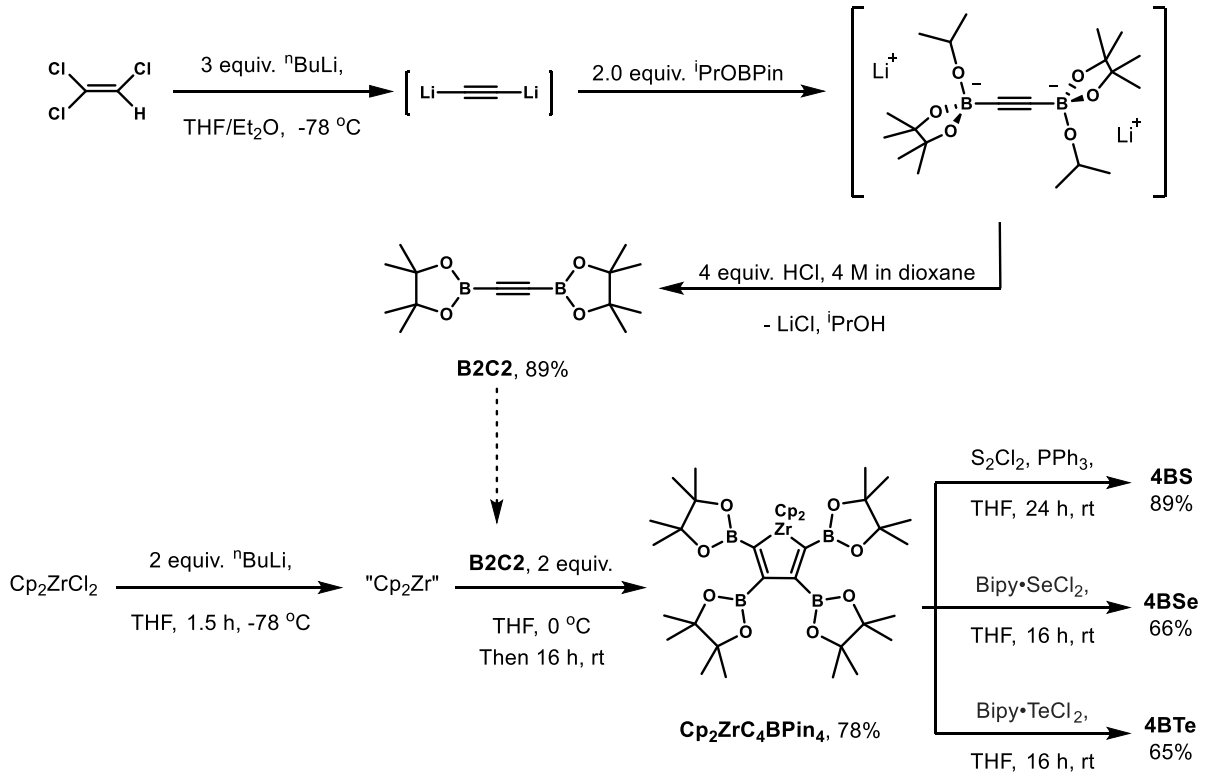

Scheme 2.1. General strategy to form tetraboryl-substituted chalcogenophenes.

2.2.1. Synthesis of tetra-boryl substituted chalcogenophenes

The synthesis of the target tetraboryl-substituted chalcogenophenes started with the synthesis of the known bis-pinacolato-diboronacetylene precursor PinBC≡CBPin (**B2C2**, Scheme 2.1). Using a modified procedure based on the literature,[22] trichloroethylene was converted efficiently into 1,2-dilithioacetylene in situ, to which was added ^{i}PrOBPin to form the diborate complex, which was then reacted with HCl to afford **B2C2** in a 89 % yield.

In the next step of the synthesis, a solution of **B2C2** in THF at 0 °C was added to a solution containing Negishi's reagent "Cp_2Zr" leading to alkyne coupling and formation of the zirconacycle complex $Cp_2ZrC_4BPin_4$.[19,21] The LiCl by-product could be easily removed by dissolving the crude product in diethyl ether and filtering the mixture to recover $Cp_2ZrC_4BPin_4$ as a dark red solid from the filtrate in a 78 % yield (see Scheme 2.1).

In the final stage of the synthesis, the sulfur and selenium-based boryl-chalcogenophenes **4BS** and **4BSe** were obtained through metallacycle transfer of $Cp_2ZrC_4BPin_4$ with the corresponding chalcogen sources, S_2Cl_2 and Bipy•$SeCl_2$, in THF (see Scheme 2.1). The thiophene analogue **4BS** was obtained as a white solid in an 89 % yield, while its selenium congener **4BSe** was recovered as an off-white solid in a 66 % yield after purification.

In the case of the tellurophene, **4BTe**, a one-pot synthetic procedure was also developed without the need to isolate the reactive zirconacycle intermediate $Cp_2ZrC_4BPin_4$. Specifically, it was possible to form **4BTe** in a 56 % overall yield starting from the borylated alkyne **B2C2** and conducting both the alkyne coupling and metallacycle transfer *in situ* in THF at room temperature under N_2 atmosphere (see Scheme 2.2). It is possible that some of the zirconacycle reactant $Cp_2ZrC_4BPin_4$ was quenched by moisture when the flask was opened to add solid Bipy•$TeCl_2$, however the final yield obtained was only on average 10 % less than the method described in Scheme 2.1; overall this procedure is an improvement as there is no need to isolate/purify the zirconacycle intermediate $Cp_2ZrC_4BPin_4$.

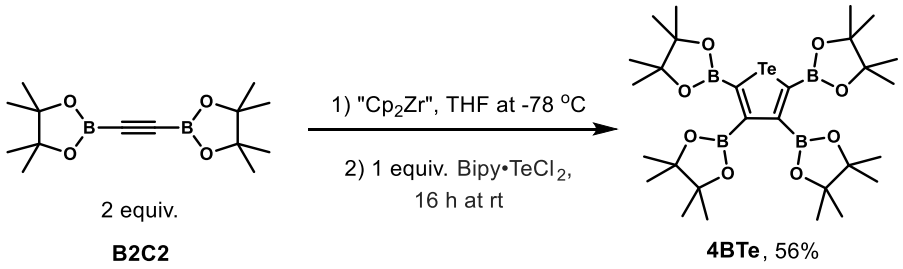

Scheme 2.2. One-pot synthesis of 2,3,4,5-tetrakis(pinacolato)tellurophene (**4BTe**).

The three chalcogenophenes **4BS**, **4BSe** and **4BTe** each show similar overall patterns in the ^1H and $^{13}C\{^1H\}$ NMR spectra. In each case, two different chemical environments for the BPin-containing methyl groups can be found at 25.2 and 24.9 ppm. Despite having two spectroscopically distinct BPin environments according to ^1H and $^{13}C\{^1H\}$ NMR, only one broad ^{11}B signal was detected for each compound; specifically, the boron resonances show a slight downfield shift from **4BS** (30.0 ppm) to **4BSe** (30.8 ppm) to **4BTe** (31.8 ppm).

Crystals of **4BSe** and **4BTe** were obtained from toluene (0 °C) with the molecular structures determined by X-ray crystallography (see Figures 2.2 and 2.3, respectively). Both structures have the BPin groups arranged around the respective chalcogenophene ring in a similar fashion, having one of the two closest BPin groups to the heavy atom almost coplanar to the chalcogenophene ring (**4BSe**: 1.6(4)°, **4BTe**: 9.2(5)°) while the other one significantly twisted (**4BSe**: 60.4(3)°, **4BTe**: 56.5(4)°). This arrangement is in contrast to what is observed in the 2,5-diborylated species **B-Se-6-B** and **B-Te-6-B** (Figure 2.1)[16] where both BPin groups are almost coplanar to the central chalcogenophene ring.

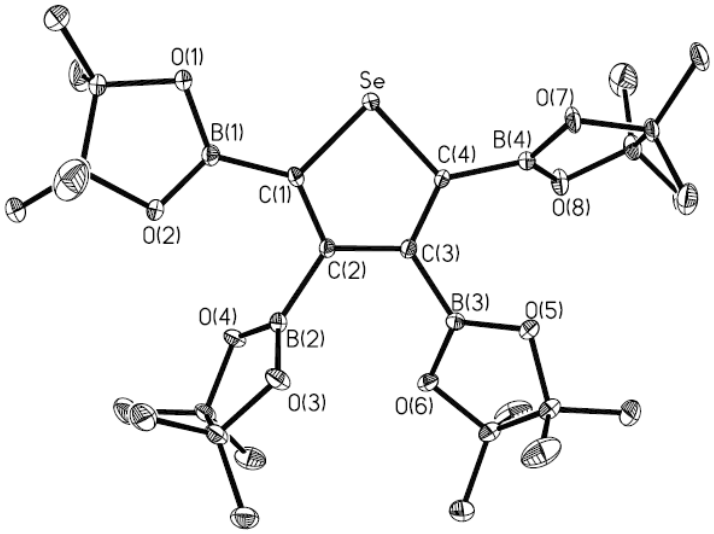

Figure 2.2. Molecular structure of **4BSe** with thermal ellipsoids presented at a 30 % probability level. Residual factor, R = 0.0264. All hydrogen atoms have been omitted for clarity. Selected bond lengths (Å) and angles (°): C(1)-C(2) 1.374(4), C(2)-C(3) 1.453(3), C(3)-C(4) 1.378(4), C(1)-B(1) 1.544(4), C(2)-B(2) 1.573(4), C(3)-B(3) 1.555(4), C(4)-B(4) 1.561(4), C(1)-Se 1.876(3), C(4)-Se 1.864(2); C(1)-Se-C(4) 88.52(11), C(1)-C(2)-C(3) 114.6(2) C(2)-C(3)-C(4) 115.1(2), C(2)-C(1)-Se 110.90(17), C(3)-C(4)-Se 110.82(17), Se-C(1)-B(1) 120.9(2), Se-C(4)-B(4) 121.65(19), C(1)-B(1)-O(1) 124.4(3), C(2)-B(2)-O(3) 124.2(3), C(3)-B(3)-O(5) 123.1(3), C(4)-B(4)-O(7) 121.8(2); O(1)-B(1)-C(1)-Se 1.6(4), O(7)-B(4)-C(4)-Se 60.4(3), C(4)-C(3)-B(3)-O(5) 33.0(4), C(1)-C(2)-B(2)-O(4) 70.7(4).

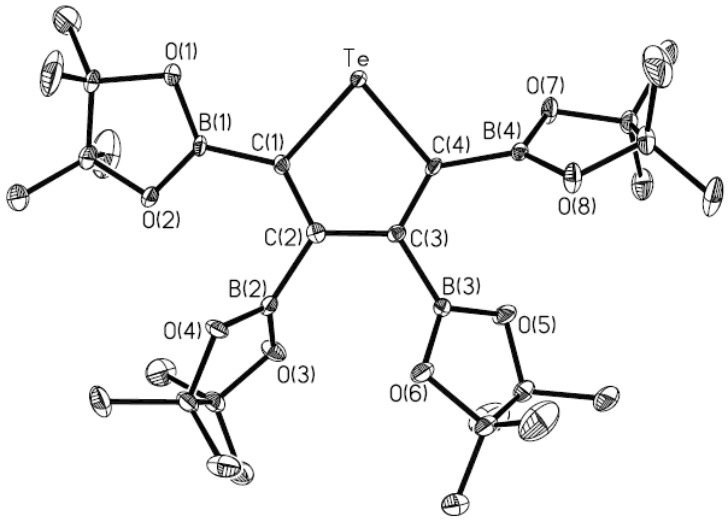

Figure 2.3. Molecular structure of **4BTe** with thermal ellipsoids presented at a 30 % probability level. Residual factor, R = 0.0342. All hydrogen atoms have been omitted for clarity. Selected bond lengths (Å) and angles (°): C(1)-C(2) 1.378(5), C(2)-C(3) 1.448(4), C(3)-C(4) 1.364(5), C(1)-B(1) 1.543(4), C(2)-B(2) 1.568(4), C(3)-B(3) 1.559(4), C(4)-B(4) 1.558(4), C(1)-Te 2.063(3), C(4)-Te 2.067(3); C(1)-Te-C(4) 82.77(12), C(1)-C(2)-C(3) 117.2(2), C(2)-C(3)-C(4) 118.6(3), C(3)-C(4)-Te 110.5(2), C(1)-B(1)-O(1) 122.8(3), C(2)-B(2)-O(3) 124.5(3), C(3)-B(3)-O(5) 123.4(3), C(4)-B(4)-O(7) 121.5(3).

2.2.2. Optical and electrochemical properties of the chalcogenophenes 4BE

The absorption spectra of **4BS**, **4BSe** and **4BTe** were measured in THF solution to see the effect the heteroatom had on the optoelectronic properties (Figure 2.4). In line with prior work in the field,[16,23,24] a progressive red-shift in the absorption maximum (λ_{max}) was noted when moving to heavier chalcogenophenes (**4BS**: 262 nm; **4BSe**: 275 nm; **4BTe**: 291 and 338 nm) along with a reduction in absorption intensity of both bands in the case of **4BTe** (see Figure 2.4, Table 2.1). The effect of solvent on the absorption profile of **4BTe** was also investigated (Figure 2.4). Based on the spectra of **4BTe** in three different solvents (THF, toluene and CH_2Cl_2) the two major absorption peaks were maintained at the same wavelength, although a decrease in intensity in CH_2Cl_2 was observed (hypochromism) (Table 2.1).

It is known that non-covalent interactions (e.g. Coulombic forces, hydrogen bonding and dipole-dipole interactions) lead to an arrangement of the molecules in certain directions and

so their respective transition dipoles can be ordered in certain directions as well, and depending on the relative orientation (parallel or collinear) of these oriented-dipoles and the induced dipoles in the neighbor molecules the absorption properties of the chromophores might decrease/increase (hypochromism/hyperchromism, respectively);[25,26] however, it is difficult to explain, based on this theory, the hypochromism observed in CH_2Cl_2, since the overall dipole change in the excited state might not be large as suggested by the lack of noticeable solvatochromic effect in **4BTe**.

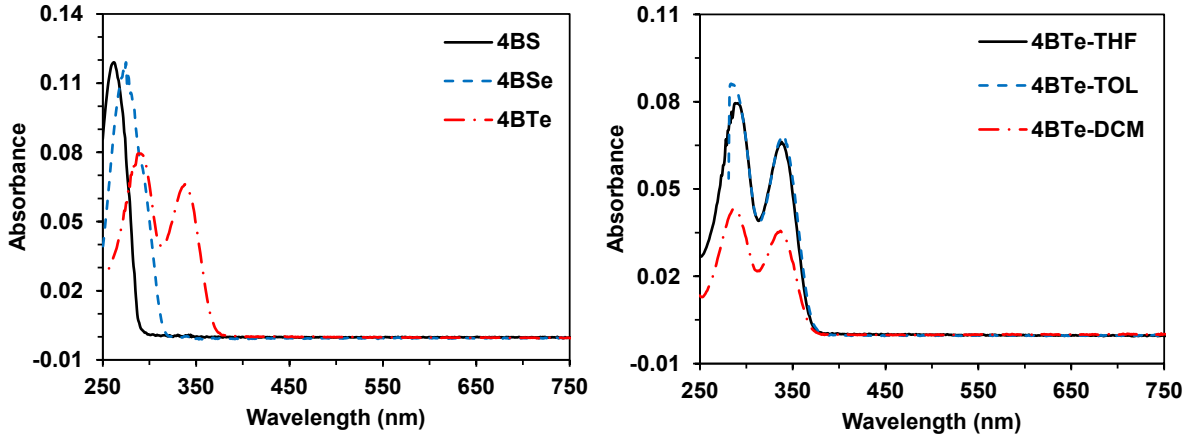

Figure 2.4. UV-Vis absorption spectra of **4BE** (E = S, Se, Te) in THF (left) and **4BTe** in different solvents (THF, toluene and CH_2Cl_2) (right); in each case, the concentration of the chalcogenophene was 11 μM.

The energy of the optical band gap (E_g) was also estimated from the UV-Vis data using Tauc's approach[27] (Equation 2.1 and Table 2.1), in which the optical band gap for a direct allowed transition (n = 1/2, in Equation 2.1) can be read directly from a graph of $(Ah\nu)^2$ versus hν by extrapolation of the straight line where the absorption is zero (A = 0) to the x-axis (hν, in eV) (Figure 2.5).

$$Ah\nu = (h\nu - E_g)^n \qquad (2.1)$$

To aid in comparison, the values of λ_{max}, λ_{em} and the estimated optical band gaps, E_g, for **4BS**, **4BSe** and **4BTe** are tabulated in Table 2.1. As can be seen in Table 2.1, the E_g values decreased when the heteroatom is changed from S to Se and Te (4.4, 4.1 and 3.4 eV, respectively), which is expected based on related examples in the literature;[3,24] this lowering of Eg is generally due to a reduction of the LUMO level.[28,29] Two electronic transitions were observed for **4BTe** in the UV-Vis spectrum, the first (288 nm) was assigned to a π-π* transition and the second absorption (338 nm) to a charge transfer absorption that will be explained below. The high energy π-π* transition is also present in tellurophenes reported in the Rivard group[17] (e.g. **B-Te-6-B** and **B-Te-5-B**).

Table 2.1. Optical properties of chalcogenophenes.

	Absorption[a]		**Photoluminescence**	**Optical band gap[c]**
	λ_{max}, nm	**ε, M^{-1} cm^{-1}**	**λ_{em}, nm**	**E_g, eV**
4BS (THF)	262	10700	-	4.4
4BSe (THF)	275	10900	-	4.1
4BTe (THF)	288	7200	516[b]	3.4
	338	6000		
4BTe (Toluene)	284	8100	-	-
	339	6400	-	-
4BTe (CH_2Cl_2)	288	4200	-	-
	337	3400	-	-

a) Concentration of chalcogenophene, 11 μM b) In THF / water (5:95), 600 μM

c) From Tauc plots

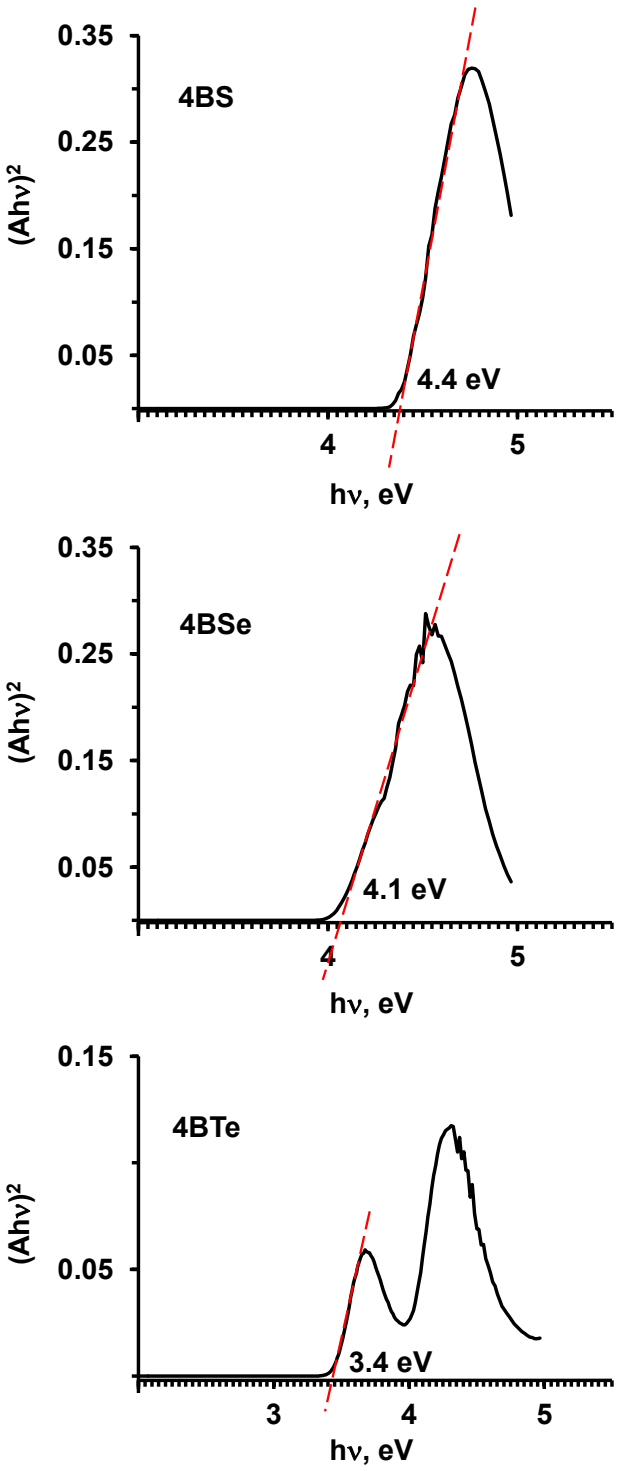

Figure 2.5. Tauc plots for **4BS**, **4BSe** and **4BTe**.

As it will be shown later, the emission profiles of **B-Te-6-B** and **4BTe** in solution (under N_2) are quenched once these samples are exposed to air. In addition the absorption profiles of **B-Te-6-B** and **4BTe** in THF were measured before and after exposure to air and the results are shown in Figure 2.6 and Table 2.2. Both tellurophenes had similar absorption properties, with two main electronic transitions in the UV spectral region (Table 2.2). Once the tellurophenes were exposed to air, a similar two band UV-Vis spectrum was seen as under N_2, indicating no change in the electronic distribution of tellurophenes in the ground state. Of note, collisional energy transfer from these tellurophenes to triplet oxygen ($^3O_2$) is only expected to occur in the excited triplet state.[30]

As mentioned before, the first absorption peak at 292 nm in **B-Te-6-B** was assigned to a π-π* transition. The lower energy absorption at 355 nm has been assigned, on the basis of TD-DFT computations[17] as an electronic transition from the HOMO (mainly localized in a lone pair on the Te^{II} center) to the LUMO (B-C π-type orbitals involving the appended BPin groups). The same assignment applies to the long wavelength UV-vis absorption in **4BTe** as confirmed via TD-DFT calculations conducted in collaboration with Prof. Brown (University of Alberta); the computed HOMO and LUMO in **4BTe** in THF are presented in Figure 2.7.

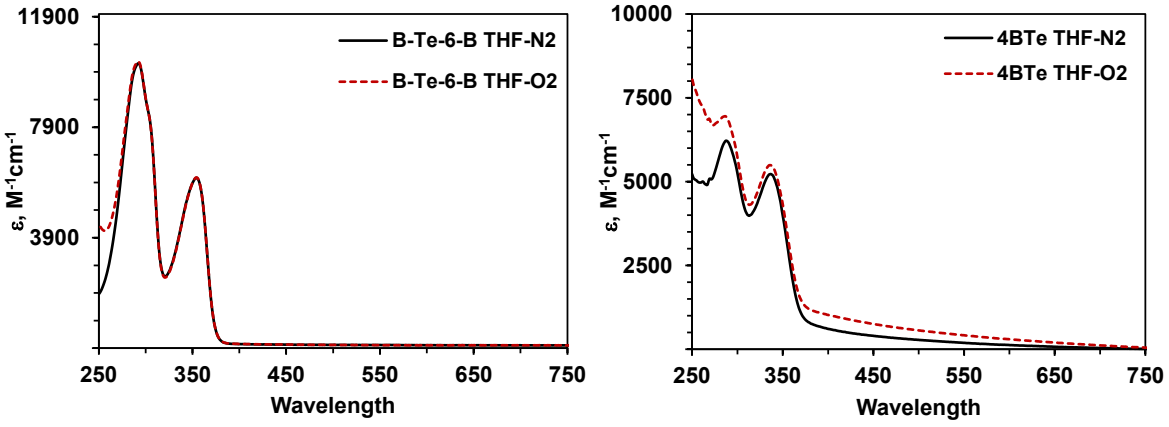

Figure 2.6. UV-Vis absorption spectra of **B-Te-6-B** and **4BTe** in THF before and after exposure to air; concentration of tellurophenes 50 μM.

Table 2.2. Absorption properties of **B-Te-6-B** and **4BTe** under N_2 and air in THF.

	λ_{max}, nm (ε, $M^{-1}cm^{-1}$)			
	B-Te-6-B		**4BTe**	
	N_2	**Air**	**N_2**	**Air**
THF	292 (10200)	292 (10300)	295 (5800)	286 (6900)
	354 (6100)	354 (6100)	342 (5000)	336 (5500)

4BS:

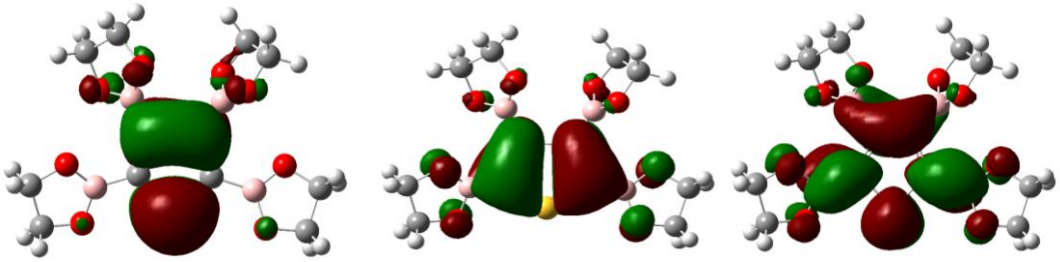

4BSe:

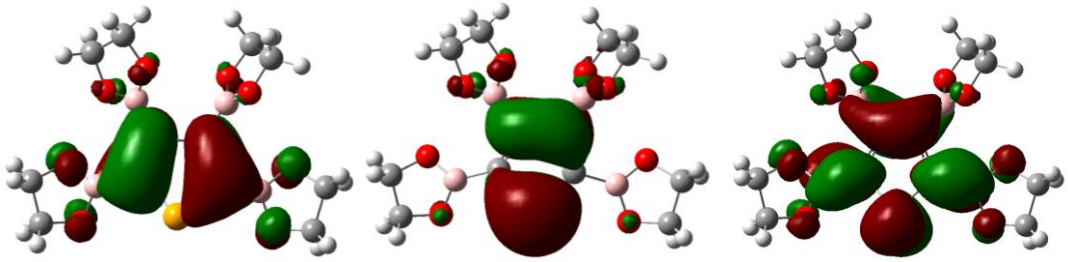

4BTe:

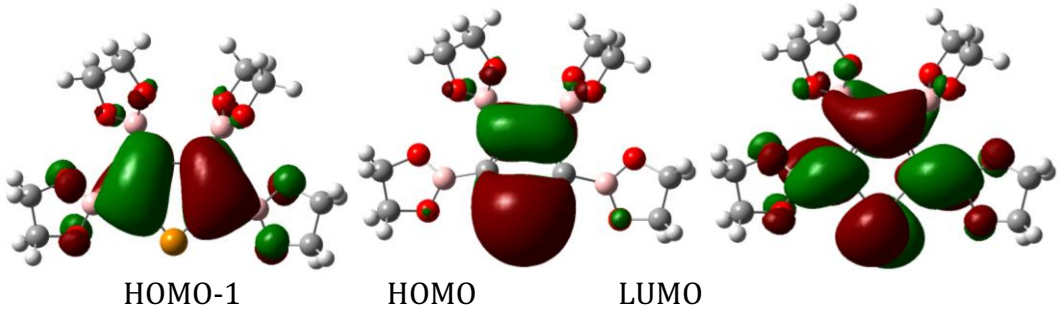

Figure 2.7. Molecular orbitals of **4BS**, **4BSe** and **4BTe**, as computed at the TD-B3LYP/aug-cc-pVTZ-(PP) level of theory in THF (IEF-PCM).

Based on the theoretical calculations for **4BS**, the most allowed transition corresponded from the HOMO localized in π-type orbitals in the C=C bonds to the LUMO localized in a B-C π-type orbitals involving the appended BPin groups, though transitions from the HOMO-1 and HOMO to the LUMO, turned out to be very close in energy (4.79 and 4.72 eV, respectively). In contrast, the most allowed transition in **4BSe** corresponded to HOMO-1 (π-type orbitals in the C=C bonds) to the LUMO (same π-type orbital located between B-C, as in **4BS**); there is also a switch in orbital character of the HOMO and HOMO-1 going from **4BS** to **4BSe**. Now the HOMO in **4BSe** and **4BTe** contains contribution from a Se^{II} or Te^{II} lone pair (Figure 2.7).

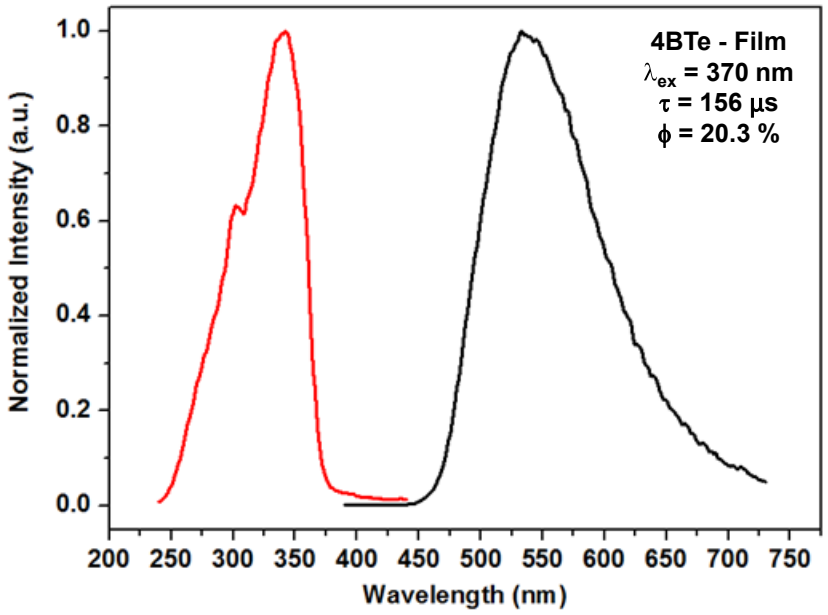

Figure 2.8. Luminescence of **4BTe** in the film state under air at λ_{ex} = 370 nm.

When UV light of 365 nm was shined on the solid **4BS**, **4BSe** and **4BTe**, only **4BTe** showed luminescence. Luminescence measurements in air (Figure 2.8) of pure films indicated green phosphorescence (λ_{em} = 536 nm) with a weighted mean luminescence lifetime of τ = 156 μs and an absolute quantum yield of ϕ = 20.3 %. Measurements under Ar

show an increase in quantum yield to ϕ = 24.4 % and a longer average lifetime (τ) of 387 μs, though with the same emission band centered at *ca.* 536 nm. The large increase in the lifetime in Ar by more than twice of the value measured in air, suggests the excited triplet states are living longer under Ar than in air and therefore, the emission from the excited triplet states in air might have being partially quenched via interaction with O_2 (also evidenced by the slight decrease in τ in air). However the packing of **4BTe** in the solid state might be preventing oxygen from diffuse entirely throughout the tellurophene film. The quenching mechanism by O_2 will be addressed later.

In collaboration with Dr. Przemyslaw Data (Durham University), prompt and delayed fluorescence studies of **B-Te-6-B** and **4BTe** in a solid 1% in Zeonex matrix - solid state under vacuum were performed. They showed two emissions in each **B-Te-6-B** and **4BTe** compound, one in fluorescence nature with lifetimes of τ = 3.02 and 1.06 ns, respectively, and the other in the phosphorescence range with lifetimes of τ = 56.56 and 242.96 μs, respectively. These results are important in the sense that the fluorescence emission had not been detected yet in both tellurophenes, probably due to its very low intensity of these emissions, which are each centered at 425 nm. The longer lifetime phosphorescence emission occurred at the same wavelength as previously reported in the solid state for **B-Te-6-B** and **4BTe** (516 and 535 nm, respectively).[17]

Solutions of **4BS** and **4BSe** in THF were irradiated at 350 nm (in the fluorimeter) and 365 nm (UV light) under N_2 and in the presence of air (O_2), however, no detectable luminescence was found (Figure 2.9, top). In contrast, THF and $CHCl_3$ solutions of the tellurophenes **4BTe** and **B-Te-6-B** under N_2 exhibited faint green-yellow luminescence upon irradiation at 365 nm (λ_{em} = 536 and 550 nm, respectively) (Figure 2.9, bottom). After these solutions were exposed to air for 5 minutes the luminescence was completely quenched as verified by the fluorimeter. The effect of air (O_2) on the emission in tellurophenes in solution is then an important factor to be considered in future luminescence studies.

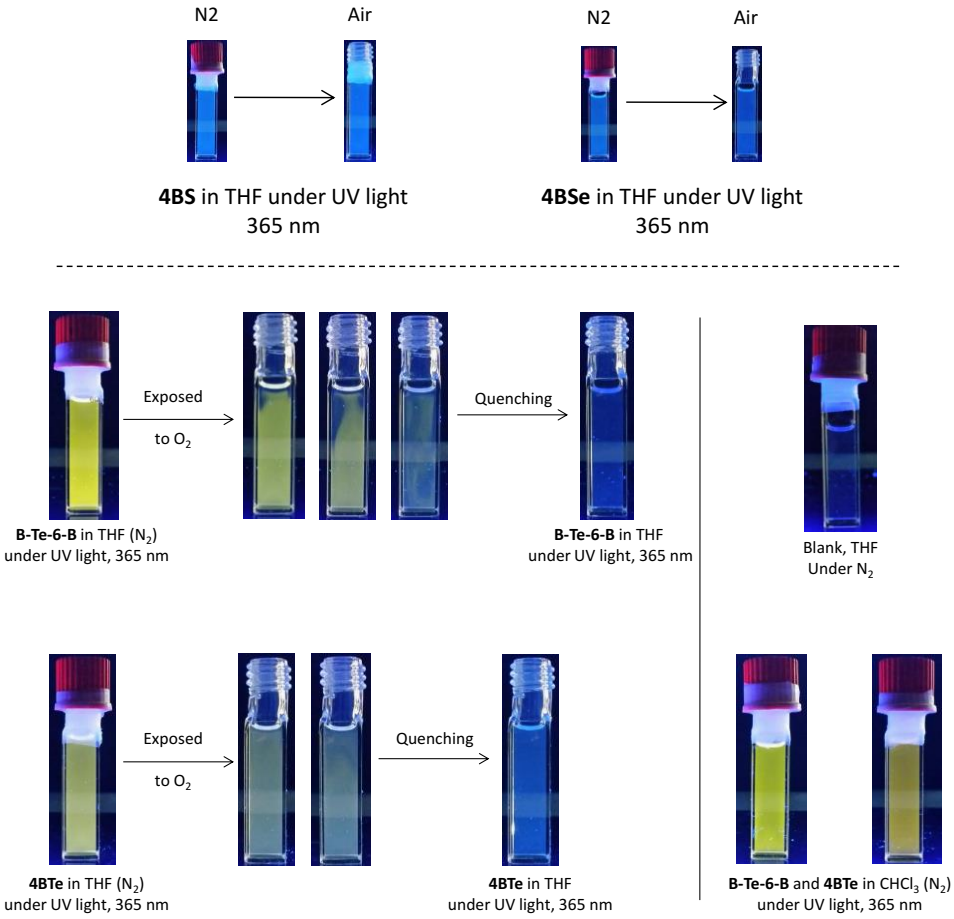

Figure 2.9. Top: no observable emission from **4BS** and **4BSe** under N_2 and O_2. Bottom: quenching process of **B-Te-6-B** and **4BTe** in THF (50 μM) under N_2 when exposed to air for 5 minutes and shined with UV light of 365 nm.

Since luminescence was observed from **B-Te-6-B** and **4BTe** in solution under N_2, it was necessary to study this effect in more detail. In collaboration with Dr. Przemyslaw Data, solutions of **B-Te-6-B** and **4BTe** in toluene and THF were measured under air and after degassing the samples (Figure 2.10). Interestingly, **B-Te-6-B** in toluene under air (top-left Figure 2.10) showed weak fluorescence emission at 460 nm, which likely corresponds to the same fluorescence emission detected in the solid state at 425 nm. In contrast, it was not possible to detect the fluorescence emission coming from **4BTe** in toluene and THF under air (Figure 2.10, bottom-left).

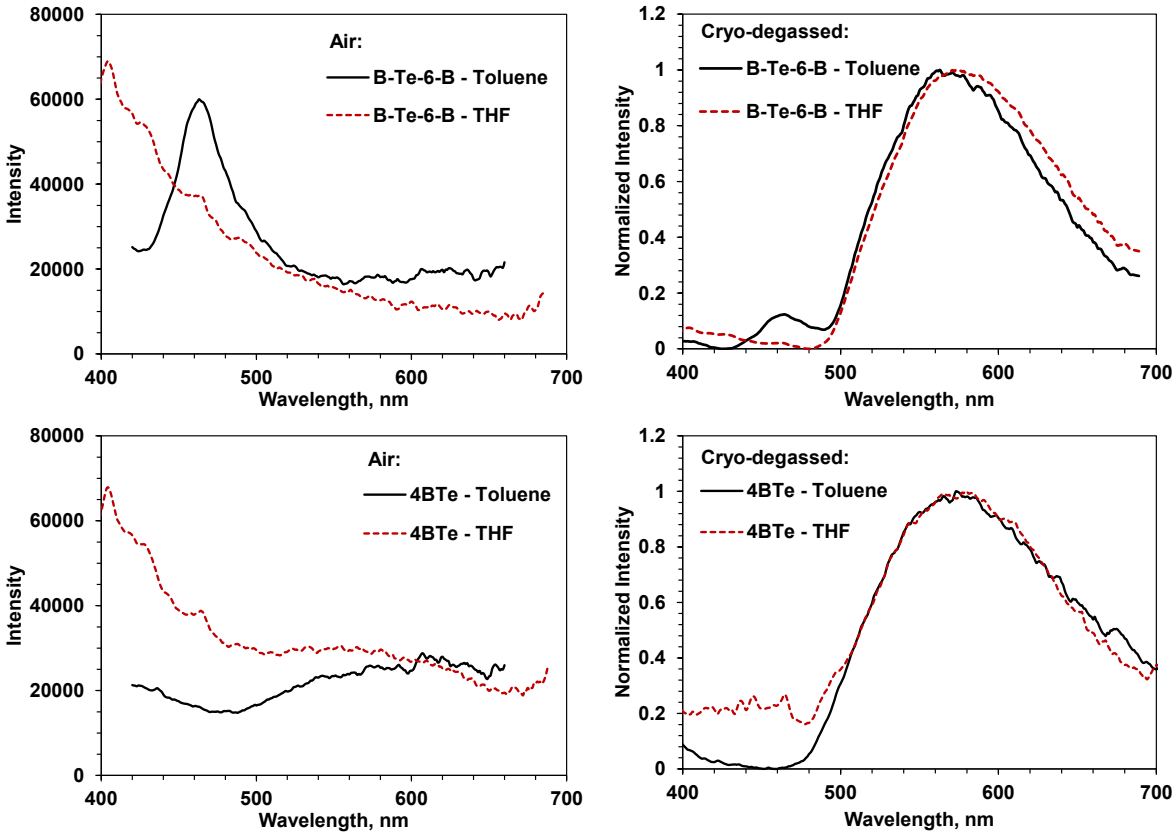

Figure 2.10. Luminescence measurements of **B-Te-6-B** and **4BTe** in toluene and THF (10 μM) under air and after degassing the samples at λ_{ex} = 350 nm.

Once the sample solutions were cryo-degassed, main broad emissions at λ_{em} = 560 and 580 nm tailing to longer wavelengths were observed in **B-Te-6-B** and **4BTe**, respectively (Figure 2.10, top and bottom-right), and a small band in **4BTe** in toluene (λ_{em} = 460 nm) corresponding to the fluorescence emission mentioned before. This is clear that quenching of phosphorescence by the presence of O_2 is a major event in air. Light emission from **4BTe** and **B-Te-6-B** in the solid state was previously shown to be phosphorescence, as evidenced by microsecond emission lifetimes, and supporting computational data was consistent with the formation of excited triplet states (T_n) via intersystem crossing from an initial singlet (S_1) state.[17,31] Thus, the noted quenching of emission in solution by O_2 is likely mediated by non-radiative collisional energy transfer from excited triplet states of the tellurophene emitters to the ground state triplet oxygen ($^3O_2$), resulting in the formation of energy singlet oxygen

($^1O_2$) and regenerating a tellurophene in its ground state (S_0).[32] This is a frequent quenching mechanism of triplet emitting compounds with emission lifetimes in the microsecond range or longer,[33] as found in Pt or Pd porphyrin-based oxygen sensors.[34]

Although the relative quantum yields of **4BTe** and **B-Te-6-B** in THF and toluene (10 μM, after cryo-degassing) were low (ϕ = 2 % for **B-Te-6-B** and **4BTe** in both solvents), the emission in solution was still strong enough to be visible to the naked eye. Accordingly, one can visually detect the quenching of luminescence after allowing the diffusion of air into the solutions as was shown in Figure 2.9. Notably, relative quantum yields of these tellurophenes in solution were very low in contrast to the absolute quantum yields (ϕ) found for **B-Te-6-B** and **4BTe** (11.5 and 20.3 %, respectively) in pure films.[17] Such a difference in values might be due to the possible hindered rotations in the solid state that avoid the excited molecule to lose its energy through non-radiative rotational pathways, in this case the rotation of the BPin groups around the B-C single bond would be restricted in the solid state.

Previous optical measurements[17] on **B-Te-6-B** showed that this tellurophene in THF/water mixtures forms aggregates after ≥ 80 wt. % water content upon which bright green luminescence in air was found. The resulting aggregation-induced emission (AIE) from **B-Te-6-B** is important as it opens the door for the possible use of **B-Te-6-B** in solid state organic light-emitting diodes (OLED) and chemical sensors;[35–38] its potential use as a sensor lies in the use of **B-Te-6-B** in the turn-on mode when they form aggregates.

Sensors usually work in the turn-off mode, that is, they are emissive in solution and upon contact with the analyte they might aggregate or precipitate showing a decrease in the emissive properties by the usual aggregation-caused quenching effect (ACQ). However, sensors working in the turn-on mode, such as AIE-based sensors, when they form aggregates their emission is increased, showing higher sensitivity and less likely to generate false-positive signals than their counterparts turn-off sensors.[35] Examples of the use AIE- based sensors have been reported (Figure 2.11) and include: selective detection of Al^{3+} in cells using a naphthalene di-imine base chelate,[39] sensing of furin activity through the detection of the emission from tetraphenylethylene (TPE)[40] aggregates formed when the enzyme furin is

cleaved, and the formation of a red emissive luminogen in the solid state based on TPE units bridged by polyyne which could be applied for the fluorescence imaging of cancer cells.[41]

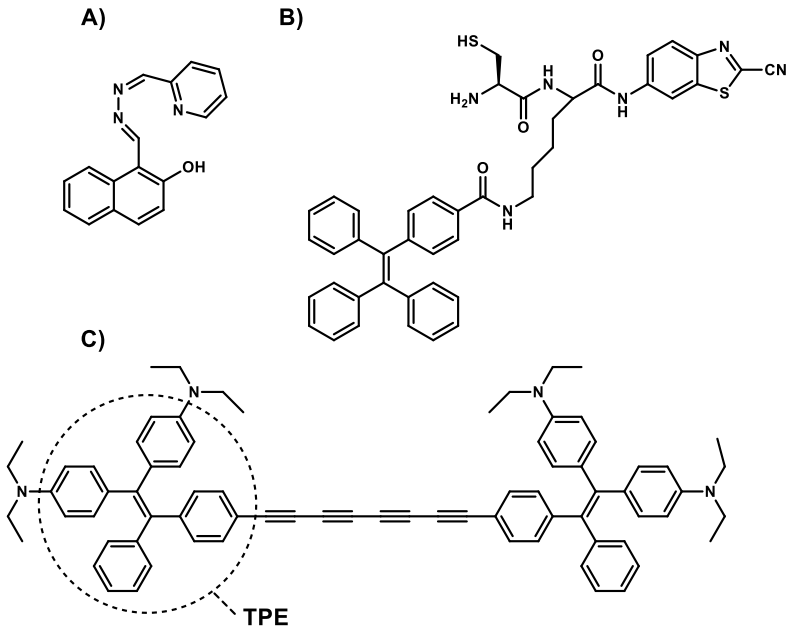

Figure 2.11. AIE-based sensors for the detection of: a) Al^{3+}, b) furin activity, and c) imaging of cancer cells.

Due to similar structural characteristics of **B-Te-6-B** with **4BTe**, the possibility of achieving AIE in air from **4BTe** was also investigated. Aggregates of **4BTe** were formed in a mixture of THF/water (5:95) and the resulting excitation and emission spectra are shown in Figure 2.12. Aggregates of **4BTe** emit at 516 nm (λ_{ex} = 365 nm). The resulting large Stokes shift (5.5×10^3 cm^{-1}) is consistent with the nature of emission from **4BTe** being phosphorescence; likewise a long lifetime (τ) of 156 μs was found in air. Usually, AIE is assigned to the restriction of intramolecular rotation (RIR) of molecular groups linked to the chromophores, along with a reduction of potentially quenching π-π stacking interactions in the solid state.[42] However since tellurophene solutions of **4BTe** (and **B-Te-6-B**) can emit in the absence of O_2, it is possible that not only restrictions in the molecular rotation of the BPin groups in the

aggregates but exclusion of O_2 in the solid/aggregated state could contribute to the phosphorescence noted in air.

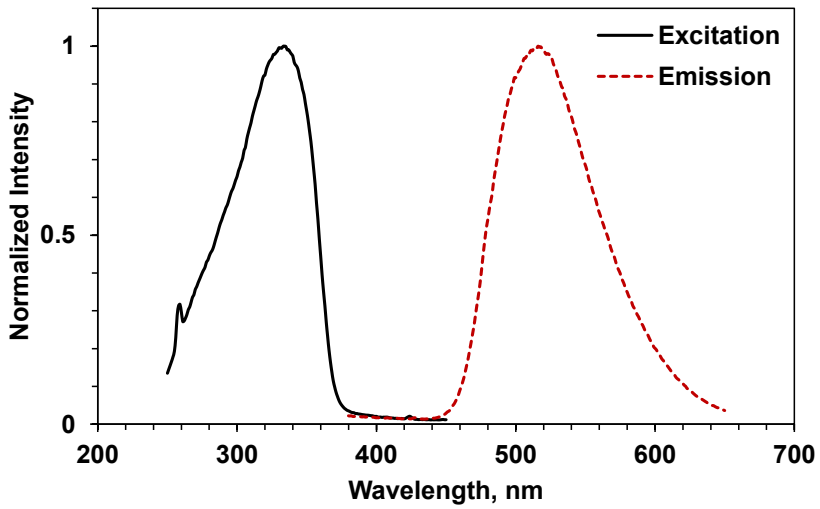

Figure 2.12. Photoluminescence excitation and emission spectra of **4BTe** in THF/water (5:95); concentration of **4BTe** = 600 μM (λ_{ex} = 365 nm).

Tellurophenes **4BTe**, **B-Te-6-B** and their phenyl/BPin mixed-substituted analogues[31] (**2,5-BPin$_2$-3,4-Ph$_2$-Te** and **2,4-BPin$_2$-3,5-Ph$_2$-Te**, see Scheme 2.3) all possess formally empty p-orbitals at the ring-bound boron centers at the 2- and/or 5-positions; these species also have one BPin group almost coplanar to the tellurophene ring, thus it is possible that all of these species share the same mechanism of phosphorescence. Accordingly, when BPin groups are found at the 2- and 5-positions of a tellurophene, the colour of emission is green (Scheme 2.3), however, when a phenyl group is also found in either the 2- or 5-position (e.g. **2,4-BPin$_2$-3,5-Ph$_2$-Te**) the emission changes from green to orange-yellow. Therefore, the emission from these compounds can be altered by modification of the substituents bound to the tellurophene. The formation and luminescent properties of unsymmetric alkyl-substituted tellurophenes will be explored in Chapter 4.

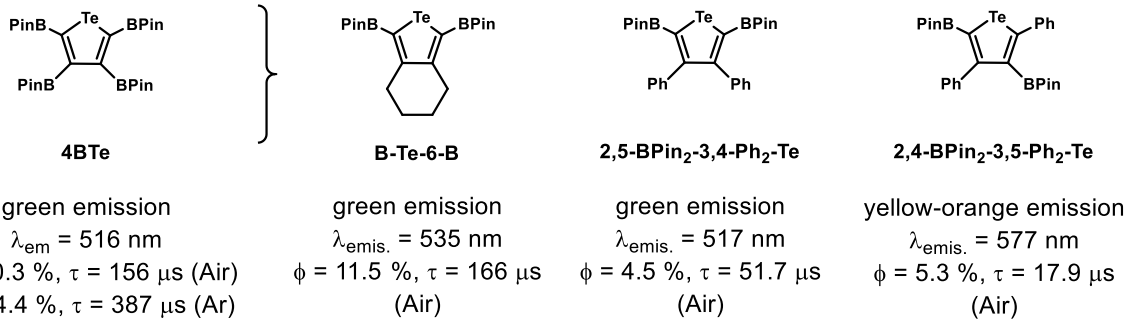

Scheme 2.3. Various BPin-substituted tellurophenes. Color of emission, absolute quantum yields and lifetimes in the solid state are shown for comparison.

Phosphorescence from **B-Te-6-B** has been rationalized as stemming from the initial population of an excited S_1 state followed by intersystem crossing (ISC), encouraged by the presence of the Te atom, to occupy triplet excited states (with emission from T_1) (Figure 2.13). Based on calculations on B-Te-6-B, the excited states S_1 and T_3 are close enough in energy (< 0.1 eV) to make intersystem crossing possible leading to eventual phosphorescence in the solid state. In contrast, it was found that in **B-S-6-B** and **B-Se-6-B** (Figure 2.1), the closest triplet state to S_1 is on average different in energy by >1 eV, making intersystem crossing highly unfavourable.[17] This is a very important finding since it stressed the importance of the presence of heavy atom (Te) in the series of chalcogenophenes to promote phosphorescence via intersystem crossing from singlet to triplet states. Furthermore, the energies of the excited triplet state (T_3) in the phenyl/BPin-substituted tellurophenes **2,5-BPin$_2$-3,4-Ph$_2$-Te** and **2,4-BPin$_2$-3,5-Ph$_2$-Te**[31] are also close to that of the first singlet excited state (S_1) allowing ISC and phosphorescence to occur.

Theoretical calculations for the chalcogenophene series **4BE** (E = S, Se and Te) are shown in Figure 2.14. As in **B-Te-6-B**, the excited states S_1 and T_3 in **4BTe** are close in energy (~ 0.12 eV) thus explaining the phosphorescence observed upon irradiation. In the case of **4BSe**, no notable emission was observed in the solid state, likely due to the difference in energy of excited states of S_1 and T_3 (0.35 eV), though the singlet excited state S_2 is relatively close in energy to the excited triplet state T_3 with a difference in energy of 0.17 eV, still large enough to hamper ISC.

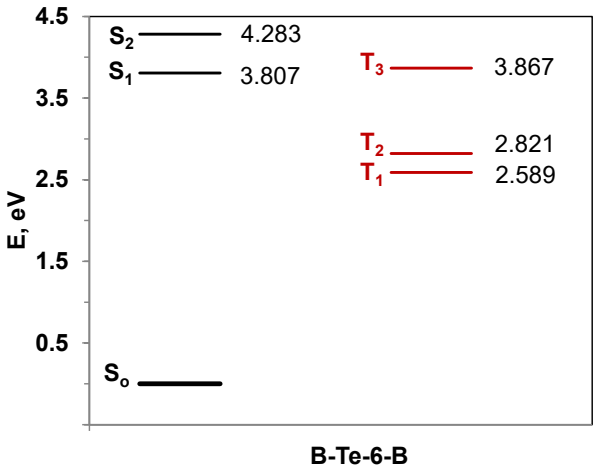

Figure 2.13. Computed vertical excitation energies to both singlet and triplet states at the TD-B3LYP/6-31G (2d, p) [LANL2DZ for Te] level of theory in the gas-phase, for **B-Te-6-B**.[17]

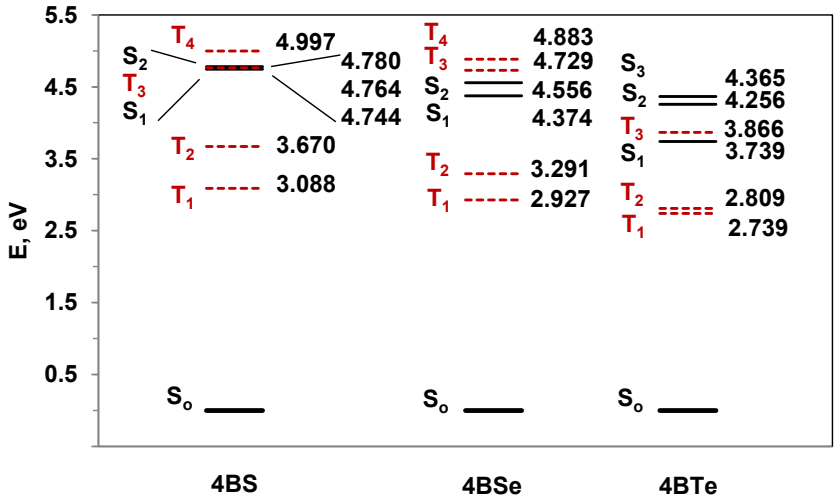

Figure 2.14. Computed vertical excitation energies to both singlet and triplet states at the B3LYP/cc-pVTZ (cc-pVTZ-pp for Te) level of theory in the gas-phase, for **4BS**, **4BSe** and **4BTe**.

The non-emissive character of **4BS** cannot be explained only by differences in energies of their excited singlet and triplet states, since S_1, S_2 and T_3 are very close in energy (~0.02

eV). However the smaller magnitude of spin-orbit coupling expected in the lighter chalcogenophene **4BS**, S could be preventing ISC from occurring. Thus the excited states in **4BS** (S_1 and S_2) likely relax by non-radiative pathways as no observable luminescence in the solid state or in solution was seen.

In order to see how the HOMO and LUMO's energies vary in the series of chalcogenophenes (**4BE**; E = S, Se and Te), cyclic voltammetry (CV) measurements were performed at a 100 mV/s scan rate using analytically pure samples of **4BE** (Figure 2.15) and ferrocene (Fc) as a standard. Scanning the potential through all the range available for the system **4BTe** and Fc (in THF: -3.0 to 1.5 V) showed reduction processes at negative potentials relative to the ferrocene standard (Fc) (Figure 2.16).

Based on the CV measurements, the peak-to-peak separation for the first reduction waves (ΔE) in **4BS**, **4BSe** and **4BTe** are more than 100 mV (0.35, 0.22, and 0.22 V, respectively), therefore these redox processes are quasi-reversible in nature. Besides these quasi-reversible redox process, **4BTe** showed an irreversible reduction wave starting at -2.92 V. Multiple cycles (up to 3 times) proved good electrochemical stability for the events (Figure 2.17). The standard potential at the maximum of the quasi-reversible waves for **4BS**, **4BSe** and **4BTe** -2.53, -2.57 and -2.50 V (vs Fc/Fc^+). According to the literature,[43] $\mathbf{4BE}^{\bullet-}$ species could be considered as strong reducing agents and even catalysts. Examples where anion radicals are used as catalysts can be found in the reductive cyclizations of unsaturated enones using dicyanoanthracenes (DCA) as the photo-catalyst precursor. DCA is reduced with PPh_3 to form the active catalytic species $DCA^{\bullet-}$ which induces cyclization by reducing the enone via an enol radical intermediate (Scheme 2.4).[44]

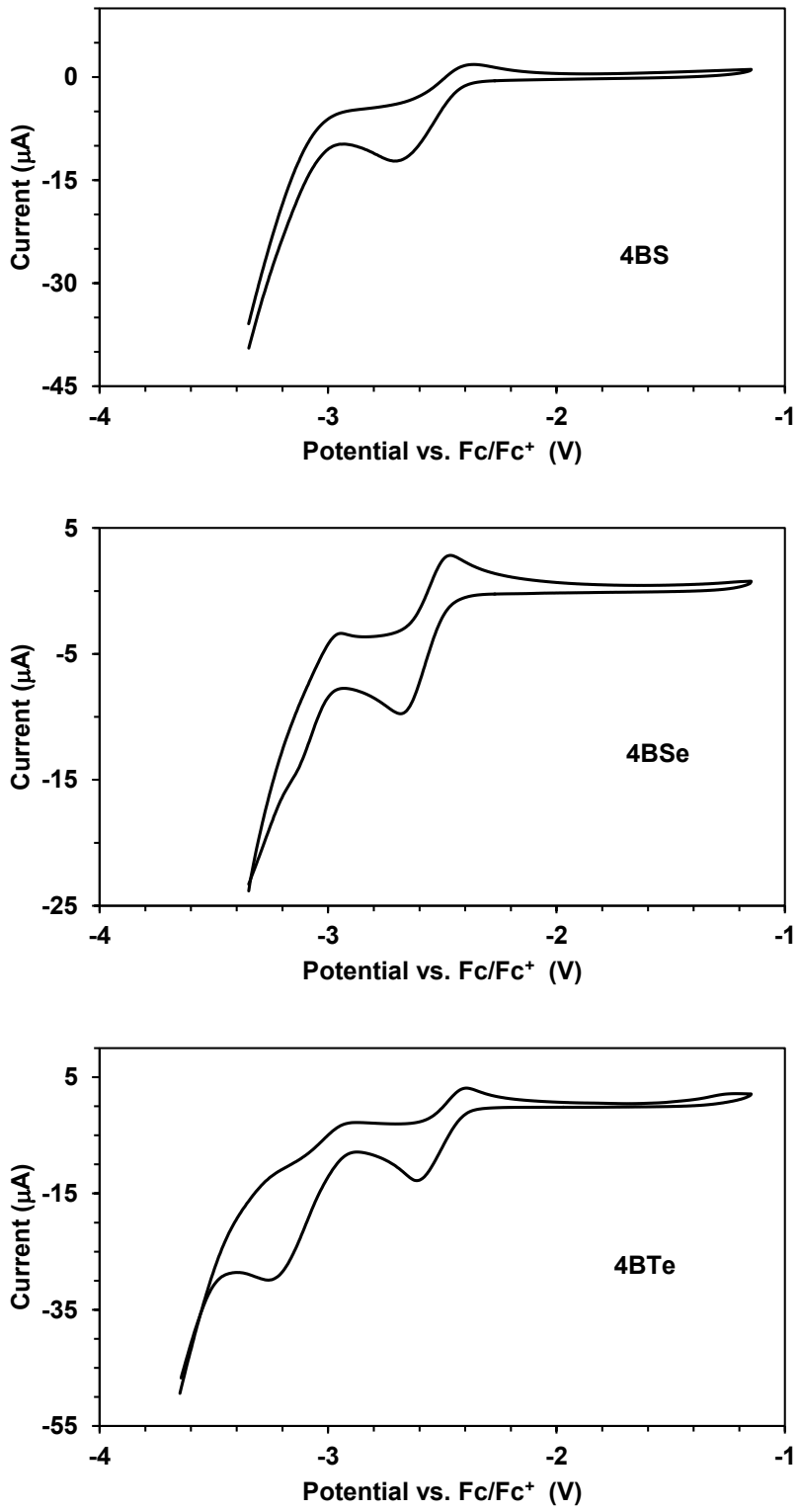

Figure 2.15. Cyclic voltammograms of **4BS** (3.7 mM), **4BSe** (3.4 mM) and **4BTe** (3.2 mM) in THF / 0.1 M $^{n}Bu_4NPF_6$ under Ar, room temperature at 100 mV/s.

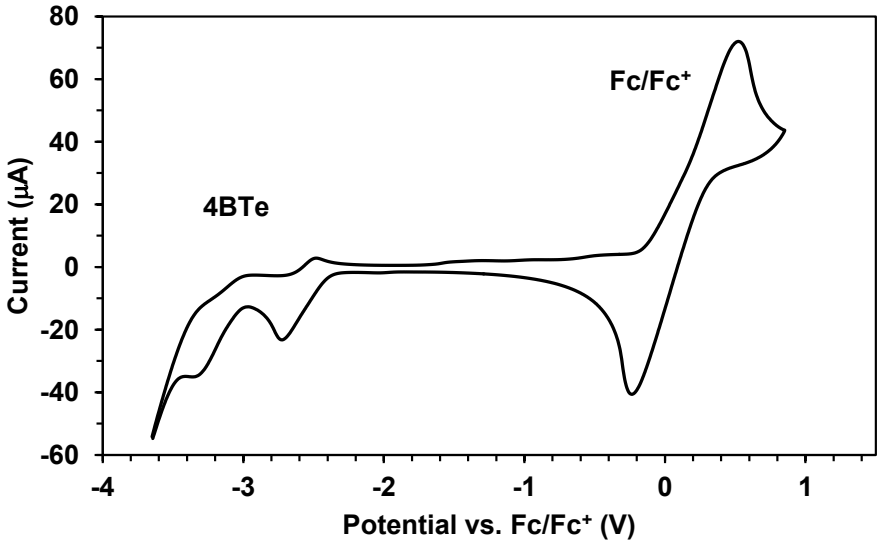

Figure 2.16. Cyclic voltammogram of **4BTe** and Fc/Fc^{+} in THF (3.2 mM and 6.1 mM, respectively) vs. Ag pseudo-reference at 100 mV/s under Ar.

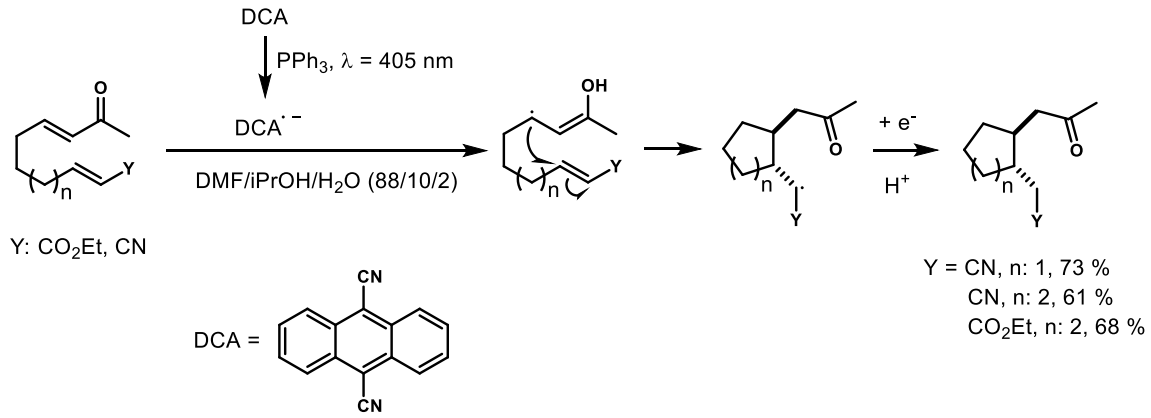

Scheme 2.4. Reductive cyclizations of unsaturated enones via anion-radical catalyst formation ($DCA^{\bullet -}$).

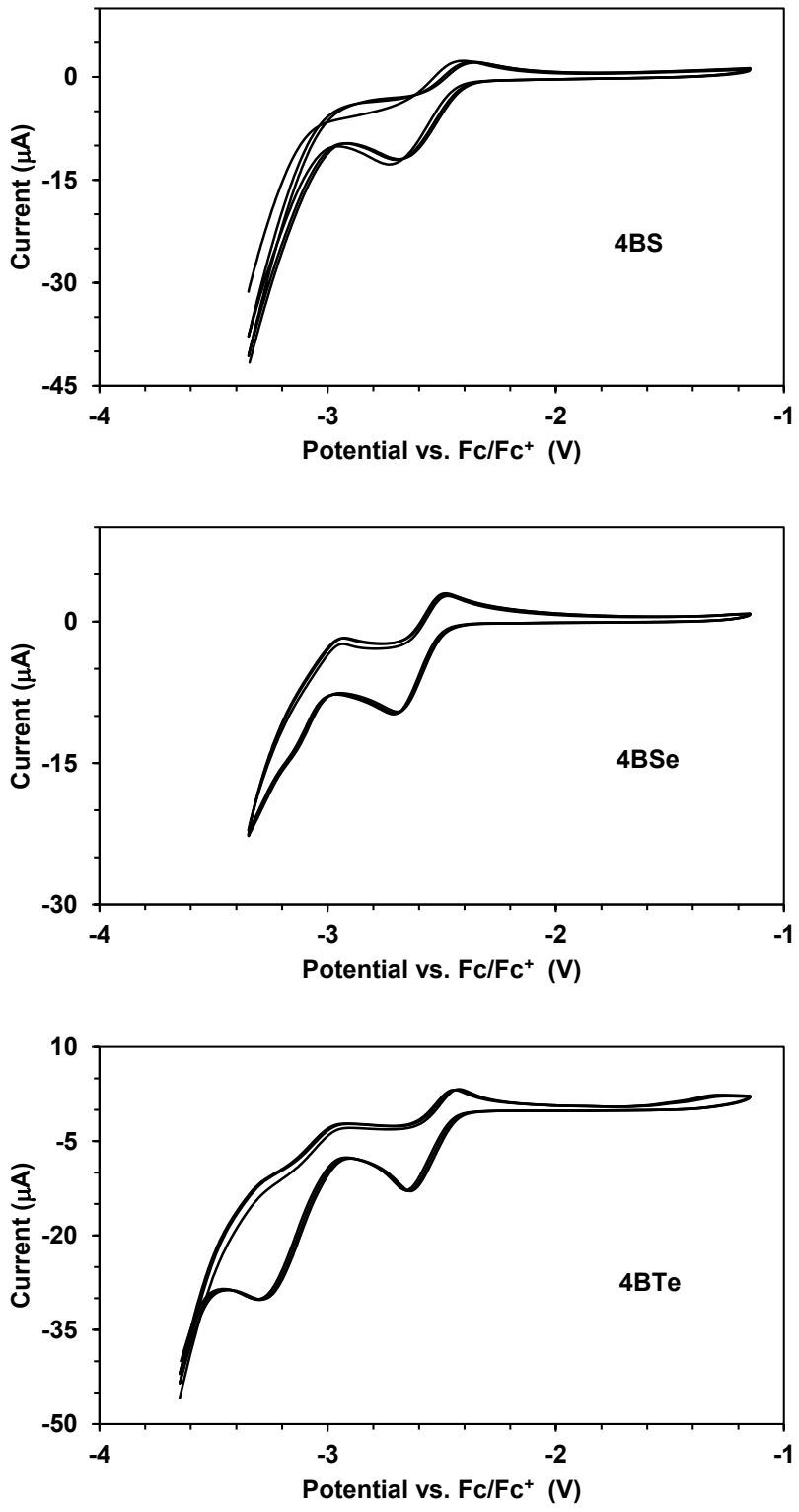

Figure 2.17. Cyclic voltammograms of **4BS**, **4BSe** and **4BTe** in THF vs. Fc/Fc^{+}. Three cycles, scan rate at 100 mV/s.

Table 2.3. Cyclic voltammetry measurements of the chalcogenophenes **4BE**.

	$E_{ox/onset}$, V	$E_{red/onset}$, V	E_{LUMO}[a], eV	E_{HOMO}[b], eV	E_g^{opt}, eV
4BS	-2.62	-2.42	-2.34	-6.74	4.4
4BSe	-2.65	-2.47	-2.29	-6.39	4.1
4BTe	-2.55	-2.40	-2.36	-5.76	3.4
	-	-2.92	-	-	-

a) $E_{LUMO} = -(4.76 + E_{red/onset})$ eV

b) E_{HOMO} (eV) = $E_{LUMO} - E_g^{opt}$

The energy of LUMO level (E_{LUMO}) in **4BTe** was calculated using the corrected reduction potential derived from the onset of the reduction wave by cyclic voltammetry (Table 2.3). The E_{HOMO} of **4BTe** was calculated from the estimated E_{LUMO} from CV and the optical bandgap found by UV-Vis measurements. It was found that the lower bandgap in **4BTe** is mainly driven by an increase in energy of the HOMO level (localized in a lone pair on the Te^{II} center, Figure 2.7). Thus **4BTe** might be more prone to oxidation than the lighter analogues **4BS** and **4BSe**.

2.2.3. Initial cross-coupling trials between 4BTe and 2-iodothiophene

4BTe is the most interesting chalcogenophene within the **4BE** series (E = S, Se and Te) in terms of optoelectronic properties; as a result, the possible functionalization of **4BTe** using Suzuki-Miyaura cross-coupling was explored. If suitable coupling conditions can be developed then the generation of tetraaryl substituted, star-type, tellurophene structures could be formed.[45,46] Star-shaped molecules have some advantages over the linear analogues.[47–49] For example, these species often have enhanced solubility and film-forming properties,[50] with enhanced and broader absorption properties leading to higher power conversion

efficiencies in photovoltaic devices.[51,52] The improved photovoltaic performance in star-shaped molecules partially stems from an increased number of chemical groups able to absorb light[49] compared to small molecules. Recently, a power conversion efficiency (PCE) value of 8.1% was achieved in an organic solar cell containing a star-shaped light absorber constructed from having benzodithiophene core (Figure 2.18).[52]

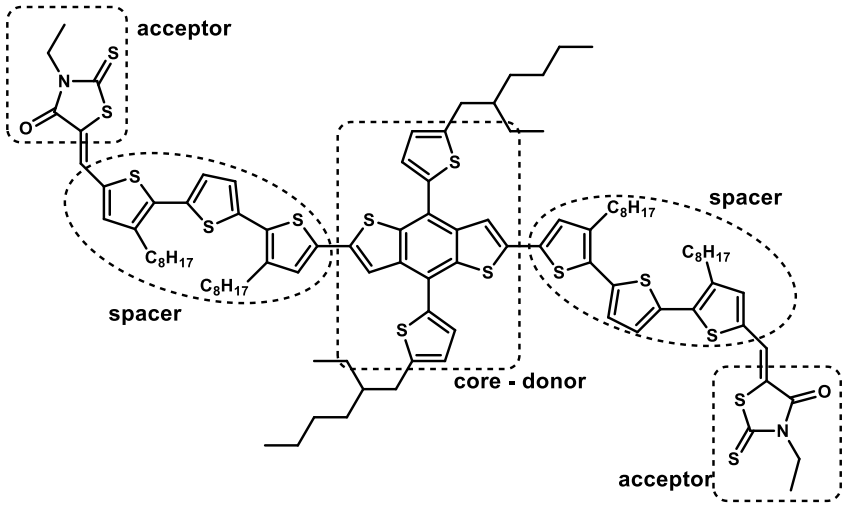

Figure 2.18. Star-shaped benzodithiophene found in a high PCE solar cell.[52]

One challenge inherent to many tellurophene-based materials is a possible reduction in solubility due to well-known Te---Te intermolecular interactions. Tellurophenes based on star-shape structures could present better solubility than their lighter precursors, however, star-shaped structures containing tellurophene cores are not known so far. Most star-shaped compounds are based on core structures such as single[53] and fused-aromatic rings, -heterocycles, and heteroatom-containing triphenylamine (TPA) and silane units (Figure 2.19).

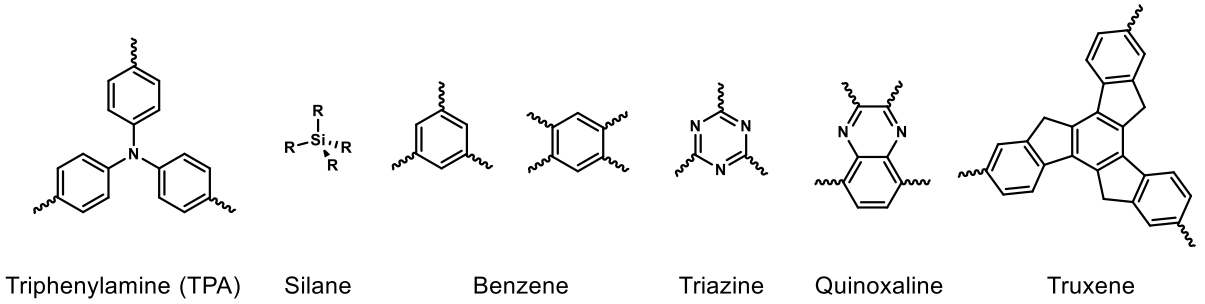

Figure 2.19. Different core units in star-shaped molecules. Examples can be found in the literature for TPA,[51,45,46] silanes,[50,54] benzene,[53] triazine,[55] quinoxaline[56] and truxene[57,58] based materials.

Suzuki-Miyaura cross-coupling reactions were tested under different conditions in order to form the tetrathienyltellurophene (**4T-Te**) (Scheme 2.5). First, the reaction was tested under different solvents (THF, DMF and toluene) (Scheme 2.5 a), then under microwave irradiation in THF at 135 °C for 45 min (Scheme 2.5 b), and finally different (pre)catalysts, $Pd(OAc)_2$ and $Pd(PPh_3)_4$, were tested under microwave conditions (80 °C for 1 h) (Scheme 2.5 c). Unfortunately none of these reactions afforded the desired tetrathienyl substituted tellurophene. At the end of each reaction it was possible to detect (by ^{1}H NMR and $^{13}C\{^{1}H\}$ NMR spectroscopy) unreacted 2-iodothiophene and by-products of protodeboronation reactions (see Chapter 3 for more details).

As stated above, the protodeboronation by-products **2BTe** and **BTe**, derived from the cleavage of BPin groups from **4BTe** (Scheme 2.6) were detected in most coupling attempts; thus it appeared that **4BTe** was very sensitive to base-induced BPin cleavage. Accordingly, the sensitivity of **4BTe** to various bases was then explored in detail and the results form the basis for much of Chapter 3.

Recently an alternate route to **4T-Te** was developed in the Rivard group[59,60] wherein the known dithienylacetylene ((2-thienyl)C≡C(2-thienyl), **TC2T)** was coupled to yield the new zirconacycle, $Cp_2ZrC_4(2\text{-thienyl})_4$; this species then underwent metallacycle transfer with Bipy•$TeCl_2$ to afford **4T-Te** in a 33 % overall yield (Scheme 2.7).

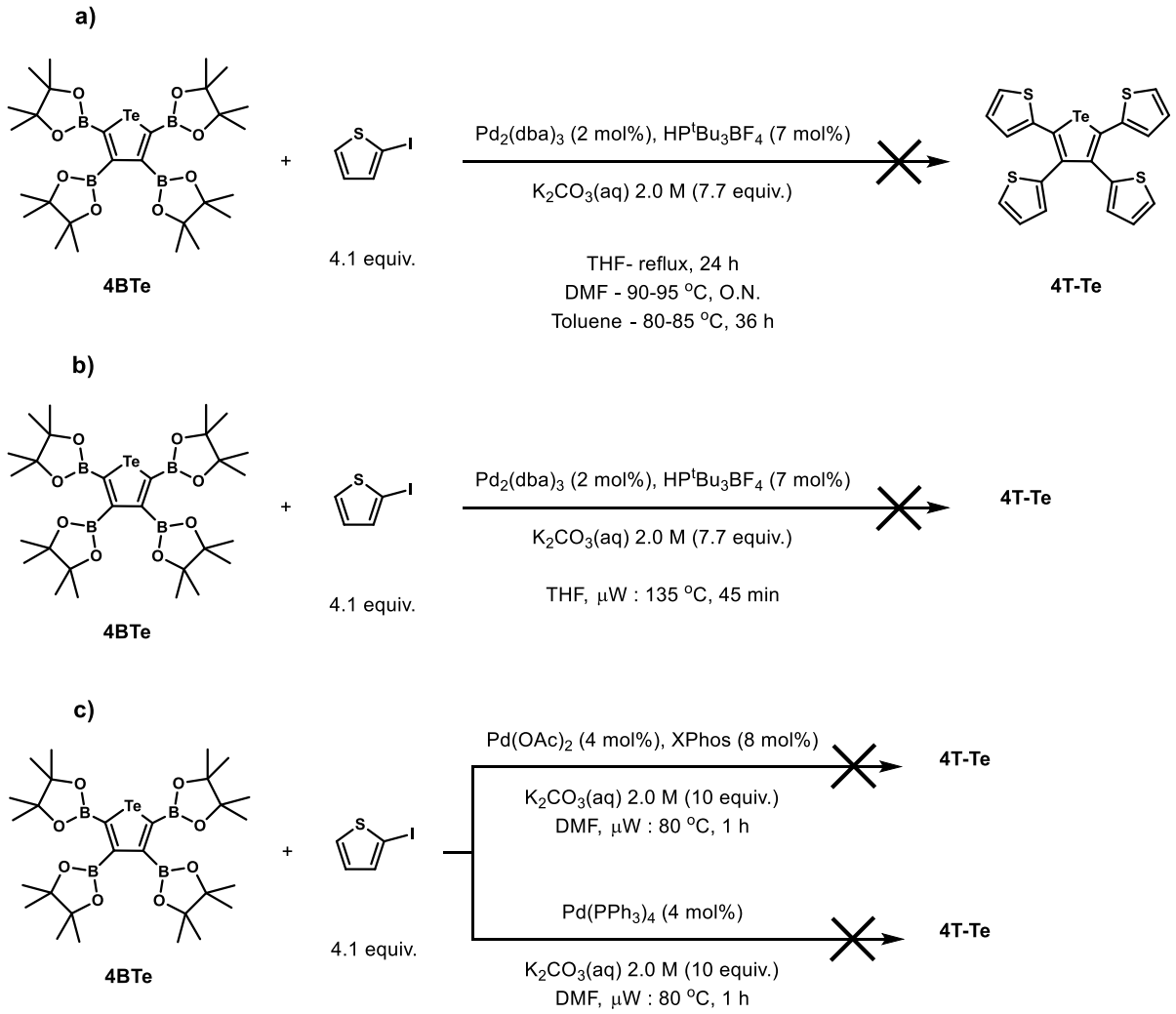

Scheme 2.5. Attempted Suzuki-Miyaura cross-coupling reactions of **4BTe** with 2-iodothiophene.

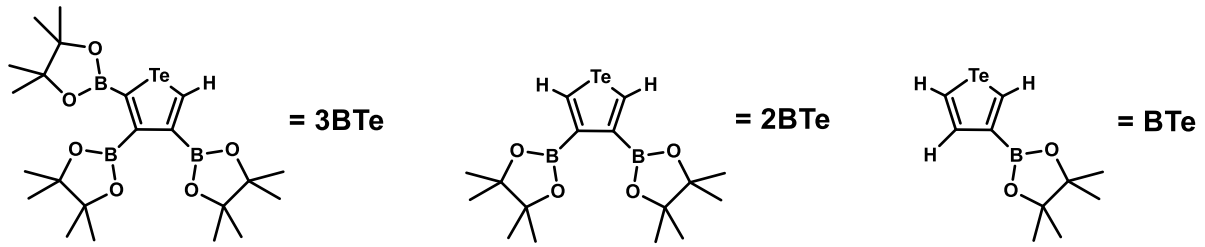

Scheme 2.6. By-products generated from the protodeboronation of **4BTe**.

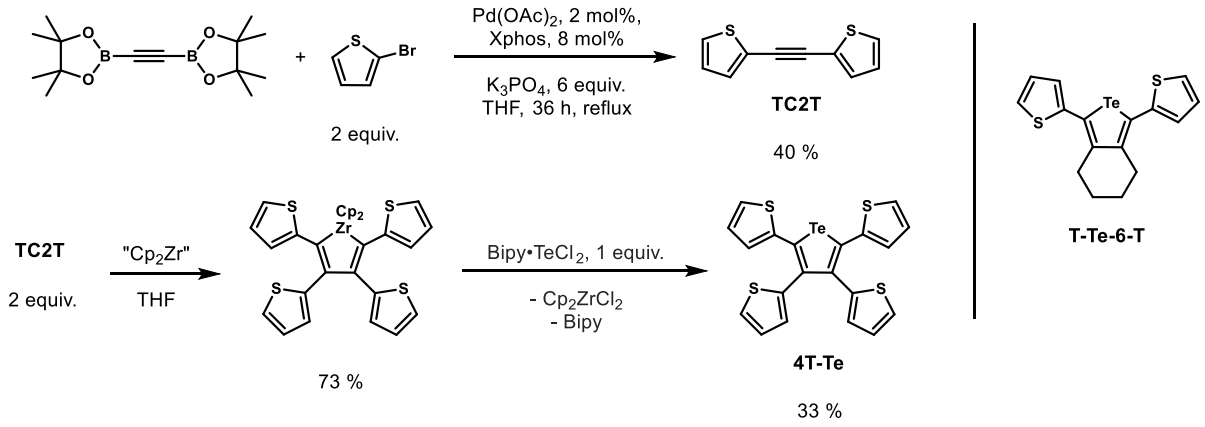

Scheme 2.7. Synthesis of **4T-Te** via dithienyl acetylene. Right side: structure of bithiophene-substituted tellurophene, **T-Te-6-T**.

2.3. CONCLUSIONS

The synthesis and characterization of the tetraborylated chalcogenophenes, **4BS**, **4BSe** and **4BTe** is reported. **4BTe** showed a smaller band gap than its lighter analogues, in addition to good electrochemical stability and aggregation-induced phosphorescence. Luminescence studies of **B-Te-6-B** and **4BTe** in solution under N_2/Ar and air proved the quenching effect of O_2 had on the phosphorescent emission of the respective tellurophenes solutions. Prompt fluorescence studies on **B-Te-6-B** and **4BTe** allowed to detect a fluorescence band with very short lifetimes. Although the functionalization of the tellurophene ring in **4BTe** proved to be challenging through Suzuki-Miyaura cross-coupling, **4BTe** could be useful as a building block to form another generic valuable BPin-capped tellurophenes, such as **2BTe** and **BTe**, through selective cleavage of the B-C single bond around the five-membered ring. **2BTe** and **BTe** might further be used as a precursors to form 3,4- or 3-substituted tellurophenes via Suzuki-Miyaura cross-coupling reactions. Further research in the synthesis of **2BTe** and **BTe** is covered in detailed in Chapter 3.

2.4. EXPERIMENTAL SECTION

2.4.1. General methods

Unless explicitly stated, all reactions were conducted with standard Schlenk and glove box (MBraun) techniques using N_2 as an inert atmosphere, with solvents that were dried using a Grubbs' type purification system manufactured by Innovative Technology Inc. 2,2′-bipyridine (Bipy) was purchased from GFS Chemicals, Cp_2ZrCl_2 was purchased from Strem Chemicals Inc., 2-isopropoxy-4,4,5,5-tetramethyl-1,3,2-dioxa-borolane (^{i}PrOBPin) was purchased from Matrix Scientific, $^{n}Bu_4NPF_6$ was purchased from Fluka-Sigma Aldrich and all other chemicals were obtained from Aldrich, and used as received. Bipy•$TeCl_2$ and Bipy•$SeCl_2$ were synthesized according to literature procedures.[21] ^{1}H and $^{13}C\{^{1}H\}$ and $^{11}B\{^{1}H\}$ NMR spectra were recorded on either a Varian Inova 500 and 400 spectrometer are referenced externally to Me_4Si (^{1}H and $^{13}C\{^{1}H\}$) and F_3B•OEt_2 (^{11}B). Melting points were measured in a MelTemp melting point apparatus and are reported without correction. Elemental analysis were performed by the Analytical and Instrumentation Laboratory at the University of Alberta, UV-visible measurements were performed with a Varian Cary 300 Scan spectrophotometer and fluorescence measurements with a Photon Technology International (PTI) MP1 fluorometer. High-resolution mass spectra were obtained on an Agilent 6220 spectrometer. Electrochemical measurements were performed in a WaveNow Potentiostat / Galvanostat System with a USB interface and AfterMath Instrument control software. The CV measurements were done using a three-electrode arrangement printed on a ceramic substrate: Pt as a working and counter electrode and a Ag pseudo-reference electrode in a 0.1 M THF solution of $^{n}Bu_4NPF_6$ as the supporting electrolyte using scan rate of 100 mV/s under Ar atmosphere in a glove box. Concentration of each chalcogenophene used in the experiment was between 3.7 and 3.2 mM. The potential at the Pt-working electrode of each sample was measured against Ag pseudo-reference electrode and corrected using the formal reduction potential (0.64 V) of the ferrocene / ferrocenium (Fc / Fc^{+}) couple measured at the same experimental conditions than those of the samples.

2.4.1.1. Modified synthesis of B2C2:

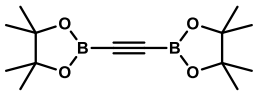

To a solution of ^{n}BuLi (50 mL, 2.5 M solution in hexanes, 125.0 mmol) in 140 mL of a 1:1 THF/Et_2O mixture at -78 °C was added 3.7 mL of trichloroethylene (42 mmol) dropwise. After stirring at room temperature overnight, the resulting solution (containing 1,2-dilithioacetylide) was cooled again to -78 °C and added via cannula to another solution of ^{i}PrOBPin (17.2 mL, 81.7 mmol) in 100 mL of Et_2O at -78 °C. The mixture was stirred at -78 °C for 4 h and at room temperature overnight. To the reaction mixture was added 42 mL of an HCl solution in dioxane (4.0 M, 167 mmol) at -78 °C and followed by stirring at room temperature for 5 h. The solids were removed by suction filtration under air and the solvent was removed from the filtrate. In order to remove any residual dioxane from the product, the remaining solid was washed with *ca.* 100 mL of cold pentane (~ 4 °C) two times and the washes collected; since the product is slightly soluble in pentane, more product can be recovered from the collected washes by removing the solvent and washing again the remaining solids with *ca*. 20 mL portions of cold pentane (~ 4 °C) two times. The collected product was dried under vacuum to afford a white powder of **B2C2** (10.139 g, 89 % yield). ^{1}H NMR (500 MHz, $CDCl_3$): δ 1.25 (s, 24H, C*H*$_3$). ^{13}C{^{1}H} NMR (500 MHz, $CDCl_3$): δ 84.7 (B*C*C*B*), 24.7 (*C*H$_3$). ^{11}B{^{1}H} NMR (400 MHz, $CDCl_3$): δ 23.2.[22]

2.4.1.2. Synthesis of $Cp_2ZrC_4BPin_4$:

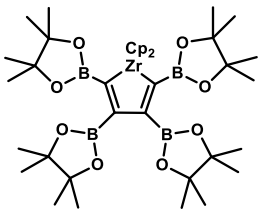

To a solution of Cp_2ZrCl_2 (2.923 g, 10.00 mmol) in 73 mL of THF at -78 °C was added dropwise a solution of ^{n}BuLi 2.5 M in hexanes (8.0 mL, 20 mmol). The mixture stirred for 1.5 h and then a cold solution of **B2C2** (5.559 g, 20.00 mmol) in THF (100 mL) (at about

4 °C) was added to the first solution via cannula transfer. The mixture was stirred overnight at room temperature. The solvent was then removed by vacuum and to the remaining solid was added 200 mL of dried Et_2O. The resulting precipitate (LiCl) was allowed to settle and the supernatant was decanted via cannula to another Schlenk flask under N_2 and the solvent evaporated. Extraction of the remaining (LiCl) precipitate with Et_2O was repeated twice (with 200 mL of Et_2O in each case). The solvent was removed from the collected Et_2O solutions to give $Cp_2ZrC_4BPin_4$ as a dark red solid (6.109 g, 78 % yield). ^1H NMR (500 MHz, C_6D_6): δ 6.17 (s, 10H, C_5H_5), 1.26 (s, 24H, CH_3), 1.25 (s, 24H, CH_3). $^{13}C\{^1H\}$ NMR (500 MHz, C_6D_6): δ 111.3 (C_5H_5), 83.1 and 82.0 (O-*C*), 25.3 and 25.0 (CH_3). $^{11}B\{^1H\}$ NMR (400 MHz, $CDCl_3$): δ 24.6 ppm. Anal. Calcd. for $C_{38}H_{58}B_4O_8Zr$: C, 58.71; H, 7.52; Found: C, 58.10; H, 7.50. Mp (°C): 165-167.

2.4.1.3. Synthesis of 2,3,4,5-tetrakis(pinacolato)thiophene (4BS):

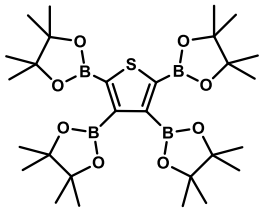

To a solution of $Cp_2ZrC_4BPin_4$ (3.059 g, 3.94 mmol) in THF (60 mL) under N_2 was added 0.4 mL of S_2Cl_2 (4.3 mmol) dropwise. After stirring at room temperature for 24 h, 4.6 mL of $P(OMe)_3$ (39 mmol) was added dropwise and the reaction mixture was stirred for another 10 min. The solvent was removed under vacuum and the resulting product was purified by column chromatography using silica gel and a 3:1 THF/hexane mixture as an eluent (2.060 g, 89 %). Colorless crystalline **4BS** could be obtained by cooling a toluene solution layered with hexanes to 4 °C (0.723 g, 31 %). ^1H NMR (400 MHz, $CDCl_3$): δ 1.37 (s, 24H, CH_3), 1.31 (s, 24H, CH_3). $^{13}C\{^1H\}$ NMR (400 MHz, $CDCl_3$): δ 84.1 and 83.8 (*C*-O), 25.1 and 24.9 (CH_3). $^{11}B\{^1H\}$ NMR (400 MHz, $CDCl_3$): δ 30.0. Anal. Calcd. for $C_{28}H_{48}B_4O_8S$: C, 57.20; H, 8.23; Found: C, 57.04; H, 8.23.

2.4.1.4. Modified preparation of Bipy•$SeCl_2$:

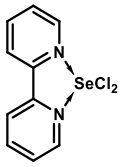

A mixture of 1.425 g of Se powder (17.95 mmol) and 1.5 mL of SO_2Cl_2 (18 mmol) under N_2 was stirred for 10 min before adding 46 mL of THF followed by stirring for 2.5 h. To this mixture was added a solution of Bipy (2.804 g, 17.95 mmol) in 70 mL of THF dropwise. After stirring for 1 h, the precipitate was allowed to settle and the supernatant decanted. The remaining solid was washed with 2 × 200 mL of Et_2O and then dried under vacuum to afford a pale yellow powder of Bipy•$SeCl_2$ (4.881 g, 88 % yield).

2.4.1.5. Synthesis of 2,3,4,5-tetrakis(pinacolato)selenophene (4BSe):

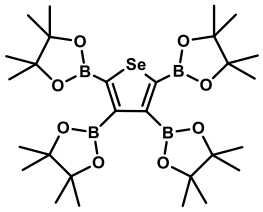

To a solution of $Cp_2ZrC_4BPin_4$ (4.897 g, 6.30 mmol) in THF (120 mL) was added Bipy•$SeCl_2$ (2.121 g, 6.93 mmol). The mixture was stirred overnight at room temperature. The solvent was then removed under reduced pressure and the product purified using column chromatography (silica gel) with a mixture of THF/hexanes (3:1) as an eluent; this afforded **4BSe** as a pale brown solid (2.674 g, 66 % yield). ^{1}H NMR (500 MHz, $CDCl_3$): δ 1.37 (s, 24H, C*H*$_3$), 1.31 (s, 24H, C*H*$_3$). ^{13}C{^{1}H} NMR (500 MHz, $CDCl_3$): δ 84.1 (*C*-O), 83.9 (*C*-O), 25.2 (*C*H$_3$), 24.9 (*C*H$_3$). ^{11}B{^{1}H} NMR (400 MHz, $CDCl_3$): δ 30.7. Anal. Calcd. for $C_{28}H_{48}B_4O_8Se$: C, 52.97; H, 7.62; Found: C, 52.87; H, 7.64.

2.4.1.6. Synthesis of 2,3,4,5-tetrakis(pinacolato)tellurophene (4BTe):

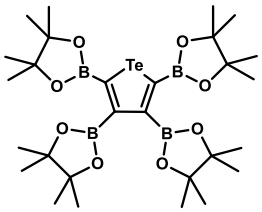

To a slurry of Cp_2ZrCl_2 (1.991 g, 6.81 mmol) in 50 mL of THF was added ^{n}BuLi (5.4 mL, 2.5 M solution in hexanes, 14 mmol) at -78 °C. After stirring for 1 h, a cold solution of **B2C2** (3.692 g, 13.28 mmol) in 70 mL of THF (at 0 °C) was added via cannula. The cold bath was removed and after stirring for 1 h, the mixture was warmed to room temperature with assistance from a warm water bath at *ca.* 35 °C; at this point the color of the mixture went from pale yellow to dark red. The reaction mixture was stirred for another 1 h at room temperature and Bipy•$TeCl_2$ (2.537, 7.15 mmol) was then added in one portion under a strong counter-flow of nitrogen, followed by additional stirring for 2 h. The volatiles were removed under vacuum and the product was purified by column chromatography (silica gel) with hexanes/THF (1:3) as an eluent to yield **4BTe** as a light brown solid (2.577 g, 56 % yield). ^{1}H NMR (500 MHz, $CDCl_3$): δ 1.36 (s, 24H, TeCBOC(CH_3)$_2$), 1.30 (s, 24H, TeCCBOC(CH_3)$_2$). ^{13}C{^{1}H} NMR (500 MHz, $CDCl_3$): δ 84.1 (*C*-O), 83.9 (*C*-O), 25.20 (*C*H_3), 24.88 (*C*H_3). ^{11}B{^{1}H} NMR (400 MHz, $CDCl_3$): δ 31.8. Anal. Calcd. for $C_{28}H_{48}B_4O_8Te$: C, 49.20; H, 7.08; Found: C, 49.29; H, 7.05.

2.4.2. X-ray details

Table 2.4. X-Ray crystallographic data for **4BSe**.

A. Crystal Data	
formula	$C_{28}H_{48}B_4O_8Se$
formula weight	634.86
crystal dimensions (mm)	0.40 × 0.31 × 0.30
crystal system	monoclinic
space group	$P2_1$ (No. 4)
unit cell parameters[a]	
a (Å)	10.4690 (11)
b (Å)	13.8325 (14)
c (Å)	11.9952 (12)
β (deg)	100.7232 (11)
V (Å^3)	1706.7 (3)
Z	2
ρ_{calcd} (g cm^{-3})	1.235
μ (mm^{-1})	1.142
B. Data Collection and Refinement Conditions	
diffractometer	Bruker D8/APEX II CCD[b]
radiation (λ [Å])	graphite-monochromated Mo Kα (0.71073)
temperature (°C)	–100
scan type	ω scans (0.4°) (10 s exposures)
data collection 2θ limit (deg)	55.16
total data collected	39904 ($-13 \le h \le 13$, $-17 \le k \le 17$, $-15 \le l \le 15$)
independent reflections	7793 (R_{int} = 0.0306)
number of observed reflections (*NO*)	7534 [$F_o^2 \ge 2\sigma(F_o^2)$]
structure solution method	Patterson/structure expansion (*DIRDIF–2008*[c])
refinement method	full-matrix least-squares on F^2 (*SHELXL–2013*[d])

absorption correction method	multi-scan (*TWINABS*)
range of transmission factors	0.7923–0.7156
data/restraints/parameters	7793 / 0 / 371
Flack absolute structure parameter[e]	0.035(3)
goodness-of-fit (S)[f] [all data]	1.030
final R indices[g]	
R_1 [$F_o^2 \geq 2\sigma(F_o^2)$]	0.0264
wR_2 [all data]	0.0668
largest difference peak and hole	0.490 and –0.791 e Å^{-3}

[a]Obtained from least-squares refinement of 9957 reflections with $4.54° < 2\theta < 55.08°$.

[b]Programs for diffractometer operation, data collection, data reduction and absorption correction were those supplied by Bruker. The crystal used for data collection was found to display non-merohedral twinning. Both components of the twin were indexed with the program *CELL_NOW* (Bruker AXS Inc., Madison, WI, 2004). The second twin component can be related to the first component by 180º rotation about the [0.2 0 1] axis in real space and about the [0 0 1] axis in reciprocal space. Integrated intensities for the reflections from the two components were written into a *SHELXL-2013* HKLF 5 reflection file with the data integration program *SAINT* (version 8.32B), using all reflection data (exactly overlapped, partially overlapped and non-overlapped). The refined value of the twin fraction (*SHELXL-2013* BASF parameter) was 0.0930(6).

[c]Beurskens, P. T.; Beurskens, G.; de Gelder, R.; Smits, J. M. M.; Garcia-Granda, S.; Gould, R. O. (2008). The *DIRDIF-2008* program system. Crystallography Laboratory, Radboud University Nijmegen, The Netherlands.

[d]Sheldrick, G. M. *Acta Crystallogr.* **2008**, *A64*, 112–122.

[e]Flack, H. D. *Acta Crystallogr.* **1983**, *A39*, 876–881; Flack, H. D.; Bernardinelli, G. *Acta Crystallogr.* **1999**, *A55*, 908–915; Flack, H. D.; Bernardinelli, G. *J. Appl. Cryst.* **2000**, *33*, 1143–1148. The Flack parameter will refine to a value near zero if the structure is in

the correct configuration and will refine to a value near one for the inverted configuration.

[f] $S = [\Sigma w(F_o^2 - F_c^2)^2/(n-p)]^{1/2}$ (n = number of data; p = number of parameters varied; $w = [\sigma^2(F_o^2) + (0.0391P)^2 + 0.0327P]^{-1}$ where $P = [\mathrm{Max}(F_o^2, 0) + 2F_c^2]/3$).

[g] $R_1 = \Sigma||F_o| - |F_c||/\Sigma|F_o|$; $wR_2 = [\Sigma w(F_o^2 - F_c^2)^2/\Sigma w(F_o^4)]^{1/2}$.

Table 2.5. X-Ray crystallographic data for **4BTe**.

A. Crystal Data	
formula	$C_{28}H_{48}B_4O_8Te$
formula weight	683.50
crystal dimensions (mm)	0.52 × 0.47 × 0.39
crystal system	monoclinic
space group	$P2_1$ (No. 4)
unit cell parameters[a]	
a (Å)	10.4971 (3)
b (Å)	14.0156 (4)
c (Å)	12.0439 (4)
β (deg)	100.4861 (6)
V (Å^3)	1742.34 (9)
Z	2
ρ_{calcd} (g cm^{-3})	1.303
μ (mm^{-1})	7.076
B. Data Collection and Refinement Conditions	
diffractometer	Bruker D8/APEX II CCD[b]
radiation (λ [Å])	Cu Kα (1.54178) (microfocus source)
temperature (°C)	–100
scan type	ω and ϕ scans (1.0°) (5 s exposures)
data collection 2θ limit (deg)	142.56

total data collected	11397 ($-12 \le h \le 11$, $-17 \le k \le 17$, $-14 \le l \le 14$)
independent reflections	6399 ($R_{int} = 0.0397$)
number of observed reflections (*NO*)	6390 [$F_o^2 \ge 2\sigma(F_o^2)$]
structure solution method	Patterson/structure expansion (*DIRDIF–2008*[c])
refinement method	full-matrix least-squares on F^2 (*SHELXL–97*[d])
absorption correction method	Gaussian integration (face-indexed)
range of transmission factors	0.1670–0.1203
data/restraints/parameters	6399 / 0 / 372
extinction coefficient (x)[e]	0.0073(4)
Flack absolute structure parameter[f]	0.373(5)
goodness-of-fit (S)[g] [all data]	1.064
final R indices[h]	
R_1 [$F_o^2 \ge 2\sigma(F_o^2)$]	0.0342
wR_2 [all data]	0.0857
largest difference peak and hole	1.401 and –1.697 e Å^{-3}

[a]Obtained from least-squares refinement of 9709 reflections with $9.78° < 2\theta < 142.52°$.

[b]Programs for diffractometer operation, data collection, data reduction and absorption correction were those supplied by Bruker.

[c]Beurskens, P. T.; Beurskens, G.; de Gelder, R.; Smits, J. M. M.; Garcia-Granda, S.; Gould, R. O. (2008). The *DIRDIF-2008* program system. Crystallography Laboratory, Radboud University Nijmegen, The Netherlands.

[d]Sheldrick, G. M. *Acta Crystallogr.* **2008**, *A64*, 112–122.

[e]$F_c^* = kF_c[1 + x\{0.001F_c^2\lambda^3/\sin(2\theta)\}]^{-1/4}$ where k is the overall scale factor.

[f]Flack, H. D. *Acta Crystallogr.* **1983**, *A39*, 876–881; Flack, H. D.; Bernardinelli, G. *Acta Crystallogr.* **1999**, *A55*, 908–915; Flack, H. D.; Bernardinelli, G. *J. Appl. Cryst.* **2000**, *33*, 1143–1148. The Flack parameter will refine to a value near zero if the structure is in

the correct configuration and will refine to a value near one for the inverted configuration. The value observed herein is indicative of a degree of racemic twinning, and was accomodated during the refinement using the *SHELXL-97* TWIN instruction (see reference *d*).

[g] $S = [\Sigma w(F_o^2 - F_c^2)^2/(n - p)]^{1/2}$ (n = number of data; p = number of parameters varied; $w = [\sigma^2(F_o^2) + (0.0598P)^2 + 0.3421P]^{-1}$ where $P = [\mathrm{Max}(F_o^2, 0) + 2F_c^2]/3$).

[h] $R_1 = \Sigma||F_o| - |F_c||/\Sigma|F_o|$; $wR_2 = [\Sigma w(F_o^2 - F_c^2)^2/\Sigma w(F_o^4)]^{1/2}$.

2.5. ADDITIONAL DATA

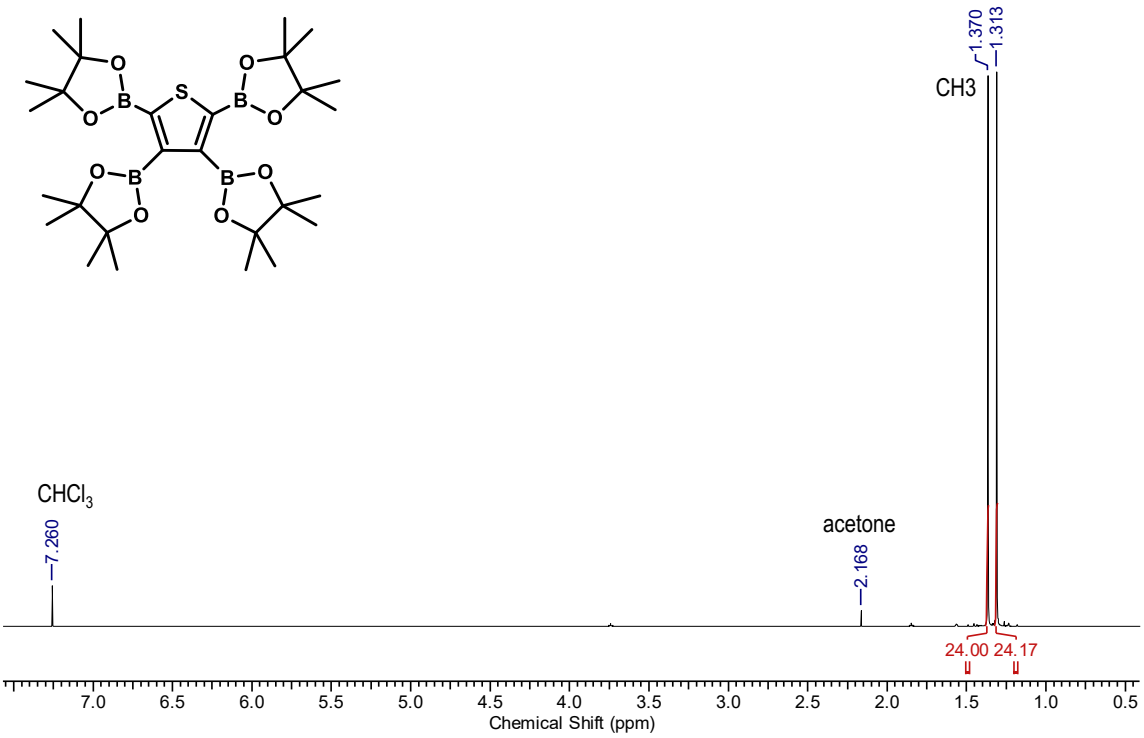

Figure 2.20. A) ^{1}H NMR spectrum of **4BS** in $CDCl_3$.

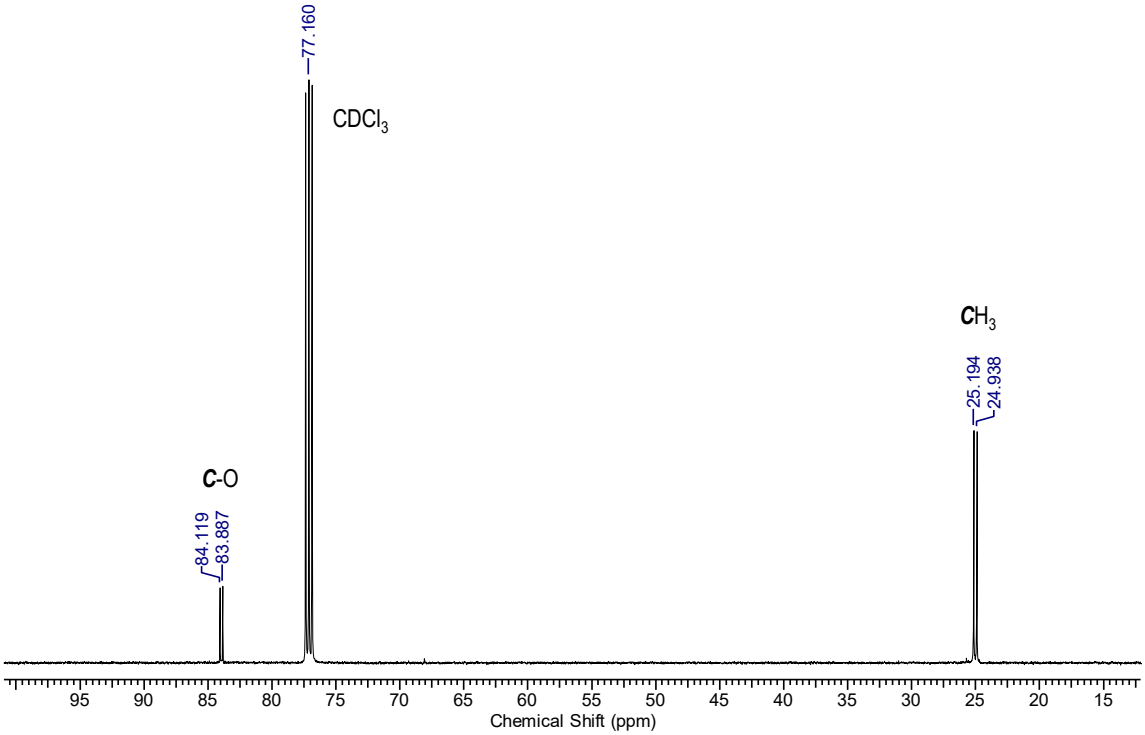

Figure 2.20. B) $^{13}C\{^{1}H\}$ NMR spectrum of **4BS** in $CDCl_3$.

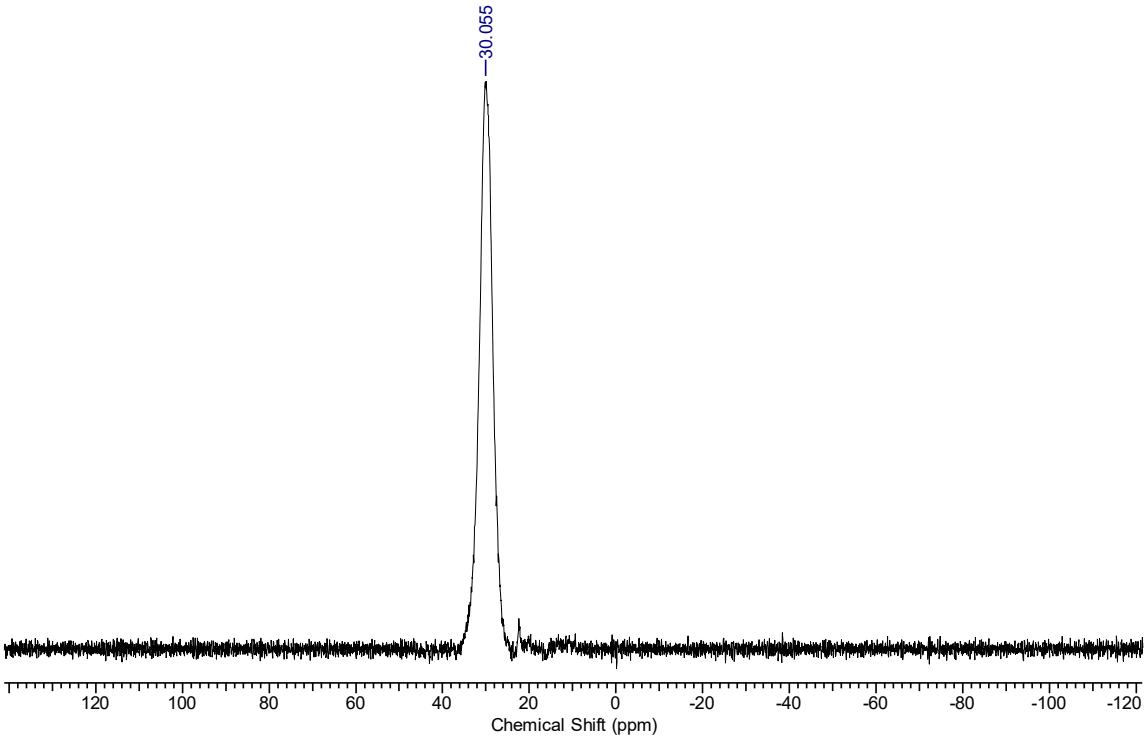

Figure 2.20. C) $^{11}B\{^{1}H\}$ NMR spectrum of **4BS** in $CDCl_3$.

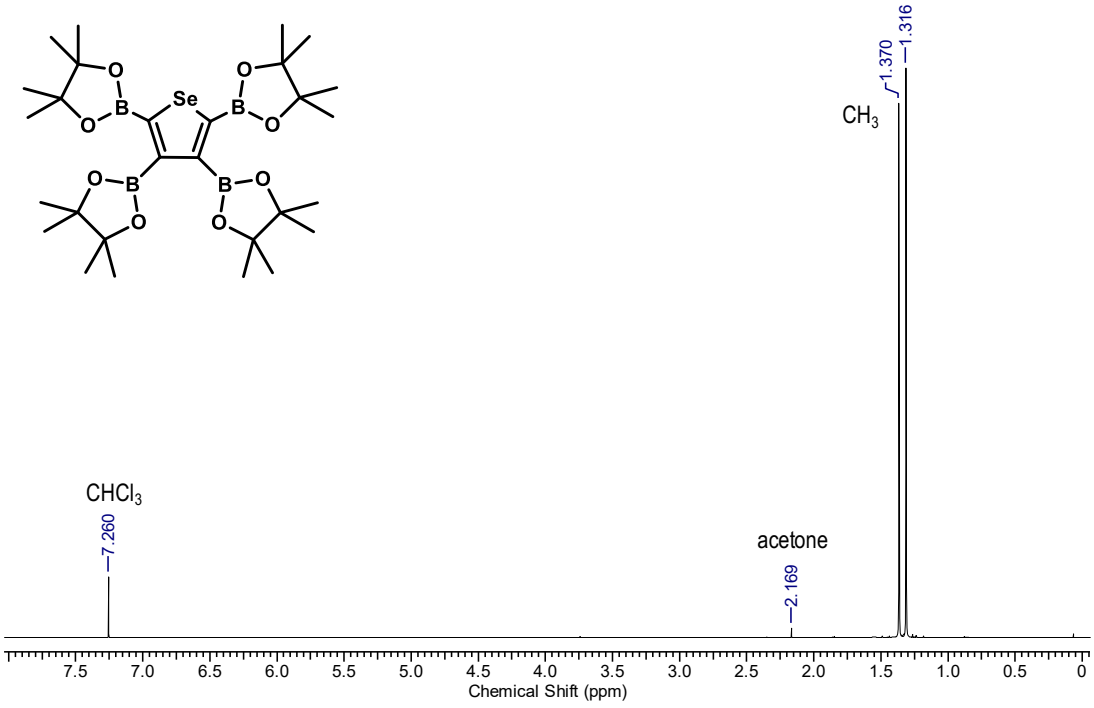

Figure 2.21. A) ^{1}H NMR spectrum of **4BSe** in $CDCl_3$.

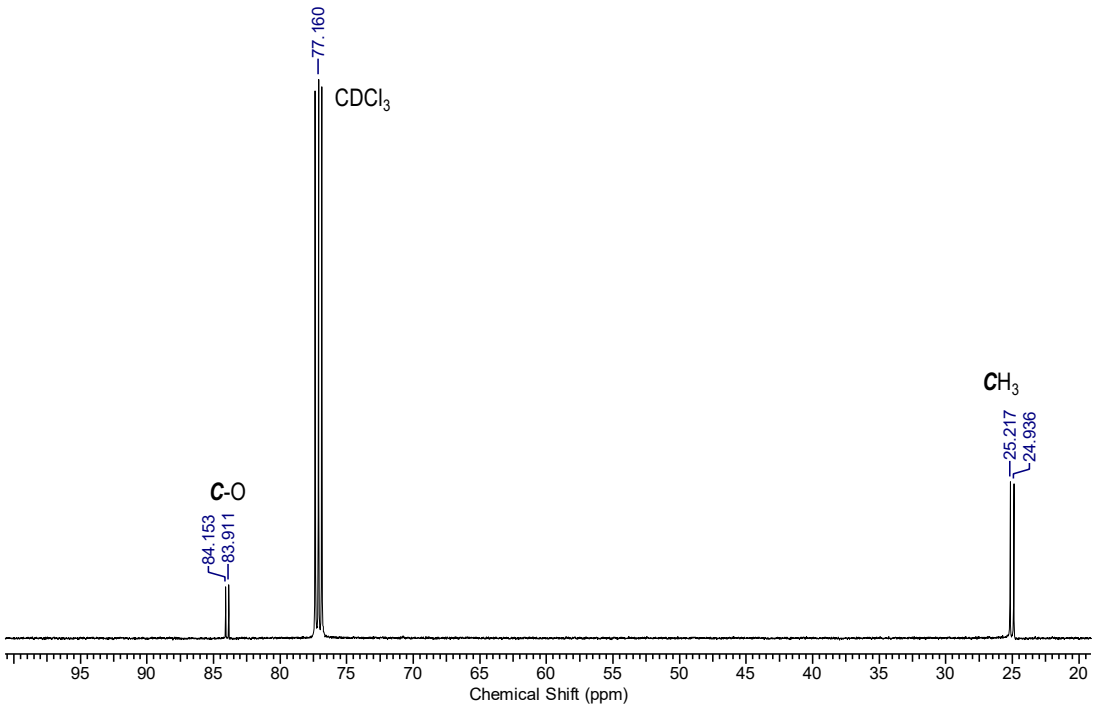

Figure 2.21. B) $^{13}C\{^{1}H\}$ NMR spectrum of **4BSe** in $CDCl_3$.

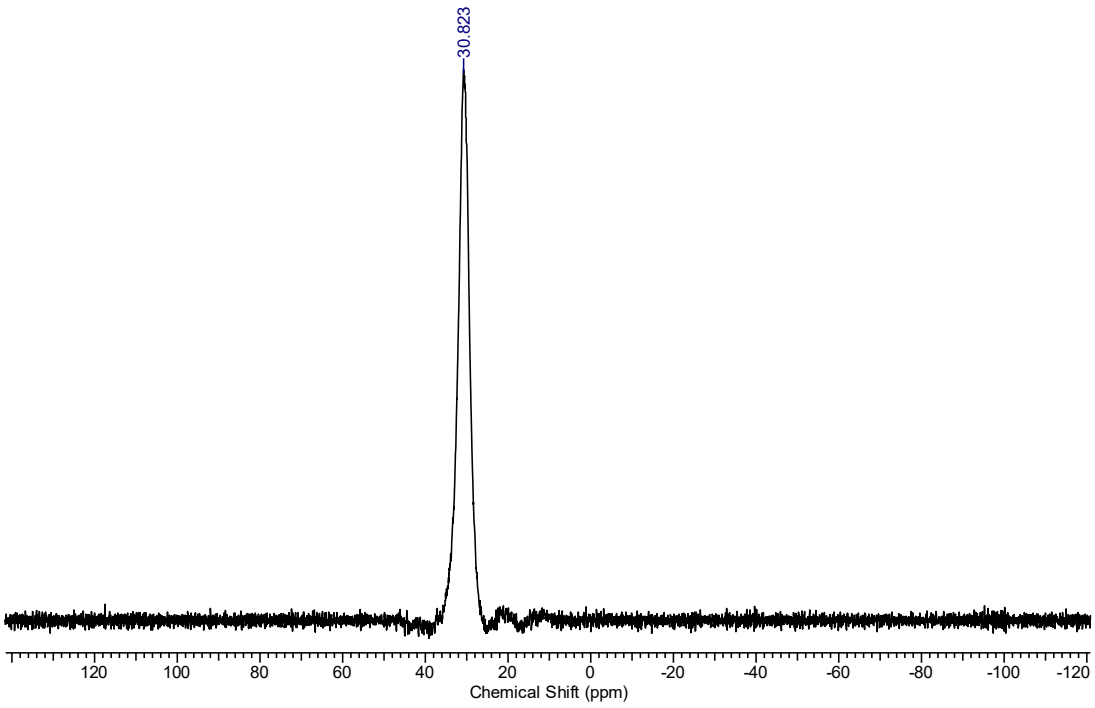

Figure 2.21. C) $^{11}B\{^{1}H\}$ NMR spectrum of **4BSe** in $CDCl_3$.

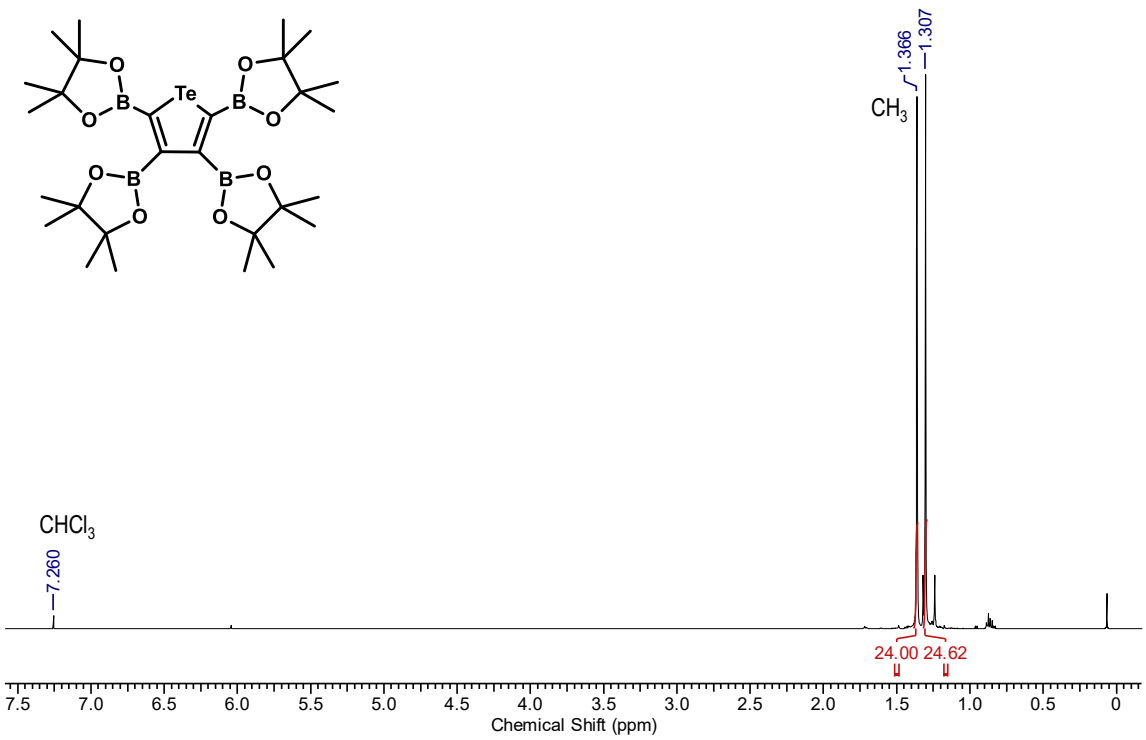

Figure 2.22. A) ^{1}H NMR spectrum of **4BTe** in $CDCl_3$.

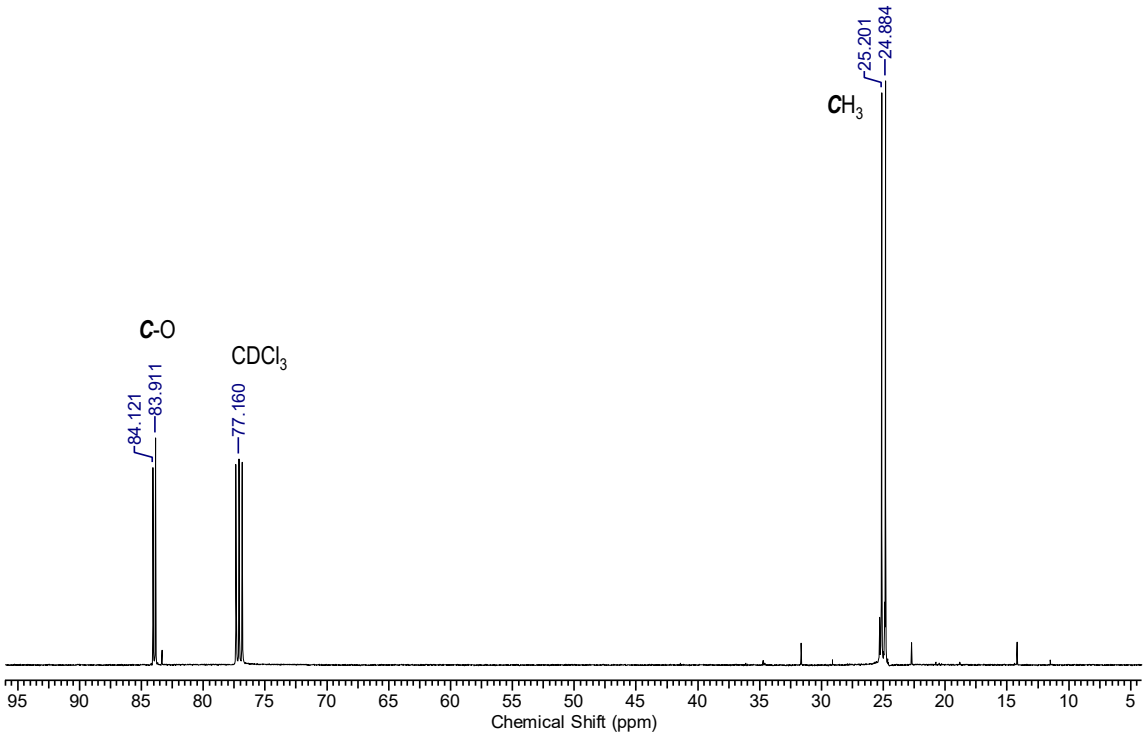

Figure 2.22. B) $^{13}C\{^{1}H\}$ NMR spectrum of **4BTe** in $CDCl_3$.

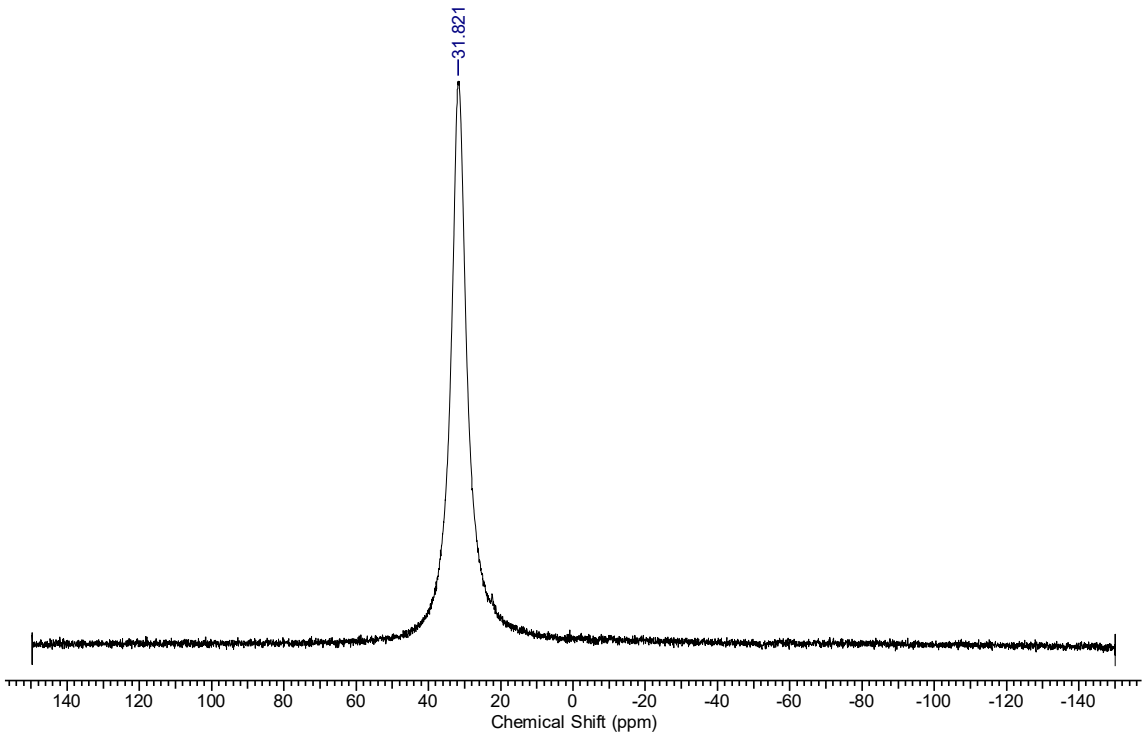

Figure 2.22. C) $^{11}B\{^{1}H\}$ NMR spectrum of **4BTe** in $CDCl_3$.

2.6. REFERENCES

1. Duhović, S.; Dincă, M. *Chem. Mater.* **2015**, *27*, 5487–5490.
2. Planells, M.; Schroeder, B. C.; McCulloch, I. *Macromolecules* **2014**, *47*, 5889–5894.
3. Park, Y. S.; Kale, T. S.; Nam, C.-Y.; Choi, D.; Grubbs, R. B. *Chem. Commun.* **2014**, *50*, 7964–7967.
4. Al-Hashimi, M.; Han, Y.; Smith, J.; Bazzi, H. S.; Alqaradawi, S. Y. A.; Watkins, S. E.; Anthopoulos, T. D.; Heeney, M. *Chem. Sci.* **2016**, *7*, 1093–1099.
5. Parke, S. M.; Boone, M. P.; Rivard, E. *Chem. Commun.* **2016**, *52*, 9485–9505.
6. Yamamoto, T.; Takimiya, K. *J. Am. Chem. Soc.* **2007**, *129*, 2224–2225.
7. Shinamura, S.; Osaka, I.; Miyazaki, E.; Takimiya, K. *Heterocycles* **2011**, *83*, 1187–1204.
8. Kremer, A.; Aurisicchio, C.; Deleo, F.; Ventura, B.; Wouters, J.; Armaroli, N.; Barbieri, A.; Bonifazi, D. *Chem. Eur. J.* **2015**, *21*, 15377–15387.
9. Manjare, S. T.; Kim, Y.; Churchill, D. G. *Acc. Chem. Res.* **2014**, *47*, 2985–2998.
10. Kaur, M.; Yang, D. S.; Choi, K.; Cho, M. J.; Choi, D. H. *Dye. Pigment.* **2014**, *100*, 118–126.
11. Kryman, M. W.; Schamerhorn, G. A.; Hill, J. E.; Calitree, B. D.; Davies, K. S.; Linder, M. K.; Ohulchanskyy, T. Y.; Detty, M. R. *Organometallics* **2014**, *33*, 2628–2640.
12. Godoi, B.; Schumacher, R. F.; Zeni, G. *Chem. Rev.* **2011**, *111*, 2937–2980.
13. Rhoden, C. R. B.; Zeni, G. *Org. Biomol. Chem.* **2011**, *9*, 1301–1313.
14. Primas, N.; Bouillon, A.; Rault, S. *Tetrahedron* **2010**, *66*, 8121–8136.
15. Borowska, E.; Durka, K.; Luliński, S.; Serwatowski, J.; Woźniak, K. *Eur. J. Org. Chem.* **2012**, 2208–2218.
16. He, G.; Kang, L.; Torres Delgado, W.; Shynkaruk, O.; Ferguson, M. J.; McDonald, R.; Rivard, E. *J. Am. Chem. Soc.* **2013**, *135*, 5360–5363.
17. He, G.; Torres Delgado, W.; Schatz, D. J.; Merten, C.; Mohammadpour, A.; Mayr, L.; Ferguson, M. J.; McDonald, R.; Brown, A.; Shankar, K.; Rivard, E. *Angew. Chem. Int. Ed.* **2014**, *53*, 4587–4591.

18. Erker, G.; Zwettler, R.; Krueger, C.; Hyla-Kryspin, I.; Gleiter, R. *Organometallics* **1990**, *9*, 524–530.
19. Negishi, E.-I.; Cederbaum, F. E.; Takahashi, T. *Tetrahedron Lett.* **1986**, *27*, 2829–2832.
20. Geng, W.; Wang, C.; Guang, J.; Hao, W.; Zhang, W. X.; Xi, Z. *Chem. Eur. J.* **2013**, *19*, 8657–8664.
21. Dutton, J. L.; Farrar, G. J.; Sgro, M. J.; Battista, T. L.; Ragogna, P. J. *Chem. Eur. J.* **2009**, *15*, 10263–10271.
22. Kang, Y. K.; Deria, P.; Carroll, P. J.; Therien, M. J. *Org. Lett.* **2008**, *10*, 1341–1344.
23. Takimiya, K.; Konda, Y.; Ebata, H.; Niihara, N.; Otsubo, T. *J. Org. Chem.* **2005**, *70*, 10569–10571.
24. Li, P.-F.; Carrera, E. I.; Seferos, D. S. *Chem Plus Chem* **2016**, *81*, 917–921.
25. Peral, F.; Gallego, E. *Spectrochim. Acta - Part A Mol. Biomol. Spectrosc.* **2000**, *56*, 2149–2155.
26. Tinoco, J. I. *J. Am. Chem. Soc.* **1960**, *82*, 4785–4790.
27. Misra, A.; Kumar, P.; Srivastava, R.; Dhawan, S. K.; Kamalasanan, M. N.; Chandra, S. *Indian J. Pure Appl. Phys.* **2005**, *43*, 921–925.
28. Je, M.; Kobilka, B. M.; Hale, B. J. *Macromolecules* **2014**, *47*, 7253–7271.
29. Planells, M.; Schroeder, B. C.; McCulloch, I. *Macromolecules* **2014**, *47*, 5889–5894.
30. Chai, J.; Wang, J.; Xu, Q.; Hao, F.; Liu, R. *Mol. Biosyst.* **2012**, *8*, 1902–1907.
31. He, G.; Wiltshire, B. D.; Choi, P.; Savin, A.; Sun, S.; Mohammadpour, A.; Ferguson, M. J.; McDonald, R.; Farsinezhad, S.; Brown, A.; Shankar, K.; Rivard, E. *Chem. Commun.* **2015**, *51*, 5444–5447.
32. Yersin, H.; Rausch, A. F.; Czerwieniec, R.; Hofbeck, T.; Fischer, T. *Coord. Chem. Rev.* **2011**, *255*, 2622–2652.
33. Ji, S.; Wu, W.; Wu, Y.; Zhao, T.; Zhou, F.; Yang, Y.; Zhang, X.; Liang, X.; Wu, W.; Chi, L.; Wang, Z.; Zhao, J. *Analyst* **2009**, *134*, 958–965.
34. Papkovsky, D. B.; Ponomarev, G. V; Trettnak, W.; Oleary, P. *Anal. Chem.* **1995**, *67*, 4112–4117.
35. Hong, Y.; Lam, J. W. Y.; Tang, B. Z. *Chem. Soc. Rev.* **2011**, *40*, 5361–5388.

36. Mei, J.; Hong, Y.; Lam, J. W. Y.; Qin, A.; Tang, Y.; Tang, B. Z. *Adv. Mater.* **2014**, *26*, 5429–5479.
37. Kwok, R. T. K.; Leung, C. W. T.; Lam, J. W. Y.; Tang, B. Z. *Chem. Soc. Rev.* **2015**, *44*, 4228–4238.
38. Dong, Y.; Lam, J. W. Y.; Qin, A.; Liu, J.; Li, Z.; Tang, B. Z.; Sun, J.; Kwok, H. S. *Appl. Phys. Lett.* **2007**, *91*, 1–4.
39. Samanta, S.; Goswami, S.; Hoque, M. N.; Ramesh, A.; Das, G. *Chem. Commun.* **2014**, *50*, 11833–11836.
40. Liu, X.; Liang, G. *Chem. Commun.* **2017**, *53*, 1037–1040.
41. Zhao, Z.; Su, H.; Zhang, P.; Cai, Y.; Kwok, R. T. K.; Chen, Y.; He, Z.; Gu, X.; He, X.; Sung, H. H.-Y.; Williams, I. D.; Lam, J. W. Y.; Zhang, Z.; Tang, B. Z. *J. Mater. Chem. B.* **2017**, *5*, 1650–1657.
42. Hong, Y.; Lam, J. W. Y.; Tang, B. Z. *Chem. Commun.* **2009**, 4332–4353.
43. Connelly, N. G.; Geiger, W. E. *Chem. Rev.* **1996**, *96*, 877–910.
44. Romero, N. A.; Nicewicz, D. A. *Chem. Rev.* **2016**, *116*, 10075–10166.
45. Roquet, S.; Cravino, A.; Leriche, P.; Aléveque, O.; Frère, P.; Roncali, J. *J. Am. Chem. Soc.* **2006**, *128*, 3459–3466.
46. Li, W.; Li, Q.; Duan, C.; Liu, S.; Ying, L.; Huang, F.; Cao, Y. *Dye. Pigment.* **2015**, *113*, 1–7.
47. Murphy, A. R.; Fréchet, J. M. J. *Chem. Rev.* **2007**, *107*, 1066–1096.
48. Pron, A.; Gawrys, P.; Zagorska, M.; Djurado, D.; Demadrille, R. *Chem. Soc. Rev.* **2010**, *39*, 2577–2632.
49. Ponomarenko, S. A.; Luponosov, Y. N.; Min, J.; Solodukhin, A. N.; Surin, N. M.; Shcherbina, M. A.; Chvalun, S. N.; Ameri, T.; Brabec, C. *Faraday Discuss.* **2014**, *174*, 313–339.
50. Ponomarenko, S. A.; Tatarinova, E. A.; Muzafarov, A. M.; Kirchmeyer, S.; Brassat, L.; Mourran, A.; Moeller, M.; Setayesh, S.; De Leeuw, D. *Chem. Mater.* **2006**, *18*, 4101–4108.
51. Dang, D.; Zhou, P.; Zhi, Y.; Bao, X.; Yang, R.; Meng, L.; Zhu, W. *J. Mater. Sci.* **2016**, *51*, 8018–8026.

52. Zhou, J. Y.; Zuo, Y.; Wan, X. J.; Long, G. K.; Zhang, Q.; Ni, W.; Liu, Y. S.; Li, Z.; He, G. R.; Li, C. X.; Kan, B.; Li, M. M.; Chen, Y. S. *J. Am. Chem. Soc.* **2013**, *135*, 8484–8487.
53. Kotwica, K.; Kostyuchenko, A. S.; Data, P.; Marszalek, T.; Skorka, L.; Jaroch, T.; Kacka, S.; Zagorska, M.; Nowakowski, R.; Monkman, A. P.; Fisyuk, A. S.; Pisula, W.; Pron, A. *Chem. Eur. J.* **2016**, *22*, 11795–11806.
54. Grana, E.; Katsigiannopoulos, D.; Avgeropoulos, A.; Goulas, V. *Int. J. Polym. Anal. Charact.* **2008**, *13*, 108–118.
55. Guzel, M.; Soganci, T.; Akgun, M.; Ak, M. *J. Electrochem. Soc.* **2015**, *162*, H527–H534.
56. Fan, Q.; Cui, J.; Liu, Y.; Su, W.; Wang, Y.; Tan, H.; Yu, D.; Gao, H.; Deng, X.; Zhu, W. *Synth. Met.* **2015**, *204*, 25–31.
57. Sun, Y.; Xiao, K.; Liu, Y.; Wang, J.; Pei, J.; Yu, G.; Zhu, D. *Adv. Funct. Mater.* **2005**, *15*, 818–822.
58. Ventura, B.; Barbieri, A.; Barigelletti, F.; Diring, S.; Ziessel, R. *Inorg. Chem.* **2010**, *49*, 8333–8346.
59. Shynkaruk, O.; He, G.; McDonald, R.; Ferguson, M. J.; Rivard, E. *Chem. Eur. J.* **2016**, *22*, 248–257.
60. Shynkaruk, O. Ph.D. Dissertation, University of Alberta, **2016**.

Chapter 3

Selective placement of bromide and pinacolboronate groups about a tellurophene: new building blocks for optoelectronic applications

3.1. INTRODUCTION

The study of tellurophene heterocycles has increased substantially recently due to the collective recognition that advantageous properties can arise from the installation of a heavy inorganic element within a ring framework.[1-5] For example the presence of Te can promote phosphorescence in some cases,[6-14] and afford lower optical band gaps in relation to thiophene and selenophene analogues.[1-5,15-18] Moreover the potential for strong Te---Te intermolecular interactions involving tellurophenes could lead to high degrees of charge mobility, making them promising candidates for photovoltaic[19,20] and thin film transistor (TFT) applications.[21-23]

One current limitation is the challenge associated with preparing and functionalizing tellurophenes, however some key breakthroughs have emerged.[24-29] Examples include the synthesis of tellurophenes via Zr/Te[6,7,26] and Sn/Te[25] atom exchange and the development of stannylated tellurophenes as building blocks[24] for efficient Stille cross-coupling methodologies. When one examines the fertile research domains of thiophenes and seleno-phenes, there are now commercially available compounds with either bromine or pinacol-boronate (BPin)-appended functional groups; these substituents are suitable for a wide range of derivatization/polymerization processes including Grignard Metathesis (GRIM), Stille, and Suzuki-Miyaura cross-coupling.[30-33] Towards this end, new synthetic routes to BPin and bromide-functionalized tellurophenes is reported. The generated library of derivatized tellurophenes should be of value to those seeking to advance the use of Te heterocycles in the development of new optoelectronic materials.[1-5]

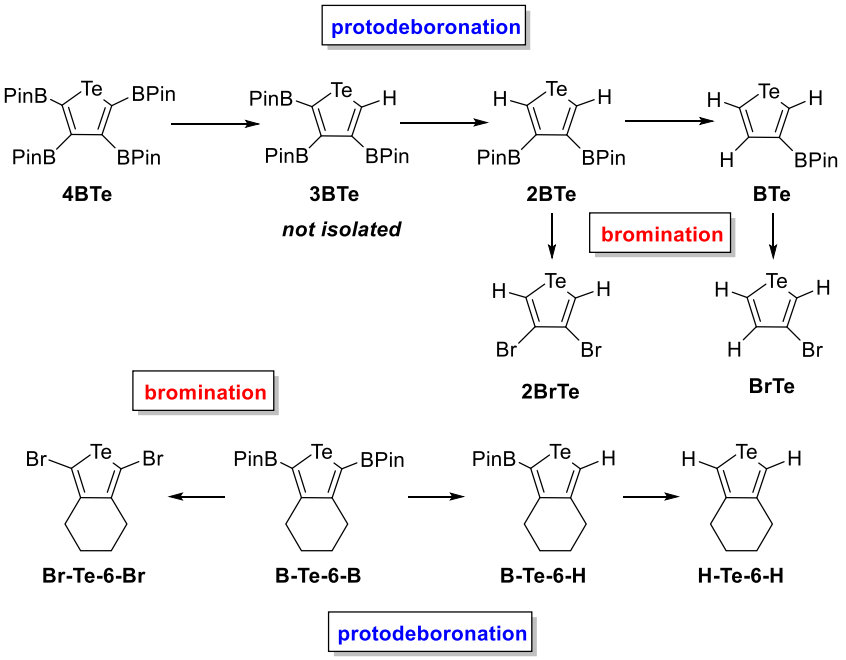

Scheme 3.1. New family of tellurophenes derived from the selective protodeboronation (PDB) or halogenation of the luminescent tellurophenes **4BTe** and **B-Te-6-B** (BPin = pinacol boronate).

3.2. RESULTS AND DISCUSSION

3.2.1. Protodeboronation (PBD) of phosphorescent tellurophenes

The research described in this thesis chapter was instigated by our group's effort to react the known green phosphorescent perborylated tellurophene **4BTe** (Scheme 3.1)[6] with various arylhalides under Suzuki-Miyaura cross-coupling conditions. It was expected that aryl-functionalized tellurophenes with color-tunable phosphorescence would be obtained in a direct fashion.[7] However it became rapidly apparent that minimal aryl-group incorporation transpired and that base-induced BPin cleavage (protodeboronation; PDB) occurred to give a variety of new BPin-containing tellurophenes, as determined by ^{1}H and ^{11}B NMR analysis. As a result, this competing reaction to Suzuki-Miyaura cross-coupling was explored in more detail. When the commonly employed base K_2CO_3 (*aq.*) was combined with 2,3,4,5-tetrakis(pinacolboronate)tellurophene **4BTe** in THF and the solvent heated to reflux for 2 h,

the predominant product obtained after work-up was the new 3,4-substituted bis(pinacolboronate)tellurophene **2BTe** in a 50 % isolated yield (Scheme 3.2). This air-stable compound afforded a high-resolution mass spectrum in accordance with the assigned overall formula, and its ^{1}H NMR spectrum showed the presence of singlet resonances at 1.34 and 9.64 ppm (24:2 ratio; in $CDCl_3$) for the BPin and tellurophene-bound protons, respectively. Moreover the latter resonance was flanked by discernable satellites ($^{2}J_{HTe}$ = 108.0 Hz) arising from coupling to a ^{125}Te nucleus (7.1 % abundance; I = ½), strongly suggesting the presence of proximal hydrogen atoms at the 2- and 5-positions of the tellurophene ring. For comparison, a similar $^{2}J_{HTe}$ coupling constant of 93.9 Hz was noted for the hydrogen atom at the 5-position in 2-tellurophenecarboxylic acid.[34]

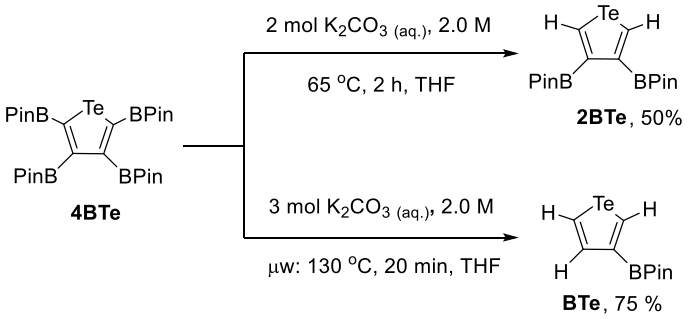

Scheme 3.2. Selective protodeboronation of **4BTe** to yield the **2BTe** and **BTe** via thermal (top) and microwave-induced conditions (bottom), respectively.

Careful analysis of the above mentioned crude reaction mixture identified the presence of an additional tellurophene-containing product with three distinct aryl-H proton environments, and one BPin group. This monopinacolato-substituted tellurophene, **BTe**, could also be obtained in pure form in 75 % yield by heating **4BTe** with aqueous K_2CO_3 for 20 min. at 130 °C under microwave conditions (Scheme 3.2). The resulting low melting beige solid (Mp = 67-69 °C) was subsequently identified as the 3-(pinacolato)tellurophene isomer by single-crystal X-ray crystallography (Figure 3.1). Thus it appears that a sequential protodeboronation process is occurring whereby the BPin groups initially positioned at the 2- and 5-positions in **4BTe** are first cleaved, followed by the loss of a third equivalent of BPin upon prolonged heating with aqueous base (Scheme 3.1). In all of the above mentioned protode-

boronation reactions, the known by-products PinBOH[35] and PinBOBPin[36] were identified by ^{1}H, ^{11}B and $^{13}C\{^{1}H\}$ NMR spectroscopy; fortunately these by-products can be readily separated from the tellurophene products by extraction with water. ^{1}H NMR analysis of the crude reaction mixtures of aliquots of the reaction between **4BTe** and K_2CO_3 (*aq*.) in THF (65 °C) taken after 10, 30 and 50 min, revealed the presence of a new product in decreasing amounts relative to **2BTe** over time, from a 3:2 ratio after 10 min down to a 1:5 ratio after 50 min. This new product afforded a singlet resonance at 10.27 ppm in $CDCl_3$ with discernable Te-H coupling ($^{2}J_{HTe}$ = 100.5 Hz; see Figure 3.17 at the end of this chapter) leading to the assignment of this product as 2,3,4-tris(pinacolboronate)tellurophene **3BTe** (Scheme 3.1).

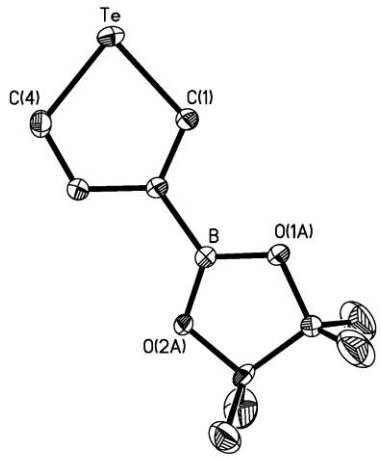

Figure 3.1. Molecular structure of **BTe** with thermal ellipsoids presented at a 30 % probability level. Residual factor, R = 0.0183. All hydrogen atoms have been omitted for clarity. Selected bond lengths (Å) and angles (°): Te-C(1) 2.0480(17), Te-C(4) 2.039(2), C(1)-C(2) 1.367(2), C(2)-C(3) 1.441(2), C(3)-C(4) 1.368(3), C(2)-B 1.554(2); C(1)-Te-C(4) 81.43(7).

The structure of **BTe** is presented in Figure 3.1 and contains a planar tellurophene ring linked to a nearly coplanar BPin unit [average C(1)-C(2)-B-O(1) torsion angle = 6.9(5)°; the BPin group is distorted over two positions]. As is common for tellurophenes, the intra-ring C(1)-Te-C(4) angle is quite narrow [81.43(7)°]. For comparison, the same C-Te-C angle in the tetra(pinacolato)tellurophene precursor **4BTe** is 82.77(12)°,[6] while the average B-C distance in each compound is the same within crystallographic error [1.554(2) Å and 1.557(8) Å *avg*. for **BTe** and **4BTe**, respectively].

Table 3.1. Optimization of conditions to form **2BTe**[a].

Entry	Time, h (temp, °C)	Base, mol equiv.	Mol %[b] **4BTe**/**2BTe**/**BTe**
1 (THF)	1 (65)		<1/92/8
2 (THF)	3 (65)	2	<1/92/8
3 (THF)	16 (65)		<1/64/36
4 (THF)	16 (65)	0	>99/<1/<1
5 (THF)	1 (65)		<1/91/9
6 (THF)	3 (65)	4	<1/73/27
7 (THF)	24 (65)		<1/49/51
8 (THF)			<1/97/3
9 (Dioxane)			<1/96/4
10 (MeCN)	24 (RT)	5	<1/95/5
11 (DMF)			<1/72/28
12 ($CHCl_3$ or Toluene)			>99/<1/<1

[a]Aqueous K_2CO_3 (2.0 M); [b]Determined by ^{1}H NMR integration.

In order to further explore the role of base, temperature and solvent on protodeboronation (PDB), the cleavage of BPin groups from **4BTe** was studied in more detail with pertinent reaction trials summarized in Table 3.1. Effective PDB occurred to yield products with > 90 % **2BTe** content when 2-4 equiv. of aqueous K_2CO_3 were combined with **4BTe** in THF followed by heating (65 °C) for 1 h. If one allows the reaction to transpire for 24 h (Entry 7, Table 3.1) then an increase in the relative amount of mono-borylated product **BTe** is observed (by ^{1}H and ^{11}B NMR).

The role of solvent in the PDB process was also examined. As a benchmark, 5 equiv. of aqueous K_2CO_3 were reacted with **4BTe** in THF for 24 h. at room temperature and noted conversion of **4BTe** into a mixture of **2BTe** and **BTe** (97:3 ratio; Entry 8). Other polar

solvents such as DMF, dioxane and acetonitrile also support the PDB of **4BTe** to give **2BTe** as a major isolated product (72 to 96 % spectroscopic yield in crude mixtures) along with minor amounts of **BTe** (Entries 9-11, Table 1). No PDB occurred when **4BTe** and $K_2CO_{3\ (aq)}$ were combined in toluene or $CHCl_3$. As a result the remaining reactivity studies were conducted in THF given its miscibility with the quantities of water present in the reaction media, and ease at which it can be removed (by evaporation) during work-up.

Given the Rivard group's prior use of microwave conditions to facilitate chemical transformations on metallole rings,[37] compound **4BTe** was treated with 3 equiv. of $K_2CO_{3\ (aq.)}$ in THF under irradiation (Table 3.2). In the first series of experiments, the temperatures were varied from 80 °C to 130 °C with a constant heating time of 20 min. As expected, mostly **2BTe** was obtained at 80 °C (90:10 ratio of **2BTe** to **BTe**), while increasing the temperature to 130 °C enabled the isolation of pure **BTe** in an isolated yield of 75 %; this reaction can be scaled to yield 1 g of product with only trace quantities (1-2 %) of **2BTe** present. Thus microwave irradiation affords **BTe** from **4BTe** in a more rapid and higher yielding fashion than with conventional heating in refluxing overnight. The role of base in promoting the PDB of **4BTe** was also examined at 130 °C under microwave irradiation of **4BTe** and it was found that pure **BTe** was obtained with both NaOH and K_2CO_3, albeit at a slightly reduced isolated yield of 63 % when aqueous sodium hydroxide was used as a reactant. $^{i}Pr_2NH$ also facilitated the protodeboronation of **4BTe** however only partial conversion occurred to give a mixture of **2BTe** and **BTe** (55:45; Entry 5, Table 3.2).

A similar deboronation methodology was applied to the chalcogenophene analogues **4BS** and **4BSe** to see if the selectivity observed for **4BTe** PDB would translate to its lighter element congeners to yield the mono-borylated thiophene (**BS**) and selenophene (**BSe**), respectively (Scheme 3.3). Initial studies of the resulting crude product mixture by NMR (see Figures 3.7 and 3.8 at the end of the chapter) indicated the formation of predominantly the mono-substituted BPin analogues **BS** and **BSe** with respect to the di-substituted BPin chalcogenophenes, **2BS** and **2BSe** (in 88:12 and 92:8 ratios, Scheme 3.3). Therefore an overall similar trend/selectivity in protodeboronation occurs within the **4BE** series (E = S, Se and Te), illustrating the generality of based-induced BPin-aryl bond scission amongst the chalcogenophenes.

Table 3.2. Optimization of conditions to form **BTe** (from **4BTe**) under microwave irradiation.

Entry	Base[a]	Temp., °C	Time, min.	Mol % (**BTe**/**2BTe**)
1		80		10/90
2	K_2CO_3	110	20	67/33
3		130		>99/<1
4	-	130	20	86/14/<1[b]
5	$^{i}Pr_2NH$			45/55
6	K_2CO_3	130	20	>99/<1
7	NaOH			>99/<1
8			10	93/7
9	K_2CO_3	130	20	>99/<1
10			40	>99/<1

[a]3 mole equiv. of base added. [b]Mol % (**4BTe**/**BTe**/**2BTe**)

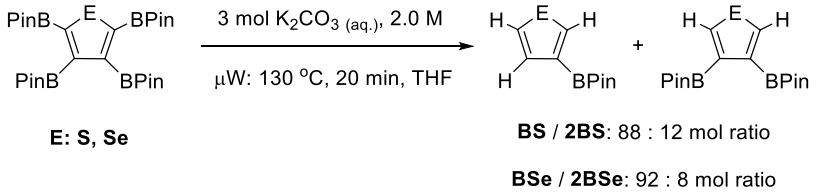

Scheme 3.3. Protodeboronation of **4BS** and **4BSe**.

Encouraged by the selective BPin-cleavage chemistry described above, I decided to explore the propensity of the first room temperature phosphorescent tellurophene **B-Te-6-B** (Scheme 3.1) to undergo protodeboronation (PDB).[6] An added driving force for studying the PDB of **B-Te-6-B** is to gain a better understanding of a potential competing reaction to the Suzuki-Miyaura cross-coupling polymerization of this tellurophene with arylhalides.[26] **B-Te-6-B** was prepared in an improved one-pot procedure in an overall yield of 63 % by first

coupling the readily available BPin-capped diyne PinBC≡C$(CH_2)_4$C≡CBPin[38] with *in situ* generated "Cp_2Zr" to yield the known zirconacycle **B-ZrCp_2-6-B**,[6,26] which is subsequently converted into **B-Te-6-B** by addition of $TeCl_2$•bipy[39] (Scheme 3.4). Furthermore, a similar one-pot procedure could be applied for the synthesis of **4BTe** (56 % overall yield) after a total of 4 h starting from the alkyne PinBC≡CBPin[40] (Scheme 3.4).

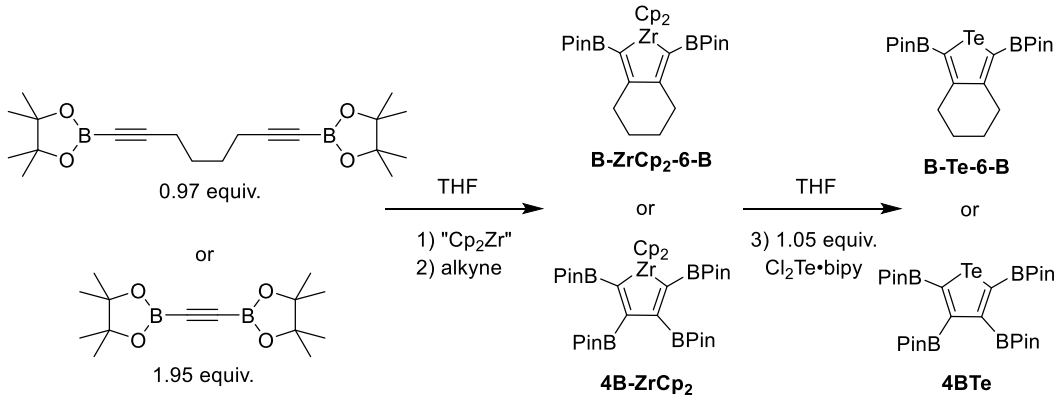

Scheme 3.4. One-pot syntheses of **B-Te-6-B** and **4BTe**.

Initial attempts to induce PDB within **B-Te-6-B** using aqueous K_2CO_3 (1 equiv.) in refluxing THF (in air) did not yield any appreciable reaction, despite heating to 65 °C for 16 h. Likewise microwave heating to 130 °C for 10 min using the same base and solvent combination did not afford any discernable PDB. These results are commensurate with aqueous K_2CO_3 being a suitable base for the Suzuki-Miyaura cross-coupling of **B-Te-6-B** with various arylhalide substrates.[26] However when the stronger base aqueous NaOH (1 equiv.) was combined with **B-Te-6-B** under microwave conditions (130 °C, 30 min.), proto-deboronation of **B-Te-6-B** transpired to yield both **B-Te-6-H** (29 % isolated yield) and small quantities of pure **H-Te-6-H** (3 % isolated yield) after separation by column chromatography. Having found that the strong base NaOH protodeboronates **B-Te-6-B**, optimization of the PBD reaction conditions was explored further. Notably, heating **B-Te-6-B** in refluxing THF for 12 h with 1.2 eq. of NaOH (aq.) afforded **B-Te-6-H** in an enhanced yield of 42 % (Scheme 3.5); the related fully deboronated product **H-Te-6-H** was obtained as a pure pale yellow oil in a 22 % yield after heating **B-Te-6-B** with 6 equiv. of 2.0 M aqueous NaOH in THF for

3 days. Crystals of **B-Te-6-H** (pale yellow solid) were obtained from toluene and the structure determined by X-ray crystallography is presented in Figure 3.2.

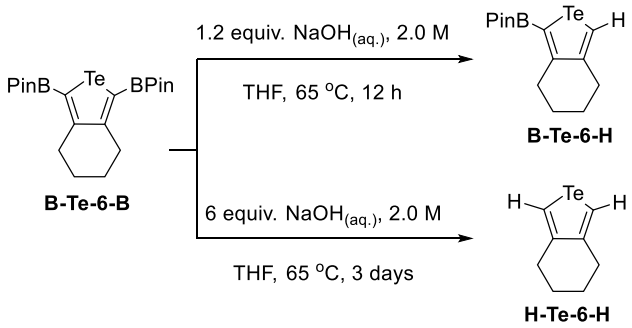

Scheme 3.5. Selective protodeboronation of **B-Te-6-B**.

The structure of the mono-borylated tellurophene **B-Te-6-H** contains many related structural features as its di-pinacolboronate-functionalized predecessor **B-Te-6-B**. For example, the planar tellurophene heterocycle in **B-Te-6-H** lies in a nearly co-planar arrangement as the flanking BO_2C_2 ring in the BPin group [Te-C(1)-B-O(1) torsion angle = -18.2(5)°]; likewise in **B-Te-6-B** the two BPin residues are aligned in a nearly coplanar geometry with the core tellurophene unit as evidenced by twist angles of 15.2(4) and 17.3(5)°. It has been noted in prior work that tellurophenes bearing co-planar BPin substituents at either the 2- or 5-positions exhibit aggregation-induced phosphorescence;[6,7] as a result, the optical properties of the new emissive tellurophene **B-Te-6-H** will be discussed towards the end of this chapter.

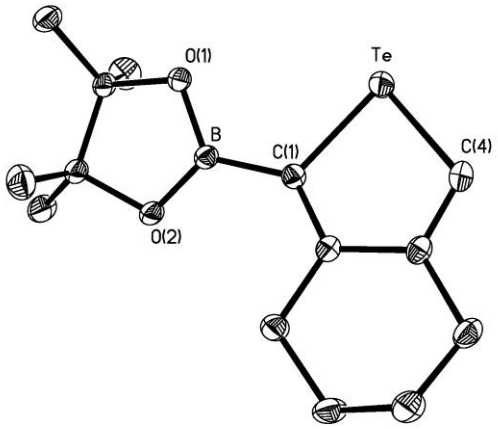

Figure 3.2. Molecular structure of **H-Te-6-B** with thermal ellipsoids presented at a 30 % probability level. Residual factor, R = 0.0226. All hydrogen atoms have been omitted for clarity. Selected bond lengths (Å) and angles (°): Te-C(1) 2.067(4), Te-C(4) 2.051(4), C(1)-C(2) 1.368(5), C(2)-C(3) 1.443(5), C(3)-C(4) 1.348(6), C(1)-B 1.541(5); C(1)-Te-C(4) 81.90(16).

From the protodeboronation studies presented it is clear that the perborylated tellurophene **4BTe** is much more prone to base-induced BPin cleavage than the partially alkylated heterocycle **B-Te-6-B**. At first glance once can attribute this fact to the more electron-rich nature of the sp^2-hybridized carbon atoms in **4BTe** in relation to **B-Te-6-B**, due to the σ-donating nature of the BPin groups. Likewise the increased reactivity of C atoms positioned next to the electropositive Te center in **4BTe** facilitate the selective protonolysis of the C-BPin linkages at the 2- and 5-positions. One needs to be cautious in over generalizing reaction trends as it has been shown that placement of ortho electron-withdrawing groups (EWGs) about arylboronates can facilitate protodeboronation,[41] while electron-donating groups (EDGs) can also facilitate this transformation.[42] In the first instance, EWGs assist in base-coordination to boron, while in the second case the EDG facilitate C-B protonolysis. In some interesting recently studies, both Cu(II) and Ag(I) salts were shown to facilitate PDB,[43,44] however as will be seen, this reaction can be suppressed under suitable reaction conditions in the case of $CuBr_2$.

3.2.2. Access to brominated tellurophenes via pinacolboronate-halide exchange

The use of brominated thiophenes is essential to many polymerization protocols with both 3-bromothiophene and later a 2,5-dibrominated thiophene used in the preparation of the widely explored conjugated material poly(3-hexylthiophene) (P3HT).[30,45] Installation of bromine atoms onto thiophene heterocycles can be accomplished via direct bromination of C-H groups with elemental Br_2 or using milder halogenating reagents such as *N*-bromo-succinimide. However the electron-rich nature of the Te(II) centers in tellurophenes leads to the competitive bromination at tellurium to yield Te(IV) dibromides.[46,47] To circumvent this possible issue, I was drawn to the mild conversion of arylboronates to arylhalides using excess $CuBr_2$.[48,49] The reaction of **B-Te-6-B** with excess $CuBr_2$ (4-6 equiv.) was first examined at *ca.* 70 °C in a 2:1 THF/water mixture. After 24 hours the target dibrominated tellurophene **Br-Te-6-Br** was obtained in a 19 % yield as a white solid after purification of the reaction mixture by column chromatography (Scheme 3.6).

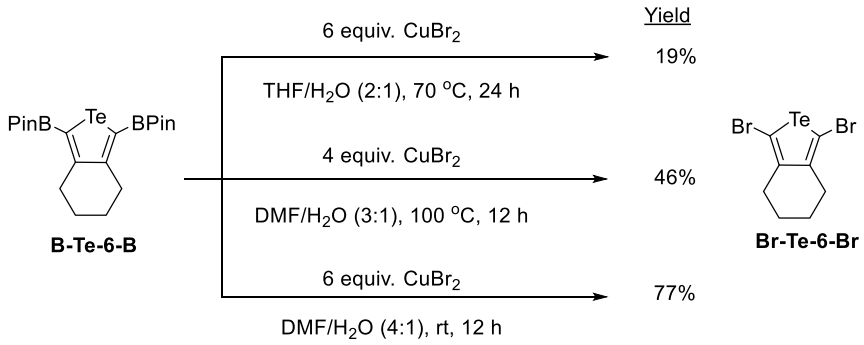

Scheme 3.6. Optimization of the BPin/Br exchange reaction to afford **Br-Te-6-Br**.

Subsequent tests were conducted to improve the yield of the BPin/Br exchange reaction outlined in Scheme 3.6. First, the effect of water on the reaction progress was examined. To my initial surprise, when $CuBr_2$ (3 equiv.) was combined with **B-Te-6-B** in MeCN (65 °C, 16 h) the direct bromination of the Te center transpired to yield the known Te(IV) dibromide **B-TeBr$_2$-6-B**[6] in an isolated yield of 53 % (Scheme 3.7) without the presence of starting material or the intended product **Br-Te-6-Br**. However when **B-Te-6-B** was heated with $CuBr_2$ to 100 °C for 12 h in DMF/H_2O (3:1), the recovery of pure **Br-Te-6-Br** in 46 % yield

was possible after purification by column chromatography (Scheme 3.6). The highest yield of **Br-Te-6-Br** (77 %) resulted from the reaction of 6 equiv. of $CuBr_2$ with **B-Te-6-B** in DMF /H_2O at room temperature for 12 h; moreover this product could be recovered in high spectroscopic purity without the need for time-consuming column chromatography (Scheme 3.6).

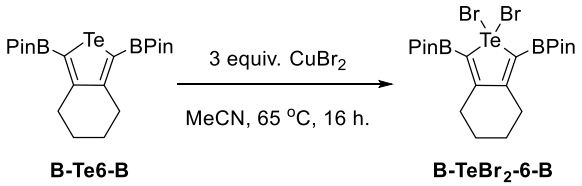

Scheme 3.7. Halogenation of **B-Te-6-B** using $CuBr_2$ to form **B-TeBr$_2$-6-B**.

The optimal conditions used to form **Br-Te-6-Br** from **B-Te-6-B** were then applied to yield the respective brominated-analogues of **2BTe** and **BTe** (3,4-dibromotellurophene and 3-bromotellurophene, respectively). When **BTe** was combined with 3 equiv. of $CuBr_2$ in DMF/H_2O (4:1) at room temperature, no discernable reaction transpired after 16 h. In the case of **2BTe**, the reaction with 6 equiv. of $CuBr_2$ at room temperature in a 4:1 DMF/H_2O mixture afforded the target dibromide **2BrTe** (Scheme 3.1) along with a new BPin-containing product that has been tentatively assigned as 3-bromo-4-pinacolatotellurophene (**BrBTe**) on the basis of ^{1}H NMR spectroscopy (see Figure 3.16 for spectral assignments). Low, yet reproducible isolated yields of pure 3,4-dibromotellurophene (**2BrTe**; 24 %) and 3-bromo-tellurophene (**BrTe**; 21 %) were obtained by heating $CuBr_2$ and **2BTe** and **BTe** respectively in MeOH/H_2O under reflux for 16 h (Scheme 3.8). Future work will involve exploring the functionalization of these new bromotellurophenes to yield new monomers for polymerization protocols.[27]

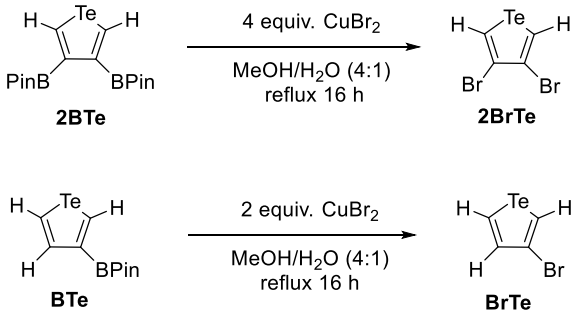

Scheme 3.8. Synthesis of 3,4-dibromo- and 3-bromotellurophene (**2BrTe** and **BrTe**).

To prove the utility of **Br-Te-6-Br** as a building block in coupling reactions, Stille cross-coupling between this heterocycle and 2-(tributylstannyl)thiophene was performed. As anticipated, heating these reagents in the presence of $Pd(PPh_3)_4$ catalyst under microwave-assisted conditions (Scheme 3.9) yielded the known thiophene-capped tellurophene (**T-Te-6-T**)[6] in a crude yield of 75 % (*ca.* 90 % purity), by washing the crude product with cold hexane; additional washings with pentane could yield analytically pure **T-Te-6-T** albeit in a reduced yield of 31 %.

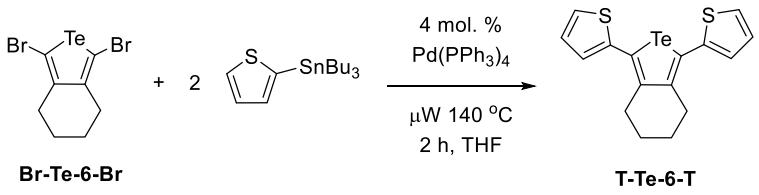

Scheme 3.9. Stille coupling involving the dibromotellurophene (**Br-Te-6-Br**).

3.2.3. Absorption and emission properties of B-Te-6-H

In general tellurophenes are non-emissive due to the "heavy-metal effect" which promotes population of long-lived excited triplet states that are generally quenched by extraneous oxygen or via self-quenching in the solid state.[1] More recently, it was found that when a BPin group was positioned adjacent to Te-center (2- or 5-positions) then solid state phosphorescence could be observed, even in the presence of O_2.[6,7] In line with prior studies **B-Te-6-H** is non-emissive in solution, due to non-radiative decay mediated by the free rotation of the

BPin group, however unlike **B-Te-6-B** or **4BTe**, this species does not emit in the solid state at room temperature, nor in presence or absence of O_2. It was difficult to obtain **B-Te-6-H** in highly crystalline form (with only one successful crystallization trial to date), so one possible theory is that at room temperature **B-Te-6-H** retains sufficient amorphous character to enable luminescence quenching/non-radiative decay by BPin rotation. As a result the emissive properties of **B-Te-6-H** were examined in frozen 2-methyl-THF at 77 K (see Figure 3.3).

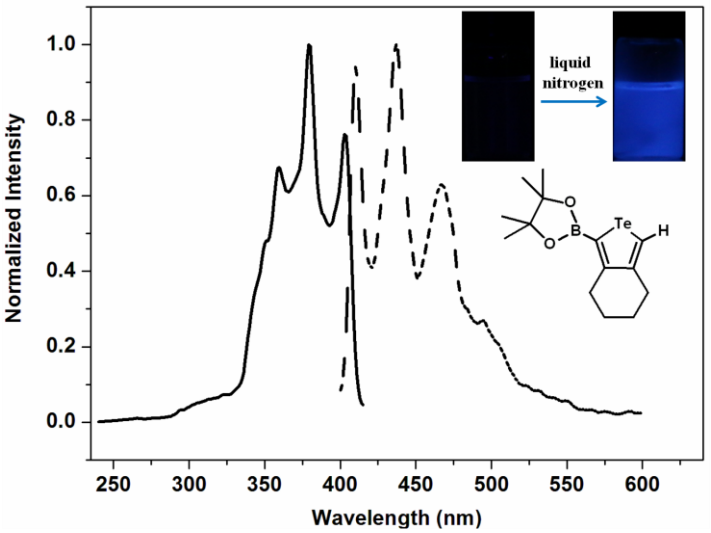

Figure 3.3. Excitation (solid lines) and emission spectra (dashed lines) of **B-Te-6-H** as a frozen glass in 2-Me-THF at 77 K. [**B-Te-6-H**] = 1×10^{-4} M. Inset shows the images of **B-Te-6-H** in 2-Me-THF at room temperature (left) and at 77 K (right) under UV lamp (λ_{ex} = 365 nm).

As shown in Figure 3.3, very weak vibrationally resolved blue emission was found, with the small Stokes shift noted suggesting that fluorescence was transpiring. Interestingly the emission of **B-Te-6-H** in film state is substantially red-shifted (λ_{em} = 580 nm) relative to in 2-methyl-THF to afford yellow emission, due to the possible formation of low excited state energy emissive excimers (Figure 3.4). The quality of the emission data unfortunately was not high enough to extract reliable lifetime data for this system and current studies are focusing on improving film crystallinity for more detailed photoluminescence studies.

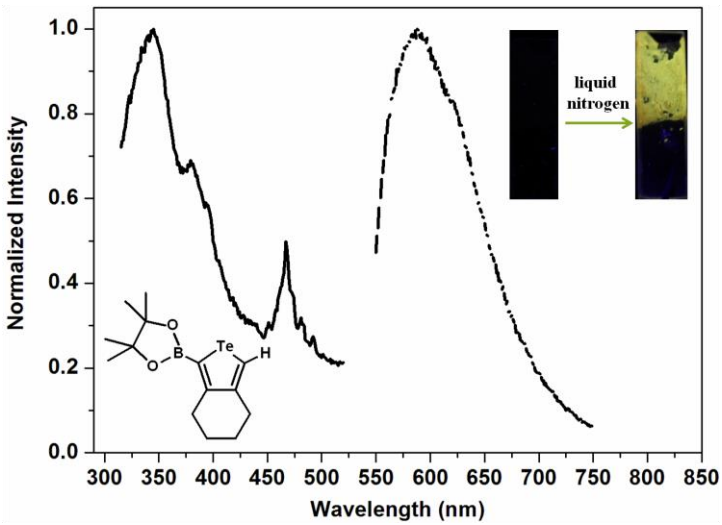

Figure 3.4. Excitation (solid lines) and emission spectra (dashed lines) of **B-Te-6-H** in film at 77 K. Inset shows the images of film of **B-Te-6-H** at room temperature (left) and at 77 K (right) under UV lamp (λ_{ex} = 365 nm).

3.3. CONCLUSIONS

General pathways to obtain both brominated and BPin-capped tellurophenes are reported. These species represent valuable building blocks for the construction of next generation materials with possibly high degrees of charge mobility and narrow optical band gaps, stemming from the presence of tellurophene heterocycles.[1-5] Future work will involve incorporating these units into polymeric structures and the continued investigation of the unusual luminescence properties of borylated tellurophenes.

3.4. EXPERIMENTAL SECTION

3.4.1. General methods

Unless explicitly stated, all reactions were conducted with standard Schlenk and glove box (MBraun) techniques using N_2 as an inert atmosphere, with solvents that were dried using a Grubbs' type purification system manufactured by Innovative Technology Inc. 1,7-Octadiyne and 2,2'-bipyridine were purchased from GFS Chemicals, Cp_2ZrCl_2 was purchased from Strem Chemicals Inc., 2-isopropoxy-4,4,5,5-tetramethyl-1,3,2-dioxa-borolane was purchased from Matrix Scientific and all other chemicals were obtained from Aldrich. Bipy•$TeCl_2$,[39] Bipy•$SeCl_2$,[39] PinBC≡CBPin,[40] PinBC≡C$(CH_2)_4$C≡CBPin,[38] $Cp_2ZrC_4BPin_4$[6] and 2-tributylstannylthiophene[50,51] were synthesized according to literature procedures, while **B-Te-6-B**,[26] and **4BTe**[6] were prepared according to modified procedures as described below and in Chapter 2, respectively. ^1H and $^{13}C\{^1H\}$ and $^{11}B\{^1H\}$ NMR spectra were recorded on either a Varian Innova 500 and 400 spectrometer are referenced externally to Me_4Si (^1H and $^{13}C\{^1H\}$) and F_3B•OEt_2 (^{11}B). Melting points were measured in a MelTemp melting point apparatus and are reported without correction. Elemental analysis were performed by the Analytical and Instrumentation Laboratory at the University of Alberta, UV-visible measurements were performed with a Varian Cary 300 Scan spectrophotometer and fluorescence measurements with a Photon Technology International (PTI) MP1 fluorometer. High-resolution mass spectra were obtained on an Agilent 6220 spectrometer.

3.4.1.1. Synthesis of B-Te-6-B:

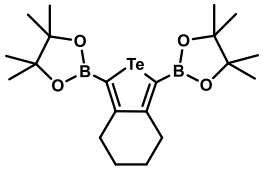

To a slurry of Cp_2ZrCl_2 (2.558 g, 8.749 mmol) in 65 mL of THF was added ^{n}BuLi (7.0 mL, 2.5 M solution in hexanes, 17.5 mmol) at -78 °C. After stirring for 1 hour at -78 °C, a cold solution of PinBC≡C$(CH_2)_4$C≡CBPin (3.039 g, 8.487 mmol) in 75 mL of THF (at 0 °C) was added via cannula. The cold bath was removed and after stirring for 1 h, the mixture was

warmed to room temperature with assistance from a warm water bath at *ca.* 35 °C; at this point the color of the mixture went from yellow to dark red. The reaction mixture was stirred for another 3 h at room temperature. Bipy•$TeCl_2$ (3.160 g, 8.911 mmol) was then added in one portion under a strong counter-flow of nitrogen, followed by additional stirring for 2 h. The volatiles were removed under vacuum and 150 mL of hexanes/pentane (1:1 mixture) was added to the remaining solids. The mixture was then filtered through a small pad (1 cm) of silica gel and the solvent was removed to give pure **B-Te-6-B** (2.588 g, 63 %) as a pale beige solid with spectroscopic data that matched those previously reported.[26]

3.4.1.2. Synthesis of 3,4-bis(pinacolato)tellurophene (2BTe):

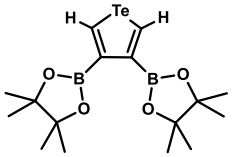

4BTe (0.342 g, 0.300 mmol) was dissolved in 4 mL of THF. 0.5 mL of aqueous K_2CO_3 (2.0 M, 1.0 mmol) was then added and the solution was heated to reflux for 2 hours. The reaction mixture was then poured into 20 mL of $CHCl_3$ and $MgSO_4$ was added, followed by filtration through a pad of Celite. After the solvent was removed from the filtrate under vacuum, the mixture was poured into 20 mL of hexanes and washed with water (3 × 50 mL of H_2O). After drying the organic layer over $MgSO_4$ and filtering, the volatiles were removed from the filtrate to afford **2BTe** (0.109 g, 50 %) as a yellow-orange oil.

*Alternate synthesis of **2BTe** under microwave conditions:* **4BTe** (0.364 g, 0.533 mmol) was dissolved in 2 mL of THF in a microwave vial under an inert atmosphere of N_2, then, 0.8 mL of aqueous K_2CO_3 (2.0 M, 1.6 mmol) was added and the vial was sealed. The reaction was left in the microwave reactor stirring for 20 min at 80 °C. The reaction mixture was poured into 20 mL of $CHCl_3$, filtered through a pad of Celite, and then the organic layer was washed with H_2O (3 × 50 mL). The organic layer was dried over $MgSO_4$, filtered and the volatiles were removed under reduced pressure. Purification was accomplished via column chromatography using silica gel with a 9:1 hexanes:THF mixture as an eluent to give **2BTe** as a deep yellow liquid (0.054 g, 23 %) in a purity of *ca.* 95 % (according to ^{1}H NMR). ^{1}H

NMR (500 MHz, $CDCl_3$): δ 9.64 (s, 2H; satellites: $^2J_{HTe}$ = 108.0 Hz, Te-C*H*), 1.34 (s, 24H, C*H*$_3$). $^{13}C\{^1H\}$ NMR (500 MHz, $CDCl_3$): δ 139.3 (Te-*C*H) 83.8, (*C*-O); 25.0 (*C*H$_3$). $^{11}B\{^1H\}$ NMR (500 MHz, $CDCl_3$): δ 30.4. HR-MS (EI) ($C_{16}H_{26}B_2O_4Te$): m/z: Calcd: 434.1079; Found: 434.1076 (Δppm = 0.9).

3.4.1.3. Synthesis of 3-pinacolatotellurophene (BTe):

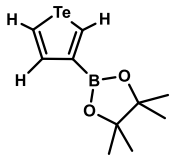

4BTe (0.455 g, 0.666 mmol) was dissolved in 4.5 mL of THF in a microwave vial under an inert atmosphere of N_2. After adding 1.0 mL of aqueous K_2CO_3 (2.0 M, 2.0 mmol) the vial was sealed. The reaction was left in the microwave reactor stirring for 20 min at 130 °C. The reaction mixture was then poured into 40 mL of $CHCl_3$ and filtered through a pad of Celite, then the organic layer washed with H_2O (3 x 70 mL) and dried over $MgSO_4$. After filtration, the volatiles were removed under vacuum to give **BTe** as a light brown solid (0.153 g, 75 %). Crystallization from toluene at 4 °C afforded colorless crystals of **BTe** that were of suitable quality for X-ray crystallography. ^1H NMR (500 MHz, $CDCl_3$): δ 9.86 (pseudo t, 1H, *J* = *ca.* 1.4 Hz; satellites: $^2J_{HTe}$ = 106.0 Hz, TeC(*H*)C(B)), 8.96 (dd, 1H, $^3J_{HH}$ = 6.6 Hz, $^4J_{HH}$ = 1.6 Hz; satellites: $^2J_{HTe}$ = 104.0 Hz, TeC(*H*)C(H)), 8.13 (dd, 1H, $^3J_{HH}$ = 6.5 Hz, $^4J_{HH}$ = 1.2 Hz; satellites: $^3J_{HTe}$ = 28.4 Hz, TeC(H)C(*H*)), 1.33 (s, 12H, C*H*$_3$). $^{13}C\{^1H\}$ NMR (500 MHz, $CDCl_3$): δ 143.2 (Te-*C*), 141.2 (Te-*C*), 126.8 (HC*C*HC(B)), 83.8 (*C*-O), 25.0 (*C*H$_3$). $^{11}B\{^1H\}$ NMR (400 MHz, $CDCl_3$): δ 29.1. HR-MS (EI) ($C_{10}H_{15}BO_2Te$): m/z: Calcd: 308.0227; Found: 308.0229 (Δppm = 0.7). Anal. Calcd. for $C_{10}H_{15}BO_2Te$: C, 39.30; H, 4.95; Found: C, 39.47; H, 4.97. Mp(°C): 67-69.

3.4.1.4. Synthesis of 3-pinacolatothiophene (BS) and 3,4-bis(pinacolato)thiophene (2BS):

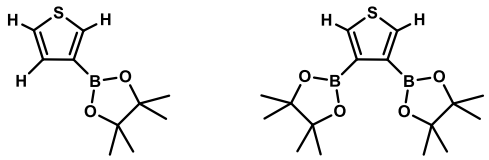

4BS (0.279 g, 0.476 mmol) was dissolved in 1.7 mL of THF in a microwave vial under an inert atmosphere of N_2. After adding 0.71 mL of aqueous K_2CO_3 (2.0 M, 1.42 mmol) the vial was sealed. The reaction mixture was left in the microwave reactor stirring for 20 min at 130 °C. The reaction mixture was then poured into 30 mL of $CHCl_3$ and filtered through a pad of Celite, then the organic layer washed with H_2O (3 x 50 mL) and dried over $MgSO_4$. After filtration, the volatiles were removed under vacuum to give a mixture of **BS** and **2BS**, in a molar ratio of 88 : 12, as a dark brown oil (0.084 g).

NMR data for **BS**: ^{1}H NMR (500 MHz, $CDCl_3$): δ 7.92 (dd, 1H, $^4J_{HH}$ = 1.1 Hz, $^4J_{HH}$ = 2.7 Hz, SC(*H*)C(B)), 7.41 (dd, 1H, $^4J_{HH}$ = 1.1 Hz, $^3J_{HH}$ = 4.9 Hz, SC(*H*)C(H)), 7.33 (dd, 1H, $^4J_{HH}$ = 2.7 Hz, $^3J_{HH}$ = 4.9 Hz, SC(H)C(*H*)), 1.33 (s, 12H, CH_3). ^{13}C{^{1}H} NMR (500 MHz, $CDCl_3$): δ 136.5 (S-*C*), 132.1 (S-*C*), 125.4 (HC*C*HC(B)), 83.7 (*C*-O), 24.9 (*C*H$_3$). ^{11}B{^{1}H} NMR (400 MHz, $CDCl_3$): δ 29.0.

NMR data for **2BS**: ^{1}H NMR (500 MHz, $CDCl_3$): δ 7.78 (s, 2H, SC(*H*)C(B)), 1.35 (s, 24H, CH_3). ^{13}C{^{1}H} NMR (500 MHz, $CDCl_3$): δ 135.5 (S-*C*), 84.7 (*C*-O), 25.0 (*C*H$_3$). ^{11}B{^{1}H} NMR (400 MHz, $CDCl_3$): δ 29.0.

3.4.1.5. Synthesis of 3-pinacolatoselenophene (BSe) and 3,4-bis(pinacolato)selenophene (2BSe):

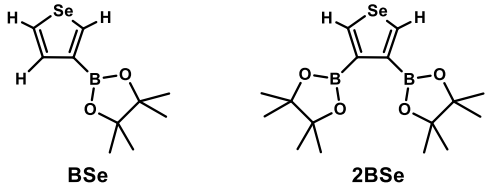

4BSe (0.247 g, 0.389 mmol) was dissolved in 1.5 mL of THF in a microwave vial under an inert atmosphere of N_2. After adding 0.58 mL of aqueous K_2CO_3 (2.0 M, 1.16 mmol) the vial was sealed. The reaction was left in the microwave reactor stirring for 20 min at 130 °C.

The reaction mixture was then poured into 30 mL of $CHCl_3$ and filtered through a pad of Celite, then the organic layer washed with H_2O (3 x 50 mL) and dried over $MgSO_4$. After filtration, the volatiles were removed under vacuum to give a mixture of **BSe** and **2BSe**, in a molar ratio of 92 : 8, as a dark brown oil (0.083 g).

NMR data for **BSe**: ^{1}H NMR (500 MHz, $CDCl_3$): δ 8.73 (dd, 1H, $^{4}J_{HH}$ = 0.9 Hz, $^{4}J_{HH}$ = 2.2 Hz; satellites: $^{2}J_{HSe}$ = 49.3 Hz, SeC(*H*)C(B)), 8.03 (dd, 1H, $^{4}J_{HH}$ = 2.2 Hz, $^{3}J_{HH}$ = 5.3 Hz; satellites: $^{2}J_{HSe}$ = 48.6 Hz, SeC(*H*)C(H)), 7.64 (dd, 1H, $^{4}J_{HH}$ = 0.9 Hz, $^{3}J_{HH}$ = 5.1 Hz; satellites: $^{3}J_{HSe}$ = 15.4 Hz, SeC(H)C(*H*)), 1.33 (s, 12H, C*H*$_3$). $^{13}C\{^{1}H\}$ (500 MHz, $CDCl_3$): δ 143.1 (satellites: $^{1}J_{SeC}$ = 118.2 Hz, Se-*C*), 134.4 (SeC(H)*C*(H)), 130.6 (satellites: $^{1}J_{SeC}$ = 111.1 Hz, Se-*C*), 83.7 (*C*-O), 24.9 (*C*H$_3$). $^{11}B\{^{1}H\}$ NMR (400 MHz, $CDCl_3$): δ 29.0.

^{1}H NMR data for **2BSe** (500 MHz, $CDCl_3$): δ 8.55 (s, 2H; satellites: $^{2}J_{HSe}$ = 49.8 Hz, SeC(*H*)C(B)), 1.35 (s, 24H, C*H*$_3$).

3.4.1.6. Synthesis of B-Te-6-H:

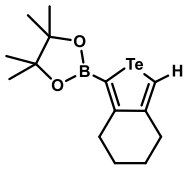

To a solution of **B-Te-6-B** (0.971 g, 2.00 mmol) in 6 mL of THF at 70 °C under air was added dropwise 1.2 mL of aqueous NaOH (2.0 M, 2.4 mmol). After heating was continued for 12 h, the reaction mixture was allowed to cool to room temperature. The mixture was then poured into 70 mL of Et_2O and extracted with a saturated brine (NaCl) solution (3 × 80 mL). The organic layer was then dried over Na_2SO_4, filtered, and the volatiles were removed under vacuum. The product was purified by column chromatography using silica gel and a 20:1 hexanes/ethyl acetate mixture as an eluent (R_f = 0.45) to give **B-Te-6-H** as a pale yellow solid (0.308 g, 42 %). Crystals of suitable quality for X-ray diffraction were grown from toluene at 0 °C. ^{1}H NMR (500 MHz, $CDCl_3$): δ 8.63 (s, 1H; satellites: $^{2}J_{HTe}$ = 93.3 Hz, Te-C*H*), 2.85 (m, 2H, C=CC*H*$_2$), 2.71 (m, 2H, C=CC*H*$_2$), 1.67 (m, 4H, C=CCH$_2$C*H*$_2$), 1.30 (s, 12H, C*H*$_3$). $^{13}C\{^{1}H\}$ NMR (500 MHz, $CDCl_3$): δ 158.3 (Te-C=*C*), 151.4 (Te-C=*C*), 125.3 (Te-*C*-H), 83.7 (*C*-O), 32.7 and 32.6 (C=C*C*H$_2$CH$_2$), 24.9 ((H$_3$*C*)$_2$C), 23.7 (C=CCH$_2$*C*H$_2$). $^{11}B\{^{1}H\}$ NMR (400 MHz, $CDCl_3$): δ 31.0. HR-MS (EI) ($C_{14}H_{21}BO_2Te$): m/z: Calcd:

362.06970; Found: 362.06999 (δ ppm = 0.8). Anal. Calcd. for $C_{14}H_{21}BO_2Te$: C, 46.74; H, 5.88; Found: C, 47.03; H, 5.81. Mp(°C): 64-66.

3.4.1.7. Synthesis of H-Te-6-H:

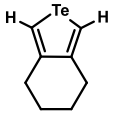

B-Te-6-B (1.363 g, 2.806 mmol) was dissolved in 9 mL of THF and 8.4 mL of aqueous NaOH (2.0 M, 17 mmol) was added dropwise under air. After heating the mixture to reflux for 3 days, the reaction mixture was left to cool to room temperature. The mixture was then poured into 60 mL of $CHCl_3$ and washed with water (3 × 80 mL). The organic layer was dried over Na_2SO_4, filtered and the volatiles were removed from the filtrate under vacuum. The product was purified by column chromatography using silica gel and a 20:1 hexanes /ethyl acetate mixture as an eluent (R_f = 0.82) to give **H-Te-6-H** as a yellow oil (0.150 g, 22 %). ^{1}H NMR (500 MHz, $CDCl_3$): δ 8.26 (s, 2H; satellites: $^2J_{HTe}$ = 101.1 Hz, Te-C*H*), 2.70 (m, 4H, C=CC*H*$_2$), 1.67 (m, 4H, C=CCH$_2$C*H*$_2$). ^{13}C{^{1}H} NMR (500 MHz, $CDCl_3$): δ 148.3 (Te-C=*C*), 117.7 (satellites: $^1J_{TeC}$ = 143.3 Hz, Te-*C*-H), 32.0 (C=C*C*H$_2$CH$_2$), 24.0 (C=CCH$_2$*C*H$_2$). HR-MS (EI) ($C_8H_{10}Te$): m/z: Calcd: 235.9845; Found: 235.9846 (Δppm = -0.5). Anal. Calcd. for $C_8H_{10}Te$: C, 41.10; H, 4.31; Found: C, 41.16; H, 4.30.

3.4.1.8. Synthesis of Br-Te-6-Br:

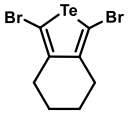

B-Te-6-B (0.124 g, 0.255 mmol) and $CuBr_2$ (0.342 g, 1.53 mmol) were dissolved in a mixture of DMF/H_2O (4 mL: 1 mL) and stirred at room temperature for 12 h. The reaction mixture was then poured into 50 mL of $CHCl_3$ and washed repeatedly with water (5 × 70 mL). The organic layer was then dried over Na_2SO_4, filtered and after removal of the solvent, the product was obtained as a white solid (0.077 g, 77 %). If purity above 90 % is necessary, the product can be further purified using column chromatography (silica gel) with petroleum ether as an eluent (R_f = 0.62) to give **Br-Te-6-Br** as a white powder. ^{1}H NMR (700 MHz, $CDCl_3$): δ 2.56 (m, 4H, Br-C=CC*H*$_2$CH$_2$), 1.65 (m, 4H, Br-C=CCH$_2$C*H*2). ^{13}C{^{1}H} NMR

(700 MHz, $CDCl_3$): δ 146.7 (Br-*C*), 102.9 (Br-C=*C*), 30.8 (C=C*C*$H_2$$CH_2$), 22.9 (C=$CCH_2$*C*$H_2$). HR-MS (EI) ($C_8H_8Br_2Te$): m/z: Calcd for $C_8H_8Br^{79}Br^{81}Te$: 391.80170; Found: 391.80258 (Δppm = 2.3). Anal. Calcd. for $C_8H_8Br_2Te$: C, 24.54; H, 2.06; Found: C, 24.98; H, 2.14. Mp(°C): 66-68.

3.4.1.9. Synthesis of B-TeBr$_2$-6-B:

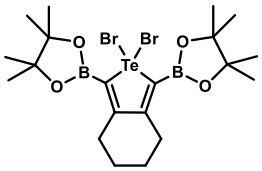

B-Te-6-B (0.124 g, 0.256 mmol) and $CuBr_2$ (0.171 g, 0.768 mmol) were dissolved in 5 mL of MeCN and stirred at 60 °C for 16 h. The reaction mixture was then poured into 20 mL of Et_2O and washed repeatedly with water (3 × 40 mL) and once with brine (40 mL). The organic layer was then dried over Na_2SO_4, filtered through a pad of Celite and after removal of the solvent, the product was obtained as a spectroscopically pure colorless solid (0.088 g, 53 %) with NMR data that matched those previously reported.[6]

3.4.1.10. Synthesis of 3,4-dibromotellurophene (2BrTe):

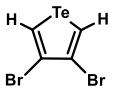

2BTe (0.255 g, 0.591 mmol) and $CuBr_2$ (0.529 g, 2.37 mmol) were dissolved in a mixture of MeOH/H2O (8 mL: 2 mL) and then heated at reflux for 16 h. The reaction mixture was dissolved in 50 mL of Et_2O and washed with water (2 × 70 mL). The organic layer was then dried over $MgSO_4$, filtered and the solvent removed under vacuum. The product was then purified using column chromatography (silica gel) with pentane/ethyl acetate (10:1) as an eluent (R_f = 0.50) to give **2BrTe** (0.048 g, 24 %) as a pure yellow liquid. ^{1}H NMR (500 MHz, $CDCl_3$): δ 8.68 (s, 2H; satellites: $^2J_{HTe}$ = 93.2 Hz, Te-C*H*). $^{13}C\{^1H\}$ NMR (500 MHz, $CDCl_3$): δ 121.8 (satellites: $^1J_{TeC}$ = 156.3 Hz, Te-*C*H), 118.5 (*C*Br). HR-MS (EI) ($C_4H_2Br_2Te$): m/z: Calcd: 337.75855; Found: 337.75554 (Δppm = 2.4). Anal. Calcd. for $C_4H_2Br_2Te$: C, 14.24; H, 0.60; Found: C, 14.81; H, 0.69.

3.4.1.11. Synthesis of 3-bromotellurophene (BrTe):

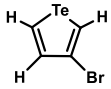

BTe (0.236 g, 0.772 mmol) and $CuBr_2$ (0.345 g, 1.54 mmol) were dissolved in a mixture of MeOH/H_2O (8 mL: 2 mL) and then heated to reflux for 16 h. The reaction mixture was dissolved in 50 mL of Et_2O and washed with water (3 × 70 mL). The organic layer was then dried over $MgSO_4$, filtered and the solvent removed. The product was then purified using column chromatography (silica gel) with hexanes/ethyl acetate (10:1) as an eluent (R_f = 0.60) to give **BrTe** (0.043 g, 21 %) as a yellow liquid with a purity of *ca.* 95 % (as determined by ^{1}H NMR spectroscopy). ^{1}H NMR (500 MHz, $CDCl_3$): δ 8.74 (dd, 1H, $^3J_{HH}$ = 6.8 Hz, $^4J_{HH}$ = 2.0 Hz; satellites: $^2J_{HTe}$ = 97.6 Hz, TeC(*H*)C(H)), 8.69 (dd, 1H, $^4J_{HH}$ = 1.5 Hz, $^4J_{HH}$ = 1.6 Hz; satellites: $^4J_{HH}$ = 95.4 Hz, TeC(*H*)C(Br)), 7.84 (dd, 1H, $^3J_{HH}$ = 6.8 Hz, $^4J_{HH}$ = 1.6 Hz; satellites: $^3J_{HH}$ = 22.6 Hz, TeC(H)C(*H*)). ^{13}C{^{1}H} NMR (500 MHz, $CDCl_3$): δ 140.1, 126.5, 120.3, 116.2 (Ar*C*).

3.4.1.12. Synthesis of T-Te-6-T:

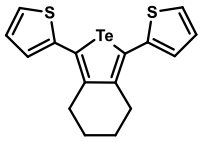

Br-Te-6-Br (0.073 g, 0.186 mmol), 2-(tributylstannyl)thiophene (0.144 g, 0.374 mmol) and $Pd(PPh_3)_4$ (0.008 g, 0.007 mmol) were dissolved in 3 mL of THF in a microwave vial under an inert atmosphere of N_2. The reaction was left in the microwave reactor stirring for 2 h at 140 °C. The reaction mixture was cooled to room temperature and then filtered through a pad of Celite and the solvent removed. The remaining solid was washed with 5 mL of cold (-30 °C) hexanes and the sample dried under vacuum to give a yellow powder of **T-Te-6-T** (0.056 g, 75 %) with a *ca.* 90 % of purity found by ^{1}H NMR spectroscopy; spectroscopic data (see Figure 3.15) that matched those previously reported.[6] Additional purification was possible by washing the crude product obtained from the above reaction 3 × 10 mL of pentane (cooled to -30 °C) affording pure **T-Te-6-T** in a 31 % yield.

3.4.2. X-ray details

Table 3.3. X-Ray crystallographic data for **BTe**.

A. Crystal Data	
formula	$C_{10}H_{15}BO_2Te$
formula weight	305.63
crystal dimensions (mm)	0.28×0.27×0.14
crystal system	tetragonal
space group	$I4_1/a$ (No. 88)
unit cell parameters[a]	
a (Å)	14.2559 (6)
c (Å)	23.5690 (10)
V (Å^3)	4789.9 (5)
Z	16
ρ_{calcd} (g cm^{-3})	1.695
μ (mm^{-1})	2.457
B. Data Collection and Refinement Conditions	
diffractometer	Bruker D8/APEX II CCD[b]
radiation (λ [Å])	graphite-monochromated Mo Kα (0.71073)
temperature (°C)	–100
scan type	ω scans (0.3°) (20 s exposures)
data collection 2θ limit (deg)	57.43
total data collected	38423 (-19≤h≤19, -19≤k≤19, -31≤l≤31)
independent reflections	3007 (R_{int} = 0.0194)
number of observed reflections (NO)	2856 [$F_o^2 \geq 2\sigma(F_o^2)$]

structure solution method	intrinsic phasing (*SHELXT*[c])
refinement method	full-matrix least-squares on F^2 (*SHELXL–2013*[c])
absorption correction method	Gaussian integration (face-indexed)
range of transmission factors	0.8166–0.5902
data/restraints/parameters	3007 / 24[d] / 199
goodness-of-fit (*S*)[e] [all data]	1.085
final *R* indices[f]	
R_1 [$F_o^2 \geq 2\sigma(F_o^2)$]	0.0183
wR_2 [all data]	0.0461
largest difference peak and hole	0.733 and –0.306 e Å^{-3}

[a]Obtained from least-squares refinement of 9769 reflections with $5.32° < 2\theta < 57.12°$.

[b]Programs for diffractometer operation, data collection, data reduction and absorption correction were those supplied by Bruker.

[c]Sheldrick, G. M. *ActaCrystallogr.* **2008**, *A64*, 112–122.

[d]The C–C, the O–C and the O–B sets of distances within the disordered tetramethyldioxaborolane group were restrained to be the same by use of the *SHELXL***SADI** instruction. Additionally, a rigid-bond restraint was applied to the anisotropic displacement parameters of the carbon atoms of the minor component by use of the *SHELXL***DELU** instruction.

[e]$S = [\Sigma w(F_o^2 - F_c^2)^2/(n-p)]^{1/2}$ (n = number of data; p = number of parameters varied; $w = [\sigma^2(F_o^2) + (0.0225P)^2 + 5.6607P]^{-1}$ where $P = [\mathrm{Max}(F_o^2, 0) + 2F_c^2]/3$).

[f]$R_1 = \Sigma||F_o| - |F_c||/\Sigma|F_o|$; $wR_2 = [\Sigma w(F_o^2 - F_c^2)^2/\Sigma w(F_o^4)]^{1/2}$.

Table 3.4. X-Ray crystallographic data for **B-Te-6-H**.

A. Crystal Data	
formula	$C_{14}H_{21}BO_2Te$
formula weight	359.72
crystal dimensions (mm)	0.30 × 0.27 × 0.19
crystal system	tetragonal
space group	$P4_32_12$ (No. 96)
unit cell parameters[a]	
a (Å)	9.1615 (2)
c (Å)	36.3296 (10)
V (Å^3)	3049.27 (18)
Z	8
ρ_{calcd} (g cm^{-3})	1.567
μ (mm^{-1})	15.32
B. Data Collection and Refinement Conditions	
diffractometer	Bruker D8/APEX II CCD[b]
radiation (λ [Å])	Cu Kα (1.54178) (microfocus source)
temperature (°C)	–100
scan type	ω and ϕ scans (1.0°) (5 s exposures)
data collection 2□ limit (deg)	148.12
total data collected	21409 (-10 ≤*h*≤ 11, -11 ≤*k*≤ 11, -45 ≤*l*≤ 45)
independent reflections	3103 (R_{int} = 0.0436)
number of observed reflections (*NO*)	3090 [$F_o^2 \geq 2\sigma(F_o^2)$]
structure solution method	Patterson/structure expansion (*DIRDIF–2008*[c])

refinement method	full-matrix least-squares on F^2 (*SHELXL–2014*[d])
absorption correction method	Gaussian integration (face-indexed)
range of transmission factors	0.2778–0.0477
data/restraints/parameters	3103 / 0 / 182
Flack absolute structure parameter[e]	0.060(9)
goodness-of-fit (*S*)[f] [all data]	1.068
final *R* indices[g]	
R_1 [$F_o^2 \geq 2\sigma(F_o^2)$]	0.0226
wR_2 [all data]	0.0563
largest difference peak and hole	0.434 and –1.102 e Å^{-3}

[a]Obtained from least-squares refinement of 9177 reflections with $4.86° < 2\theta < 147.34°$.

[b]Programs for diffractometer operation, data collection, data reduction and absorption correction were those supplied by Bruker.

[c]Beurskens, P. T.; Beurskens, G.; de Gelder, R.; Smits, J. M. M.; Garcia-Granda, S.; Gould, R. O. (2008). The *DIRDIF-2008* program system. Crystallography Laboratory, RadboudUniversityNijmegen, The Netherlands.

[d]Sheldrick, G. M. *ActaCrystallogr.***2015**, *C71*, 3–8.

[e]Flack, H. D. *Acta Crystallogr.***1983**, *A39*, 876–881; Flack, H. D.; Bernardinelli, G. *ActaCrystallogr.***1999**, *A55*, 908–915; Flack, H. D.; Bernardinelli, G. *J. Appl. Cryst.***2000**, *33*, 1143–1148. The Flack parameter will refine to a value near zero if the structure is in the correct configuration and will refine to a value near one for the inverted configuration.

[f]$S = [\Sigma w(F_o^2 - F_c^2)^2/(n-p)]^{1/2}$ (n = number of data; p = number of parameters varied; $w = [\sigma^2(F_o^2) + (0.0249P)^2 + 2.8836P]^{-1}$ where $P = [\mathrm{Max}(F_o^2, 0) + 2F_c^2]/3$).

[g]$R_1 = \Sigma||F_o| - |F_c||/\Sigma|F_o|$; $wR_2 = [\Sigma w(F_o^2 - F_c^2)^2/\Sigma w(F_o^4)]^{1/2}$.

3.5. ADDITIONAL DATA

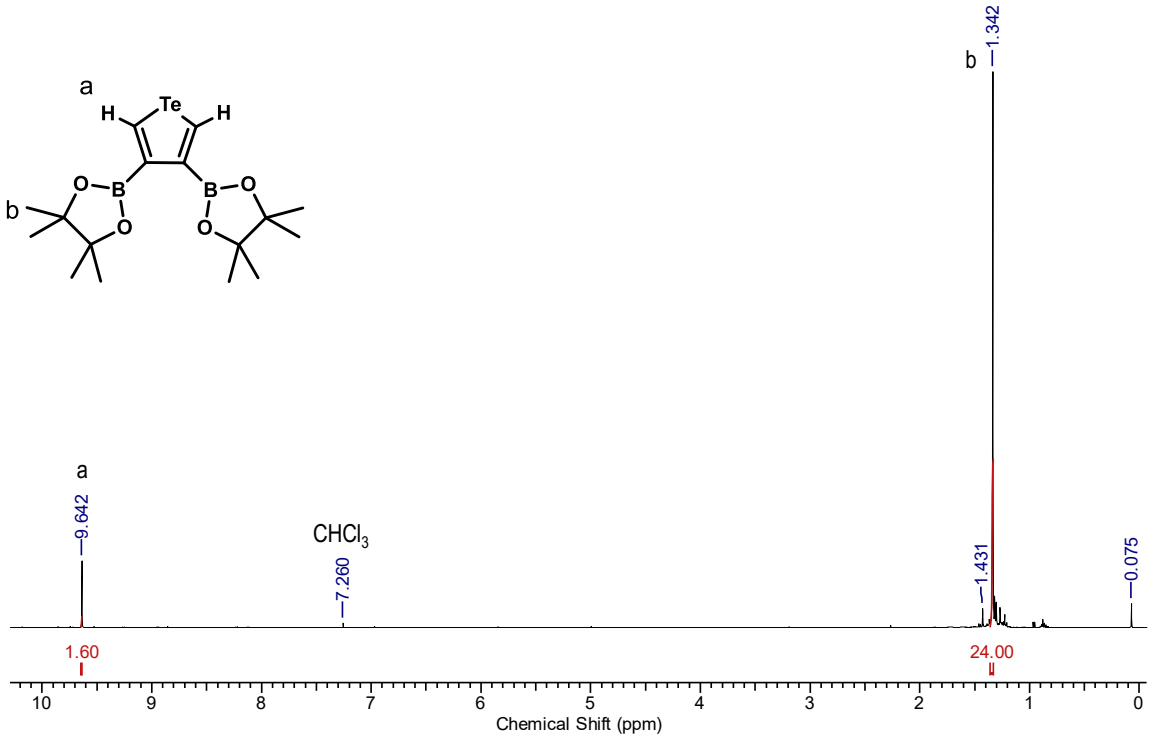

Figure 3.5. A) ^{1}H NMR spectrum of **2BTe** in $CDCl_3$.

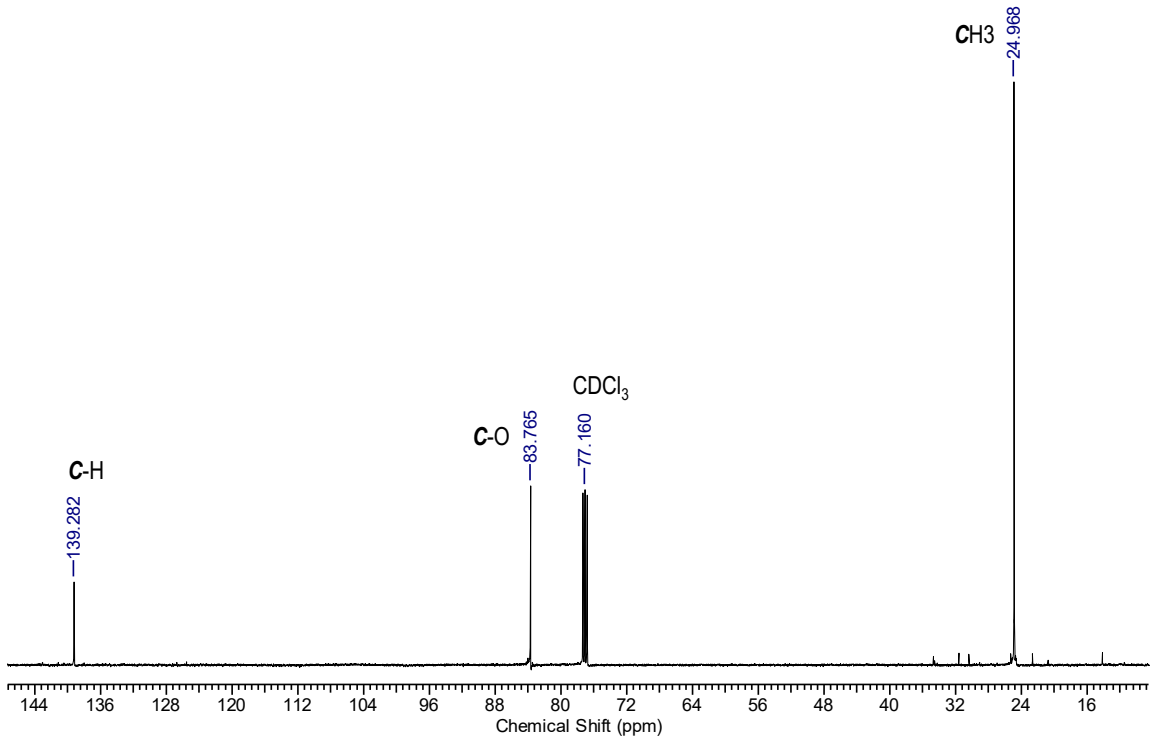

Figure 3.5. B) $^{13}C\{^{1}H\}$ NMR spectrum of **2BTe** in $CDCl_3$.

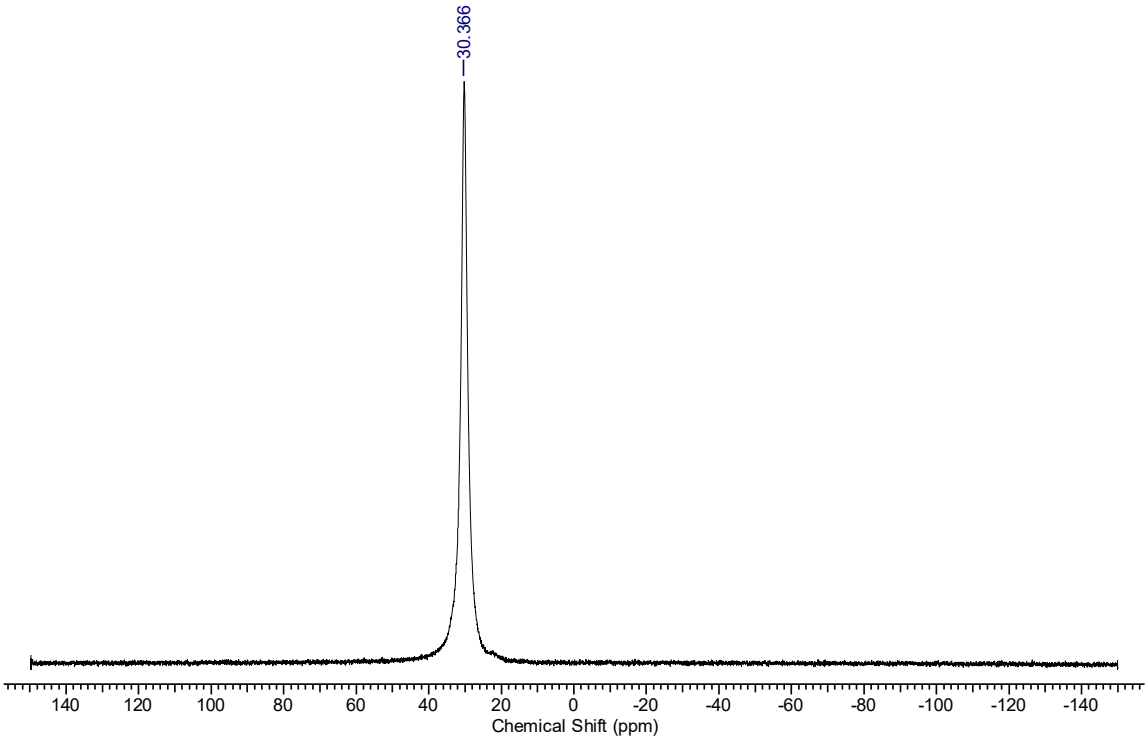

Figure 3.5. C) $^{11}B\{^{1}H\}$ NMR spectrum of **2BTe** in $CDCl_3$.

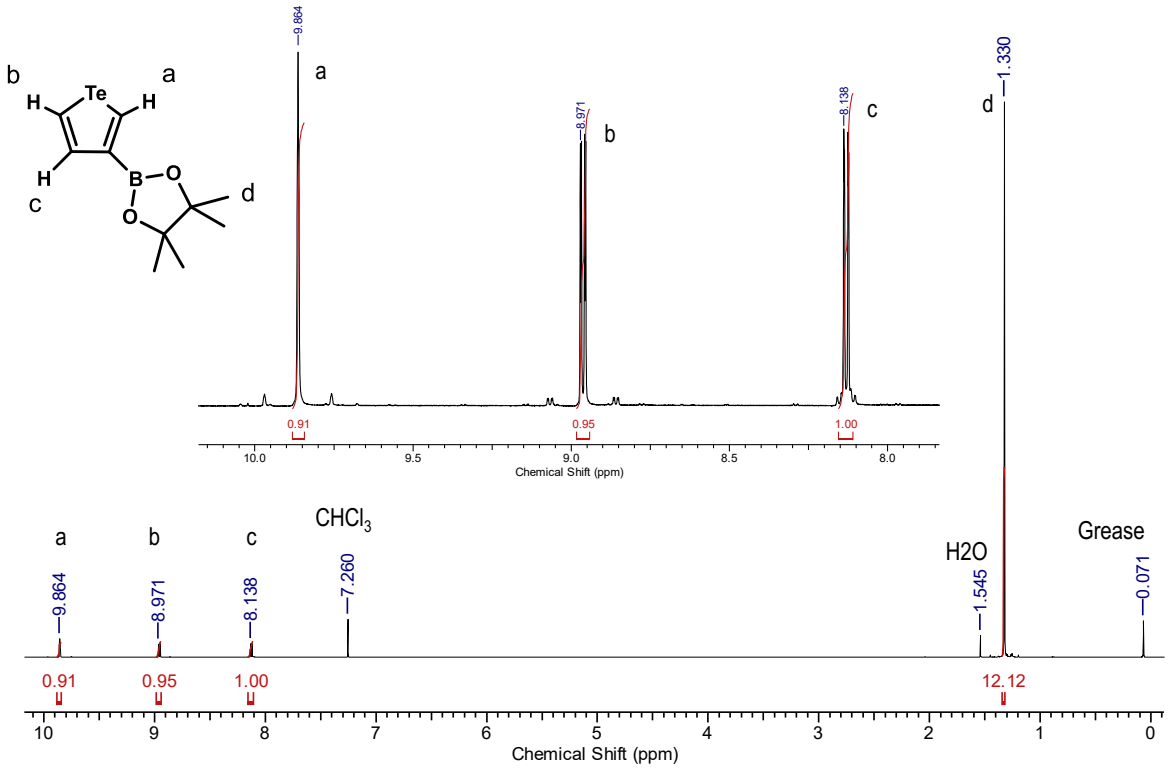

Figure 3.6. A) ^{1}H NMR spectrum of **BTe** in $CDCl_3$.

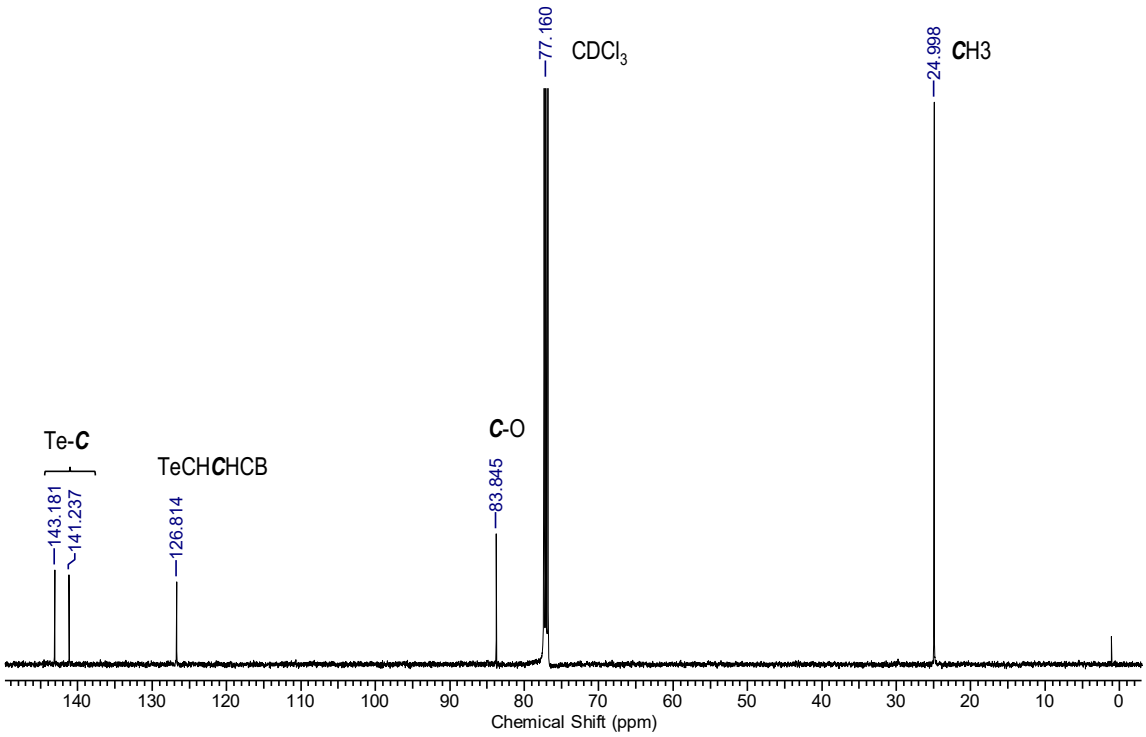

Figure 3.6. B) $^{13}C\{^{1}H\}$ NMR spectrum of **BTe** in $CDCl_3$.

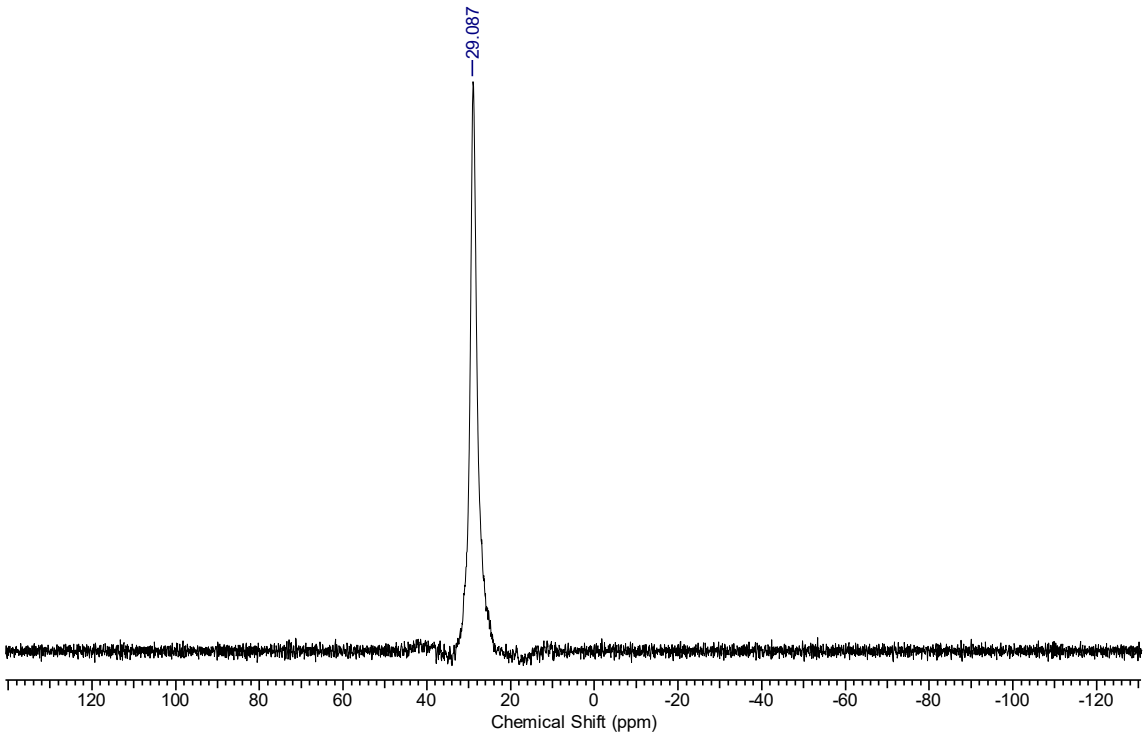

Figure 3.6. C) $^{11}B\{^{1}H\}$ NMR spectrum of **BTe** in $CDCl_3$.

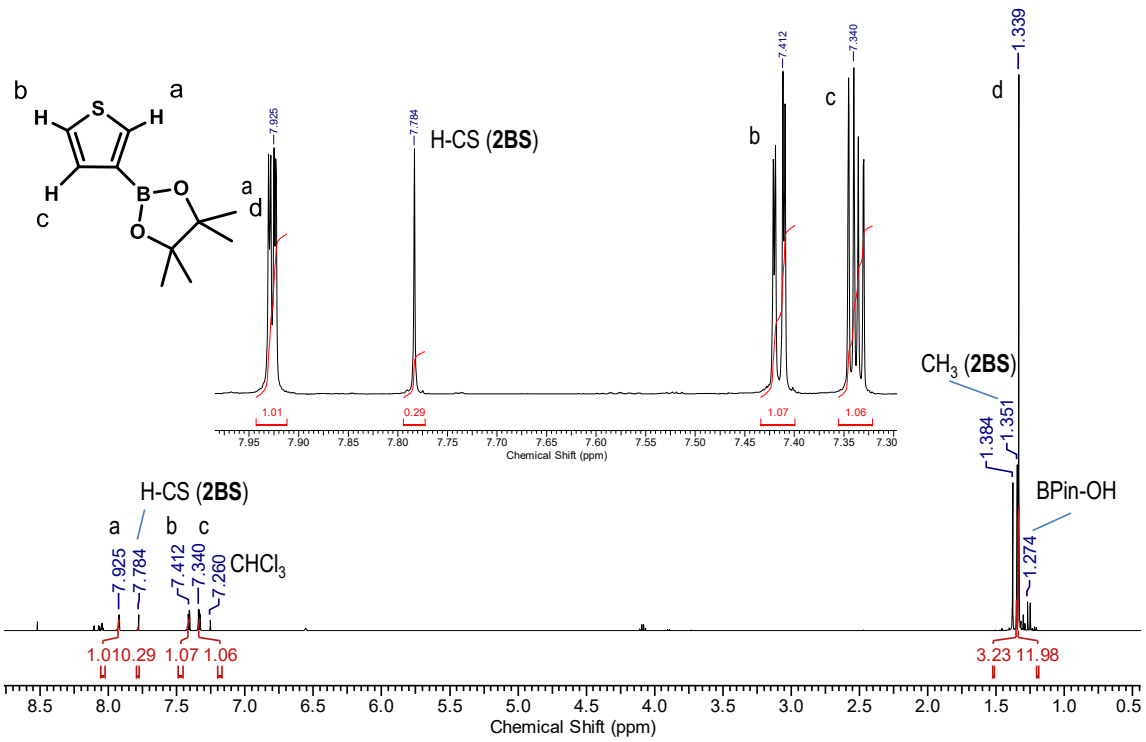

Figure 3.7. A) ^{1}H-NMR spectrum of a mixture of **BS** and **2BS** in $CDCl_3$.

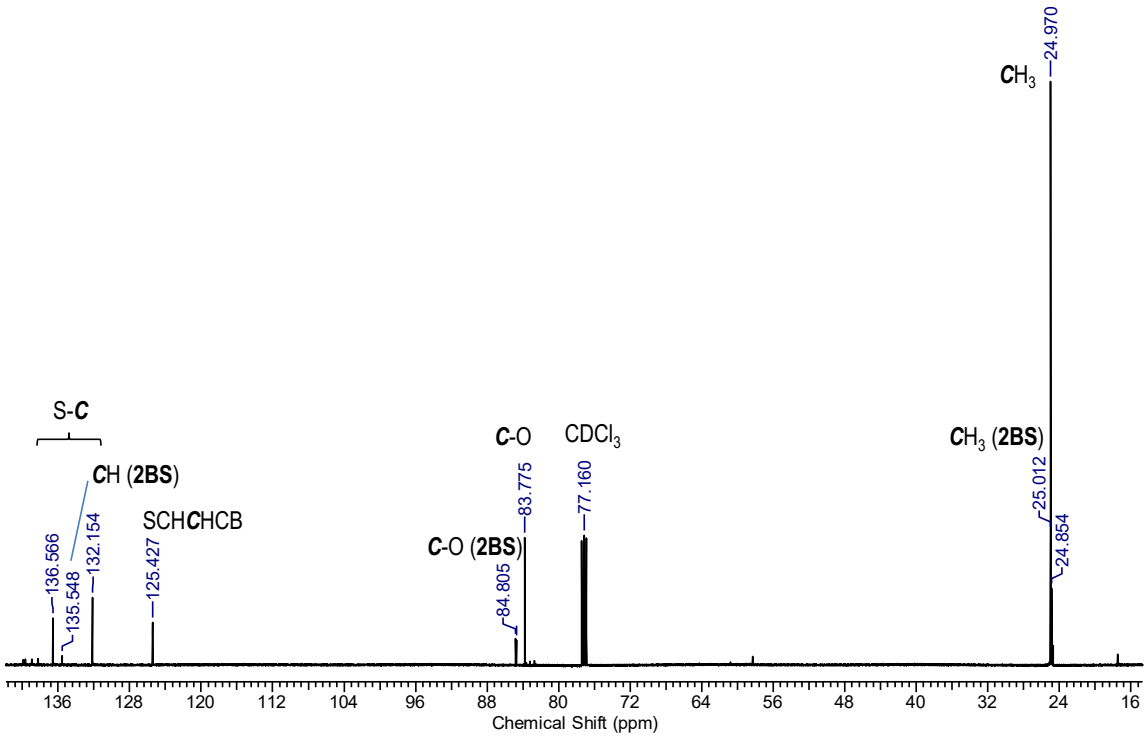

Figure 3.7. B) $^{13}C\{^{1}H\}$ NMR spectrum of a mixture of **BS** and **2BS** in $CDCl_3$.

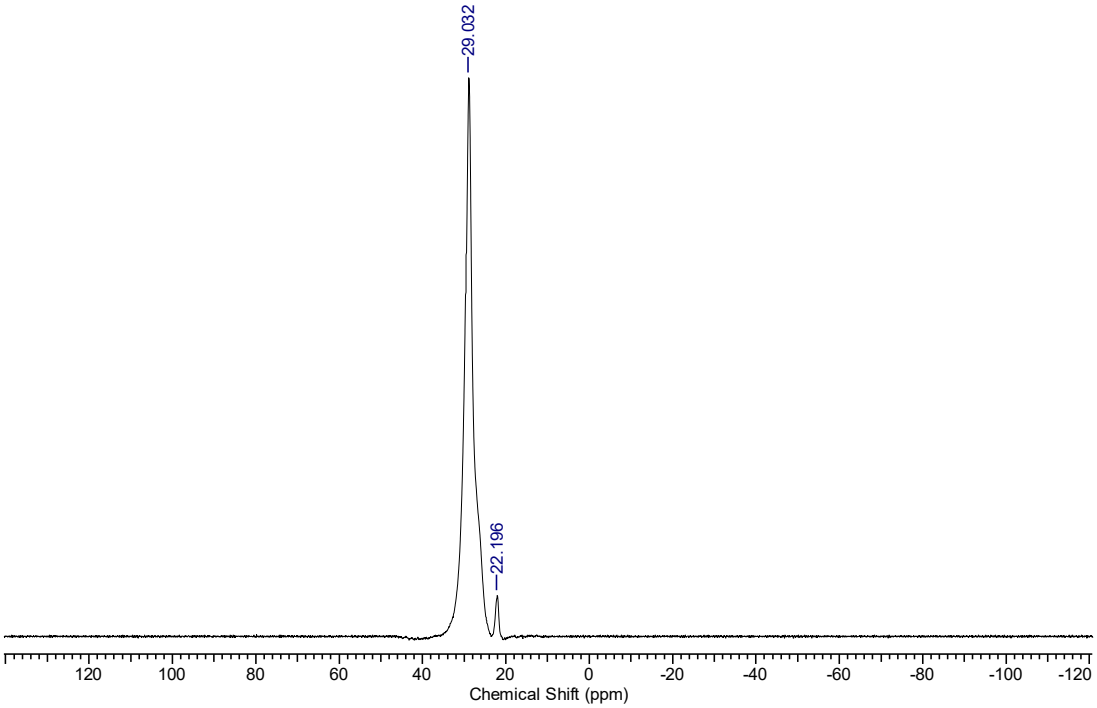

Figure 3.7. C) $^{11}B\{^{1}H\}$ NMR spectrum of a mixture of **BS** and **2BS** in $CDCl_3$.

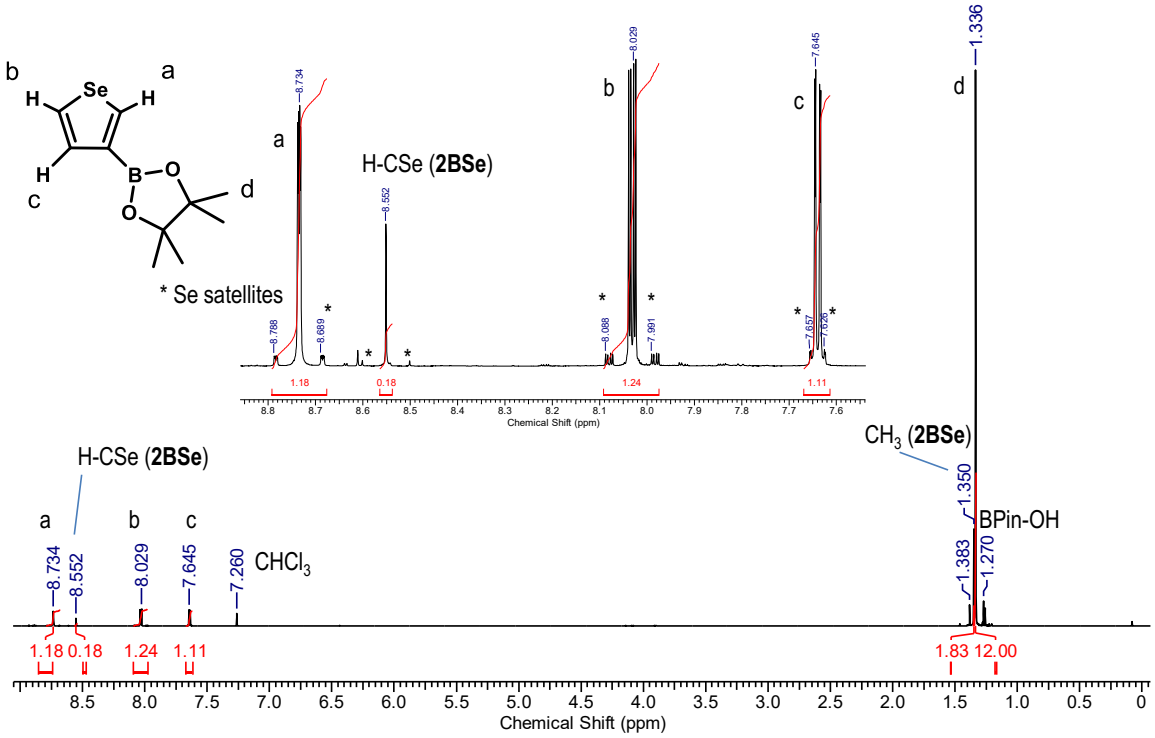

Figure 3.8. A) ^{1}H NMR spectrum of a mixture of **BSe** and **2BSe** in $CDCl_3$.

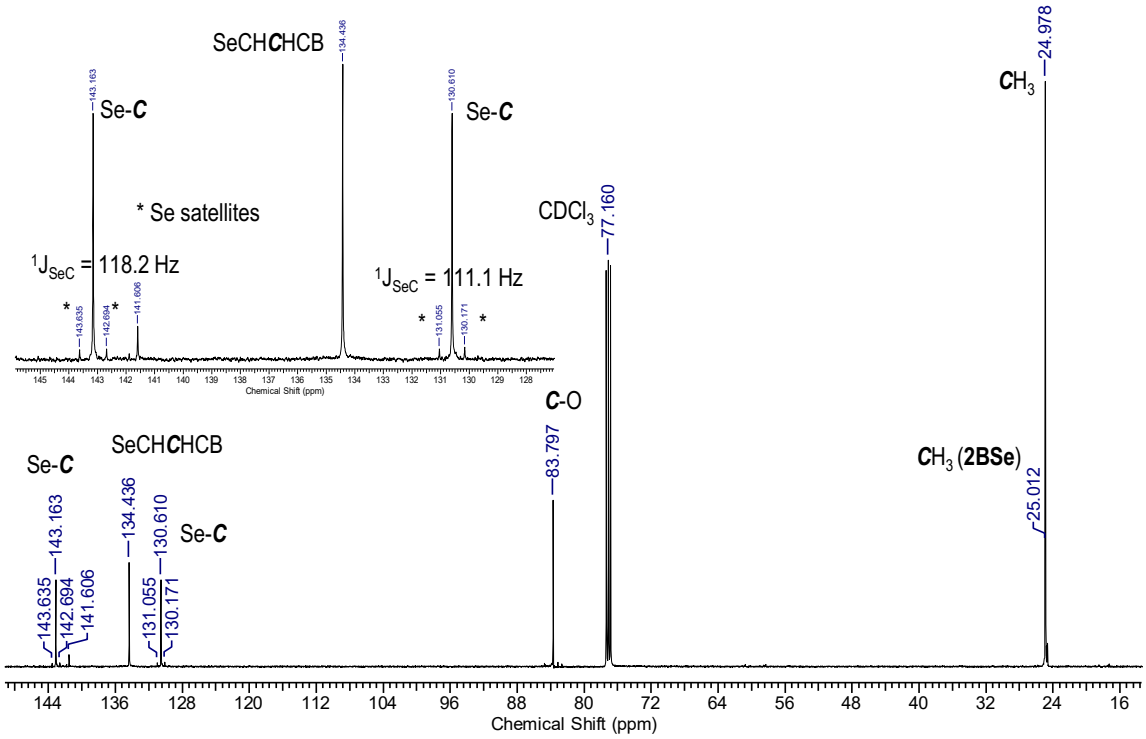

Figure 3.8. B) $^{13}C\{^1H\}$ NMR spectrum of a mixture of **BSe** and **2BSe** in $CDCl_3$.

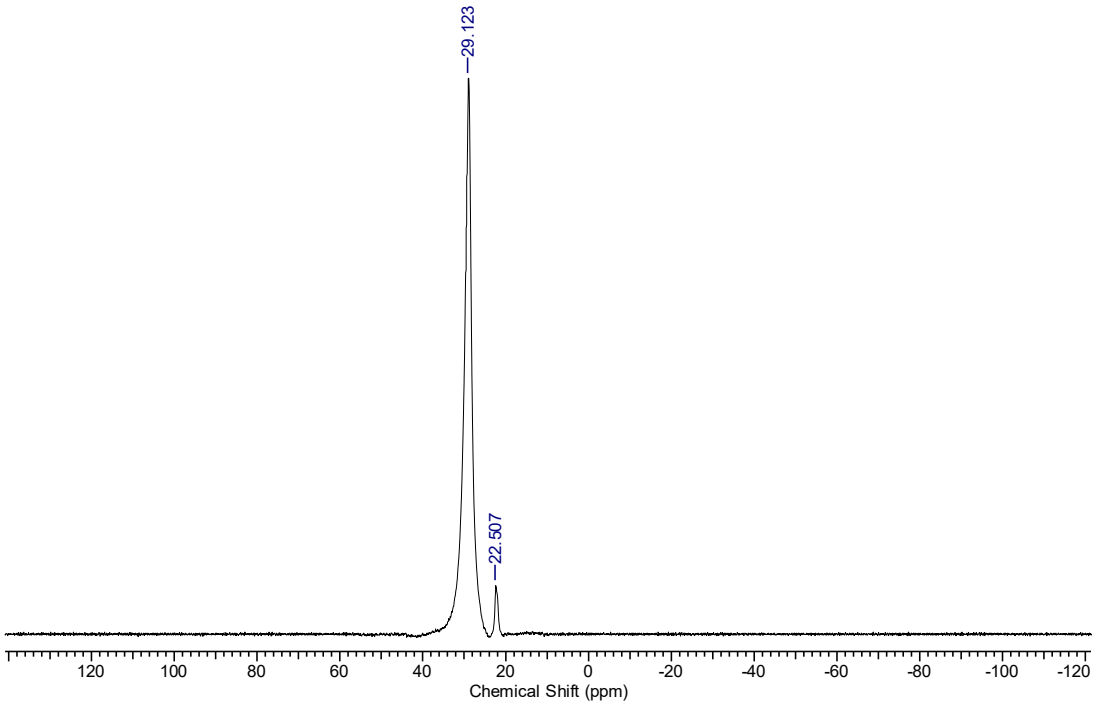

Figure 3.8. C) $^{11}B\{^1H\}$ NMR spectrum of **BSe** and **2BSe** in $CDCl_3$.

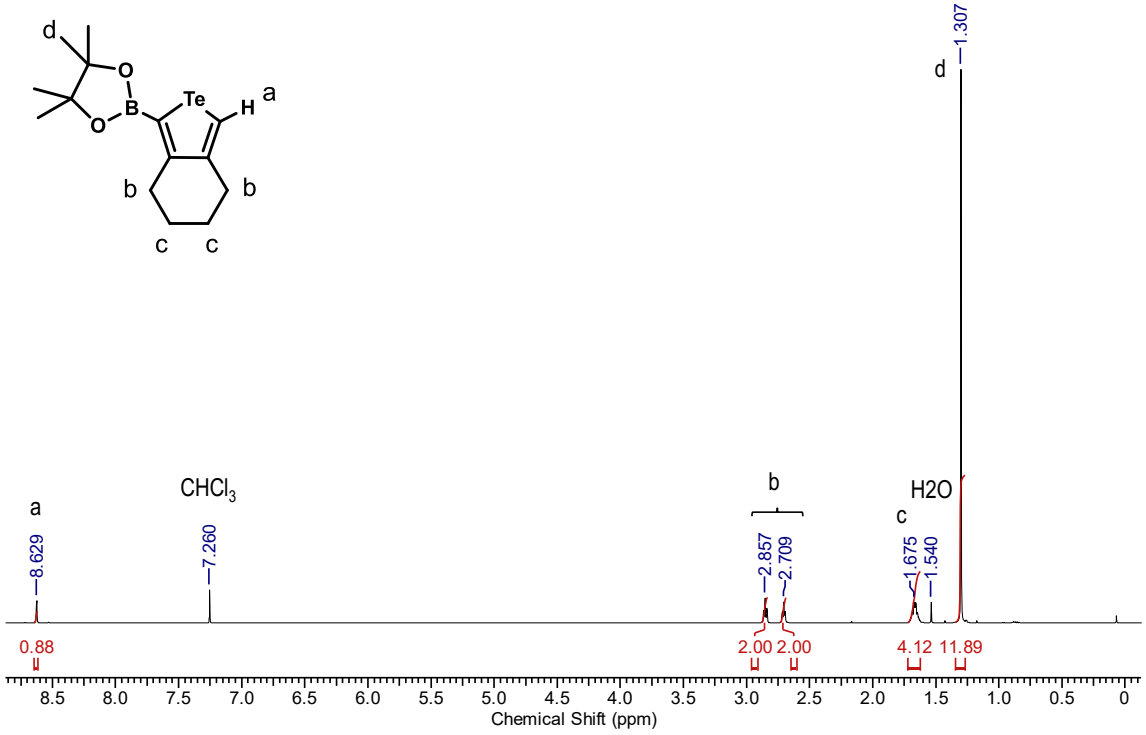

Figure 3.9. A) ^{1}H NMR spectrum of **B-Te-6-H** in $CDCl_3$.

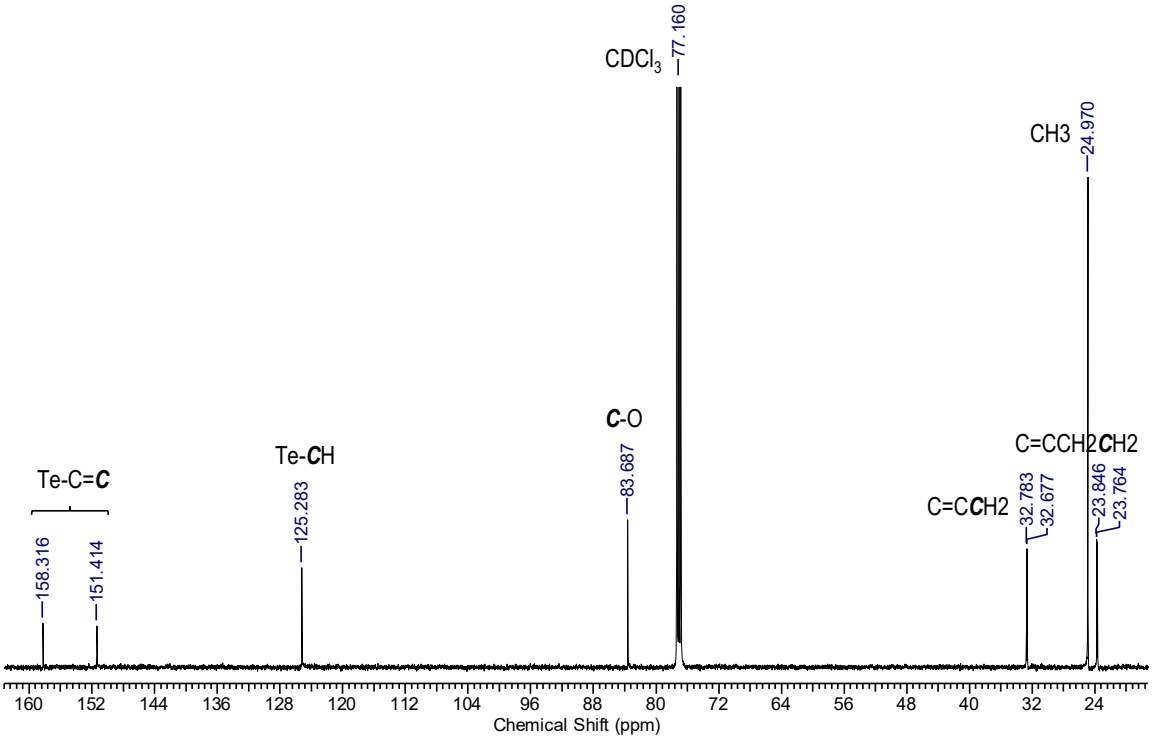

Figure 3.9. B) $^{13}C\{^{1}H\}$ NMR spectrum of **B-Te-6-H** in $CDCl_3$.

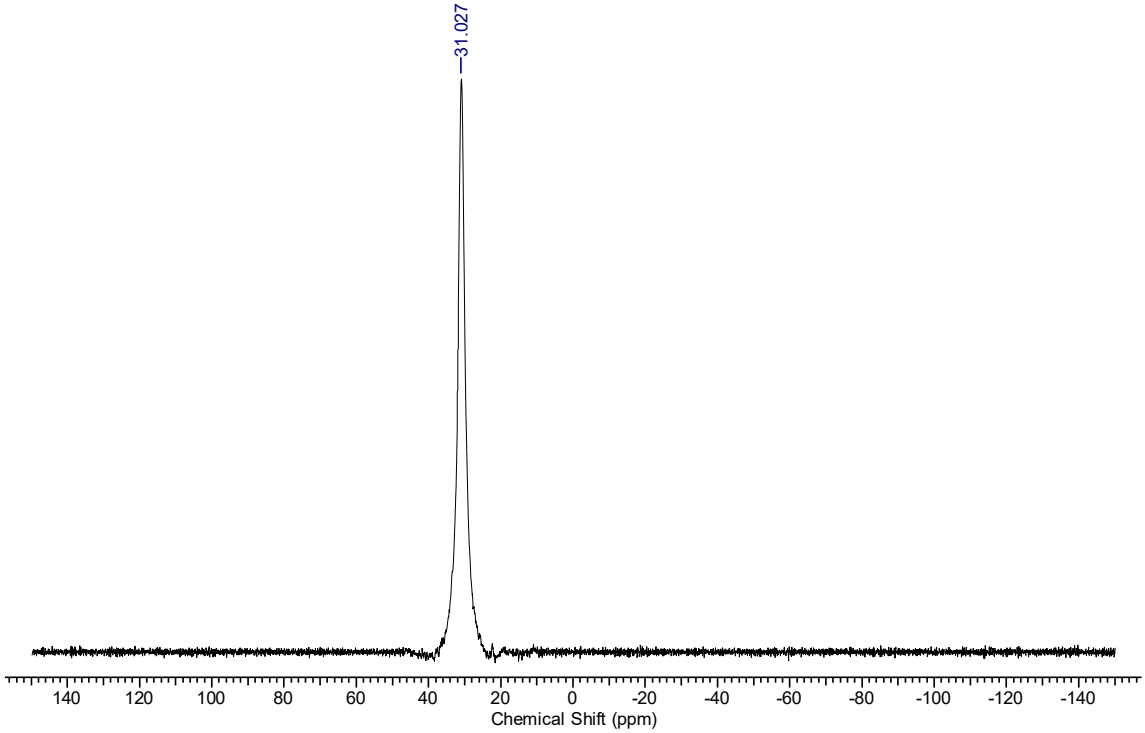

Figure 3.9. C) $^{11}B\{^{1}H\}$ NMR spectrum of **B-Te-6-H** in $CDCl_3$.

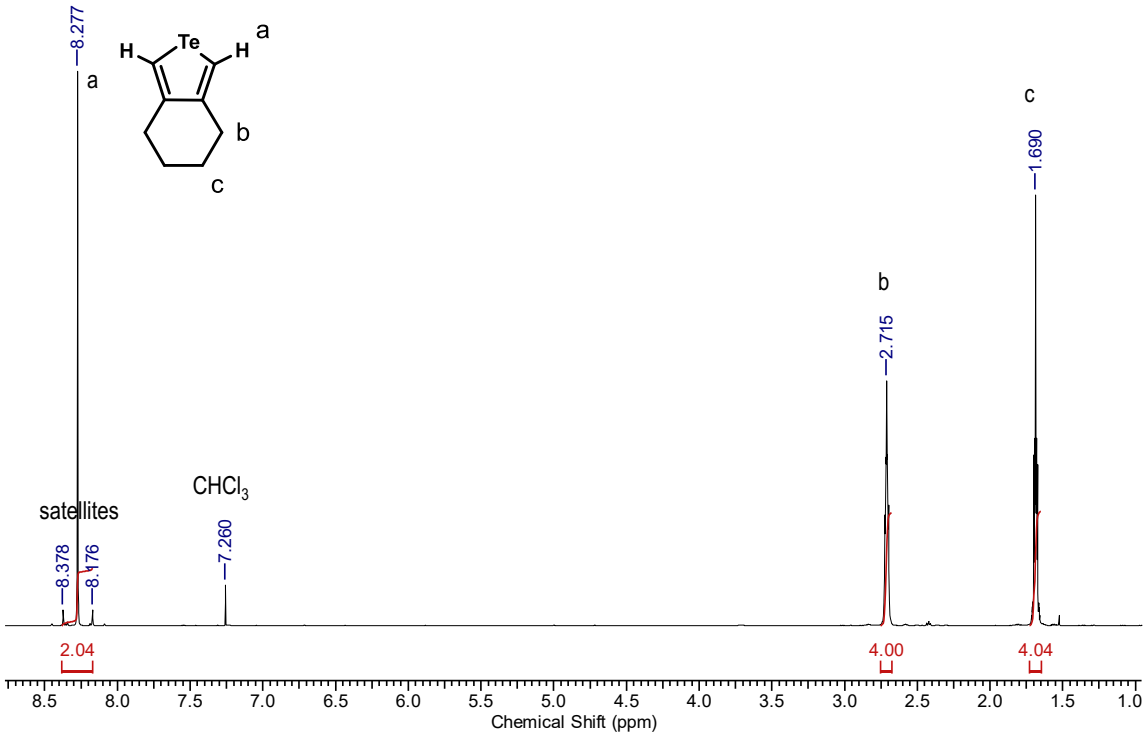

Figure 3.10. A) ^{1}H NMR spectrum of **H-Te-6-H** in $CDCl_3$.

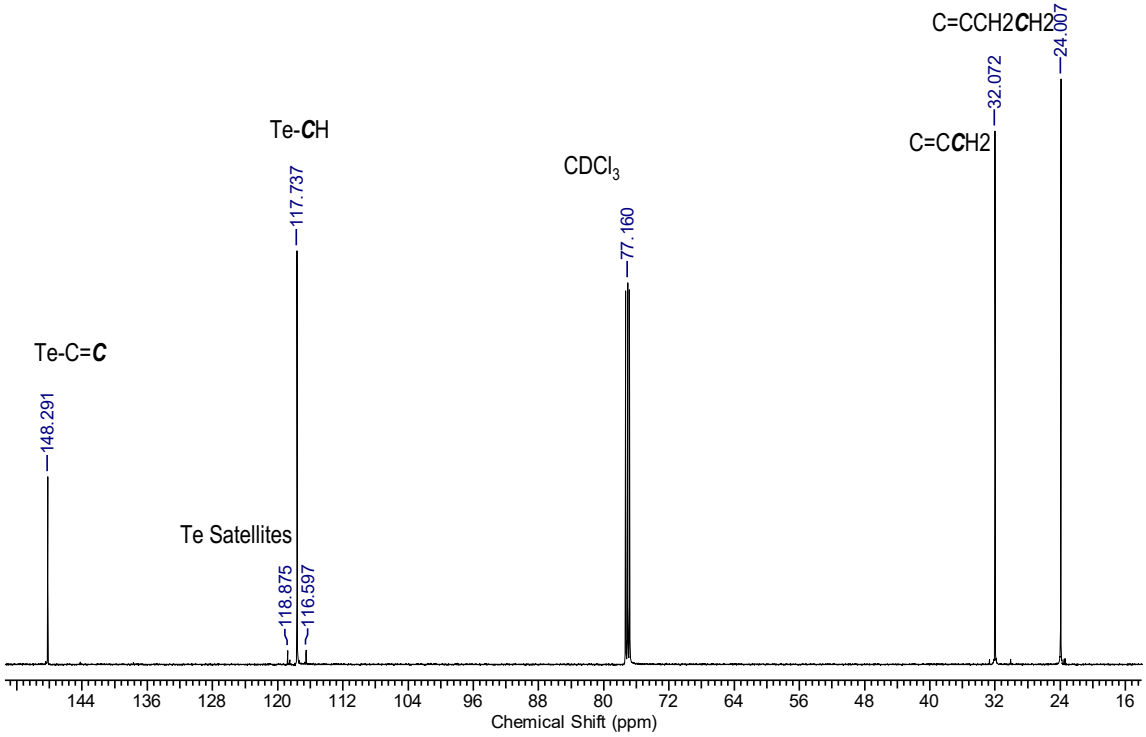

Figure 3.10. B) $^{13}C\{^{1}H\}$ NMR spectrum of **H-Te-6-H** in $CDCl_3$.

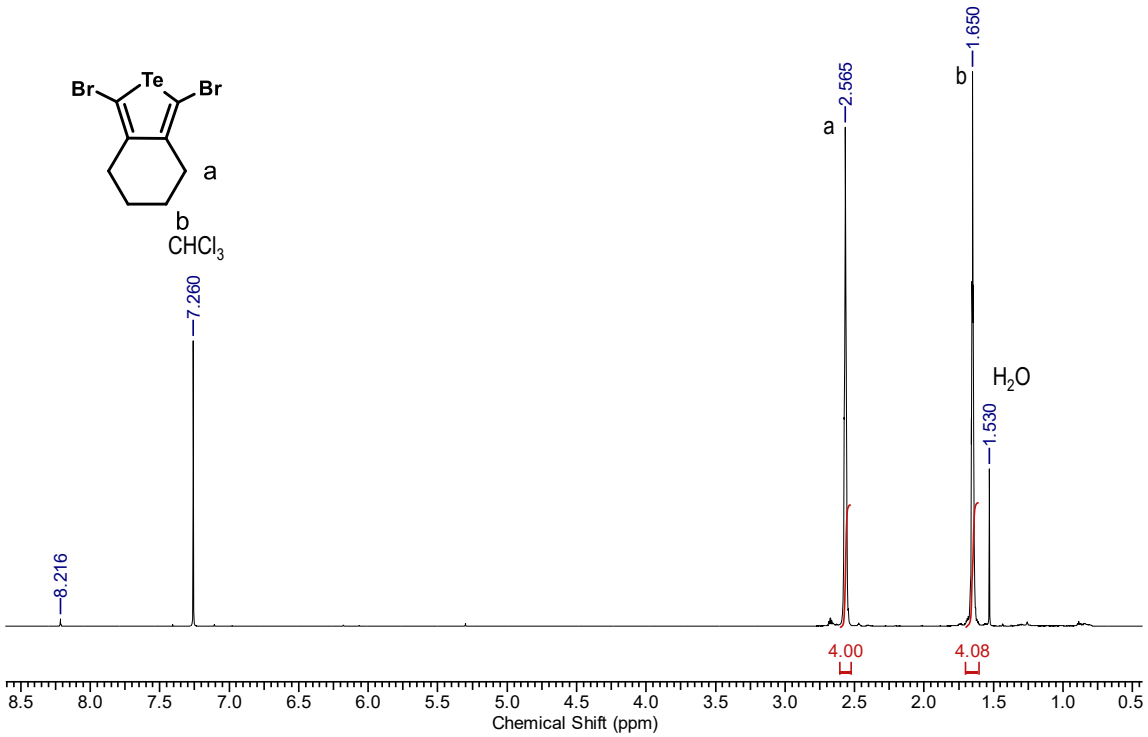

Figure 3.11. A) ^{1}H NMR spectrum of **Br-Te-6-Br** in $CDCl_3$.

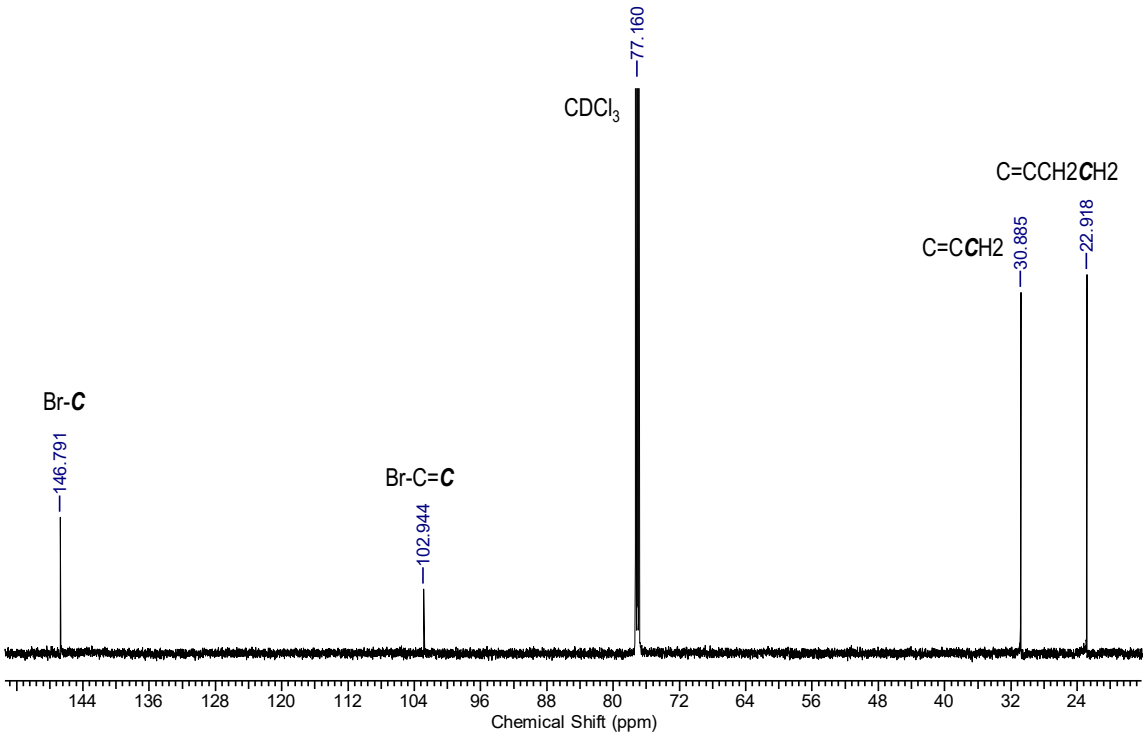

Figure 3.11. B) $^{13}C\{^{1}H\}$ NMR spectrum of **Br-Te-6-Br** in $CDCl_3$.

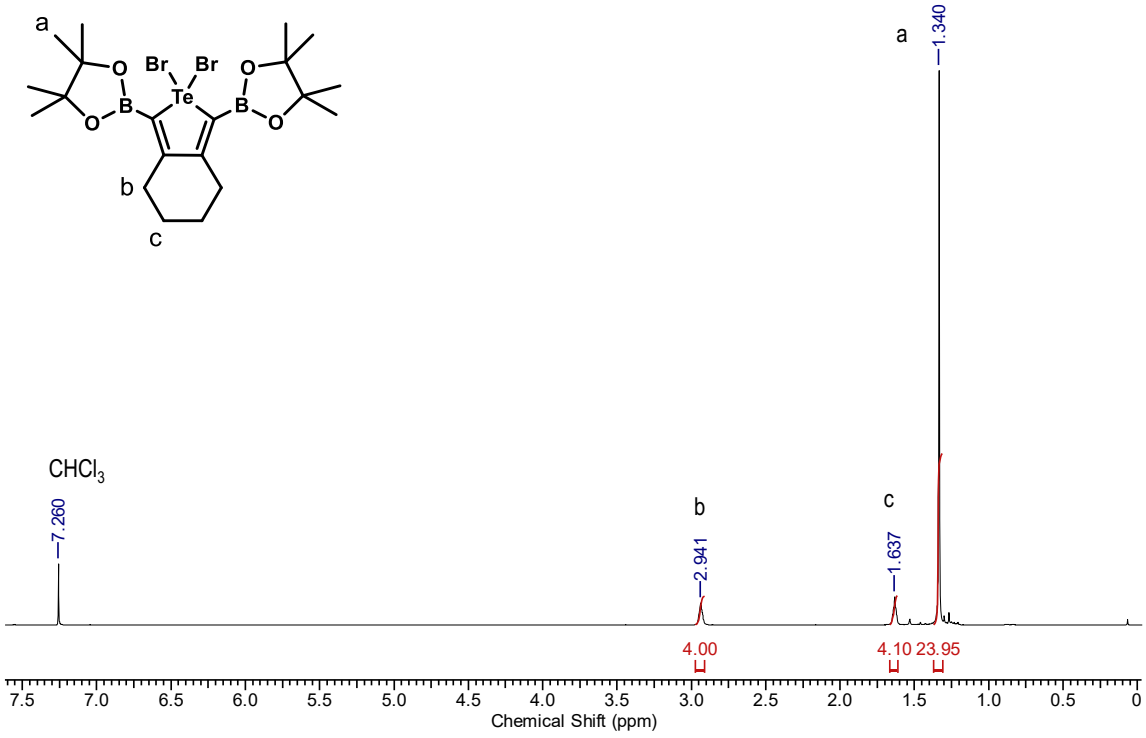

Figure 3.12. A) ^{1}H NMR spectrum of **B-TeBr$_2$-6-B** in $CDCl_3$.

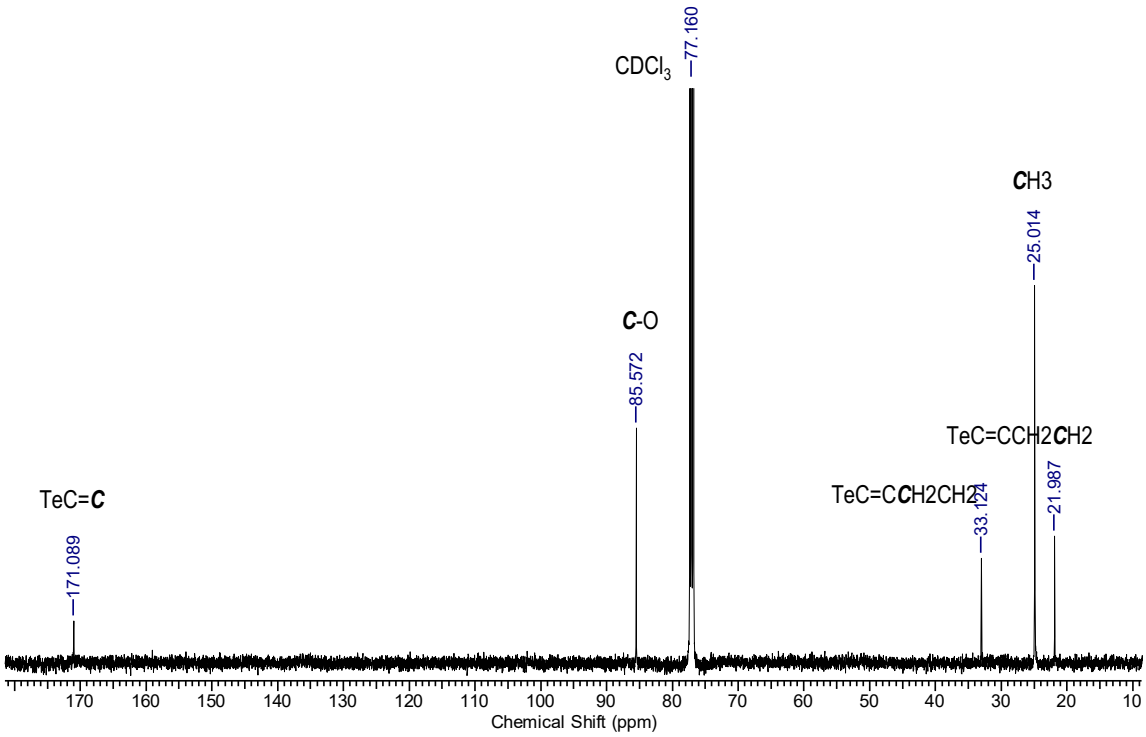

Figure 3.12. B) $^{13}C\{^{1}H\}$ NMR spectrum of **B-TeBr$_2$-6-B** in $CDCl_3$.

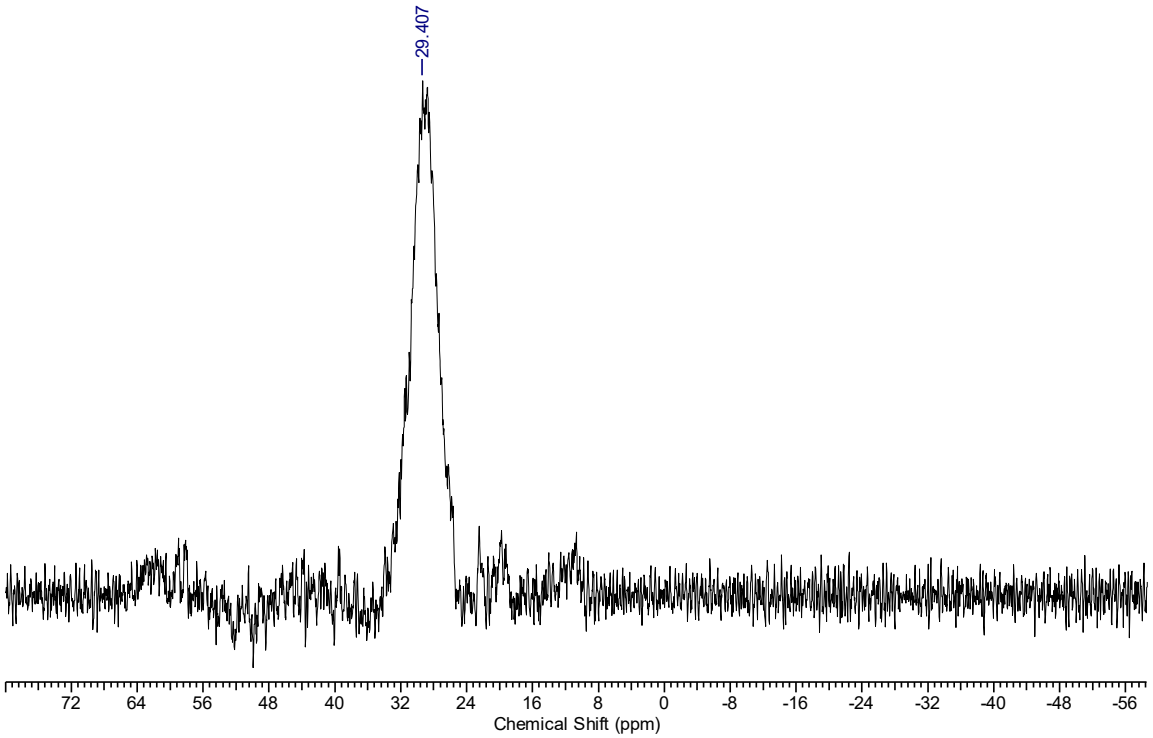

Figure 3.12. C) $^{11}B\{^{1}H\}$ NMR spectrum of **B-TeBr$_2$-6-B** in $CDCl_3$.

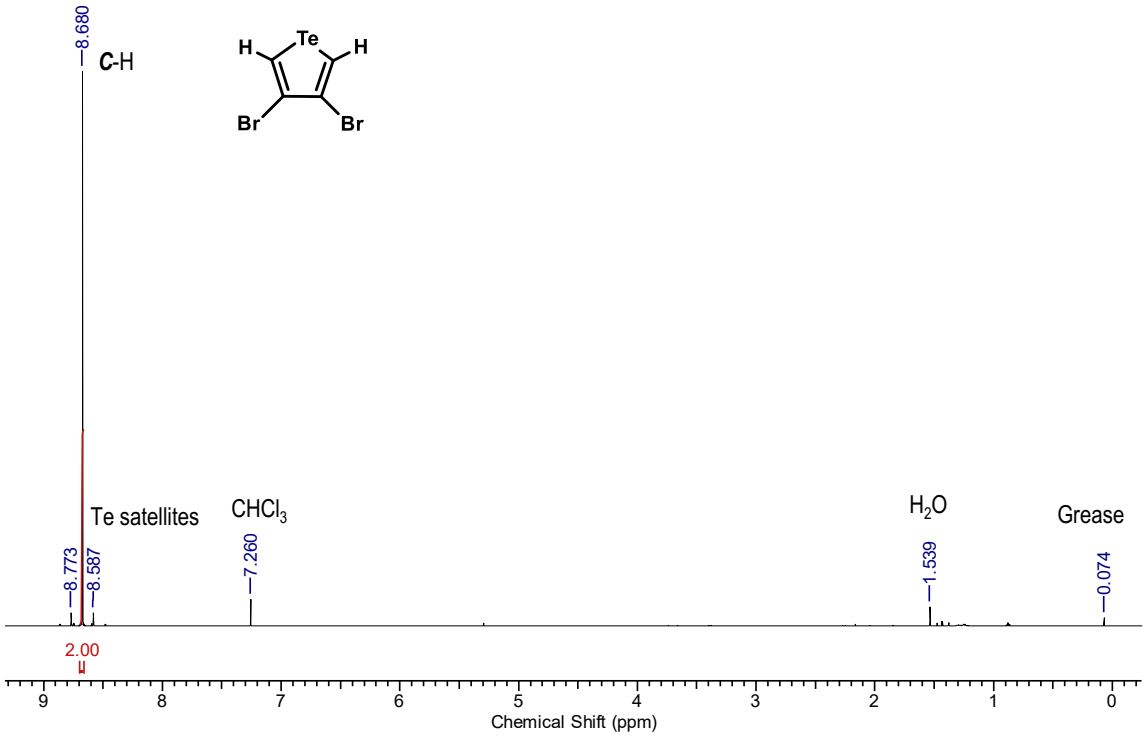

Figure 3.13. A) ^{1}H NMR spectrum of **2BrTe** in $CDCl_3$.

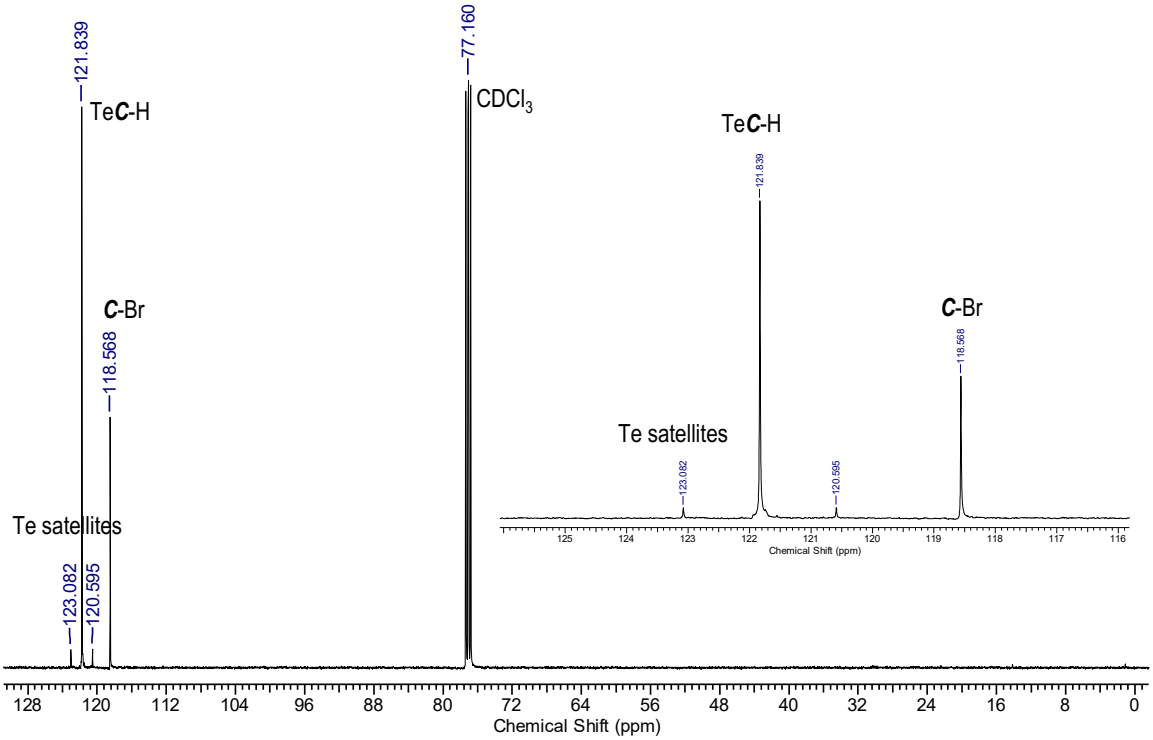

Figure 3.13. B) $^{13}C\{^{1}H\}$ NMR spectrum of **2BrTe** in $CDCl_3$.

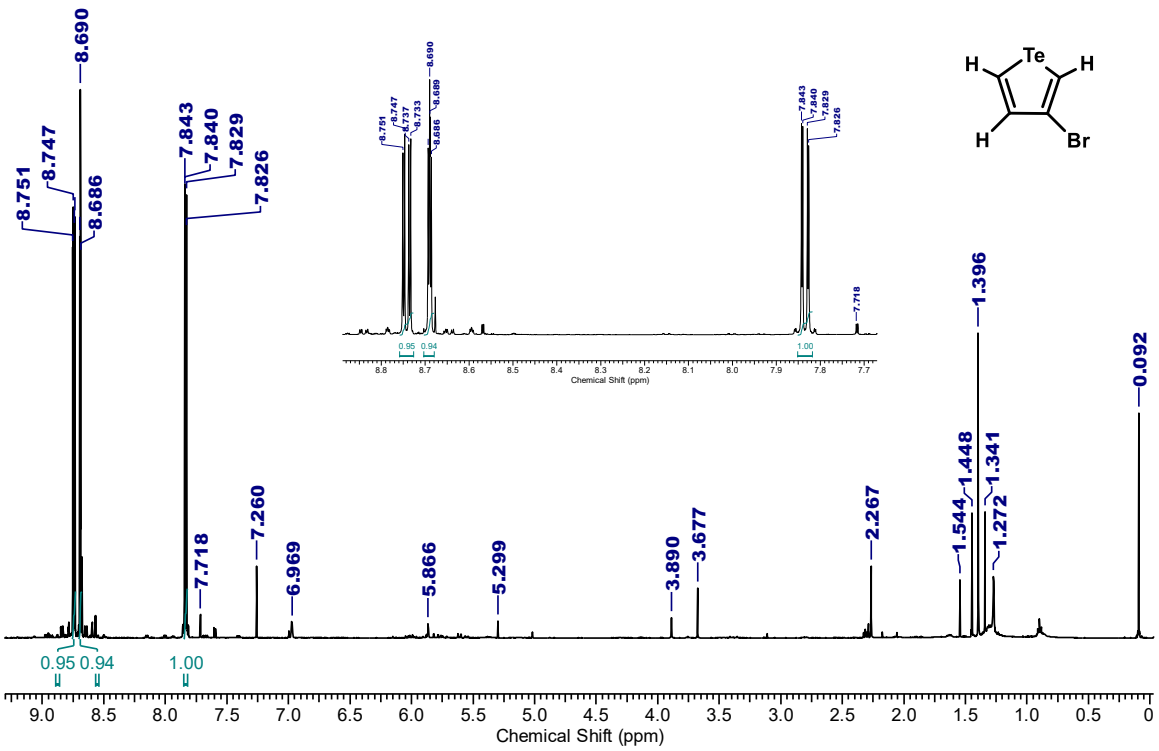

Figure 3.14. A) ^{1}H NMR spectrum of **BrTe** in $CDCl_3$.

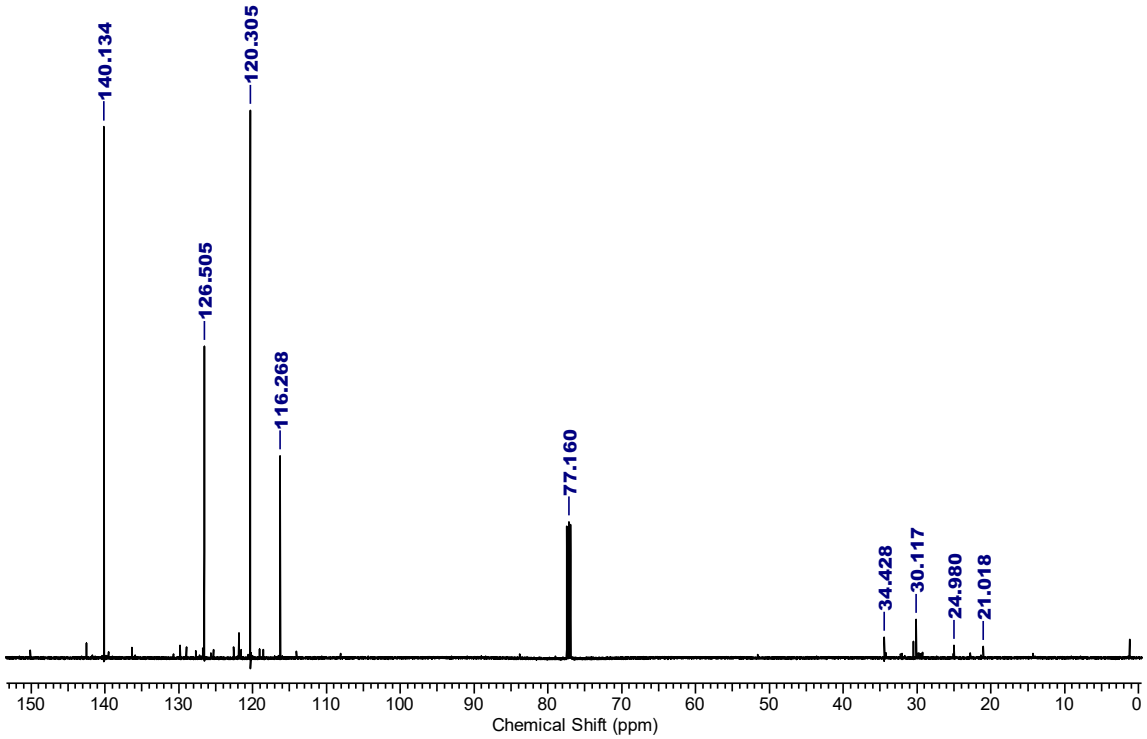

Figure 3.14. B) $^{13}C\{^{1}H\}$ NMR spectrum of **BrTe** in $CDCl_3$.

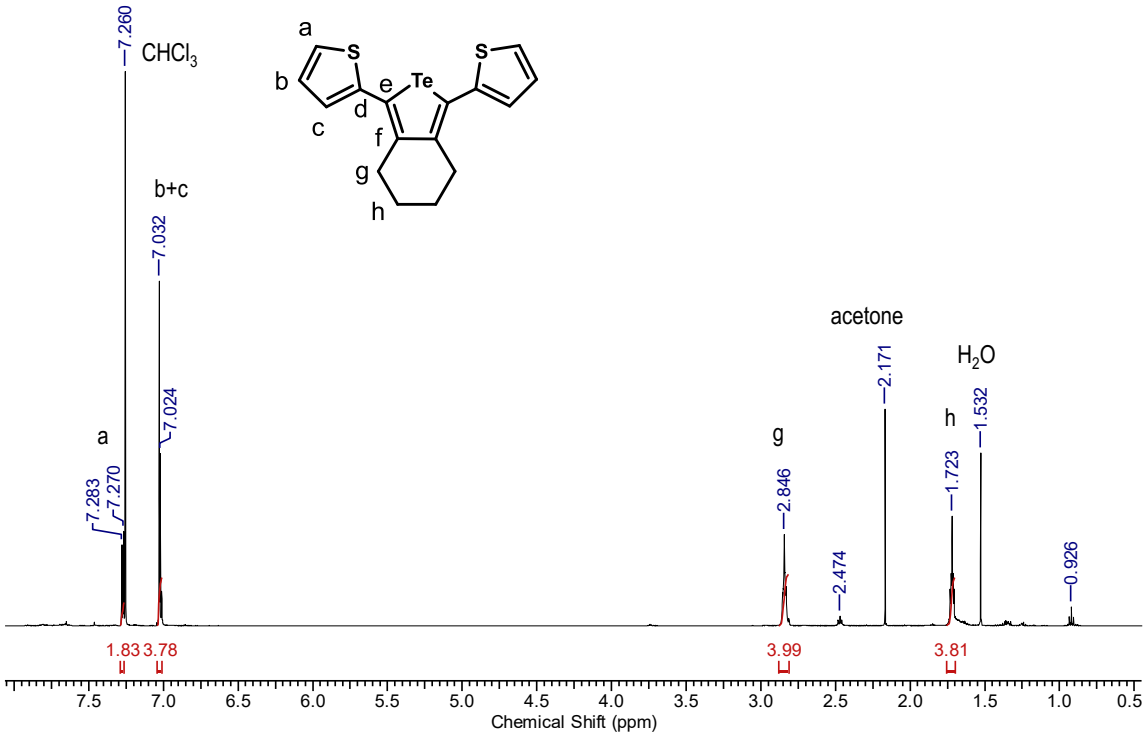

Figure 3.15. A) ^{1}H NMR spectrum of **T-Te-6-T** in $CDCl_3$.

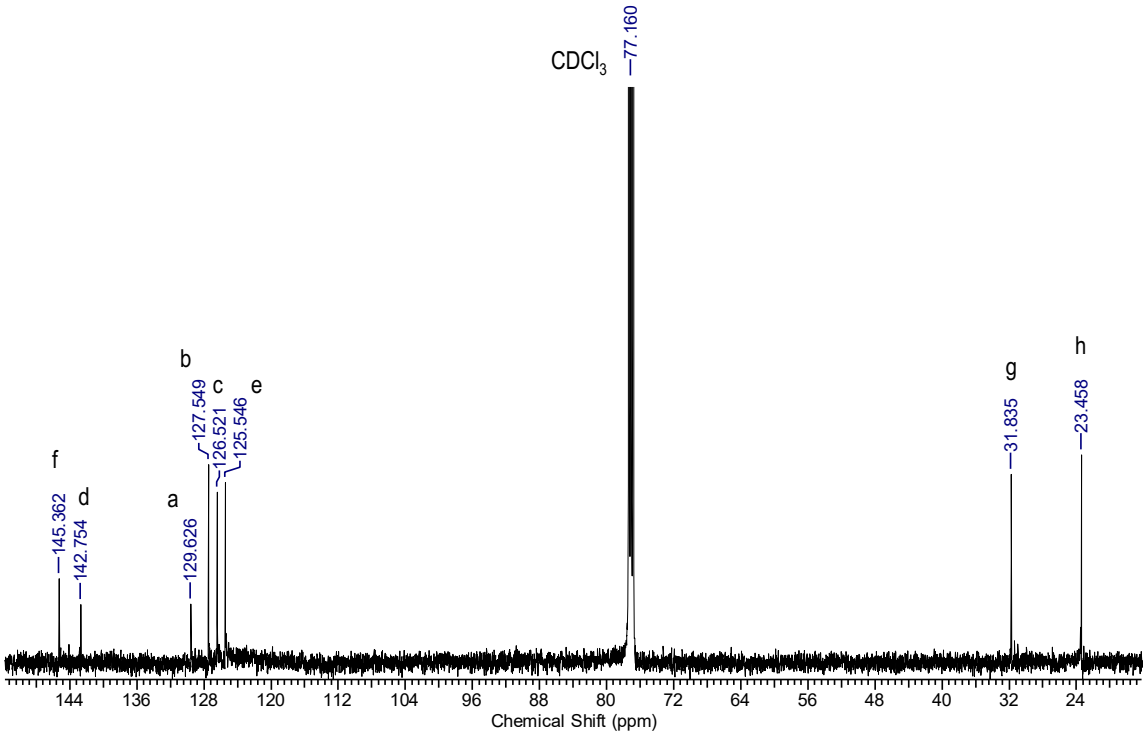

Figure 3.15. B) $^{13}C\{^{1}H\}$ NMR spectrum of **T-Te-6-T** in $CDCl_3$.

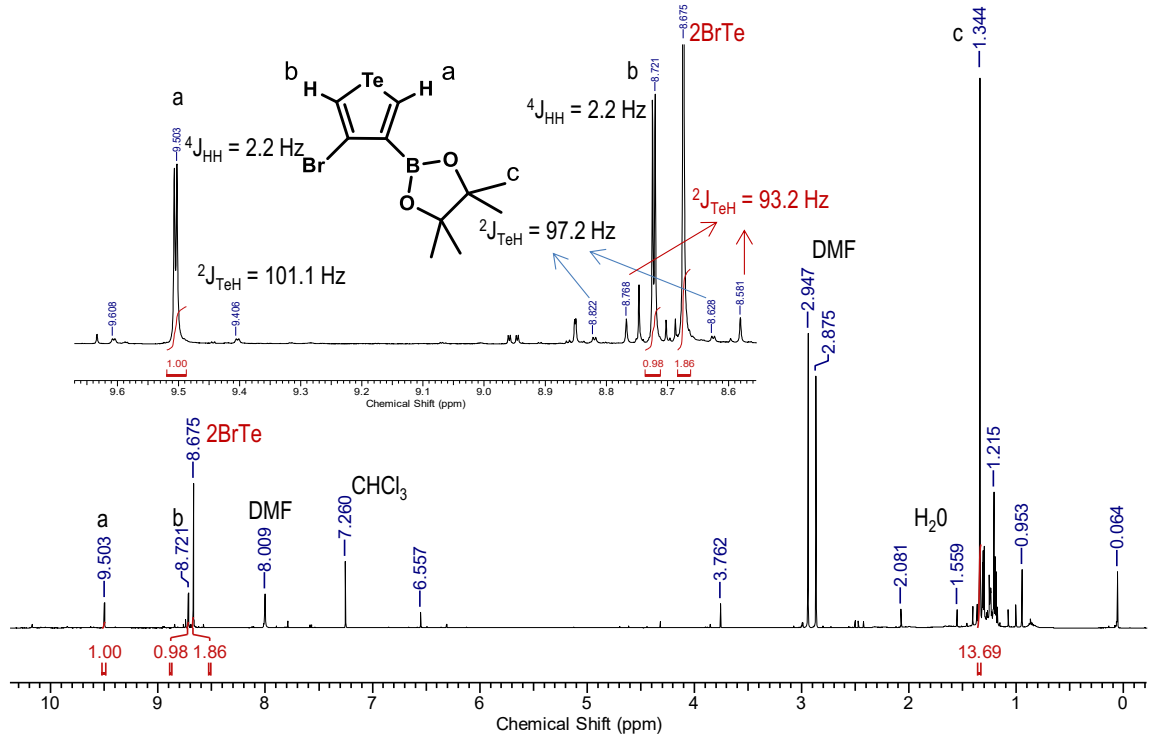

Figure 3.16. ^{1}H NMR spectrum of a reaction mixture containing **BrBTe** and **2BrTe** in $CDCl_3$.

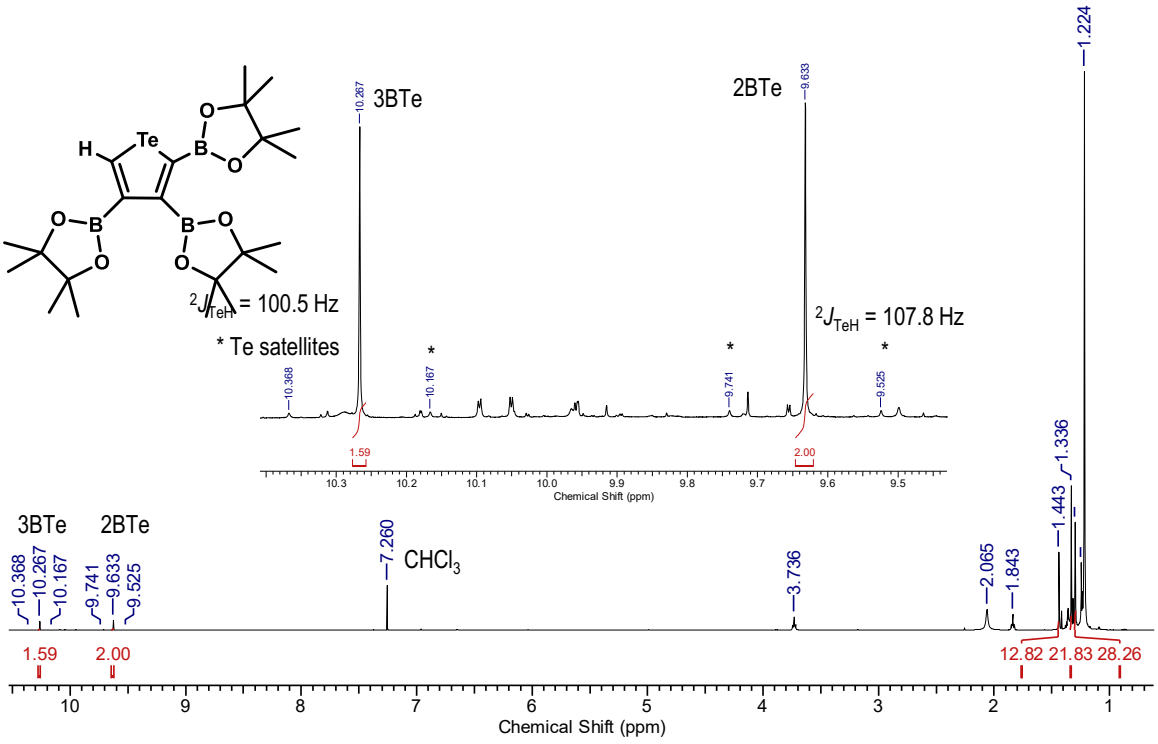

Figure 3.17. ^{1}H NMR spectrum of a reaction mixture containing **3BTe** and **2BTe** in $CDCl_3$.

3.6. REFERENCES

1. Rivard, E. *Chem. Lett.* **2015**, *44*, 730-736.
2. Carrera, E. I.; Seferos, D. S. *Macromolecules* **2015**, *48*, 297-308.
3. He, G.; Shynkaruk, O.; Lui, M. W.; Rivard, E. *Chem. Rev.* **2014**, *114*, 7815-7880.
4. Jahnke, A. A.; Seferos, D. S. *Macrom. Rapid Commun.* **2011**, *32*, 943-951.
5. Chivers, T.; Laitinen, R. S. *Chem. Soc. Rev.* **2015**, *44*, 1725-1739.
6. He, G.; Torres Delgado, W.; Schatz, D. J.; Merten, C.; Mohammadpour, A.; Mayr, L.; Ferguson, M. J.; McDonald, R.; Brown, A.; Shankar, K.; Rivard, E. *Angew. Chem. Int. Ed.* **2014**, *53*, 4587-4591.
7. He, G.; Wiltshire, B. D.; Choi, P.; Savin, A.; Sun, S.; Mohammadpour, A.; Ferguson, M. J.; McDonald, R.; Farsinezhad, S.; Brown, A.; Shankar, K.; Rivard, E. *Chem. Commun.* **2015**, *51*, 5444-5447.
8. Kryman, M. W.; Schamerhorn, G. A.; Yung, K.; Sathyamoorthy, B.; Sukumaran, D. K.; Ohulchanskyy, T. Y.; Benedict, J. B.; Detty, M. R. *Organometallics* **2013**, *32*, 4321-4333.
9. Zander, M.; Kirsch, G. *Z. Naturforsch. A* **1989**, *44*, 205-209.
10. Lapkowski, M.; Motyka, R.; Suwinski, J.; Data, P. *Macromol. Chem. Phys.* **2012**, *213*, 29-35.
11. Kaur, M.; Yang, D. S.; Choi, K.; Cho, M. J.; Choi, D. H. *Dyes Pigments* **2014**, *100*, 118-126.
12. Annaka, T.; Nakata, N.; Ishii, A. *Organometallics* **2015**, *34*, 1272-1278.
13. Kremer, A.; Fermi, A.; Biot, N.; Wouters, J.; Bonifazi, D. *Chem. Eur. J.* **2016**, *22*, 5665-5675.
14. Carrera, E. I.; Lanterna, A. E.; Lough, A. J.; Scaiano, J. C.; Seferos, D. S. *J. Am. Chem. Soc*. **2016**, *138*, 2678-2689.
15. Inoue, S.; Jigami, T.; Nozoe, H.; Otsubo, T.; Ogura, F. *Tet. Lett.* **1994**, *35*, 8009-8012.
16. Planells, M.; Schroeder, B. C.; McCulloch, I. *Macromolecules* **2014**, *47*, 5889-5894.
17. Li, P. -F.; Schon, T. B.; Seferos, D. S. *Angew. Chem., Int. Ed.* **2015**, *54*, 9361-9366.

18. Mahrok, A. K.; Carrera, E. I.; Tilley, A. J.; Ye, S.; Seferos, D. S. *Chem. Commun.* **2015**, *51*, 5475-5478.
19. Park, Y. S.; Kale, T. S.; Nam, C. -Y.; Grubbs, R. B. *Chem. Commun.* **2014**, *50*, 7964 7967.
20. Jung, E. H.; Bee, S.; Yoo, T. W.; Jo, W. H. *Polym. Chem.* **2014**, *5*, 6545-6550.
21. Kaur, M.; Yang, D. S.; Shin, J.; Lee, T. W.; Choi, K.; Cho, M. J.; Choi, D. H. *Chem. Commun.* **2013**, *49*, 5495-5497.
22. Ashraf, R. S.; Meager, I.; Nikolka, M.; Kirkus, M.; Planells, M.; Schroeder, B. C.; Holliday, S.; Hurhangee, M.; Nielsen, C. B.; Sirringhaus, H.; McCulloch, I. *J. Am. Chem. Soc.* **2015**, *137*, 1314-1321.
23. Al-Hashimi, M.; Han, Y.; Smith, J.; Bazzi, H. S.; Alqaradawi, S. Y. A.; Watkins, S. E.; Anthopoulos, T. D.; Heeney, M. *Chem. Sci.* **2016**, *7*, 1093-1099.
24. Sweat, D. P.; Stephens, C. E. *Synthesis* **2009**, *19*, 3214-3218.
25. Sashida, H.; Kaname, M.; Ohyanagi, K. *Heterocycles* **2010**, *82*, 441-447.
26. He, G.; Kang, L.; Torres Delgado, W.; Shynkaruk, O.; Ferguson, M. J.; McDonald, R.; Rivard, E. *J. Am. Chem. Soc.* **2013**, *135*, 5360-5363.
27. Jahnke, A. A.; Djukic, B.; McCormick, T. M.; Domingo Buchaca, E.; Hellmann, C.; Lee, Y.; Seferos, D. S. *J. Am. Chem. Soc.* **2013**, *135*, 951-954.
28. Park, Y. S.; Wu, Q.; Nam, C. -Y.; Grubbs, R. B. *Angew. Chem., Int. Ed.* **2014**, *53*, 10691-10695.
29. Aprile, A.; Iversen, K. J.; Wilson, D. J. D.; Dutton, J. L. *Inorg. Chem.* **2015**, *54*, 4934-4939.
30. Osaka, I.; McCullough, R. D. *Acc. Chem. Res.* **2008**, *41*, 1202-1214.
31. Patra, A.; Bendikov, M. *J. Mater. Chem.* **2010**, *20*, 422-433.
32. Stefan, M. C.; Bhatt, M. P.; Sista, P.; Magurudeniya, H. D. *Polym. Chem.* **2012**, *7*, 1693-1701.
33. Higashihara, T.; Ueda, M. *Macromol. Res.* **2013**, *21*, 257-271.
34. Martin, M. L.; Trierweiler, M.; Galasso, V.; Fringuelli, F.; Taticchi, A. *J. Magn. Res.* **1981**, *42*, 155-158.
35. Bagherzadeh, S.; Mankad, N. P. *J. Am. Chem. Soc.* **2015**, *137*, 10898-10901.
36. Hawkeswood, S.; Stephan, D. W. *Dalton Trans.* **2005**, 2182-2187.

37. Shynkaruk, O.; He, G.; McDonald, R.; Ferguson, M. J.; Rivard, E. *Chem. Eur. J.* **2016**, *22*, 248-257.
38. Gandon, V.; Leca, D.; Aechtner, T.; Vollhardt, K. P. C.; Malacria, M.; Aubert, C. *Org. Lett.* **2014**, *6*, 3405-3407.
39. Dutton, J. L.; Farrar, G. J.; Sgro, M. J.; Battista, T. L.; Ragogna, P. J. *Chem. Eur. J.* **2009**, *15*, 10263-10271.
40. Kang, Y. K.; Deria, P.; Carroll, P. J.; Therein, M. J. *Org. Lett.* **2008**, *10*, 1341-1344.
41. Lozada, J.; Liu, Z.; Perrin, D. M. *J. Org. Chem.* **2014**, *79*, 5365-5368.
42. Ahn, S. -J.; Lee, C. -Y.; Kim, N. -K.; Cheon, C. -H. *J. Org. Chem.* **2014**, *79*, 7277-7285.
43. Liu, C.; Li, X.; Wu, Y.; Qiu, J. *RSC Adv.* **2014**, *4*, 54307-54311.
44. Liu, C.; Li, X.; Wu, Y. *RSC Adv.* **2015**, *5*, 15354-15358.
45. Li, G.; Shrotriya, V.; Huang, J. S.; Yao, Y.; Moriarty, T.; Emery, K.; Yang, Y. *Nature Mater.* **2005**, *4*, 864-868.
46. Jahnke, A. A.; Howe, G. W.; Seferos, D. S. *Angew. Chem., Int. Ed.* **2010**, *49*, 10140-10144.
47. Carrera, E. I.; McCormick, T. M.; Kapp, M. J.; Lough, A. J.; Seferos, D. S. *Inorg. Chem.* **2013**, *52*, 13779-13790.
48. Thompson, A. L.; Kabalka, G. W.; Akula, M. R.; Huffman, J. W. *Synthesis* **2005**, 547-550.
49. Shi, H.; Babinski, D. J.; Ritter, T. *J. Am. Chem. Soc.* **2015**, *137*, 3775-3778.
50. Jiang, Q.; Zhen, S.; Mo, D.; Lin, K.; Ming, S.; Wang, Z.; Liu, C.; Xu, J.; Yao, Y.; Duan, X.; Zhu, D.; Shi, H. *J. Polym. Sci. Part A Polym. Chem.* **2016**, *54*, 325–334.
51. Zhu, S. S.; Swager, T. M. *J. Am. Chem. Soc.* **1997**, *119*, 12568–12577.

Chapter 4

Synthesis of unsymmetric tellurophenes and study of the effect of electron withdrawing / donating groups on their luminescence properties

4.1. INTRODUCTION

The synthesis of fluorophores that can emit/absorb in different regions of the UV-vis spectrum is a highly researched topic in materials chemistry. A wide range of possible applications of those compounds such as in displays,[1] photovoltaics[2,3] and sensors[4] can be found in the literature. Of great interest to this Thesis, the search for stable phosphors for energy efficient LED has led to important breakthroughs, however there still exists challenges in relation to the ease of synthesis, stability and processability of these compounds.[5,6]

One well-known strategy for achieving efficient color-tunable emission is the push-pull concept.[7] Specifically, by placing strong electron-donating (push) or electron-withdrawing (pull) groups in conjugation within a molecule can lead to charge imbalance thereby enabling charge transfer upon excitation. Moreover, the wavelength (and colour) of emission can be tuned by varying the nature of the donor and/or acceptor groups present in the molecule. Commonly used donor groups include the amine-based triphenylamine (TPA) substituent and heterocyclic benzodithiophene. Common acceptor units include nitro, nitrile and trifluoromethyl substituents, and electron deficient heterocycles such as benzothiadiazole and quinoxaline. The optoelectronic properties of the design donor-acceptor (D-A) can also be modulated by the presence of aromatic spacers or linkers to give D-π-A type structures.[8–10]

Over the past decade, researchers have used the electron deficient nature of three-coordinated boron center as part of acceptor arrangements.[11] For example, Yamaguchi and coworkers[12,6] have formed different highly emissive D-π-A solids (Figure 4.1) with bis(dimesitylboryl)-phenyleneethynylene and dimesitylborylbithiophene groups as the acceptor unit and different electron-donating amino groups to tune the fluorescence emission of these solids from green to red. These compounds were also fluorescent in solution and are stable in the presence of air and water, and have high thermal stability (>350 °C). Moreover, the steric

bulk provided by the mesityl (Mes = 2,4,6-$Me_3C_6H_2$) groups on boron and the large Stokes shift arising from intramolecular charge transfer proved to be useful for avoiding quenching such as Dexter electron transfer (DET) and/or Förster resonance energy transfer in the solid state.[13–18]

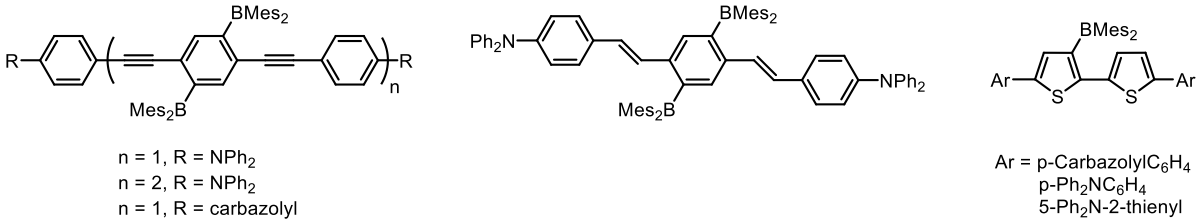

Figure 4.1. Emissive dimesitylboryl-substituted phenylene and bithiophene compounds.

The synthesis of unsymmetric (push-pull) tellurophenes has been explored by different research teams. For example, a tellurophene containing p-NO_2-C_6H_4 and p-$Bu_2NC_6H_4$ groups at 2- and 5-positions has been prepared by Seferos and coworkers (Figure 4.2) as part of a general study of on the addition of halogens to the Te centers in tellurophenes (and the latter photoelimination of X_2).[19] The donor capabilities of a series of D-A-D benzochalcogenophenes compounds (Figure 4.2) within photovoltaic devices has been reported.[20] By incorporating benzotellurophenes as the donor components, red-shifted absorption and increased external quantum efficiencies were noted in compared related compounds bearing lighter benzochalcogenophene analogues. In both reports, ipso-arylative cross-coupling was used to functionalize the Te heterocycles.

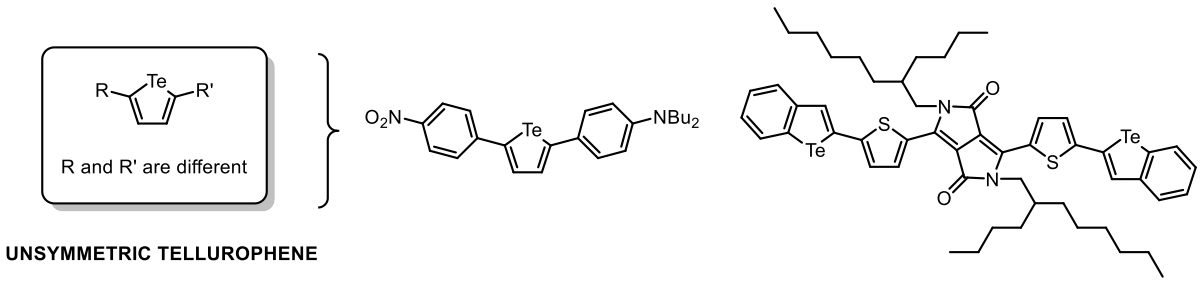

Figure 4.2. Examples of unsymmetric tellurophenes structures.

Recently, the Rivard group have synthesized a series of air stable phosphorescent BPin-substituted tellurophenes (Figure 4.3).[21,22] One of the unsymmetrically-substituted tellurophenes **2,4-BPin$_2$-3,5-Ph$_2$-Te** displayed yellow-orange phosphorescence (λ_{em} = 577 nm, τ = 17.9 μs) which was different from the usual green emission (λ_{em} = 517-535 nm) observed in pre-existing tellurophenes containing BPin groups at the 2- and 5- positions (**2,5-BPin$_2$-3,4-Ph$_2$-Te**). This observation opened the question about the possibility of tuning the luminescence of BPin-capped tellurophenes through placing groups with different electron donating/withdrawing abilities at the opposite side of the BPin substitution, promoting possible electronic changes in the charge transfer between tellurium and the boron centers (Figure 4.4).

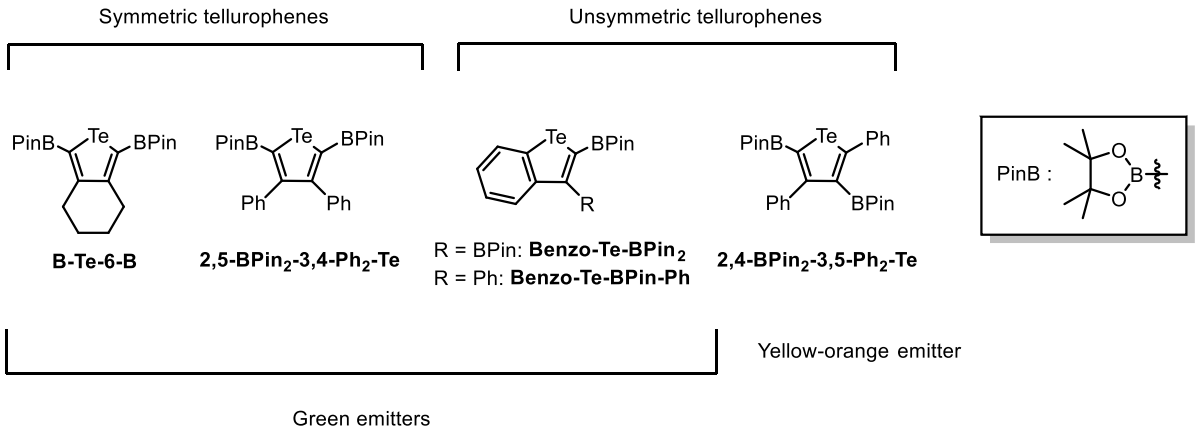

Figure 4.3. Tellurophenes phosphors containing BPin groups as substituents.

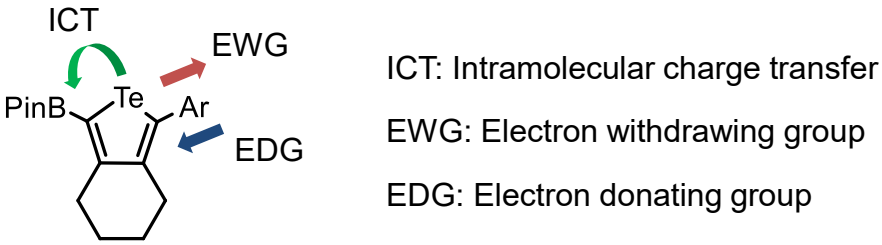

Figure 4.4. Strategy to tune the luminescence of BPin-substituted tellurophenes.

Recently, Dr. Shynkaruk[23] from the Rivard group attempted to form tetra-substituted unsymmetric tellurophenes via selective reductive coupling of two different alkynes via the known[24,25] zirconium complexes $Cp_2Zr(PhCCPh)DMAP$ and $Cp_2Zr(DMAP)_2$ (Scheme 4.1). The goal was to selectively insert alkynes to yield five membered zirconacycles and then form unsymmetric tellurophenes after transmetallation with $Bipy{\bullet}TeCl_2$; however, in each case starting materials were recovered.

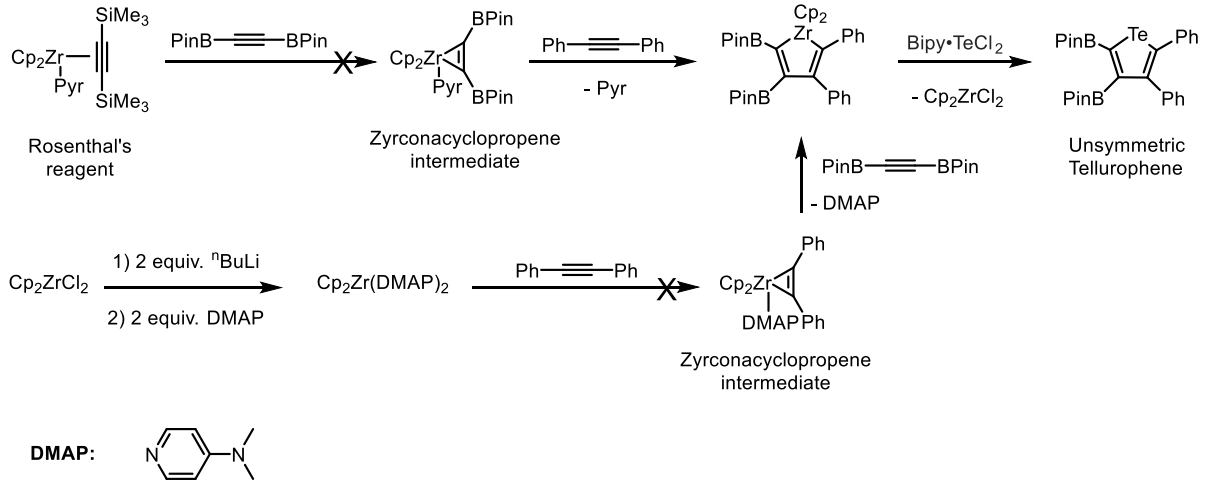

Scheme 4.1. Attempted synthesis of unsymmetric tellurophenes via zirconocene-based intermediates.

If one desires to use tellurophenes in OLEDs, it is necessary that the emissive tellurophenes can operate at high temperatures and have high luminescence quantum yields in the solid state.[14] Moreover such species should emit one of the three primary colors (blue, green and red) for a full-color display. There are intrinsic challenges to overcome associated to blue and red emitters, such as a lack of stability in blue emitters[26,27] and low quantum yields in the case of red emitters.[28] In this context, having efficient emissive tellurophenes in the solid state along with high color tunability is of great importance.

In order to obtain color tunable tellurophenes that are highly efficient emissive tellurophenes in the solid state, the synthesis of unsymmetric tellurophenes was explored. As shown in Scheme 4.2, a general synthetic route to unsymmetrically-substituted tellurophenes (**B-Te-6-Ar**) was investigated. In each structure, one pinacolborate ester (BPin) group is present

along with a different aromatic (Ar) side group such as 1,3-bis(trifluoromethyl)phenyl (Ar^F) and naphthalene (Naph). In addition, direct emission from the naphthalene and fluorene substituents could also be possible. The steric bulk associated with some of these groups might prevent close packing in the solid state and therefore avoiding aggregation-caused quenching effects such as electronic charge transfer (excimer formation) and energy charge transfers by dipole-dipole coupling (Förster resonance energy transfer). In order to compare the emission properties, the synthesis of the respective di-substituted symmetric tellurophenes (**Ar-Te-6-Ar**) was also explored.

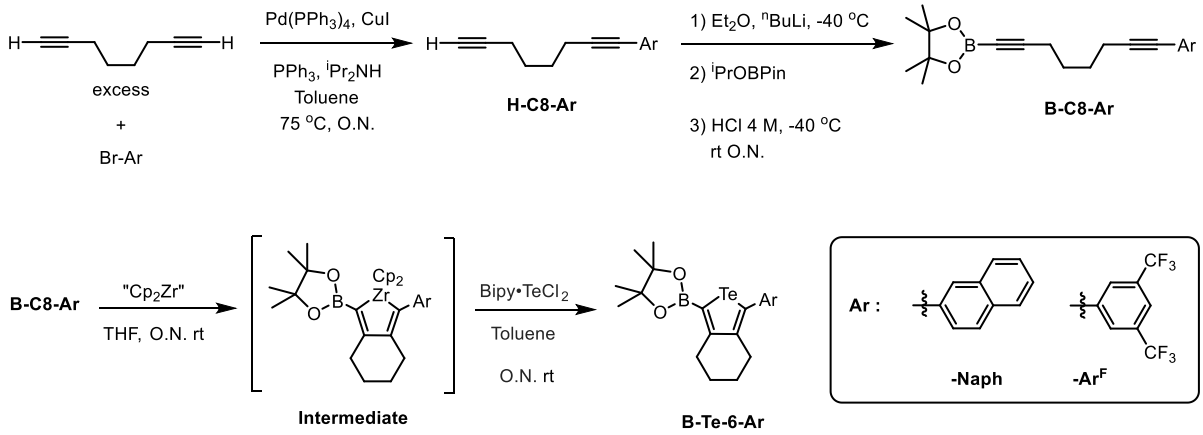

Scheme 4.2. General synthetic protocol to unsymmetric tellurophenes.

4.2. RESULTS AND DISCUSSION

Different strategies for the synthesis of unsymmetric tellurophenes (**B-Te-6-Ar**, Scheme 4.3) were explored in this chapter. The first one was through the direct reaction of one equivalent of an aryl halide (ArBr) with **B-Te-6-B** using Suzuki-Miyaura cross-coupling. The other routes involved the initial syntheses of unsymmetric alkyne functionalized octadiynes, **B-C8-Ar**, followed by the formation of the target tellurophenes **B-Te-6-Ar** via alkyne cyclization with Negishi's reagent "Cp_2Zr" (made in situ from Cp_2ZrCl_2 and 2 equiv. of ^{n}BuLi), and transmetallation with Bipy•$TeCl_2$. In order to prepare the requisite diynes, **B-C8-Ar**, either the BPin group can be installed onto the diyne first (to form **B-C8-H**) or the diyne is initially arylated to yield **H-C8-Ar** as a synthetic intermediate (Scheme 4.2).

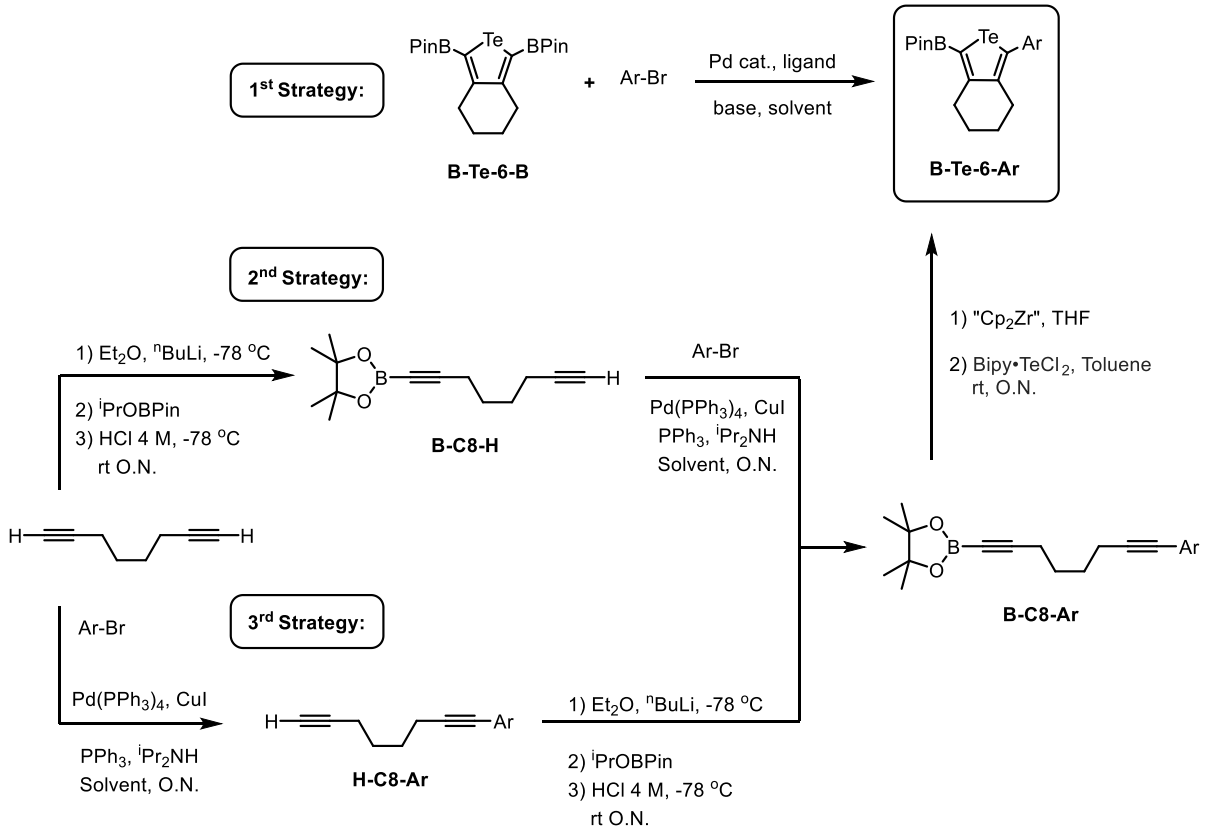

Scheme 4.3. Strategies explored to form unsymmetrically-substituted tellurophenes.

4.2.1. Synthesis of unsymmetric / symmetric tellurophenes via direct cross-coupling of 2-bromonaphthalene and B-Te-6-H (1st strategy)

Microwave and thermal reaction conditions were tested in the attempted synthesis of **B-Te-6-Naph** (Scheme 4.4). $Pd(OAc)_2$ was used in most cases as a pre-catalyst and the type of ligand, base and solvent was varied. Under thermal conditions the symmetric tellurophene **Naph-Te-6-Naph** was mainly formed (entries 3 and 4, Table 4.1) along with the previously known by-products (**B-Te-6-H** and **H-Te-6-H**),[29] resulting from the protodeboronation (PDB) of **B-Te-6-B**. The target product (**B-Te-6-Naph**) was also formed in a small yield (12 %, calculated by ^{1}H NMR integration) using $Pd_2(dba)_3$ as a pre-catalyst in THF (entry 2, Table 4.1).

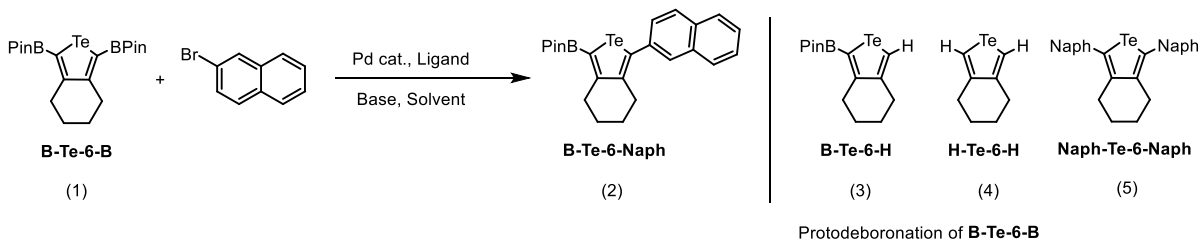

Scheme 4.4. Synthesis of unsymmetric tellurophenes through Suzuki-Miyaura cross-coupling conditions (1st strategy).

Table 4.1. Reaction conditions tested to form **B-Te-6-Naph** using one equivalent of 2-bromonaphthalene and **B-Te-6-B** through Suzuki-Miyaura coupling (1st strategy).

Entry	Pd cat., mol%	Ligand, equiv.	Base, equiv.	Solvent	Reaction Conditions	Products[b] 1 / 2 / 3 / 4 / 5 mol %
1	$Pd(OAc)_2$ / 2	-	K_2CO_3 / 2	DMF	120 °C, 16 h	0 / 0 / 85 / 15 / 0
2	$Pd_2(dba)_3$ / 2	$[HP^tBu_3]BF_4$ / 0.08	K_2CO_3 aq. / 2	THF	70 °C, 24 h	63 / 12 / 21 / 4 / 0
3	$Pd(OAc)_2$ / 4	Xphos / 0.08	K_2CO_3 aq. / 3	MeCN	85 °C, 36 h	0 / 0 / 0 / 33 / 67
4[a]	$Pd(OAc)_2$ / 5	dppf / 0.1	Cs_2CO_3 / 2	DMF	100 °C,16 h	32 / 0 / 0 / 28 / 40
5	$Pd(OAc)_2$ / 4	Xphos / 0.08	K_2CO_3 aq. / 1	MeCN	μW: 110 °C, 2 h	0 / 11 / 12 / 0 / 77
6			K_2CO_3 / 1			6 / 9 / 18 / 10 / 57
7			-			100 / 0 / 0 / 0 / 0
8			K_2CO_3 / 1	THF		58 / 6 / 20 / 16 / 0
9			K_2CO_3 / 1	Toluene		54 / 6 / 27 / 13 / 0
10			K_2CO_3 / 1	DMF		47 / 8 / 38 / 7 / 0
11			NaOH / 1	MeCN		58 / 3 / 39 / 0 / 0
12			K_3PO_4 / 1			92 / 8 / 0 / 0 / 0
13			Cs_2CO_3 / 1			18 / 22 / 13 / 3 / 44

a) 2 equiv. **B-Te-6-B** and 1 equiv. of CuCl b) See Scheme 4.4 for reference numbers

The effect of solvent in the coupling reaction under microwave irradiation was also investigated. When **B-Te-6-B** was combined with 2-bromonaphthalene under microwave irradiation in THF, toluene or DMF, using a mild base such as K_2CO_3 at 110 °C (entries 8, 9

and 10, Table 4.1) by-products of PDB and starting materials were recovered along with a trace amount of the main product **B-Te-6-Naph** (6 %). However, when MeCN was used as a solvent and either aqueous or anhydrous K_2CO_3 as a base (entries 5 and 6, Table 4.1) double arylation occurred to yield **Naph-Te-6-Naph** as a major product (77 and 57 % yield). Based on these results, MeCN seemed to be a more suitable solvent for Suzuki-Miyaura in comparison to THF, toluene and DMF.

Having found the most adequate solvent for coupling, the effect of other bases, such as NaOH, $CsCO_3$ and K_3PO_4 was explored. The reactions carried out with NaOH and $CsCO_3$ in MeCN (entries 11 and 13, Table 4.1) afforded by-products of PDB as well as **Naph-Te-6-Naph** (44 %) and **B-Te-6-Naph** (22 %) in low yields. When K_3PO_4 was used as a base, protodeboronation was suppressed however **B-Te-6-Naph** was only formed in 8 % yield (as determined by NMR spectroscopy) after 2 hours of reaction time.

Under the abovementioned conditions it was not possible to form the target mono-arylated tellurophene **B-Te-6-Naph** as a main product under Suzuki-Miyaura coupling conditions. 2-Bromonaphthalene could be coupled to both sides of a tellurophene to give **Naph-Te-6-Naph** in a 44 % yield after work-up (entry 5, Table 4.1) in MeCN using K_2CO_3 as a base; this result transpired when only 1 equivalent of 2-bromonaphthalene was added. It is expected that this disubstituted tellurophene could be formed in a better yield of 44 % if at least 2 equivalents of 2-bromonaphthalene were used in the reaction.

In general, the symmetric tellurophene **Naph-Te-6-Naph** formed in a higher yield versus the unsymmetric **B-Te-6-Naph** under the microwave-assisted Suzuki-Miyaura coupling conditions (Scheme 4.4). It is possible that once **B-Te-6-Naph** is formed, it re-enters the catalytic cycle to undergo coupling with the BPin group during the long reaction times used in each trial. It would be interesting for future work, to prove the previous statement by doing the reaction under the conditions of entry 5 (Table 4.1) but tracking the reaction starting with small reaction times, e.g. 10 minutes under microwave irradiation at 110 °C. In some cases, the mono-arylated product **H-Te-6-Naph** could be seen by ^{1}H NMR (Figure 4.5), which likely forms via the PDB of **B-Te-6-Naph**. The detection of small satellites with a coupling constant ($^2J_{HTe}$) of 97.8 Hz is in agreement with previous coupling constants detected in related tellurophenes.[29] The formation of **H-Te-6-Naph** would contribute to decrease the

yield of **B-Te-6-Naph** even more. Unfortunately, it was not possible to isolate **H-Te-6-Naph** in pure form.

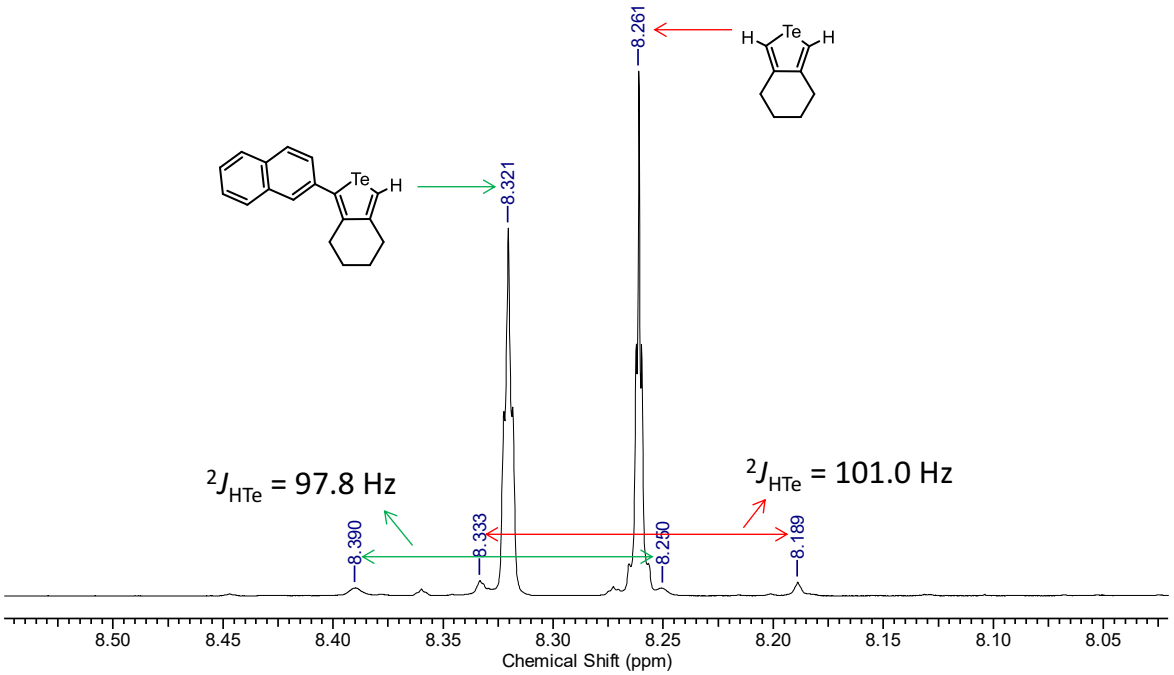

Figure 4.5. Identification of **H-Te-6-Naph** during the attempted synthesis of **B-Te-6-Naph** through Suzuki-Miyaura conditions (Table 4.1).

Fagnou and coworkers[30] reported the direct arylation of electron rich heterocycles such as thiophene using pivalic acid (PivOH) as a cocatalyst and $Pd(OAc)_2$ as a pre-catalyst in dimethylacetamide (DMA). Pivalic acid in the presence of base such as K_2CO_3 forms potassium pivalate, which could serve as a soluble proton transfer agent from the arene to the insoluble K_2CO_3 in a concerted metalation-deprotonation pathway described by the authors.[30] Accordingly similar reaction conditions were tested in the hope that **B-Te-6-H** (Scheme 4.5, Table 4.2) could be selectively arylated to give **B-Te-6-Ar**. However, using the reaction conditions shown in entry 1 (Table 4.2) protodeboronation of **B-Te-6-H** was observed. Using Cs_2CO_3 as a base (entry 3, Table 4.2), **H-Te-6-H** and **H-Te-6-Naph** (Figure 4.5) formed in a mole ratio of 40/60, along with some unreacted 2-bromonaphthalene detected by ^{1}H NMR spectroscopy.

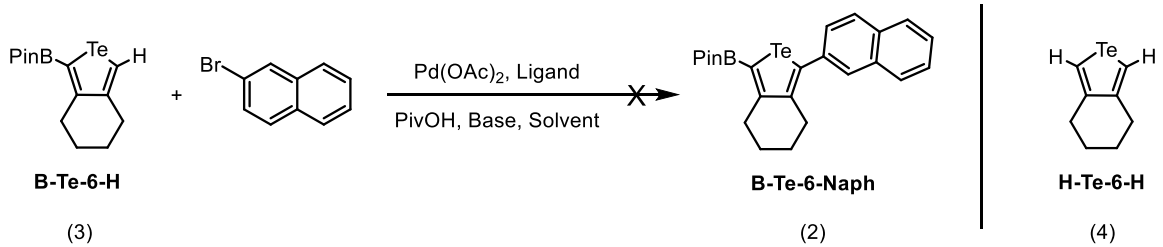

Scheme 4.5. Attempted synthesis of the unsymmetric tellurophene **B-Te-6-Ar** through direct arylative coupling.

Table 4.2. Reaction conditions used in the attempted direct arylative coupling of one equivalent of 2-bromonaphthalene with **B-Te-6-H**.

Entry	$Pd(OAc)_2$, mol%	Ligand, equiv.	Base, equiv.	PivOH, equiv.	Reaction Conditions	Product[a]
1	2	$[HP^tBu_3]BF_4$ / 0.04	K_2CO_3 / 1.5	0.3	DMF, 100 °C, 36 h	4
2	5	$^tBu_3P$ / 0.05	K_2CO_3 / 0.75	0.25	Toluene, 120 °C, 16 h	3, 4
3	5	Xphos / 0.1	Cs_2CO_3 / 1	0	Toluene 120 °C, 22 h	4
4	4	Xphos / 0.08	K_2CO_3 aq. / 0.5	0	MeCN, μW: 110 °C, 2 h	No rxn.

a) See Scheme 4.5 for reference numbers.

Motivated by the results summarized in Table 4.1, where **Naph-Te-6-Naph** was formed as a by-product, the reaction conditions were then altered to give a good yield of this disubstituted symmetric tellurophene (Scheme 4.6, Table 4.3); the optoelectronic properties of this species will be discussed (along with those of the unsymmetric analogue **B-Te-6-Naph**) later in this Chapter. Using toluene and THF as solvents (entries 2 to 6, Table 4.3) led to the conversion (0-22 % according to ^1H NMR spectroscopy) of 2-bromonaphthalene into **Naph-Te-6-Naph**, plus unreacted **B-Te-6-B**, along with PDB by-products and **H-Te-6-Naph**. However using conventional heating to 80 °C (entry 1, Table 4.3) in MeCN, it was possible to recover **Naph-Te-6-Naph** in a 36 % yield.

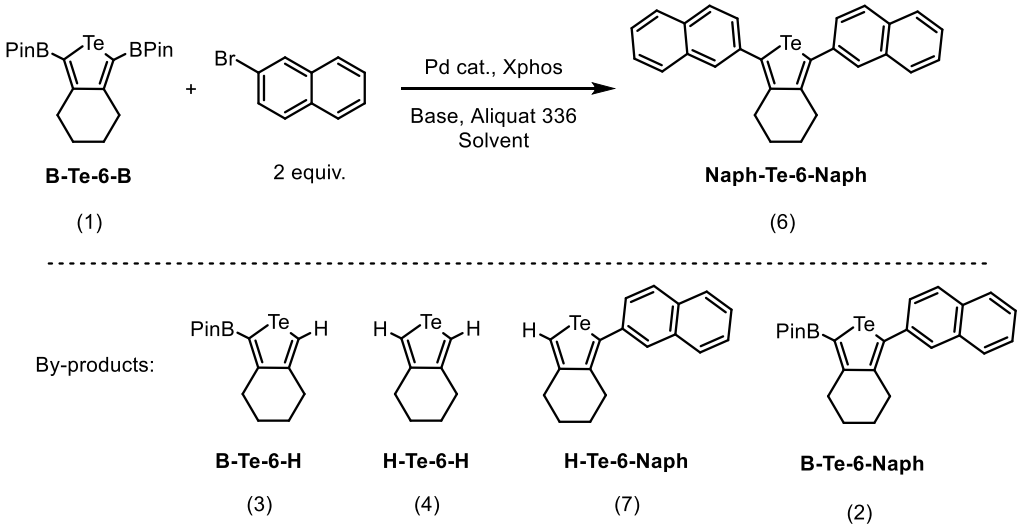

Scheme 4.6. Synthesis of **Naph-Te-6-Naph** using Suzuki-Miyaura cross-coupling conditions.

Table 4.3. Optimization of Suzuki-Miyaura conditions to form **Naph-Te-6-Naph**.

Entry	Pd cat., mol%	Xphos, equiv.	Base, equiv.	Reaction Conditions, (Isolated Yield of 2[c], %)	Products[c] 1 / 6 / 3 / 4 / 7 / 2 mol %
1	$Pd(OAc)_2$ / 4	0.08	K_2CO_3 aq. / 4	MeCN, 80 °C, 60 h / **36 %**	0 / 34 / 0 / 10 / 56 / 0
2[a]	$Pd(OAc)_2$ / 4	0.08	K_2CO_3 aq. / 4	Toluene, 90 °C, 72 h	0 / 21 / 24 / 20 / 35 / 0
3[a]	$Pd(PPh_3)_4$ / 5	-	K_2CO_3 aq. / 2	Toluene, µW: 90 °C, 1 h	20 / 22 / 27 / 8 / 23 / 0
4[a]	$Pd(PPh_3)_4$ / 5	-	Na_2CO_3 aq. / 4	Toluene, 90 °C, 96 h	0 / 0 / 0 / 56 / 44 / 0
5			K_2CO_3 aq. / 5	THF, µW: 150 °C, 1 h	10 / 12 / 30 / 13 / 22 / 13
6			K_2CO_3 aq. / 5	THF, µW: 130 °C, 2 h	16 / 12 / 26 / 6 / 17 / 23
7	$Pd(OAc)_2$ / 4	0.08	K_2CO_3 aq. / 5	MeCN, µW: 150 °C, 1 h	0 / 14 / 0 / 47 / 39 / 0
8			K_2CO_3 aq. / 5	MeCN, µW: 130 °C, 2 h / **20 %**	2 / 30 / 9 / 17 / 41 / 1
9[b]			K_2CO_3 aq. / 1	MeCN, µW: 110 °C, 2 h / **44 %**	0 / 64 / 10 / 3 / 15 / 8

a) Plus Aliquat 336, 1.3 equiv. b) 1 equiv. of 2-bromonaphthalene, c) See Scheme 4.6 for reference compounds

Given the long time of reaction (60 h) used to prepare **Naph-Te-6-Naph** in MeCN, microwave conditions were then used to shorten the reaction time, leading to an increase in product yield to 44 %, despite of only one equivalent of 2-bromonaphthalene in the reaction

(entry 9, Table 4.3). By decreasing the temperature from 150 to 110 °C under microwave conditions, and lowering the equivalents of K_2CO_3 base from 5 to 1 in MeCN (entries from 7 to 9, Table 4.3) the amount of the PDB by-products **B-Te-6-H** and **H-Te-6-H** were greatly reduced, affording a higher isolated yield of **Naph-Te-6-Naph**.

Crystals of **Naph-Te-6-Naph** suitable for single-crystal X-ray diffraction were obtained from CH_2Cl_2 (0 °C) and the molecular structure is presented in Figure 4.6. In contrast to what is seen within the boryl-capped tellurophene **B-Te-6-B**, the two naphthalene units are not coplanar with the central tellurophene ring, as evidenced by the respective torsion angles of 140.8(6)° (Te-C7-C12-C11) and -60.7(9)° (Te-C8-C22-C21). The non-coplanar naphthalene-tellurophene-naphthalene configuration might have a significant impact on the optoelectronic properties in the solid state, as optimal charge transfer between the Te center and the π* framework of the naphthalene system could be suppressed.

Using similar reaction conditions to form **Naph-Te-6-Naph** found in entry 1 (MeCN, 80 °C), Table 4.3, 2-bromofluorene was successfully coupled with **B-Te-6-B** (Scheme 4.7) to afford **Fl-Te-6-Fl** as a solid in a 58 % isolated yield.

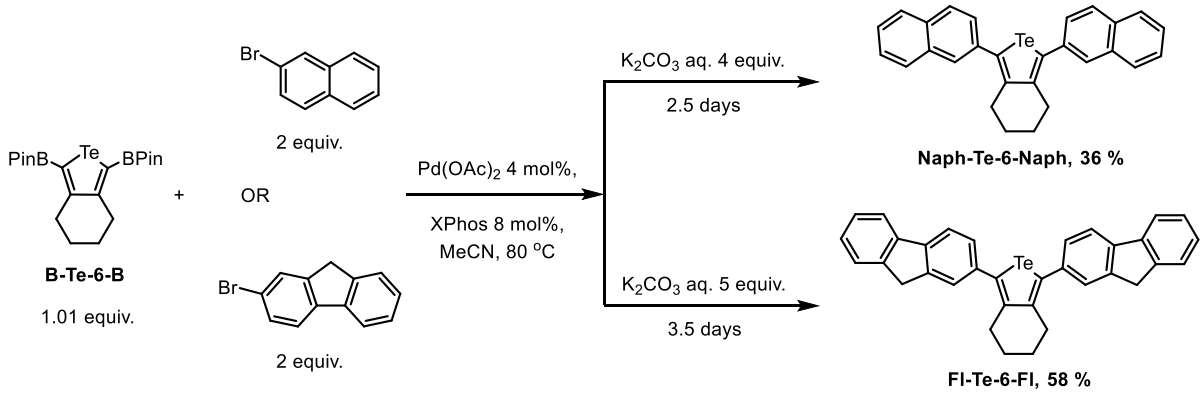

Scheme 4.7. Synthesis of **Naph-Te-6-Naph** and **Fl-Te-6-Fl** through Suzuki-Miyaura coupling.

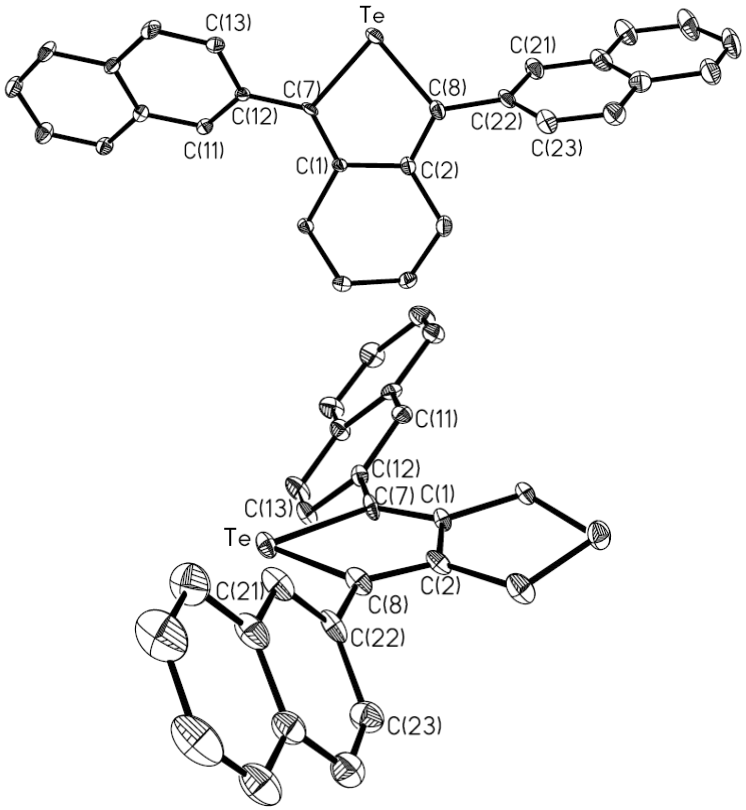

Figure 4.6. Molecular structure of **Naph-Te-6-Naph** (two views shown) with thermal ellipsoids presented at a 30 % probability level. Residual factor, R = 0.0653. All hydrogen atoms have been omitted for clarity. Selected bond lengths (Å) and angles (°): C(1)-C(2) 1.463(10), C(2)-C(8) 1.349(10), C(8)-Te 2.079(8), C(1)-C(7) 1.359(10), C(7)-Te 2.088(7), C(7)-C(12) 1.474(10), C(11)-C(12) 1.379(9), C(12)-C(13) 1.415(10), C(8)-C(22) 1.488(10), C(21)-C(22) 1.361(12), C(22)-C(23) 1.423(13); C(7)-Te-C(8) 81.5(3), Te-C(8)-C(2) 112.3(5), C(8)-C(2)-C(1) 116.8(7), C(2)-C(1)-C(7) 118.4(6), C(1)-C(7)-Te 110.8(5), Te-C(7)-C(12) 118.9(5), Te-C(8)-C(22) 120.7(6), Te-C(7)-C(12)-C(11) 140.8(6), Te-C(7)-C(12)-C(13) -42.1(9), Te-C(8)-C(22)-C(21) -60.7(9), Te-C(8)-C(22)-C(23) 119.9(8).

The coupling of 5-bromo-1,3-bis(trifluoromethyl)benzene and 4-bromo-N,N-dimethylaniline with **B-Te-6-B** under microwave-assisted Suzuki-coupling (110 °C in MeCN; Table 4.3) was also explored. The desired fluoroaryl-capped tellurophene **Ar^{F}-Te-6-Ar^{F}** was formed as a dark brown solid and recovered after purification in a 15 % yield (Scheme 4.8). On the other hand, coupling of 4-bromo-N,N-dimethylaniline with **B-Te-6-B** was not possible and starting materials were recovered after heating the reagents with catalyst and base at 110 °C for 2 hours under microwave conditions.

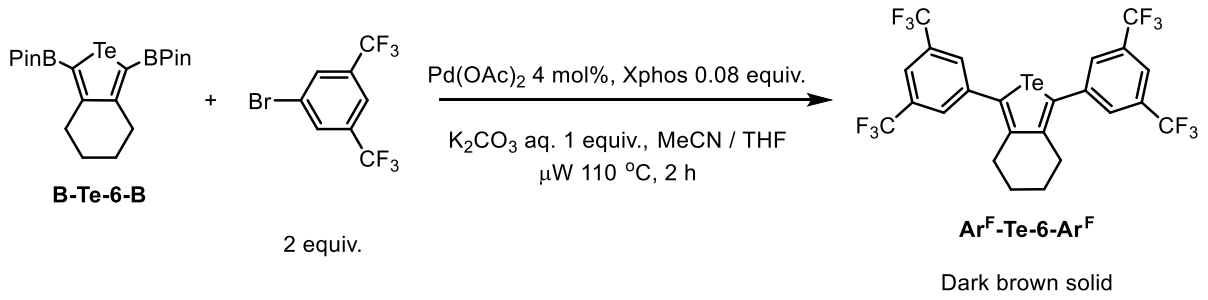

Scheme 4.8. Synthesis of **Ar^F-Te-6-Ar^F** through Suzuki-Miyaura coupling under microwave irradiation.

Crystals of **Ar^F-Te-6-Ar^F** suitable for single-crystal X-ray diffraction were obtained from a mixture of hexanes and CH_2Cl_2 (0 °C) and the molecular structure is presented in Figure 4.7. A similar non-coplanar configuration of the $(CF_3)_2C_6H_3$, (Ar^F) group and the central tellurophene unit exists as noted in **Naph-Te-6-Naph**. Accordingly, torsion angles of -61.4(4)° (Te-C7-C11-C12) and -69.1(4)° (Te-C8-C21-C26) are present.

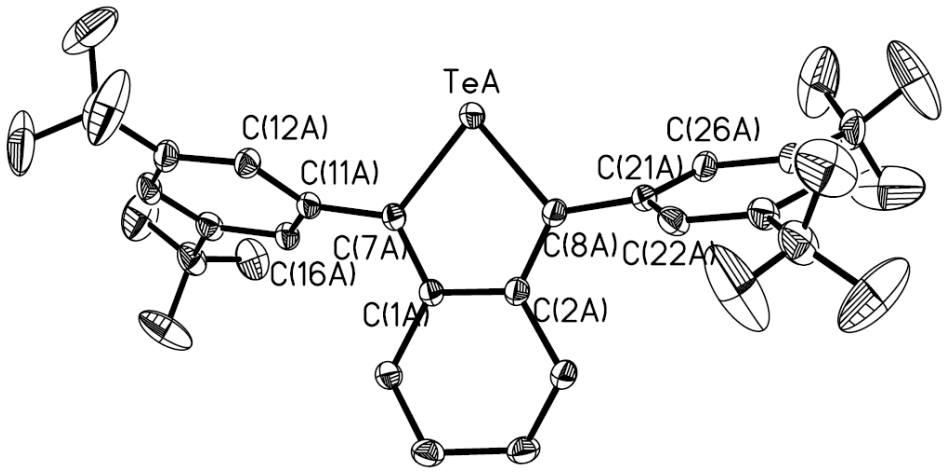

Figure 4.7. Molecular structure of **Ar^F-Te-6-Ar^F** with thermal ellipsoids presented at a 30 % probability level. Residual factor, R = 0.0387. All hydrogen atoms have been omitted for clarity. Selected bond lengths (Å) and angles (°): C(1)-C(2) 1.449(4), C(2)-C(8) 1.366(4), C(8)-Te 2.068(3), C(1)-C(7) 1.366(4), C(7)-Te 2.068(3), C(7)-C(11) 1.474(4), C(11)-C(12) 1.395(5), C(11)-C(16) 1.391(5), C(8)-C(21) 1.477(4), C(21)-C(26) 1.390(5), C(21)-C(22) 1.394(4); C(7)-Te-C(8) 81.66(12), Te-C(8)-C(2) 111.8(2), C(8)-C(2)-C(1) 117.4(3), C(2)-C(1)-C(7) 117.2(3), C(1)-C(7)-Te 111.9(2), Te-C(7)-C(11) 122.3(2), Te-C(8)-C(21) 123.4(2), Te-C(7)-C(11)-C(12) -61.4(4), Te-C(7)-C(11)-C(16) 120.4(3), Te-C(8)-C(21)-C(22) 114.5(3), Te-C(8)-C(21)-C(26) -69.1(4).

4.2.2. Synthesis of unsymmetric octadiynes via initial lithiation-borylation (2nd strategy, Scheme 4.3)

With the goal of gaining access to unsymmetrically-substituted tellurophenes (**B-Te-6-Ar**) in higher yield, a second approach starting from unsymmetrically-functionalized diynes (Scheme 4.3) was investigated. Following a similar procedure reported in the literature,[31] **B-C8-H** was synthesized in 87 % yield (Scheme 4.9). It is important to start with an excess of 1,7-octadiyne followed by the slow addition of ^{n}BuLi in order to prevent the formation of the known diborylated diyne PinB-C≡C-$(CH_2)_4$-C≡C-BPin.

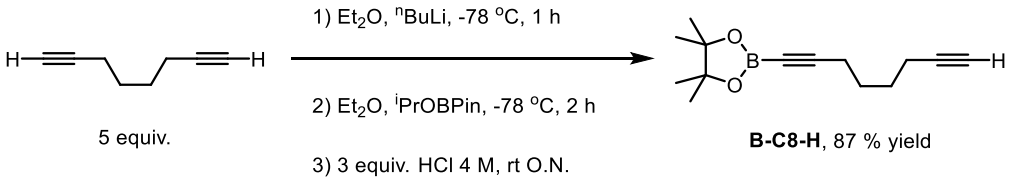

Scheme 4.9. Synthesis of the monoborylated 1,7-octadiyne, **B-C8-H**.

Once **B-C8-H** was formed, selective Sonogashira coupling of the terminal acetylenic C-H group to yield the arylated diyene PinB-C≡C-$(CH_2)_4$-C≡C-Naph was attempted (Scheme 4.10, Table 4.4). Selective Sonogashira over Suzuki coupling reaction has been reported[32] in the synthesis of ethynylarylboronic esters under microwave conditions; although in those cases the boronate ester and the halide were part of the same aromatic structure. Several Sonogashira cross-coupling conditions were attempted (Table 4.4) in order to form **B-C8-Naph** from **B-C8-H**, including similar protocols as that reported in the literature.[32] Despite trying various reaction conditions, there was no indication that the coupling of 2-bromo-naphthalene occurred exclusively at an acetylenic C-H position; instead, coupling at both sites to form **Naph-C8-Naph** and the resulting homocoupling product **Naph-C8-C8-Naph** as the main products detected according to ^{1}H NMR spectroscopy (also confirmed by mass spectrometry).

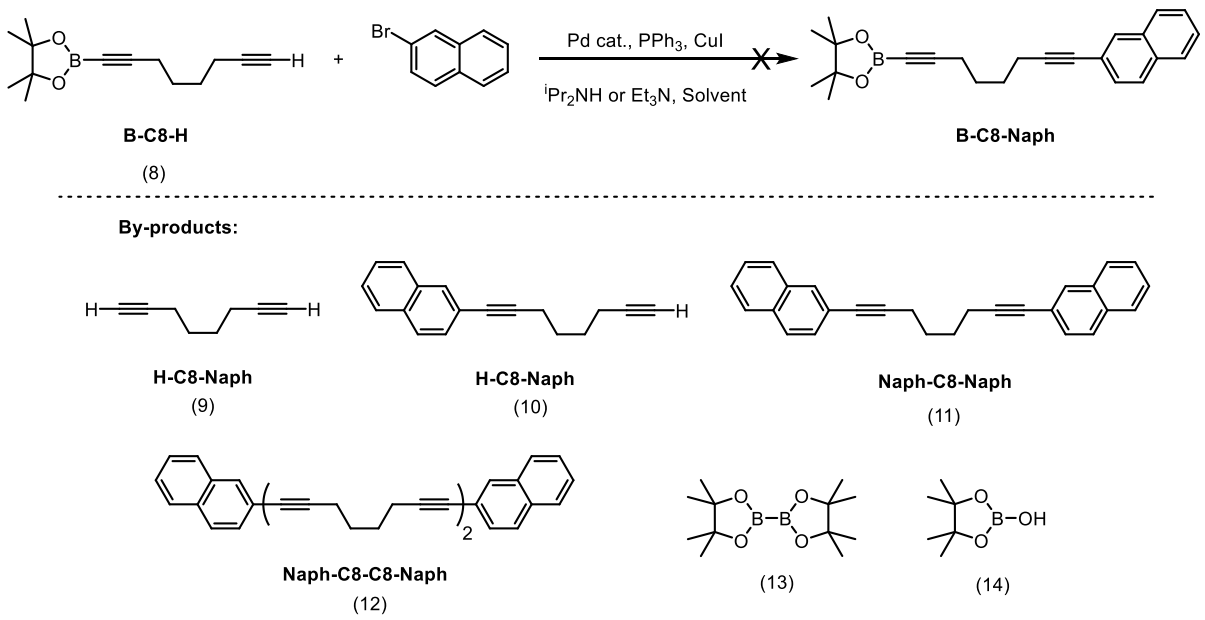

Scheme 4.10. Attempted synthesis of **B-C8-Naph** through Sonogashira cross-coupling.

Table 4.4. Reaction conditions tested to form **B-C8-Naph** through Sonogashira cross-coupling.

Entry	Pd cat., mol%	PPh_3, equiv.	CuI, equiv.	$^iPr_2NH$, equiv.	Solvent	Reaction Conditions	Products[a]
1	$Pd(OAc)_2$ / 5	0.18	0.05	13.6	DMF	μW: 120 °C, 20 min	11, 12, 13, 14
2	$Pd(PPh_3)_4$ / 5	0.18	0.05	13.6	DMF		8, 11, 12, 13, 14
3	$Pd(PPh_3)_2Cl_2$ / 3	0	0.06	Et_3N / 5.2	THF	40 °C, 16 h	9, 14, 13
4	$Pd(PPh_3)_4$ / 5	0.18	0.05	13.6	Toluene	μW: 100 °C, 1 h	8, 10, 11, 12, 14
5	$Pd(PPh_3)_4$ / 5	0.18	0.05	1	Toluene	rt, 16 h	9, 10, 14
6	$Pd(PPh_3)_4$ / 5	0.18	0.05	-	Toluene	rt, 16 h	9, 14
7	$Pd(PPh_3)_4$ / 5	0.18	0.05	2	Toluene	μW: 70 °C, 20 min	9, 10, 14
8	$Pd(PPh_3)_4$ / 5	0.1	0.1	100	Toluene	80 °C, 16 h	10, 11, 12, 14

a) See Scheme 4.10 for reference numbers. Major products underline.

In the reaction between **B-C8-H** and 2-bromonaphthalene, it is not clear which site of **B-C8-H** the coupling occurs first, since the by-product **H-C8-Naph** could be formed by two concurrent pathways (Scheme 4.10). The first pathway is through Suzuki-Miyaura cross-coupling (coupling of naphthalene at the BPin site) and the second one is via Sonogashira coupling of naphthalene at the acetylenic site, followed by PDB, as described in Scheme 4.11. Finally, by the action of some residual O_2 in the reaction media, Pd(0) could be oxidized back to Pd(II), which might catalyze the homocoupling by the double transmetallation of in situ formed Naph-C≡C-$(CH_2)_4$-C≡C-Cu at a Pd(II) center, followed by the reductive elimination of two octadiyne-naphthalene units from the Pd complex to finally form the homocoupled by-product **Naph-C8-C8-Naph**, as described in the literature.[33]

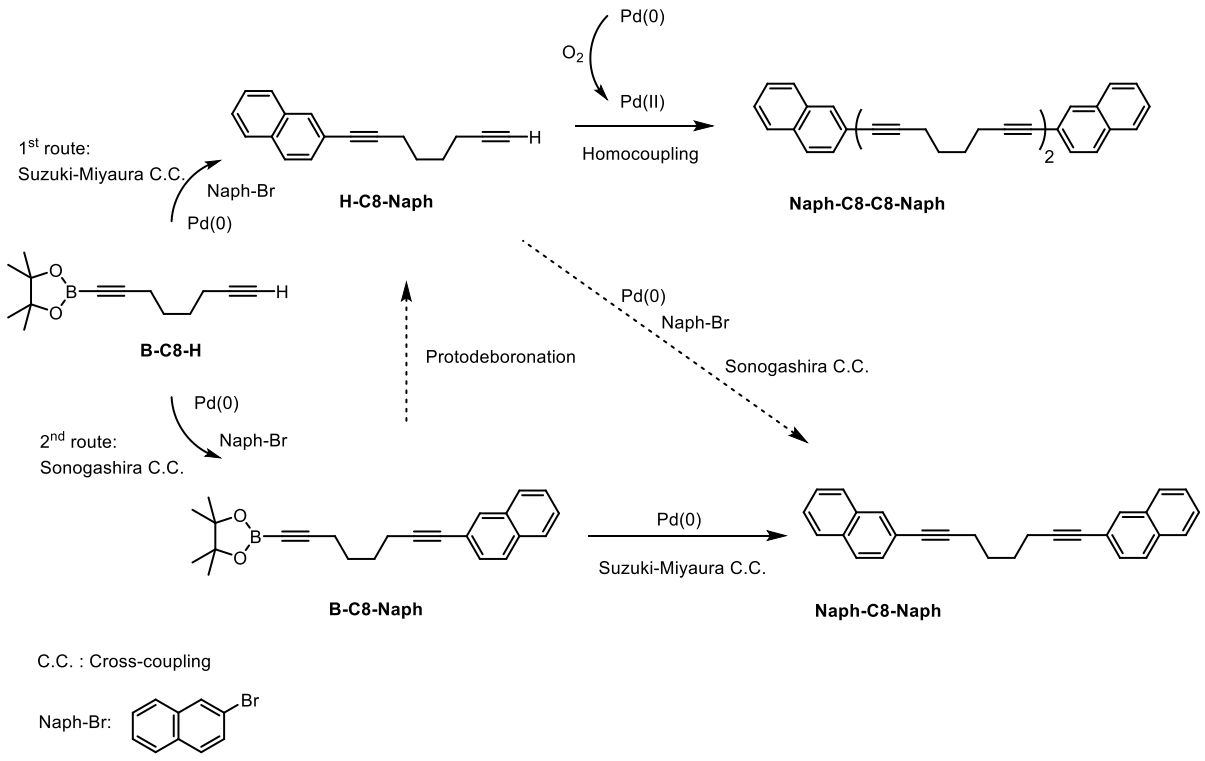

Scheme 4.11. Possibly pathways in the formation of by-products in the synthesis of **B-C8-Naph**.

In order to avoid protodeboronation (PDB) and try to recover some **B-C8-Naph** at the end of the reaction, the base $^{i}Pr_2NH$ was not added to the reaction mixture described in entry

6, Table 4.4 (in toluene with 16 h of stirring at room temperature), however, PDB still occurred under these conditions and 1,7-octadiyne was detected at the end of the reaction. Based on these results, BPin-capped 1,7-octadiyne is very sensitive to PDB under Sonogashira conditions, likely due to the presence of CuI. CuI might be inducing PDB of the BPin-capped species; notably, PDB of arylboronic acids promoted by different copper salts, including CuI, has been reported.[34]

Using the same reactants as in Scheme 4.10, but now under Suzuki-Miyaura conditions, the synthesis of **H-C8-Naph** was attempted (Scheme 4.12 and Table 4.5). Under these conditions it was possible to form **H-C8-Naph** in higher ratio (> 62 %) than the disubstituted product **Naph-C8-Naph**.

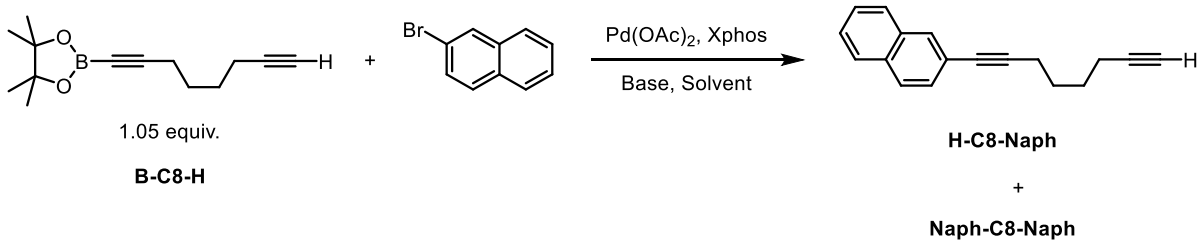

Scheme 4.12. Synthesis of **H-C8-Naph** and **Naph-C8-Naph** via coupling of **B-C8-H** with 2-bromonaphthalene through Suzuki-Miyaura coupling reactions.

Conversion of **B-C8-H** under Suzuki-Miyaura cross-coupling conditions to form exclusively **H-C8-Naph** was not possible. Under the reactions explored, there was always generation of the disubstituted by-product **Naph-C8-Naph** detected in addition to the target product **H-C8-Naph** (entries 4-6, Table 4.5). The use of KOH as a base in toluene or ethanol (entries 1, 2 and 3, Table 4.5) promoted the PDB of **B-C8-H** (to give **H-C8-H**) along with the formation of unidentified by-products. When the reactions of 2-bromonaphthalene and **B-C8-H** were conducted in THF / H_2O in the presence of mild bases, the formation of **H-C8-Naph** (entries 5 and 6, Table 4.5) transpired to give up to 79 % NMR yield.

In conclusion, **B-C8-H** is very sensitive to Sonogashira conditions, since the use of $^{i}Pr_2NH$ as a base and CuI as a co-catalyst can also promote the PDB of **B-Te-6-H**. Better results were found using Suzuki-Miyaura conditions in terms of less amount of by-products and some selectivity towards the formation of **H-C8-Naph** over **Naph-C8-Naph**.

Table 4.5. Reaction conditions tested in the synthesis of **H-C8-Naph** through Suzuki-Miyaura coupling reactions.

Entry	$Pd(OAc)_2$ mol%	Xphos, equiv.	Base, equiv.	Reaction Conditions	Products H-C8-Naph / Naph-C8-Naph, mol %
1	1	0.02	KOH / 3	Toluene, 90 °C, O.N.	0 / 0
2	2	0.04	KOH / 3	EtOH / H_2O (1:1), μW: 150 °C, 10 min	0 / 0
3	2	0.04	KOH / 3	EtOH / H_2O (1:1), μW: 110 °C, 10 min	0 / 0
4	1	0.02	KOH aq. / 3		62 / 38
5	1	0.02	Na_2CO_3 aq. / 3	THF / H_2O (2:1), μW: 100 °C, 30 min	79 / 21
6	1	0.02	K_3PO_4 aq. / 3		76 / 24

4.2.3. Synthesis of unsymmetric octadiynes via initial Sonogashira coupling (3rd strategy, Scheme 4.3)

The synthesis of unsymmetrically-substituted diynes using Sonogashira coupling reactions has been reported.[35] Specifically, it was possibly to couple 2-iodothiophene or 2-iodobenzene with 1,6-heptadiyne at room temperature to form the respective unsymmetric aromatic-substituted heptadiynes in good yields of 75 % and 80 %, respectively. Scheme 4.13).

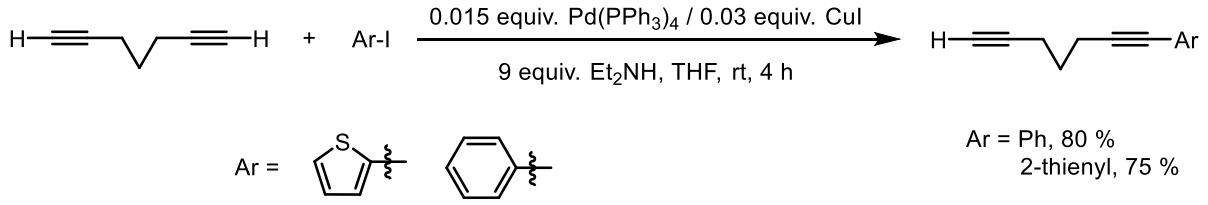

Scheme 4.13. Reported synthesis of unsymmetric 1,7-heptadiyene using Sonogashira coupling conditions.[35]

Motivated by these results, use of lower base loadings of $^{i}Pr_2NH$ (5-7 equiv.) along with an excess of 1,7-octadiyene as a reagent, it was possible to form the unsymmetric diyne **H-C8-Naph** in yields up to 70 % after purification by column chromatography (Scheme 4.14). It is likely that using less $^{i}Pr_2NH$ in the synthesis (Table 4.6) prevented further deprotonation from occurring and therefore lowering the amount of disubstituted **Naph-Te-6-Naph** formed as a by-product. Conversely, by altering the ratio of 1,7-octadiyne to 2-bromonaphthalene to 1:2, **Naph-Te-6-Naph** was synthesized as a solid in 61 % yield (Scheme 4.15).

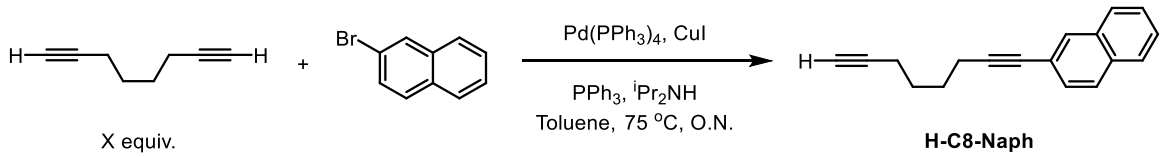

Scheme 4.14. Synthesis of **H-C8-Naph** through Sonogashira coupling reaction.

Table 4.6. Optimization of the Sonogashira coupling conditions to form **H-C8-Naph**.

Entry	Alkyne, equiv.	$Pd(PPh_3)_4$, mol%	PPh_3, equiv.	CuI, equiv.	$^{i}Pr_2NH$, equiv.	Yield % of H-C8-Naph[a]
1[b]	5	3	0.06	0.06	100	12
2	1	3	0.06	0.06	10	28
3	5	2	0.04	0.04	5	61
4	7	2	0.04	0.04	7	70

a) Isolated yield after column chromatography

b) Toluene / $^{i}Pr_2NH$ (1:1)

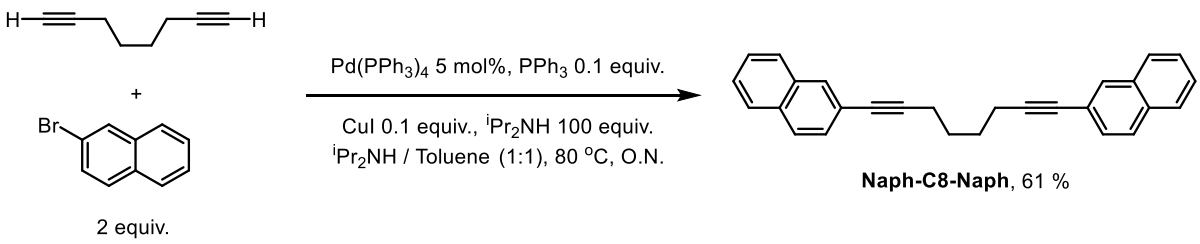

Scheme 4.15. Synthesis of the symmetric diyne **Naph-C8-Naph** via Sonogashira coupling.

By applying a similar protocol as used to prepare **H-C8-Naph**, the monoarylated 1,7-octadiyne **H-C8-Ar^F** could be synthesized in a 57 % isolated yield (Scheme 4.16). However, attempts to couple 4-bromo-N,N-dimethylaniline with 1,7-octadiyene under the same conditions led to no reaction.

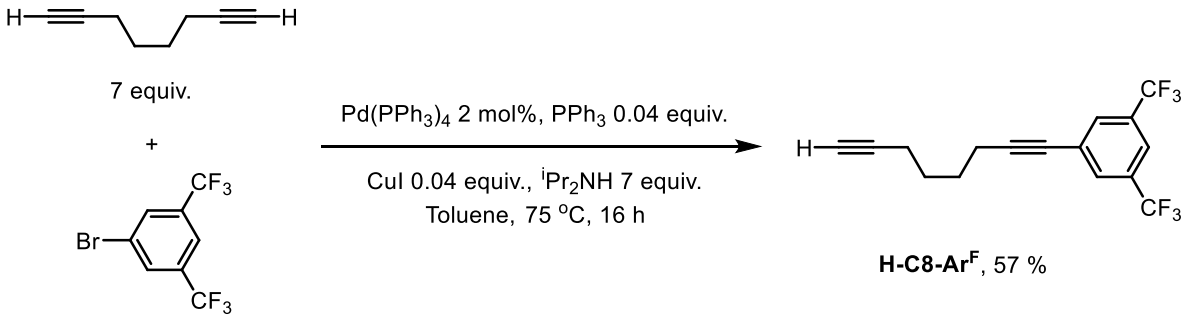

Scheme 4.16. Synthesis of the unsymmetric diyne **H-C8-Ar^F** via Sonogashira coupling.

Subsequent borylation of the respective aromatic-substituted 1,7-octadiynes were performed using the common technique of lithiation of a terminal alkyne, followed by the formation of the boronate ester, and then quenching of the reaction mixture with HCl. Good yields and purity of more than 75 % were obtained after the respective work-ups to form **B-C8-Naph** (Scheme 4.17) and **B-C8-Ar^F** (Scheme 4.18). No further purifications were attempted; instead, these diynes were used directly as is in the respective preparations of unsymmetric tellurophenes.

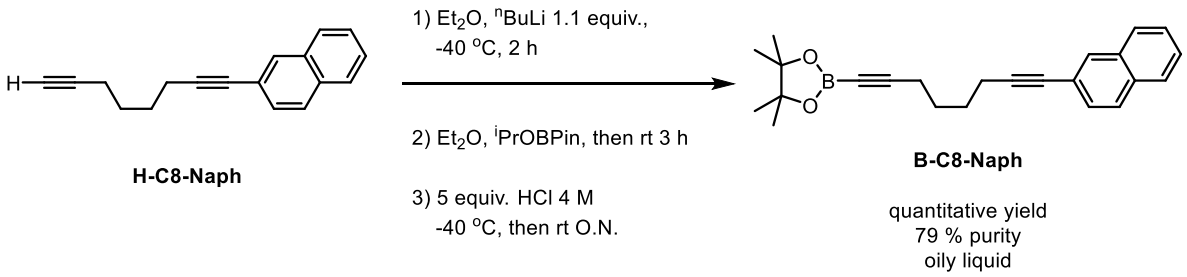

Scheme 4.17. Synthesis of the unsymmetric diyne **B-C8-Naph**.

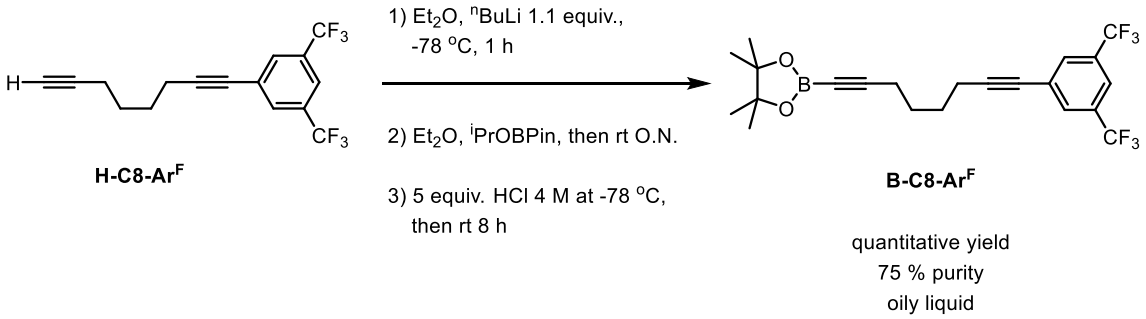

Scheme 4.18. Synthesis of the unsymmetric diyne **B-C8-Ar^F**.

4.2.4. Synthesis of unsymmetric tellurophenes B-Te-6-Naph and B-Te-6-Ar^F

B-Te-6-Naph and **B-Te-6-Ar^F** (Scheme 4.19) were prepared in a one-pot procedure by first coupling the respective BPin-capped diyne, **B-C8-Naph** or **B-C8-Ar^F**, with in situ generated "Cp_2Zr" to yield the five-membered zirconacycles; these intermediates were subsequently converted into **B-Te-6-Naph** or **B-Te-6-Ar^F** by addition of Bipy•$TeCl_2$ as a Te(II) source. After removal of the Cp_2ZrCl_2 by-product, good crude yields (> 70 %) of the tellurophenes were obtained. The presence of the respective tellurophene was confirmed first by mass spectrometric analysis and then by ^{1}H, ^{13}C {^{1}H} and ^{11}B NMR spectroscopy. Purification of **B-Te-6-Naph** and **B-Te-6-Ar^F** by column chromatography lowered the yields drastically (6-9 %), partially because **B-Te-6-Naph** decomposed in the column using silica gel, as evidence by the possible presence of the PDB by-product **H-Te-6-Naph** after column chromatography. The presence of this by-products was postulated by the appearance of a singlet resonance with their respective satellites in the aromatic region of ^{1}H NMR with chemical

shift at 8.33 ppm assigned to the hydrogen atom attached to the five-membered ring in **H-Te-6-Naph** (Figure 4.5). Despite the low yield of **B-Te-6-Naph**, this species was obtained in sufficient quantities in pure form to perform optical measurements. Unfortunately, this was not the case for **B-Te-6-Ar^F**.

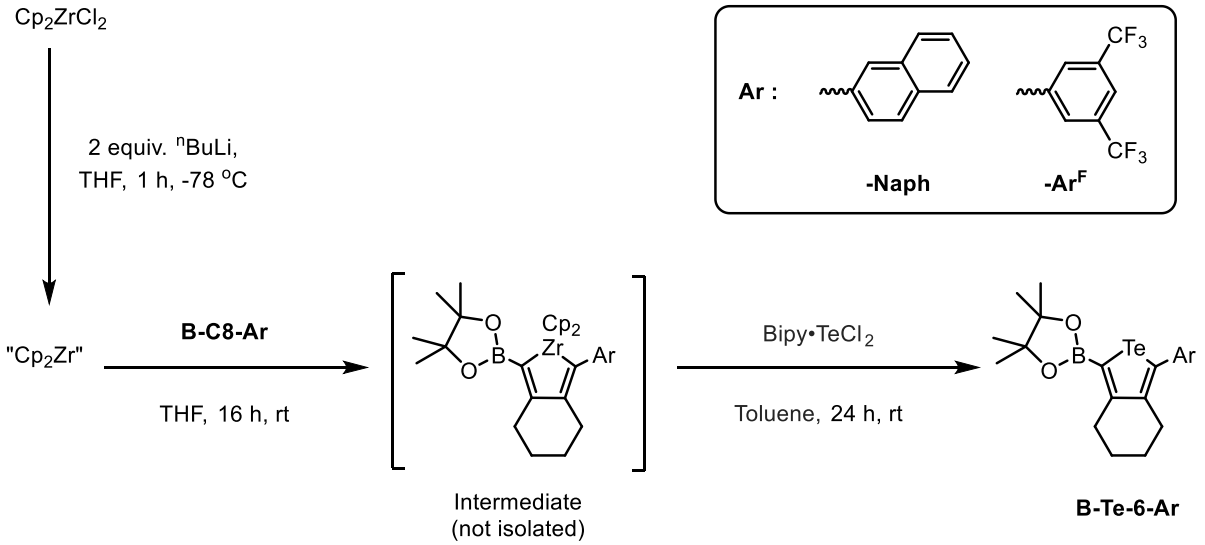

Scheme 4.19. Synthesis of the unsymmetric tellurophenes, **B-Te-6-Naph** and **B-Te-6-Ar^F**.

The abovementioned syntheses (Scheme 4.19) were carried out in one-pot to yield **B-Te-6-Naph** and **B-Te-6-Ar^F**, however, having pure products proved to be a challenge, since some decomposition occurred during silica gel column chromatography. Other methods to purify and extract the main products were tested, such as trituration and crystallization in different solvents at -30 °C, however, they did not work, obtaining at the end of the process the same oily mixtures. Sublimation might be an alternative way to consider in the future for recovering **B-Te-6-Naph** and **B-Te-6-Ar^F** as pure solids.

4.2.5. Optical properties of tellurophenes: Naph-Te-6-Naph, Fl-Te-6-Fl, Ar^F-Te-6-Ar^F and Naph-Te-6-B

Naph-Te-6-Naph, **Fl-Te-6-Fl**, and **Naph-Te-6-B** present the same set of two absorption bands in the range of 250 and 350 nm (Figure 4.9 and Table 4.7) in contrast with the single absorption band found in **Ar^F-Te-6-Ar^F** (λ_{max} = 312 nm). In order to explain the origin of these bands, the absorption properties of the single molecules of naphthalene and fluorene should be addressed first, along with the optical properties of some related molecules such as naphthalene-thiophene-naphthalene: **Naph-S1-Naph**,[36,37] **2,4-BPin$_2$-3,5-Ph$_2$-Te** (Figure 4.3) and 2,5-bis(2-(9,9-dihexylfluorene))tellurophene[38] (Figure 4.8).

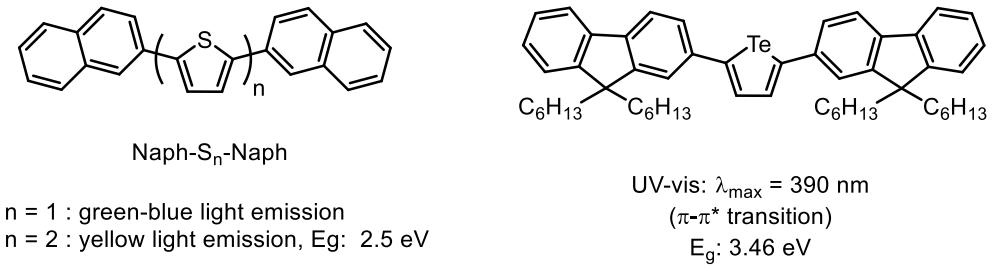

Figure 4.8. Analogues of **Naph-Te-6-Naph** and **Fl-Te-6-Fl**: Naphthalene-capped oligothiophenes.[36,37] and 2,5-bis(2-(9,9-dihexylfluorene)) tellurophene,[38] respectively.

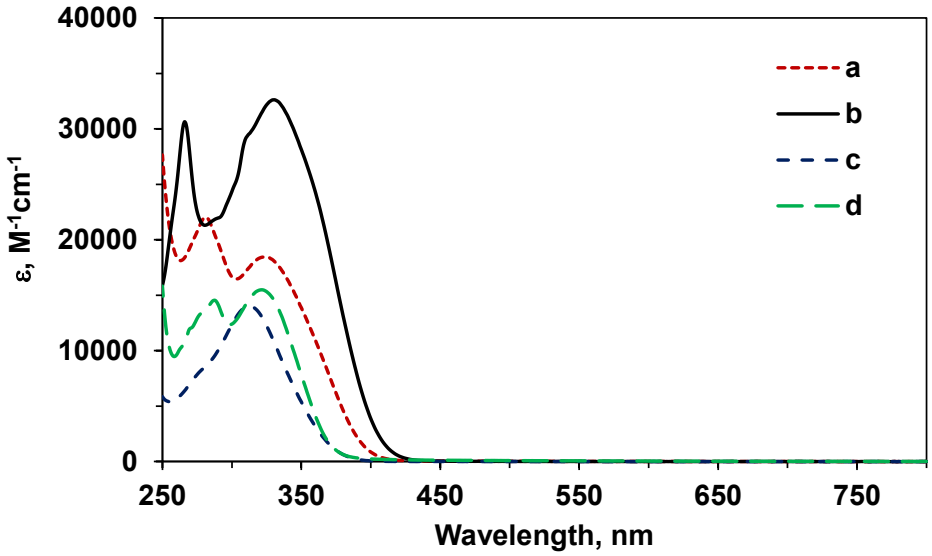

Figure 4.9. UV-vis absorption of a) **Naph-Te-6-Naph**, b) **Fl-Te-6-Fl**, c) **Ar^F-Te-6-Ar^F** and d) **Naph-Te-6-B** in THF (30 μM) at room temperature under N_2.

Table 4.7. Optical properties of tellurophenes.

	Absorption		
	λ_{max}, nm	ε, $M^{-1}cm^{-1}$	Eg, eV[a]
Naph-Te-6-Naph	281	22100	3.3
	324	18500	
Fl-Te-6-Fl	266	30700	3.2
	330	32600	
Ar^F-Te-6-Ar^F	312	14000	3.5
Naph-Te-6-B	287	14500	3.4
	322	15500	

a) Calculated using Tauc plots, see Figure 4.10

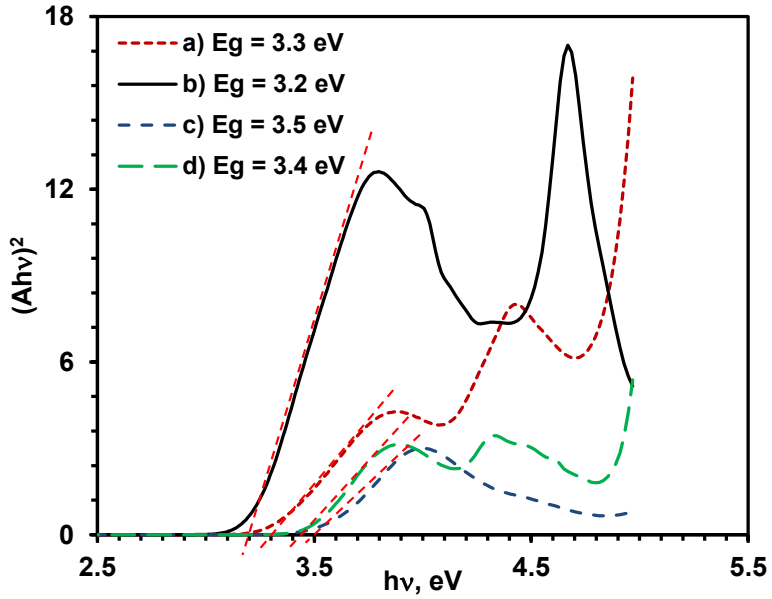

Figure 4.10. Tauc plots of tellurophenes: a) **Naph-Te-6-Naph**, b) **Fl-Te-6-Fl**, c) **Ar^F-Te-6-Ar^F** and d) **Naph-Te-6-B** in THF (30 μM) at room temperature under N_2.

Optical band gaps were calculated from the Tauc plots (Figure 4.10). Interestingly, the value for **Fl-Te-6-Fl** (Eg = 3.2 eV) is smaller than the one reported by Seferos' 2,5-bis(2-(9,9-dihexylfluorene)) tellurophene (Eg = 3.46 eV),[38] indicating a likely more delocalized structure in **Fl-Te-6-Fl** and more planar configuration provided by the absence of alkyl chains in the fluorene unit compared to 2,5-bis(2-(9,9-dihexylfluorene)) tellurophene.

Different studies have shown the absorption maximum for a single molecule of naphthalene occurs at 219 nm with another absorption band at 275 nm;[39,40] these spectral features have been assigned to π-π* transitions.[41] According to this, the high energy absorptions observed in the naphthalene-substituted tellurophenes **Naph-Te-6-B** and **Naph-Te-6-Naph** (287 and 281 nm, respectively) could also be attributed to a π-π* transition from the naphthalene units themselves; in line with this postulate, there is a reduction in intensity of this band in **Naph-Te-6-B** (ε = 14500 $M^{-1}cm^{-1}$) compared to **Naph-Te-6-Naph** (ε = 22100 $M^{-1}cm^{-1}$), since less naphthalene groups are available to absorb and contribute to the intensity of the band compared to the disubstituted **Naph-Te-6-Naph**. The second band observed in **Naph-Te-6-Naph** and **Naph-Te-6-B** at 322 and 324 nm, respectively is tentatively assigned as a Te (lone pair) to π* transition (with quinodal C-C π-bonding character). In the case of the closest analogue naphthalene-substituted chalcogenophene (**Naph-S1-Naph**) reported[36,37] (Figure 4.8), two similar bands in the UV-vis spectrum at 282 and 352 nm, however, no specific assignment was reported.

Theoretical calculations on **2,4-BPin$_2$-3,5-Ph$_2$-Te**[21] (Figure 4.3) showed that the electron density in the HOMO level is located on Te lone pair atom and a π-bonding manifold between carbons C3 and C4 in the tellurophene ring. The LUMO level has orbital density located at two sites: one is a delocalized π-orbital between the ipso-carbon of the Ph substituent and the tellurophene ring and the other site is a π overlap between the carbon and the empty p-orbital on boron. Based on this data, it is possible to that in **Naph-Te-6-Naph** and **Naph-Te-6-B** a related HOMO-LUMO transition is contributing to the second absorption bands located at 322-324 nm. In the case of **Naph-Te-6-B** two charge transfer absorptions from Te to the naphthalene and BPin groups could be responsible for the observed lower energy absorption, and computational studies are underway to gain more insight into this process.

In the case of **Fl-Te-6-Fl**, two intense absorption bands were observed at 266 (ε = 30700 $M^{-1}cm^{-1}$) and 330 nm (ε = 32600 $M^{-1}cm^{-1}$) with a shoulder around 310 nm. Looking at the absorption properties of a single fluorene molecule,[42] three absorption bands can be distinguished (260, 290 and 300 nm) and all correspond to transitions of π-π* character.[43,38] Based on this assignment, all absorption bands in **Fl-Te-6-Fl** could have contribution from the single fluorene unit, however, due to the broadness of the band at 330 nm is possible that other transitions involving the tellurophene ring could be contributing to the broad signal observed. The Seferos group reported theoretical and experimental results on 2,5-bis(2-(9,9-dihexylfluorene))tellurophene (Figure 4.8) and of fluorene itself.[38] In this study, the UV-vis spectrum of the fluorene-substituted tellurophene was found to have a broad band at 390 nm, which by their theoretical calculations, it was assigned to a transition from the HOMO level localized at the carbon atoms in the tellurophene ring (π in character) to a LUMO level, where orbital density is delocalized in a π-type orbital between the fluorene units and the core tellurophene ring. Due to similar structural characteristics of 2,5-bis(2-(9,9-dihexylfluorene))tellurophene and **Fl-Te-6-Fl**, the same type of transition at 330 nm might be occurring in **Fl-Te-6-Fl**.

In the case of the assignment of the absorption band in **Ar^F-Te-6-Ar^F** at 312 nm, the lack of available data in the absorption properties of the fluoroarene *m*-$(CF_3)_2C_6H_4$ or any related chalcogenophene makes the assignment uncertain at this time. However, given that *m*-$(CF_3)_2C_6H_3$ is a good electron-withdrawing group, it is possible that a transition between the π orbitals localized in the tellurophene center to orbitals located on the Ar^F could be occurring, in a similar fashion as postulated for **Naph-Te-6-Naph** and **Fl-Te-6-Fl**.

The emission properties of **Naph-Te-6-Naph**, **Fl-Te-6-Fl**, **Ar^F-Te-6-Ar^F** and **Naph-Te-6-B** were first tested in the solid state under UV-light (irradiation at ca. 365 nm at room temperature) under aerated conditions. It was found that only **Ar^F-Te-6-Ar^F** and **Naph-Te-6-B** showed visible photoluminescence with intense yellow and faint red-orange emission, respectively (see Figure 4.11).

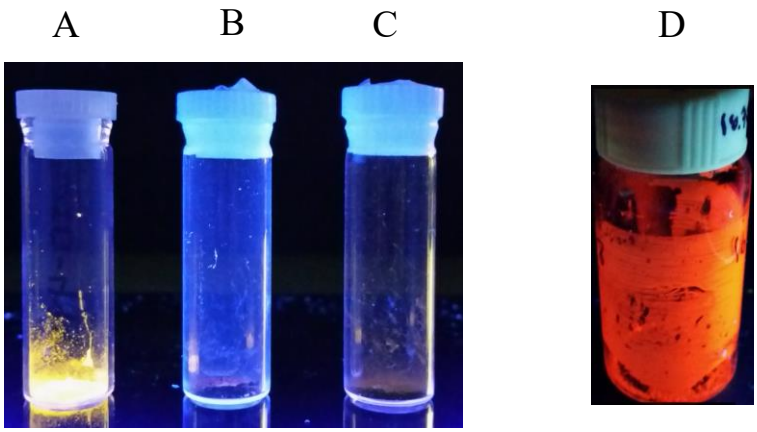

Figure 4.11. Solid state luminescence of A) **Ar^F-Te-6-Ar^F** (under air) and D) **Naph-Te-6-B** (under air) and the lack of visually discernable emission from B) **Naph-Te-6-Naph** (under N_2) and C) **Fl-Te-6-Fl** (under N_2) at room temperature, when irradiated with UV light at λ = 365 nm.

More detailed photoluminescence studies on **Ar^F-Te-6-Ar^F** indicated that the nature of the yellow emission at 600 nm (Figures 4.11 and 4.12) to be phosphorescence with a lifetime of τ = 29.3 μs measured in air at room temperature, with an absolute quantum yield of (ϕ) of 9.4 %. Interestingly, when films of **Naph-Te-6-Naph** and **Fl-Te-6-Fl** were frozen in liquid N_2 and exposed immediately to UV light of 365 nm, faint orange-red and yellow-orange luminescence was detected in each solid sample, respectively, however, their intensity was too low to obtain reliable lifetime and quantum yield data; however the large Stokes shifts noted are consistent with phosphorescence. Initial attempts to get the emission profile of the unsymmetric red-emitter **Naph-Te-6-B** in the solid state have been difficult, given the very low nature of its red emission. An explanation for this process is the retention of some molecular in the amorphous films of these tellurophenes at room temperature which are suppressed upon cooling, thus leading to less non-radiative quenching via a restriction of intramolecular rotation.

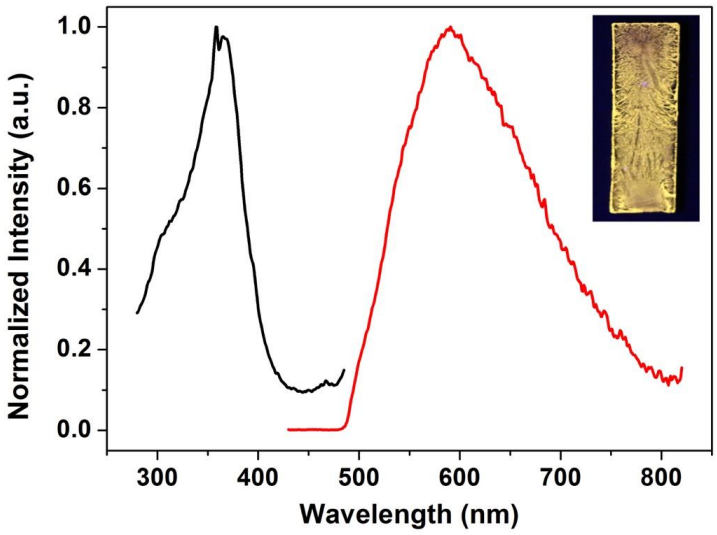

Figure 4.12. Luminescence measurements of **Ar^{F}-Te-6-Ar^{F}** in film at room temperature, λ_{exc} = 375 nm.

None of the tellurophenes reported in this chapter were found to be emissive in THF under air or N_2 atmosphere at room temperature. It is likely that a non-radiative relaxation mechanism is occurring, such as intramolecular rotations of the appended groups.

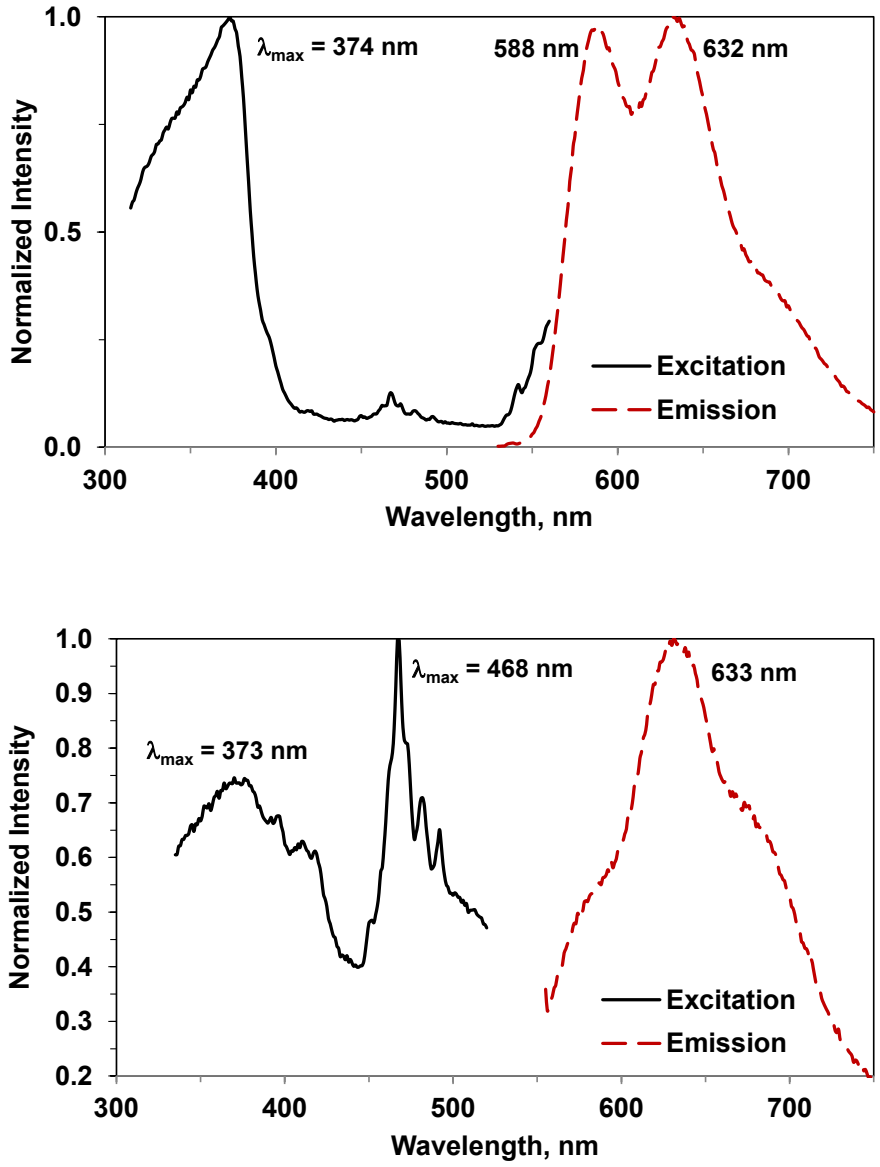

Figure 4.13. Luminescence measurements of **Naph-Te-6-Naph** (top, λ_{exc} = 375 nm) and **Fl-Te-6-Fl** (bottom, λ_{exc} = 475 nm) in film at low temperature (77 K).

Additional theoretical calculations are underway in order to know the possible energy distribution of the different excited singlet and triplet states available in **Naph-Te-6-Naph**, **Fl-Te-6-Fl** and **Ar^F-Te-6-Ar^F**, and to explain the phosphorescence observed in each case.

Table 4.8. Excitation and emission properties of symmetric tellurophenes.

	STATE	λ_{max}, nm	λ_{em}, nm
Naph-Te-6-Naph[a]	FILM	374	588, 632
Fl-Te-6-Fl[a]	FILM	373, 468	633
Ar^F-Te-6-Ar^F[b]	FILM	370	600

Measures at a) low temperature, 77 K and b) r.t.

Overall, the luminescence studies showed some interesting trends. While the symmetric tellurophene (**Naph-Te-6-Naph**) is practically not luminescent at room temperature, its un-symmetric counterpart, **Naph-Te-6-B**, is a faint red-orange emitter at room temperature. It is likely that for **Naph-Te-6-B** the presence of the acceptor group, BPin creates a donor-acceptor (D-A) type structure that red-shifts the emission. The low quantum yield in these species could be due to a lack of crystallinity in the solid state that enables quenching by O_2 to occur more readily (via diffusion through the film); moreover there is a chance for molecular motion in these amorphous films, which also could lead to a reduction in quantum yield. Lastly the red-emitting **Naph-Te-6-B** would have a faster rate of non-radiative decay due to the Energy Gap Law.[44]

Low quantum yields in solid red emitters could be partially overcome by using bulky substituents in the fluorophores to prevent quenching by close packing; this strategy has been reported with perylene bisimides and naphthalenes moieties as a fluorophores and tetraphenylethene (TPE) as a bulky substituent (Figure 4.14).[45] Accordingly, it could be interesting to study the optical properties of tellurophenes using more bulky and conjugated systems than the substituent naphthalene, such as anthracene, with the goal to obtain more intense red emission and high quantum yields by preventing close intermolecular contacts from forming, thus mitigating triplet-triplet annihiliation.

In order to have red-shift emission (generally fluorescence), it is often necessary to couple several aromatic units to form long conjugated systems (Figure 4.14). In the case of **Naph-Te-6-B** such extended levels of conjugation are not needed due to effective intersystem crossing (ISC) between excited singlet, S_n, and triplet, T_n, states, leading to the resulting large Stokes shift associated with phosphorescence (and red emission). Thus one can achieve red emission without complex synthetic procedures.

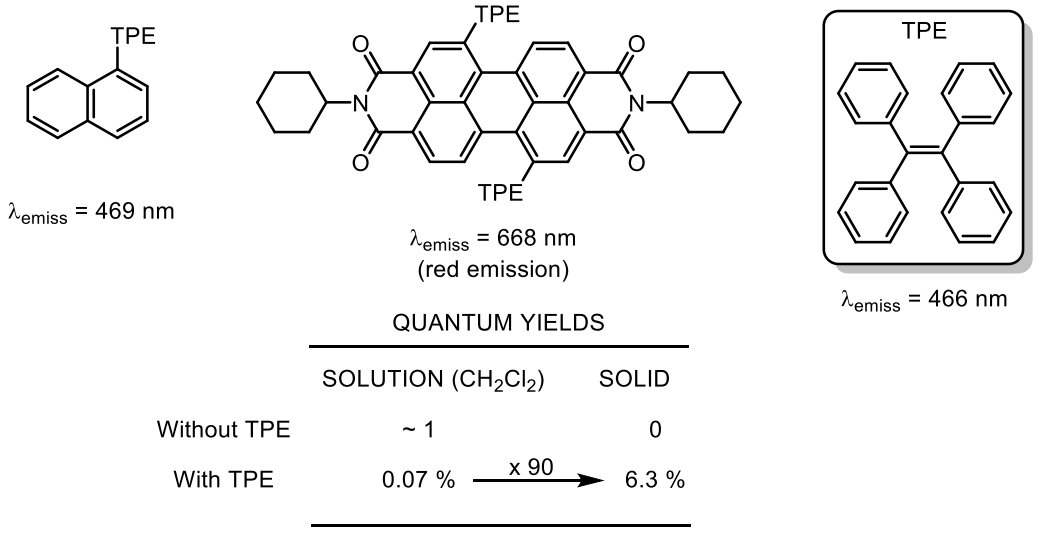

Figure 4.14. TPE-substituted fluorophores with increasing quantum yields in the solid state by attaching TPE moiety.

Another observation, related to the intense yellow phosphorescence emission of **Ar^F-Te-6-Ar^F** is that it seems that the combination of electron withdrawing groups (such as *m*-$(CF_3)_2C_6H_3$) attached to the electron-rich tellurophene in **Ar^F-Te-6-Ar^F** forms a good couple acceptor-donor-acceptor (A-D-A) to yield intensely phosphorescent tellurophenes in the solid state at room temperature. Here the aryl-bound CF_3 groups might be preventing close intermolecular packing in the solid state and so helping to avoid self-quenching of triplet emission. In terms of the easy synthesis of symmetric tellurophenes compared to the unsymmetric derivatives, the discovery that symmetric tellurophenes could still be phosphorescent in solid state at room temperature is an important finding, which could open a door to

a new class of easy accessible emitters. Given the high quantum yield noted when electron-withdrawing Ar^F groups are appended onto a tellurophene, it would be interesting to prepare analogues Te heterocycles containing $(CHO)C_6H_4$, $(CN)C_6H_4$ and $(COOMe)C_6H_4$ as side groups (Figure 4.15).

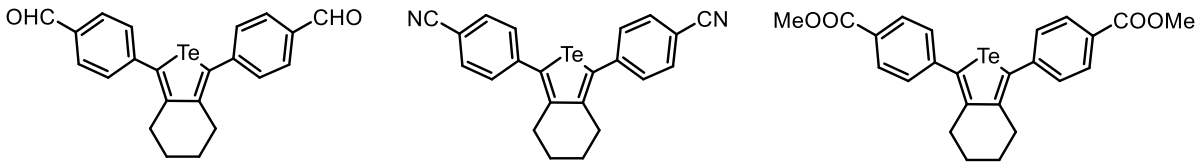

Figure 4.15. Possible luminescence symmetric tellurophenes with different electron withdrawing substituents appended to the tellurophene.

4.3. CONCLUSIONS

Synthetic protocols have been developed to obtain phosphorescent symmetrically and unsymmetrically-substituted tellurophenes through Suzuki-Miyaura and Sonogashira cross-coupling reactions. The electron-deficient species **Ar^F-Te-6-Ar^F** was strongly emitting in the solid state despite the lack of BPin groups, thus it is now possible to achieve phosphorescence using readily available diarylated tellurophenes. Future work will involve the synthesis of another symmetric tellurophenes with different electron withdrawing groups attached at the 2- and 5-positions of the five-membered tellurophenes and study their optoelectronic properties.

4.4. EXPERIMENTAL SECTION

4.4.1. General methods

Unless explicitly stated, all reactions were conducted with standard Schlenk and glove box (MBraun) techniques using N_2 as an inert atmosphere, with solvents that were dried using a Grubbs' type purification system manufactured by Innovative Technology Inc. 1,7-octadiyne and 2,2'-bipyridine (Bipy) were purchased from GFS Chemicals, Cp_2ZrCl_2 was purchased from Strem Chemicals Inc., 2-isopropoxy-4,4,5,5-tetramethyl-1,3,2-dioxaborolane (^{i}PrOBPin), 1-bromo-3,5-bis(trifluoromethyl)benzene and 4-bromo-N,N-dimethylaniline were purchased from Matrix Scientific and all other chemicals were obtained from Aldrich. Bipy•$TeCl_2$ was synthesized according a literature procedure.[46] ^{1}H, $^{13}C\{^{1}H\}$, $^{11}B\{^{1}H\}$ and ^{19}F NMR spectra were recorded on either a Varian Innova 500 and 400 spectrometer and referenced externally to Me_4Si (^{1}H and $^{13}C\{^{1}H\}$), F_3B•OEt_2 (^{11}B) and $CFCl_3$ (^{19}F). Melting points were measured in a MelTemp apparatus and are reported without correction. Elemental analysis were performed by the Analytical and Instrumentation Laboratory at the University of Alberta, UV-visible measurements were performed with a Varian Cary 300 Scan spectrophotometer and fluorescence measurements with a Photon Technology International (PTI) MP1 fluorometer. High resolution mass spectra were obtained on an Agilent 6220 spectrometer.

4.4.1.1 Synthesis of B-C8-H:

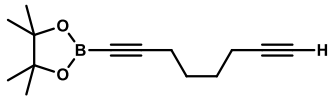

To a solution of 15 mL (113 mmol) of 1,7-octadiyne in 225 mL of Et_2O at -78 °C under N_2, was added slowly a ^{n}BuLi solution (2.5 M in hexanes, 9.0 mL, 23 mmol). The mixture was then stirred for 1 h at -78 °C, followed by addition via cannula to another Schlenk flask containing a solution of ^{i}PrOBPin (4.7 mL, 23 mmol) in 100 mL of Et_2O at -78 °C. The reaction mixture was stirred for 2 h at -78 °C. After stirring at room temperature overnight, a solution of HCl was added (4.0 M in dioxane, 16.8 mL, 68 mmol) at -78 °C and followed by stirring at room temperature overnight. The mixture was filtered in air and the

solvent removed from the filtrate. The excess of 1,7-octadiyne and dioxane were removed under vacuum at 80 °C to afford **B-C8-H** as a colorless oil (4.708 g, 87 % yield). ^{1}H NMR (400 MHz, $CDCl_3$): δ 2.31-2.23 (m, 2H, BC≡CCH_2), 2.21-2.16 (m, 2H, HC≡CCH_2), 1.92 (t, 1H, $^{4}J_{HH}$ = 2.7 Hz, HC≡CCH$_2$), 1.68-1.59 (m, 4H, HC≡CCH$_2$(CH_2)$_2$), 1.25 (s, 12H, CH_3). ^{13}C{^{1}H} NMR (400 MHz, $CDCl_3$): δ 84.17 and 84.15 (CH$_2$$C$≡CB and H$C$≡C), 84.1 ((H$_3$C)$_2$$C$), 68.7 (HC≡$C$), 27.5, 27.1 (C≡CCH$_2$($CH_2$)$_2$), 24.8 ($CH_3$), 19.2, 18.0 (C≡C$CH_2$(CH$_2$)$_2$). ^{11}B{^{1}H} NMR (400 MHz, $CDCl_3$): δ 23.6.

4.4.1.2. Synthesis of H-C8-Naph:

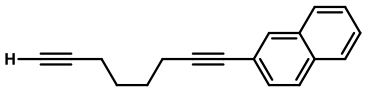

$Pd(PPh_3)_4$ (0.198 g, 0.17 mmol), CuI (0.065 g, 0.34 mmol), PPh_3 (0.090 g, 0.34 mmol), diisopropylamine (8.4 mL, 60 mmol) and 1,7-octadiyne (7.8 mL, 60 mmol) were dissolved in 57 mL of toluene under N_2. Once the solution was warmed up to 75 °C, a solution of 2-bromonaphthalene (1.837 g, 8.60 mmol) in 10 mL of toluene was added over 10 minutes and the mixture was stirred overnight at 75 °C. The reaction mixture was filtered through a pad of silica gel at room temperature and the filtrate was washed twice with 200 mL portions aqueous saturated of NH_4Cl and the organic layer was recovered and dried over $MgSO_4$. After another filtration, the solvent was removed under reduced pressure at room temperature, followed by exposure to dynamic vacuum with stirring for 3 h at 60 °C. The remaining oily was re-dissolved in 100 mL of cold pentane (0 °C) and then filtered to remove the possible by-product of **Naph-C8-Naph**, which is insoluble in cold pentane. The solvent was removed under vacuum and the resulting product was purified by column chromatography using silica gel (75:1 hexanes/ethyl acetate mixture as an eluent) to give **H-C8-Naph** as a pale yellow oil (1.608 g, 70 %). ^{1}H NMR (500 MHz, $CDCl_3$): δ 7.93 (s, 1H, ArH), 7.83-7.74 (m, 3H, ArH), 7.51-7.44 (m, 3H, ArH), 2.51 (t, 2H, $^{3}J_{HH}$ = 6.7 Hz, ArC≡CCH_2), 2.33-2.28 (m, 2H, HC≡CCH_2), 2.00 (t, 1H, $^{4}J_{HH}$ = 2.7 Hz, HC≡CCH$_2$), 1.83-1.73 (m, 4H, HC≡CCH$_2$(CH_2)$_2$). ^{13}C{^{1}H} NMR (500 MHz, $CDCl_3$): δ 133.2, 132.6, 131.2, 128.8, 127.9, 127.8, 127.7, 126.5,

126.4 and 121.4 (Ar*C*), 90.2 (Ar*C*≡C), 84.3 (H*C*≡C), 81.4 (ArC≡*C*), 68.7 (HC≡*C*), 27.9 and 27.8 (C≡CCH$_2$(*C*H$_2$)$_2$), 19.2 and 18.2 (C≡C*C*H$_2$(CH$_2$)$_2$). HR-MS (EI) ($C_{18}H_{16}$): m/z: Calcd: 232.12520; Found: 232.12507 (Δppm = 0.6). Anal. Calcd. for $C_{18}H_{16}$: C, 93.06; H, 6.94; Found: C, 92.71; H, 6.93.

4.4.1.3. Synthesis of H-C8-Ar^F:

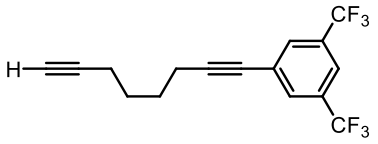

Pd(PPh$_3$)$_4$ (0.298 g, 0.25 mmol), CuI (0.098 g, 0.51 mmol), PPh$_3$ (0.135 g, 0.51 mmol), diisopropylamine (12.6 mL, 90.4 mmol), 1,7-octadiyne (12.0 mL, 90.4 mmol) and 1-bromo-3,5-bis(trifluoromethyl)benzene (3.862 g, 12.9 mmol) were dissolved in 86 mL of toluene under N_2. The final solution was stirred for 36 h at 75 °C. The reaction mixture was filtered through a pad of silica gel at room temperature and the filtrate was washed twice with 300 mL portions aqueous saturated of NH_4Cl and the organic layer was recovered and dried over $MgSO_4$. After another filtration, the solvent was removed under reduced pressure at room temperature, followed by exposure to dynamic vacuum with stirring for 3 h at 60 °C. The residue was mixed with 100 mL of cold pentane (0 °C) and then filtered. The solvent was removed from the filtrate under vacuum and the resulting product was purified by column chromatography using silica gel and a 75:1 hexanes/ethyl acetate mixture as an eluent (R_f = 0.45) to give **H-C8-Ar^F** as an oil (2.379 g, 57 %). ^{1}H NMR (500 MHz, $CDCl_3$): δ 7.81 (s, 2H, Ar*H*), 7.75 (s, 1H, Ar*H*), 2.47 (t, 2H, $^3J_{HH}$ = 6.8 Hz, ArC≡CC*H*$_2$), 2.30-2.25 (m, 2H, HC≡CC*H*$_2$), 1.97 (t, 1H, $^4J_{HH}$ = 2.7 Hz, *H*C≡CCH$_2$), 1.80-1.67 (m, 4H, HC≡CCH$_2$(C*H*$_2$)$_2$). ^{13}C{^{1}H} NMR (500 MHz, $CDCl_3$): δ 131.9 (q, $^2J_{CF}$ = 33.5 Hz, *C*CF$_3$), 131.6 (Ar*C*), 126.4 (Ar*C*), 123.2 (q, $^1J_{CF}$ = 272.7 Hz, *C*F$_3$C;), 121.1 (Ar*C*), 94.0 (Ar*C*≡C), 84.0 (H*C*≡C), 78.6 (ArC≡*C*), 68.8 (HC≡*C*), 27.7 and 27.5 (C≡CCH$_2$(*C*H$_2$)$_2$), 19.1 and 18.1 (C≡C*C*H$_2$(CH$_2$)$_2$). HR-MS (EI) ($C_{16}H_{12}F_6$): m/z: Calcd: 318.08432; Found: 318.08441 (Δppm = 0.3). Anal. Calcd. for $C_{16}H_{12}F_6$: C, 60.38; H, 3.80; Found: C, 60.50; H, 3.75.

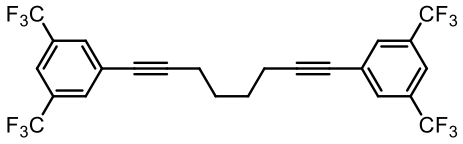

In one of the first fractions eluted from column, the by-product **Ar^F-C8-Ar^F** was recovered (0.076 g). **Ar^F-C8- Ar^F**: ^{1}H NMR (500 MHz, $CDCl_3$): δ 7.81 (s, 4H, Ar*H*), 7.75 (s, 2H, Ar*H*), 2.53 (m, 4H, C≡CCH_2CH$_2$), 1.82 (m, 4H, C≡CCH$_2$CH_2). ^{13}C{^{1}H} NMR (500 MHz, $CDCl_3$): δ 132.0 (q, $^2J_{CF}$ = 33.5 Hz, *C*CF$_3$,), 131.6 (Ar*C*), 126.3 (Ar*C*), 123.1 (q, $^1J_{CF}$ = 272.7 Hz, *C*F$_3$), 121.2 (Ar*C*), 93.8 (Ar*C*≡C), 78.8 (ArC≡*C*), 27.7 (C≡CCH$_2$(*C*H$_2$)$_2$) and 19.1 (C≡C*C*H$_2$(CH$_2$)$_2$). HR-MS (EI) ($C_{24}H_{14}F_{12}$): m/z: Calcd: 530.09039; Found: 530.08982 (Δppm = 1.1). Anal. Calcd. for $C_{24}H_{14}F_{12}$: C, 54.35; H, 2.66; Found: C, 54.34; H, 2.84.

4.4.1.4. Synthesis of B-C8-Naph:

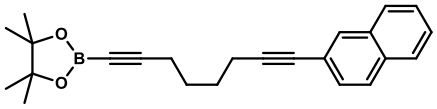

To a solution of **H-C8-Naph** (0.791 g, 3.41 mmol) in 68 mL of Et_2O at -40 °C was added dropwise an ^{n}BuLi solution (2.5 M in hexanes, 1.5 mL, 3.8 mmol). After the mixture was stirred for 2 h at -40 °C, neat ^{i}PrOBPin (0.72 mL, 3.4 mmol) was added. The reaction mixture was stirred for 3 h at room temperature and then quenched with 4.3 mL (17 mmol) of 4.0 M HCl in dioxane at -40 °C. The resultant mixture was then stirred at room temperature overnight followed by filtration in air. The volatiles were removed from the filtrate under vacuum to give **B-C8-Naph** as an oil in quantitative mass yield with 79 % purity estimated by ^{1}H NMR spectroscopy. ^{1}H NMR (500 MHz, $CDCl_3$): δ 7.89 (s, 1H, Ar*H*), 7.80-7.72 (m, 3H, Ar*H*), 7.48-7.42 (m, 3H, Ar*H*), 2.51-2.45 (m, 2H, ArC≡CCH_2), 2.38-2.33 (m, 2H, PinBC≡CCH_2), 1.80-1.72 (m, 4H, PinBC≡CCH$_2$(CH_2)$_2$), 1.27 (s, 12H, CH_3). ^{13}C{^{1}H} NMR (500 MHz, $CDCl_3$): δ 133.2, 132.6, 131.2, 128.8, 127.9, 127.8, 127.7, 126.4, 126.4 and 121.4 (Ar*C*), 90.1 (Ar*C*≡C), 84.2 (BC≡*C*) and 81.4 (ArC≡*C*), 27.9 and 27.4 (C≡CCH$_2$(*C*H$_2$)$_2$), 24.8 (*C*H$_3$), 19.3 and 19.2 (C≡C*C*H$_2$(CH$_2$)$_2$). ^{11}B {^{1}H} NMR (500 MHz, $CDCl_3$): δ 23.7. HR-MS (EI) ($C_{24}H_{27}BO_2$): m/z: Calcd: 358.21042; Found: 358.21002 (Δppm = 1.1).

4.4.1.5. Synthesis of B-C8-Ar^F:

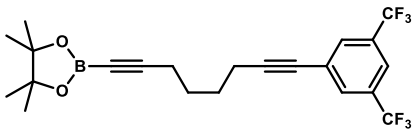

To a solution of **H-C8-Ar^F** (0.943 g, 2.73 mmol) in 109 mL of Et_2O at -78 °C was added dropwise ^{n}BuLi (2.5 M solution in hexanes, 1.2 mL, 3.0 mmol). After stirring for 1 h at -78 °C, neat ^{i}PrOBPin (0.57 mL, 2.7 mmol) was added by syringe. The mixture was stirred at room temperature overnight and then HCl (4.0 M solution in dioxane, 3.4 mL, 14 mmol) was added at -78 °C. The resulting mixture was then stirred at room temperature for 8 h. The reaction mixture was filtered in air and the volatiles were removed under reduced pressure to give **B-C8-C$_6$H$_3$(CF$_3$)$_2$** with 75 % of purity as estimated by ^{1}H NMR spectroscopy. ^{1}H NMR (500 MHz, $CDCl_3$): δ 7.81 (s, 2H, Ar*H*), 7.74 (s, 1H, Ar*H*), 2.48-2.43 (m, 2H, ArC≡CC*H*$_2$), 2.37-2.32 (m, 2H, PinBC≡CC*H*$_2$), 1.79-1.67 (m, 4H, PinBC≡CCH$_2$(C*H*$_2$)$_2$), 1.27 (s, 12H, C*H*$_3$). ^{13}C{^{1}H} NMR (500 MHz, $CDCl_3$): δ 131.9 (q, $^2J_{CF}$ = 33.5 Hz, *C*CF$_3$), 131.6 (Ar*C*), 126.4 (Ar*C*), 123.2 (q, $^1J_{CF}$ = 273.2 Hz, *C*F$_3$;), 121.1 (Ar*C*), 93.9 (Ar*C*≡C), 84.3 (BC≡*C*), 78.6 (ArC≡*C*), 27.5 and 27.3 (C≡CCH$_2$(*C*H$_2$)$_2$), 24.8 (*C*H$_3$), 19.3 and 19.1 (C≡C*C*H$_2$(CH$_2$)$_2$). ^{11}B{^{1}H} NMR (500 MHz, $CDCl_3$): δ 23.6. HR-MS (EI) ($C_{16}H_{12}F_6$): m/z: Calcd: 444.16953; Found: 444.16989 (Δppm = 0.8).

4.4.1.6. Synthesis of Naph-Te-6-Naph:

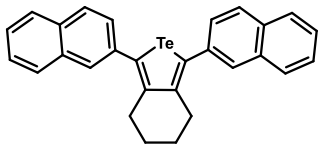

B-Te-6-B (0.201 g, 0.41 mmol), 2-bromonaphthalene (0.175 g, 0.82 mmol), $Pd(OAc)_2$ (3.7 mg, 4 mol%), Xphos (0.016 g, 8 mol%) were dissolved in 5.0 mL of MeCN. After adding 0.82 mL of aqueous K_2CO_3 (2.0 M solution, 1.6 mmol), the reaction mixture was stirred at 80 °C for 60 h. The final product was not soluble in MeCN, thus the supernatant was decanted and 50 mL of $CHCl_3$ was added to dissolve the precipitate. The resulting

solution was filtered through a pad of Celite. After the volatiles were removed from the filtrate, the remaining solid was washed three times with 20 mL aliquots of pentane to remove the residues of Xphos and dried under reduced pressure to afford **Naph-Te-6-Naph** as a brown solid (0.072 g, 36 %). ^{1}H NMR (600 MHz, $CDCl_3$): δ 7.89 (s, 2H, Ar*H*), 7.88-7.82 (m, 6H, Ar*H*), 7.61-7.57 (m, 2H, Ar*H*), 7.53-7.47 (m, 4H, Ar*H*), 2.82 (br, 4H, C=CC*H*$_2$), 1.69 (br, 4H, C=CCH$_2$C*H*$_2$). ^{13}C{^{1}H} NMR (500 MHz, $CDCl_3$): δ 144.9, 139.7, 137.9, 133.5, 132.3, 128.1, 128.01, 127.96, 127.9, 127.8, 126.5 and 126.1 (Ar*C* and Te-*C*=*C*), 30.8 (C=CCH$_2$*C*H$_2$) and 23.5 (C=C*C*H$_2$CH$_2$). UV/Vis (THF): λ_{max} (ε) = 281 nm (2.21×10^4 M^{-1} cm^{-1}), 324 nm (1.85×10^4 $M^{-1}cm^{-1}$). HR-MS (EI) ($C_{28}H_{22}Te$): m/z: Calcd: 488.07837; Found: 488.07782 (Δppm = 1.3). Anal. Calcd. for $C_{28}H_{22}Te$: C, 69.19; H, 4.56; Found: C, 68.47; H, 4.59. Mp(°C): 171-174.

4.4.1.7. Synthesis of Fl-Te-6-Fl:

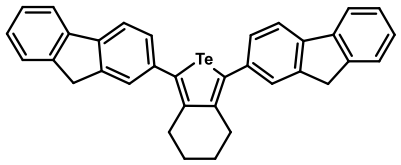

B-Te-6-B (0.392 g, 0.81 mmol), 2-bromofluorene (0.413 g, 1.60 mmol), $Pd(OAc)_2$ (7.3 mg, 4 mol%), Xphos (0.031 g, 8 mol %) were dissolved in 10 mL of MeCN. After adding 1.6 mL of aqueous K_2CO_3 (2.0 M solution, 3.2 mmol), the reaction mixture was stirred at 80 °C for 12 h. The resulting mixture was filtrated and the precipitate washed four times with 20 mL portions of MeCN and three times with 20 mL portions of hexanes. The remaining solid was dissolved in 5 mL of CH_2Cl_2, filtered through small pad of Celite and the volatiles removed under reduced pressure to yield **Fl-Te-6-Fl** as a yellow-green powder (0.177 g, 39 %). ^{1}H NMR (500 MHz, $CDCl_3$): δ 7.78 (pseudo t, 4H, J_{HH} = ca. 8.1 Hz, Ar*H*), 7.61 (pseudo s, 2H, J_{HH} = ca. 0.9 Hz, Ar*H*), 7.55 (d, 2H, J_{HH} = ca. 7.2 Hz, Ar*H*), 7.47 (dd, 2H, J_{HH} = ca. 7.8 Hz, J_{HH} = ca. 1.7 Hz, Ar*H*), 7.39 (pseudo t, 2H, J_{HH} = ca. 7.3 Hz, Ar*H*), 7.31 (pseudo t, 2H, J_{HH} = ca. 7.3 Hz, J_{HH} = ca. 1.2 Hz, Ar*H*), 3.94 (s, 4H, C*H*$_2$ in Fl), 2.79 (m, 4H, C=CC*H*$_2$CH$_2$), 1.68 (m, 4H, C=CCH$_2$C*H*$_2$). ^{13}C{^{1}H} NMR (500 MHz, $CDCl_3$): δ 144.6, 143.6, 143.5, 141.5, 140.6, 139.8, 139.0, 128.3, 127.0, 126.9, 126.1, 125.2, 120.0 and 119.7

(Ar*C*), 37.1 (*C*H$_2$), 30.8 (C=C*C*H$_2$CH$_2$), 23.5 (C=CCH$_2$*C*H$_2$). UV/Vis (THF): λ_{max} (ε) = 266 nm (3.07×10^4 M^{-1} cm^{-1}), 330 nm (3.26×10^4 M^{-1} cm^{-1}). HR-MS (EI) ($C_{34}H_{26}Te$): m/z: Calcd: 564.10913; Found: 564.10883 (Δppm = 0.52). Anal. Calcd. for $C_{34}H_{26}Te$: C, 72.64; H, 4.66; Found: C, 71.99; H, 4.82. Mp(°C): > 250.

4.4.1.8. Synthesis of Ar^F-Te-6-Ar^F:

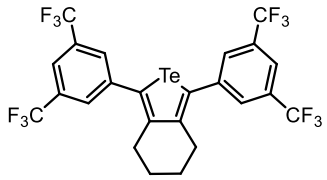

B-Te-6-B (0.196 g, 0.40 mmol), 5-bromo-1,3-bis(trifluoromethyl)benzene (0.239 g, 0.80 mmol), Pd(OAc)$_2$ (3.6 mg, 4 mol%), Xphos (0.016 g, 8 mol %) were dissolved in 5.5 mL of a solvent mixture of MeCN / THF (10:1) in a vial suitable for microwave reactions. After adding 0.2 mL of aqueous K_2CO_3 (2.0 M solution, 0.4 mmol), the reaction mixture was stirred at 110 °C for 3 h in a microwave reactor. The resulting mixture was poured into 60 mL of $CHCl_3$ while stirring, filtered through a pad of Celite and the solvent removed under reduced pressure. The remaining solid was dissolved in 50 mL of toluene and wash four times with 50 mL portions of water. The organic layer dried over $MgSO_4$, filtered and the volatiles removed under reduced pressure to yield the product as a light yellow solid (0.190 g, 72 %). The resulting crude product was purified by column chromatography using silica gel and petroleum ether as an eluent to give **Ar^F-Te-6-Ar^F** as a light yellow solid (0.114 g, 43 %). ^{1}H NMR (500 MHz, $CDCl_3$): δ 7.82 (s, 6H, Ar*H*), 2.65 (m, 4H, C=CC*H*$_2$CH$_2$), 1.68 (m, 4H, C=CCH$_2$C*H*$_2$). ^{13}C{^{1}H} NMR (500 MHz, $CDCl_3$): δ 143.3, 142.2, 137.0 (Ar*C*), 132.0 ($^2J_{CF}$ = 33.5 Hz, *C*CF$_3$), 129.2 (ArC), 123.3 ($^1J_{CF}$ = 272.7 Hz, *C*F$_3$), 30.4 (C=C*C*H$_2$CH$_2$), 23.0 (C=CCH$_2$*C*H$_2$). ^{19}F NMR (500 MHz, $CDCl_3$): δ 62.8. UV/Vis (THF): λ_{max} (ε) = 312 nm (1.40×10^4 M^{-1} cm^{-1}). HR-MS (EI) ($C_{24}H_{14}F_{12}Te$): m/z: Calcd: 659.99606; Found: 659.99554 (Δppm = 0.79) Anal. Calcd. for $C_{24}H_{14}F_{12}Te$: C, 43.81; H, 2.14; Found: C, 43.99; H, 2.29.

4.4.1.9. Synthesis of B-Te-6-Naph:

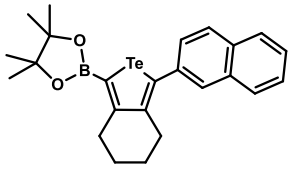

To a solution of Cp_2ZrCl_2 (0.675 g, 2.31 mmol) in 23 mL of THF was added ^{n}BuLi (1.8 mL, 4.6 mmol, 2.5 M solution in hexanes) at -78 °C. After stirring for 1 h, a solution of **B-C8-Naph** (0.802 g, 2.24 mmol) in 10 mL of THF was added via cannula. After stirring overnight at room temperature, a solution of Bipy•$TeCl_2$ (0.876 g, 2.47 mmol) in 20 mL of toluene was added dropwise under inert atmosphere and followed by stirring at room temperature for 24 h. The volatiles were removed under reduced pressure and the resulting solid was dissolved in 50 mL of toluene and filtered through a small pad of silica gel (under air). The filtrate was concentrated to a volume of *ca.* 10 mL and then stored at 4 °C for 2 days in order to precipitate the Cp_2ZrCl_2 by-product. The mother liquor was decanted and collected. The remaining precipitate was washed three times with 2 mL portions of cold toluene (~ 0 °C). The organic fractions were combined and the solvent was removed to give an oil. In order to remove any remaining Cp_2ZrCl_2 that might still be present, a 10 mL mixture of CH_2Cl_2 / hexanes (1:1) was added to the oily product and the mixture cooled to 0 °C for 16 h; this cold solution was then passed through a small pad of silica gel to effectively remove Cp_2ZrCl_2. The solvent was removed from the filtrate under vacuum to get an oily mixture of products (0.770, 70 %). The resulting product was purified by column chromatography using silica gel and a 25:1 hexanes/Et_2O mixture as an eluent (R_f = 0.15) to give **B-Te-6-Naph** as a yellow solid (0.096 g, 9 %).^{1}H NMR (500 MHz, $CDCl_3$): δ 7.83 (m, 4H, Ar*H*), 7.53 (m, 1H, Ar*H*), 7.48 (m, 2H, Ar*H*), 2.94 (t, 2H, $^{3}J_{HH}$ = 6.6 Hz, C=CCH_2), 2.72 (t, 2H, $^{3}J_{HH}$ = 6.2 Hz, C=CCH_2), 1.74 (m, 2H, C=CCH$_2$CH_2), 1.62 (m, 2H, C=CCH$_2$CH_2), 1.33 (s, 12H, CH_3). ^{13}C{^{1}H} NMR (500 MHz, $CDCl_3$): δ 147.1, 146.7, 138.6, 133.3, 132.4, 128.1, 127.8, 127.7, 127.5, 126.5, 126.1 (Ar*C* and Te-*C*=*C*), 83.7 (*C*-O), 33.4 (C=C*C*H$_2$), 31.0 (C=C*C*H$_2$), 24.9 (*C*H$_3$), 23.6 (C=CCH$_2$*C*H$_2$) and 23.4 (C=CCH$_2$*C*H$_2$). ^{11}B{^{1}H} NMR (500 MHz, $CDCl_3$): δ 31.3. UV/Vis (THF): λ_{max} (ε) = 287 nm (1.45×10^4 M^{-1} cm^{-1}), 312 nm (1.4×10^4 $M^{-1}cm^{-1}$). HR-MS (EI) ($C_{24}H_{27}BO_2Te$): m/z: Calcd: 488.11663; Found: 488.11685

(Δppm = -0.4). Anal. Calcd. for $C_{24}H_{27}BO_2Te$: C, 59.33; H, 5.60; Found: C, 60.26; H, 5.74. Mp(°C): 132-134.

4.4.1.10. Synthesis of B-Te-6-Ar^F:

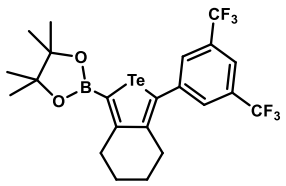

To a solution of Cp_2ZrCl_2 (0.522 g, 1.79 mmol) in 20 mL of THF was added ^{n}BuLi (1.4 mL, 3.5 mmol, 2.5 M solution in hexanes) at -78 °C. After stirring for 1 h, a solution of **B-C8-Ar^F** (0.770 g, 1.73 mmol) in 10 mL of THF was added via cannula. After stirring overnight at room temperature, a solution of Bipy•$TeCl_2$ (0.678 g, 1.91 mmol) in 20 mL of toluene was added dropwise under inert atmosphere, followed by stirring at room temperature for 24 h. The volatiles were removed under reduced pressure and the resulting solid was dissolved in 50 mL of toluene and filtered through a small pad of silica gel (under air). The filtrate was concentrated to a volume of *ca.* 10 mL and then stored at 4 °C for 2 days in order to precipitate the Cp_2ZrCl_2 by-product. The mother liquor was decanted and collected. The remaining precipitate was washed three times with 2 mL portions of cold toluene (~ 0 °C). The organic fractions were combined and the solvent was removed to give an oil. In order to remove any remaining Cp_2ZrCl_2 that might still be present, a 10 mL mixture of CH_2Cl_2 / hexanes (1:1) was added to the oily product and the mixture cooled to 0 °C; this cold solution was then passed through a small pad of silica gel to effectively remove Cp_2ZrCl_2. The solvent was removed from the filtrate under vacuum to get an oily mixture of products (1.025, 103 %). The solvent was removed from the filtrate under vacuum and the resulting product was purified by column chromatography using silica gel and a 30:1 hexanes/THF mixture as an eluent to give a **B-C8-Ar^F** as a solid (0.059 g, 6 %). ^{1}H NMR (500 MHz, $CDCl_3$): δ 7.79 (3H, Ar*H*), 2.93 (t, 2H, $^3J_{HH}$ = 6.6 Hz, C=CCH_2), 2.59 (t, 2H, $^3J_{HH}$ = 6.4 Hz, C=CCH_2), 1.73 (m, 2H, C=CCH$_2$CH_2), 1.62 (m, 2H, C=CCH$_2$CH_2), 1.33 (s, 12H, CH_3). ^{13}C{^{1}H} NMR (500 MHz, $CDCl_3$): δ 159.1, 148.1, 143.5, 131.6, 128.9, 124.5, 122.3, 120.5 (Ar*C* and Te-*C*=*C*), 84.0 (*C*-O), 33.2 (C=C*C*H$_2$), 30.7 (C=C*C*H$_2$), 24.9 (*C*H$_3$), 23.3 (C=CCH$_2$*C*H$_2$) and 23.1

(C=CCH$_2$*C*H$_2$). ^{11}B{^{1}H} NMR (400 MHz, $CDCl_3$): δ 30.5. ^{19}F NMR (400 MHz, $CDCl_3$): δ 62.8. HR-MS (EI) ($C_{22}H_{23}BF_6O_2Te$): m/z: Calcd: 574.07575; Found: 574.07562 (Δppm = 0.2).

4.4.2. X-ray details

Table 4.9. X-Ray crystallographic data for **Naph-Te-6-Naph**.

A. Crystal Data	
formula	$C_{28}H_{22}Te$
formula weight	486.05
crystal dimensions (mm)	0.20 × 0.17 × 0.04
crystal system	orthorhombic
space group	*Pbca* (No. 61)
unit cell parameters[a]	
a (Å)	16.0968 (3)
b (Å)	7.3295 (2)
c (Å)	35.3537 (8)
V (Å^3)	4171.08 (17)
Z	8
ρ_{calcd} (g cm^{-3})	1.548
μ (mm^{-1})	11.32
B. Data Collection and Refinement Conditions	
diffractometer	Bruker D8/APEX II CCD[b]
radiation (λ [Å])	Cu Kα (1.54178) (microfocus source)
temperature (°C)	–100
scan type	ω and ϕ scans (1.0°) (5 s exposures)

data collection 2θ limit (deg)	148.03
total data collected	23232 ($-20 \le h \le 19$, $-9 \le k \le 8$, $-34 \le l \le 41$)
independent reflections	4108 ($R_{int} = 0.0673$)
number of observed reflections (*NO*)	3772 [$F_o^2 \ge 2\sigma(F_o^2)$]
structure solution method	Patterson/structure expansion (*DIRDIF–2008*[c])
refinement method	full-matrix least-squares on F^2 (*SHELXL–2014*[d])
absorption correction method	Gaussian integration (face-indexed)
range of transmission factors	0.7190–0.1931
data/restraints/parameters	4108 / 0 / 262
goodness-of-fit (*S*)[e] [all data]	1.334
final *R* indices[f]	
R_1 [$F_o^2 \ge 2\sigma(F_o^2)$]	0.0653
wR_2 [all data]	0.1463
largest difference peak and hole	1.208 and –2.466 e Å^{-3}

[a]Obtained from least-squares refinement of 9456 reflections with $7.42° < 2\theta < 147.54°$.

[b]Programs for diffractometer operation, data collection, data reduction and absorption correction were those supplied by Bruker.

[c]Beurskens, P. T.; Beurskens, G.; de Gelder, R.; Smits, J. M. M.; Garcia-Granda, S.; Gould, R. O. (2008). The *DIRDIF-2008* program system. Crystallography Laboratory, Radboud University Nijmegen, The Netherlands.

[d]Sheldrick, G. M. *Acta Crystallogr.* **2015**, *C71*, 3–8.

[e]$S = [\Sigma w(F_o^2 - F_c^2)^2/(n - p)]^{1/2}$ (n = number of data; p = number of parameters varied; $w = [\sigma^2(F_o^2) + 50.7994P]^{-1}$ where $P = [\text{Max}(F_o^2, 0) + 2F_c^2]/3$).

$^{f}R_1 = \Sigma||F_o| - |F_c||/\Sigma|F_o|$; $wR_2 = [\Sigma w(F_o^2 - F_c^2)^2/\Sigma w(F_o^4)]^{1/2}$.

Table 4.10. X-Ray crystallographic data for **Ar^{F}-Te-6-Ar^{F}**.

A. Crystal Data	
formula	$C_{24}H_{14}F_{12}Te$
formula weight	657.95
crystal dimensions (mm)	0.42 × 0.24 × 0.08
crystal system	triclinic
space group	$P\bar{1}$ (No. 2)
unit cell parameters[a]	
a (Å)	11.6764 (8)
b (Å)	14.6438 (11)
c (Å)	15.8273 (11)
α (deg)	68.5869 (8)
β (deg)	72.8467 (8)
γ (deg)	73.0843 (8)
V (Å^3)	2355.7 (3)
Z	4
ρ_{calcd} (g cm^{-3})	1.855
μ (mm^{-1})	1.369
B. Data Collection and Refinement Conditions	
diffractometer	Bruker D8/APEX II CCD[b]
radiation (λ [Å])	graphite-monochromated Mo Kα (0.71073)
temperature (°C)	–100
scan type	ω scans (0.3°) (15 s exposures)
data collection 2θ limit (deg)	56.48
total data collected	22229 (-15 ≤ h ≤ 15, -19 ≤ k ≤ 19, -21 ≤ l ≤ 21)
independent reflections	11350 (R_{int} = 0.0173)
number of observed reflections (NO)	9459 [$F_o^2 \geq 2\sigma(F_o^2)$]

structure solution method	Patterson/structure expansion (*DIRDIF–2008*[c])
refinement method	full-matrix least-squares on F^2 (*SHELXL–2014*[d])
absorption correction method	Gaussian integration (face-indexed)
range of transmission factors	0.9279–0.6886
data/restraints/parameters	11350 / 0 / 667
goodness-of-fit (S)[e] [all data]	1.055
final R indices[f]	
R_1 [$F_o^2 \geq 2\sigma(F_o^2)$]	0.0387
wR_2 [all data]	0.1051
largest difference peak and hole	1.428 and –0.768 e Å^{-3}

[a]Obtained from least-squares refinement of 9986 reflections with $4.76° < 2\theta < 50.60°$.

[b]Programs for diffractometer operation, data collection, data reduction and absorption correction were those supplied by Bruker.

[c]Beurskens, P. T.; Beurskens, G.; de Gelder, R.; Smits, J. M. M.; Garcia-Granda, S.; Gould, R. O. (2008). The *DIRDIF-2008* program system. Crystallography Laboratory, Radboud University Nijmegen, The Netherlands.

[d]Sheldrick, G. M. *Acta Crystallogr.* **2015**, *C71*, 3–8.

[e]$S = [\Sigma w(F_o^2 - F_c^2)^2/(n - p)]^{1/2}$ (n = number of data; p = number of parameters varied; $w = [\sigma^2(F_o^2) + (0.0497P)^2 + 3.2965P]^{-1}$ where $P = [\mathrm{Max}(F_o^2, 0) + 2F_c^2]/3$).

[f]$R_1 = \Sigma||F_o| - |F_c||/\Sigma|F_o|$; $wR_2 = [\Sigma w(F_o^2 - F_c^2)^2/\Sigma w(F_o^4)]^{1/2}$.

4.5. ADDITIONAL DATA

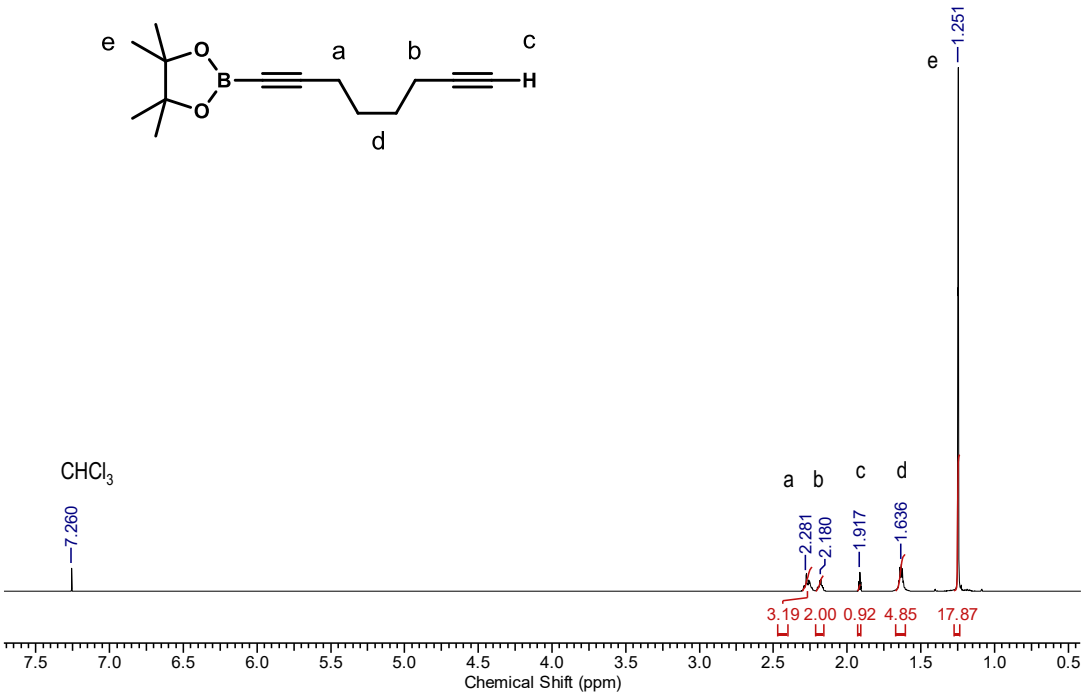

Figure 4.16. A) ^{1}H NMR spectrum of **B-C8-H** in $CDCl_3$.

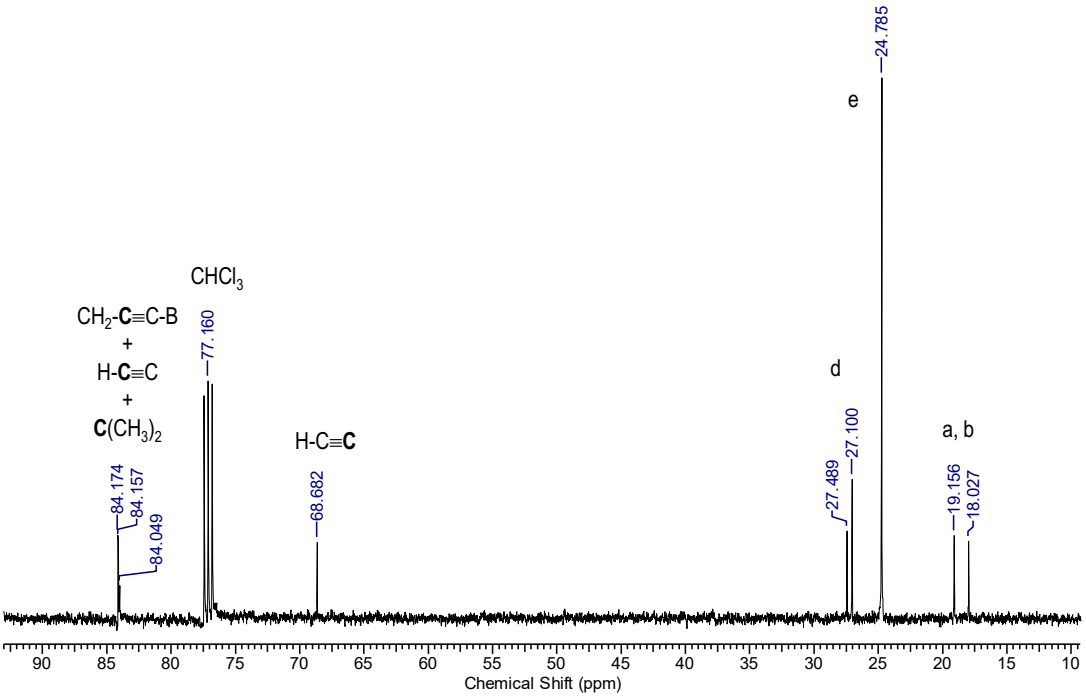

Figure 4.16. B) $^{13}C\{^{1}H\}$ NMR spectrum of **B-C8-H** in $CDCl_3$.

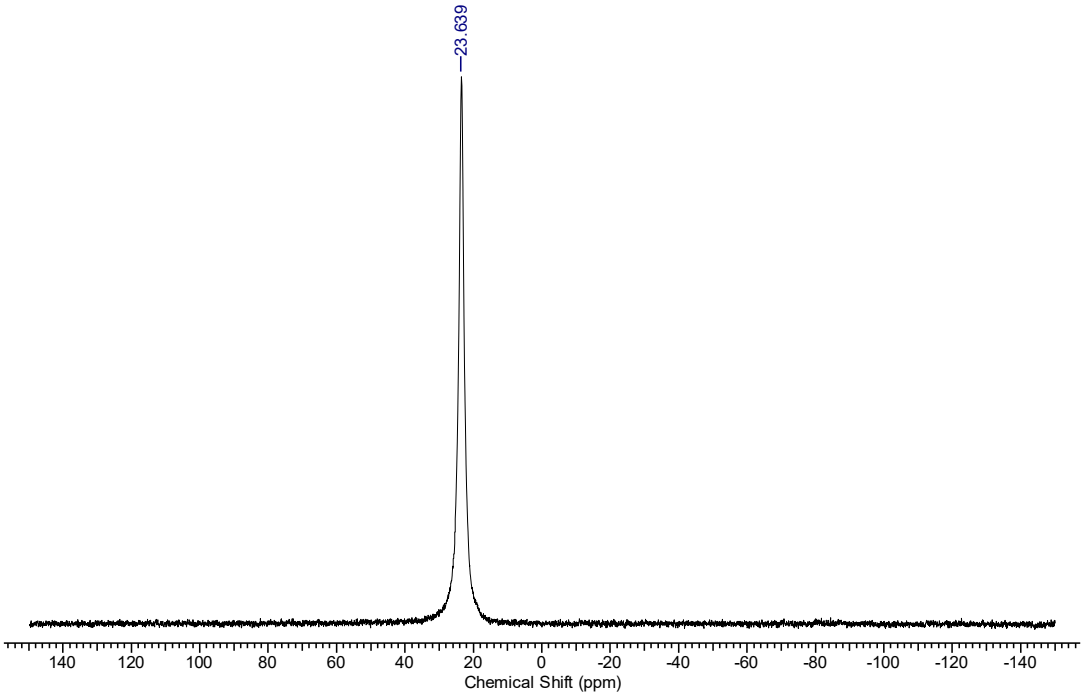

Figure 4.16. C) $^{11}B\{^{1}H\}$ NMR spectrum of **B-C8-H** in $CDCl_3$.

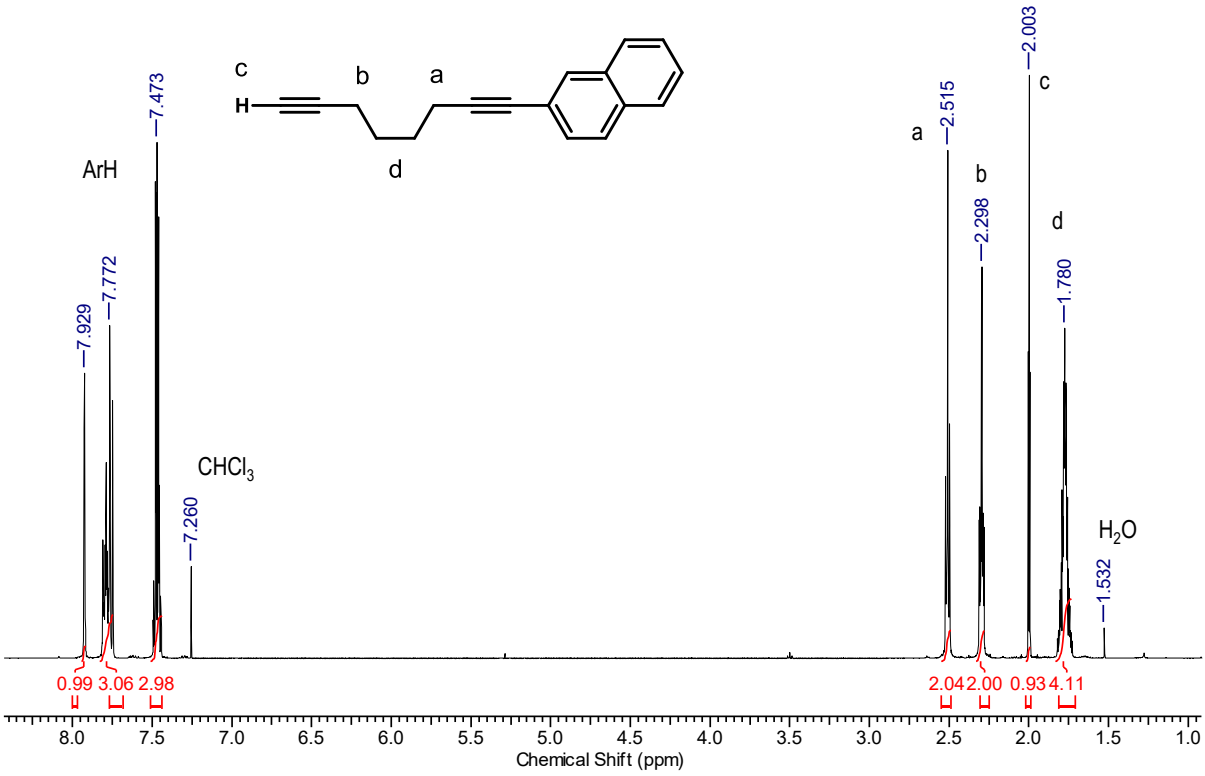

Figure 4.17. A) ^{1}H NMR spectrum of **H-C8-Naph** in $CDCl_3$.

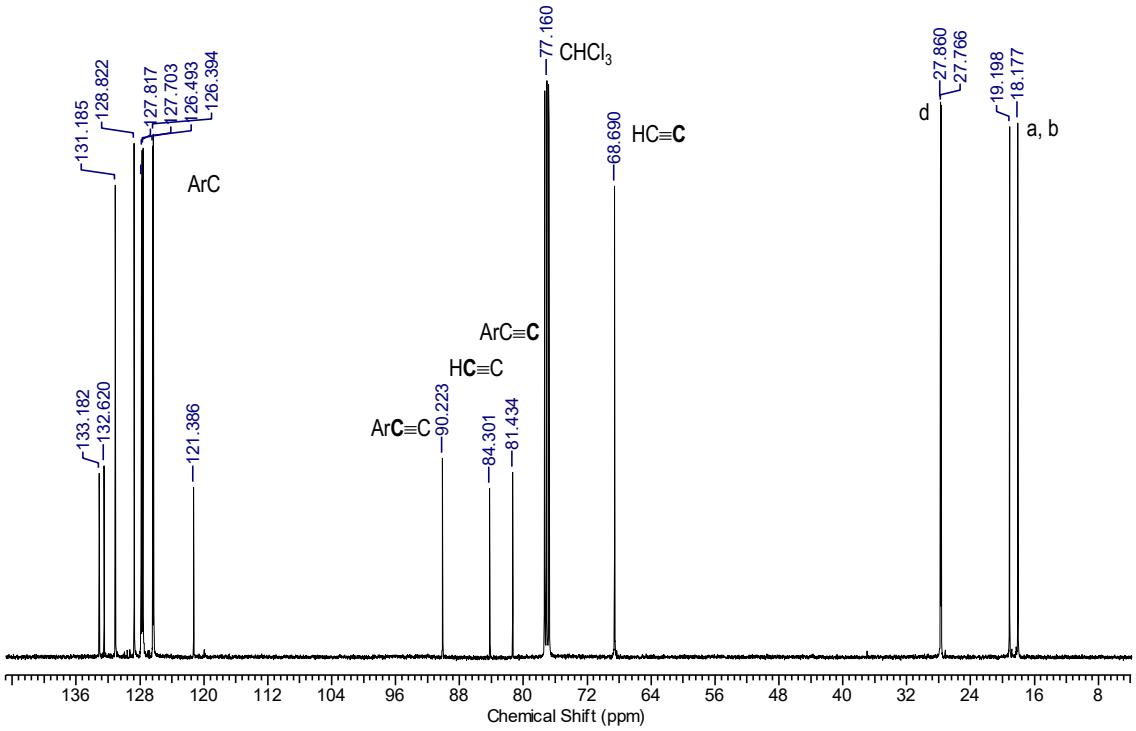

Figure 4.17. B) $^{13}C\{^{1}H\}$ NMR spectrum of **H-C8-Naph** in $CDCl_3$.

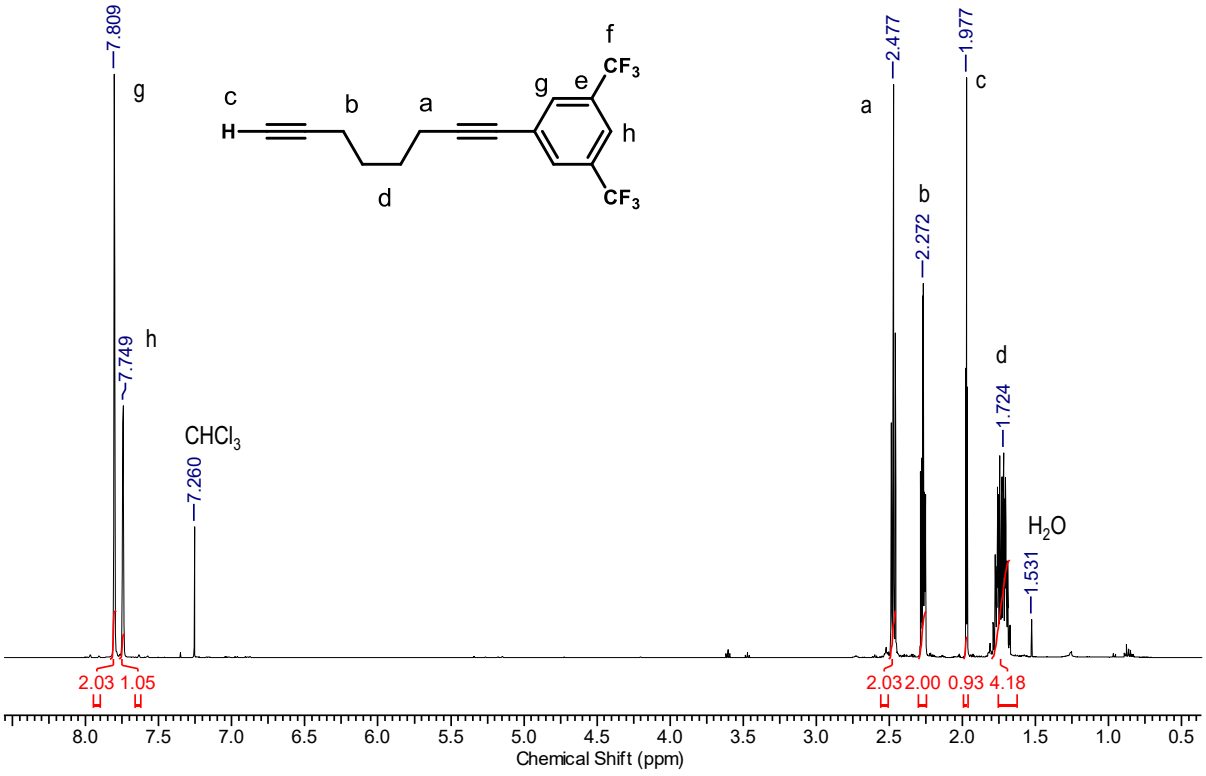

Figure 4.18. A) ^{1}H NMR spectrum of **H-C8-Ar^{F}** in $CDCl_3$.

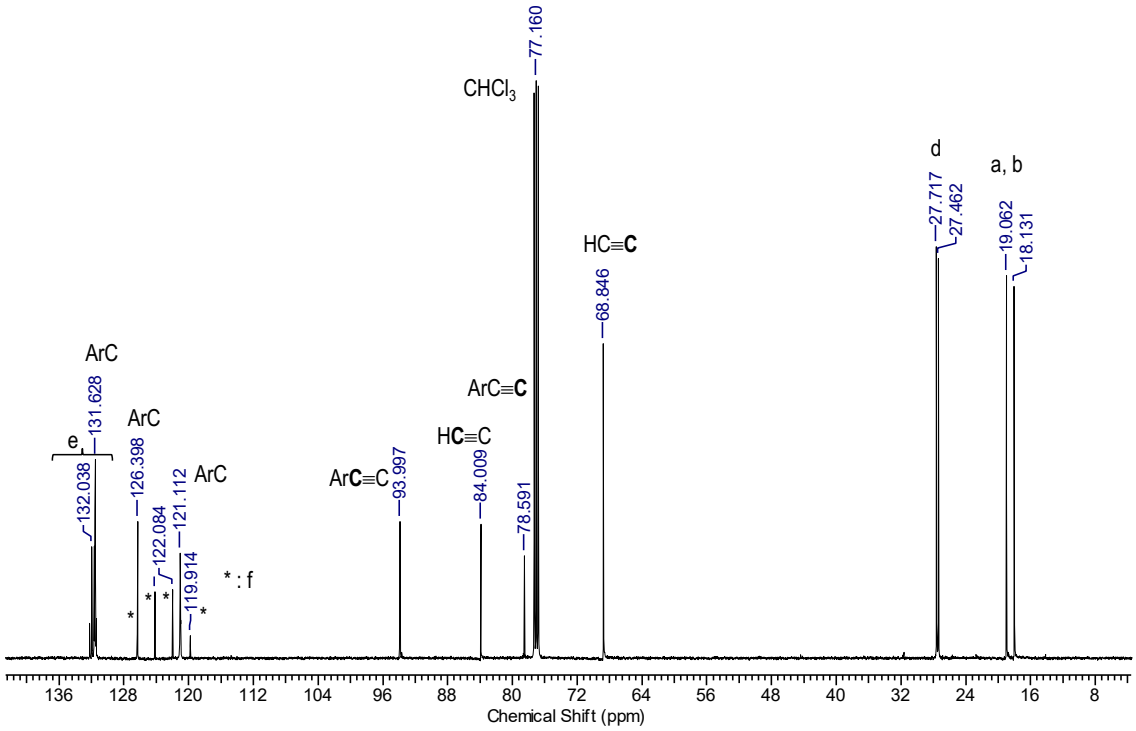

Figure 4.18. B) $^{13}C\{^{1}H\}$ NMR spectrum of **H-C8-Ar^{F}** in $CDCl_3$.

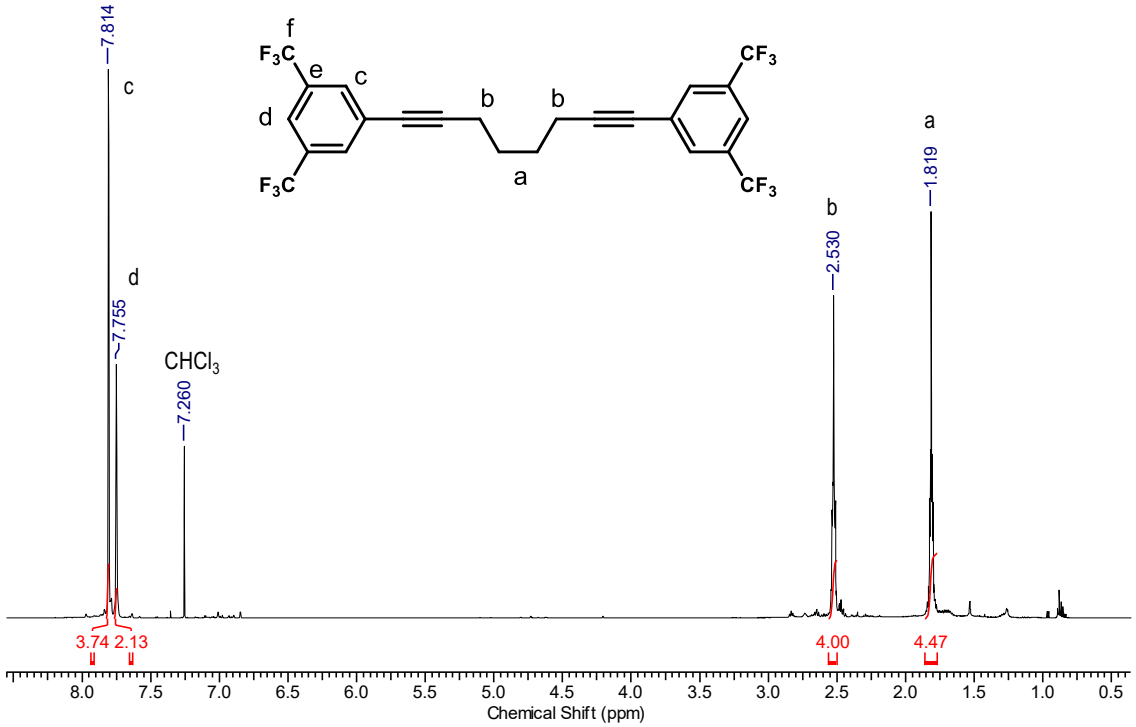

Figure 4.19. A) ^{1}H NMR spectrum of **Ar^{F}-C8-Ar^{F}** in $CDCl_3$.

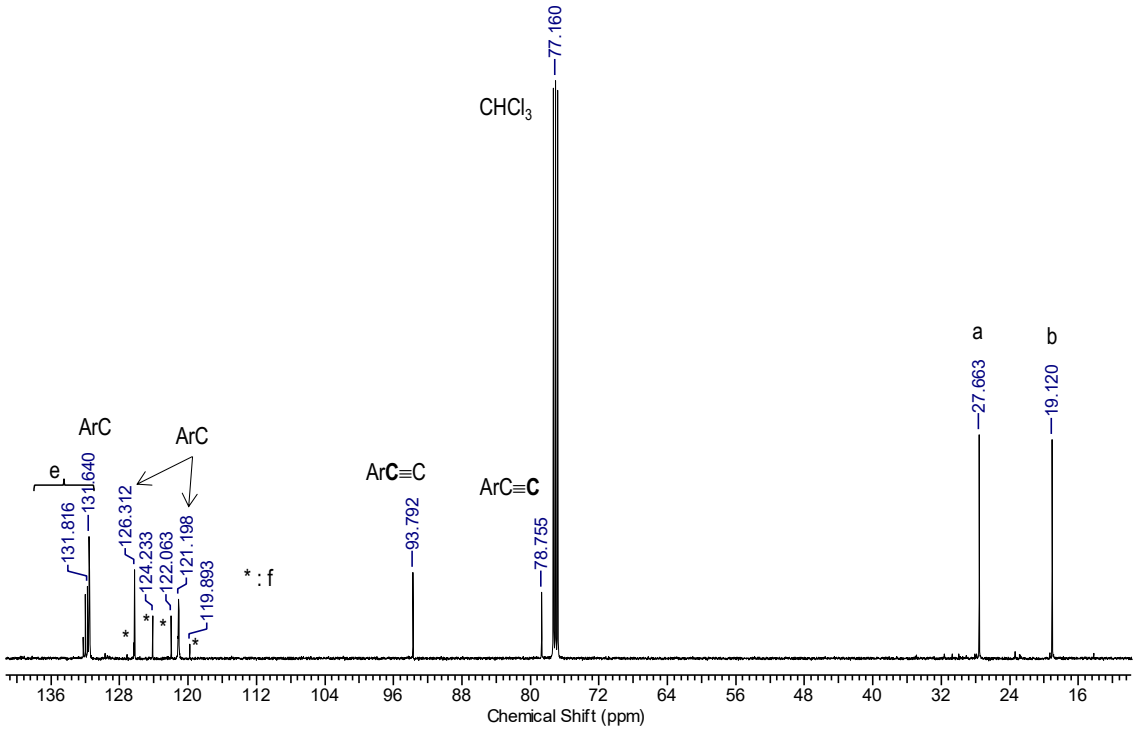

Figure 4.19. B) $^{13}C\{^{1}H\}$ NMR spectrum of **Ar^{F}-C8-Ar^{F}** in $CDCl_3$.

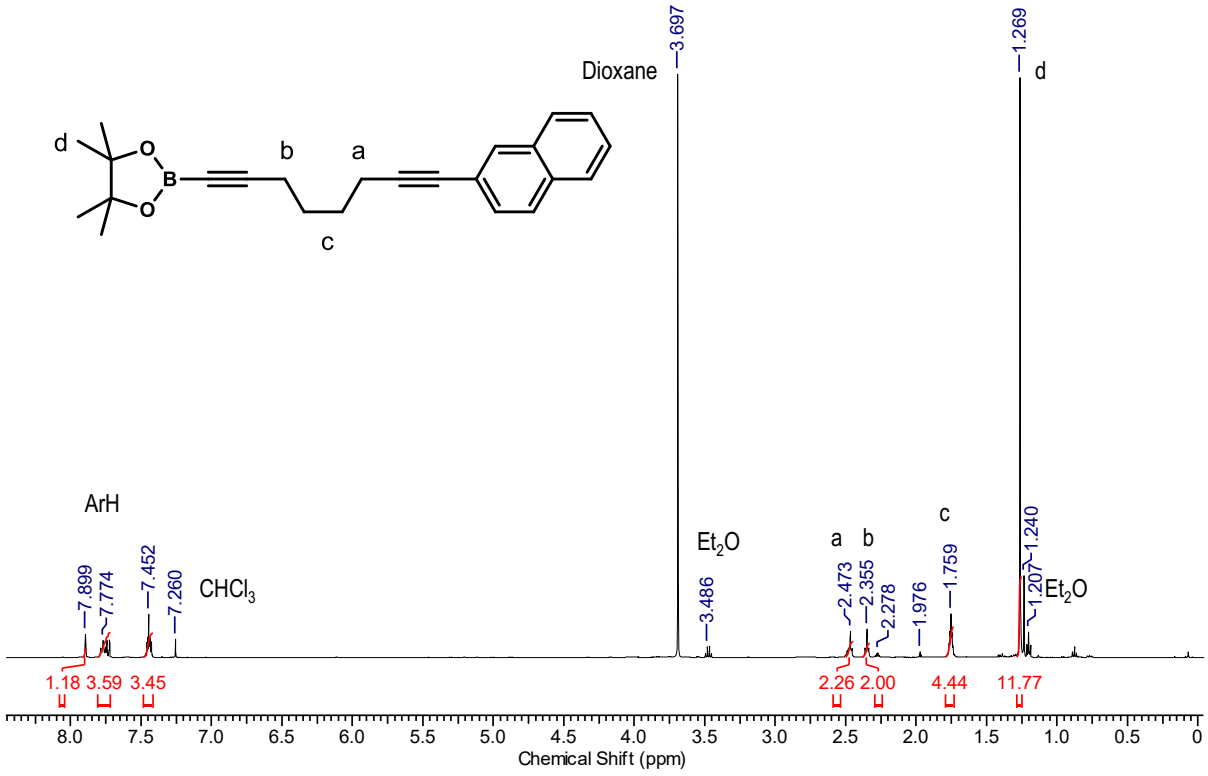

Figure 4.20. A) ^{1}H NMR spectrum of **B-C8-Naph** in $CDCl_3$.

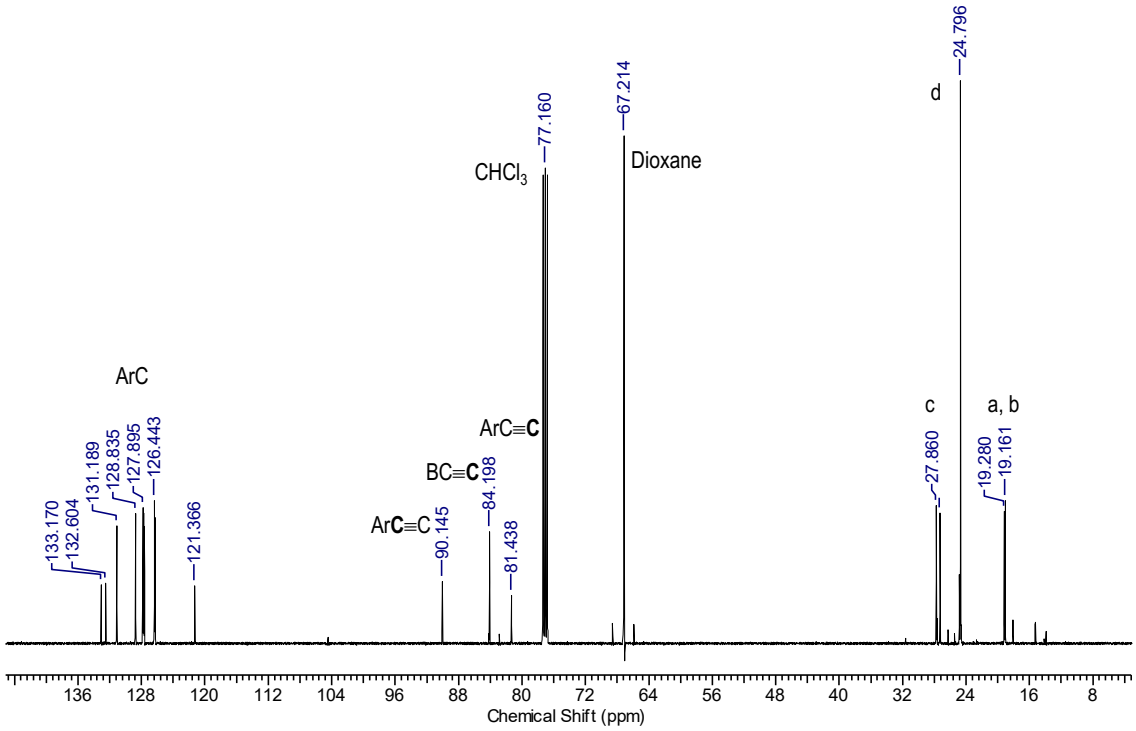

Figure 4.20. B) $^{13}C\{^{1}H\}$ NMR spectrum of **B-C8-Naph** in $CDCl_3$.

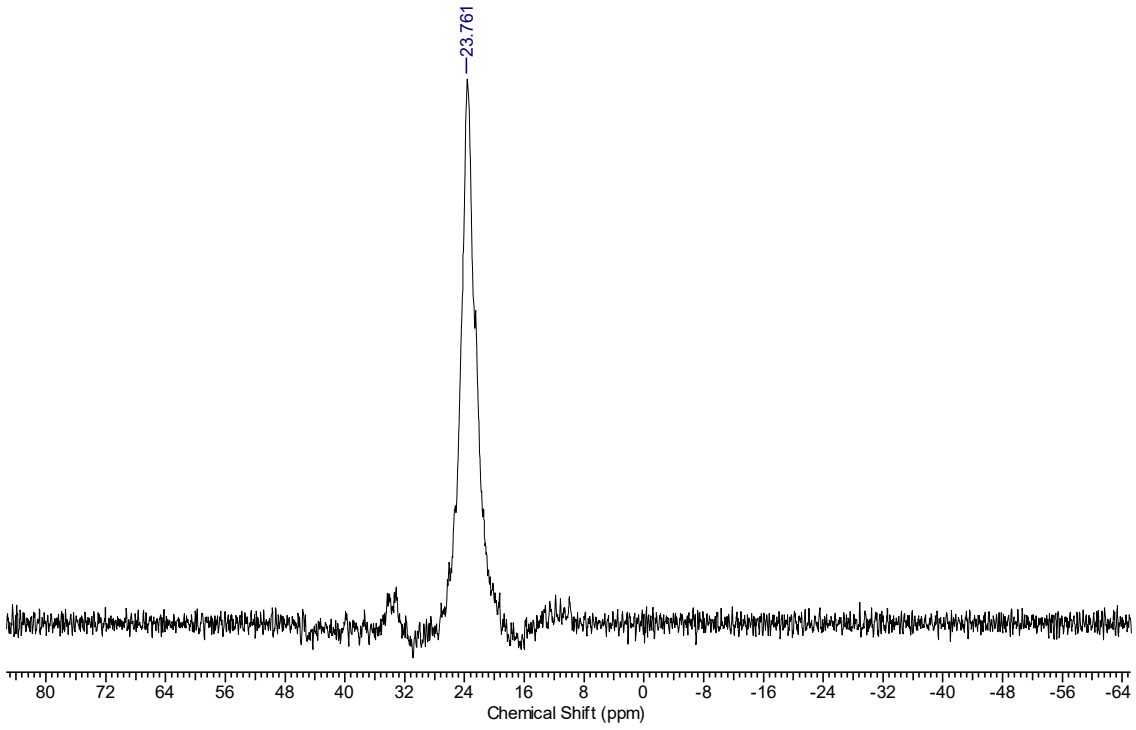

Figure 4.20. C) $^{11}B\{^{1}H\}$ NMR spectrum of **B-C8-Naph** in $CDCl_3$.

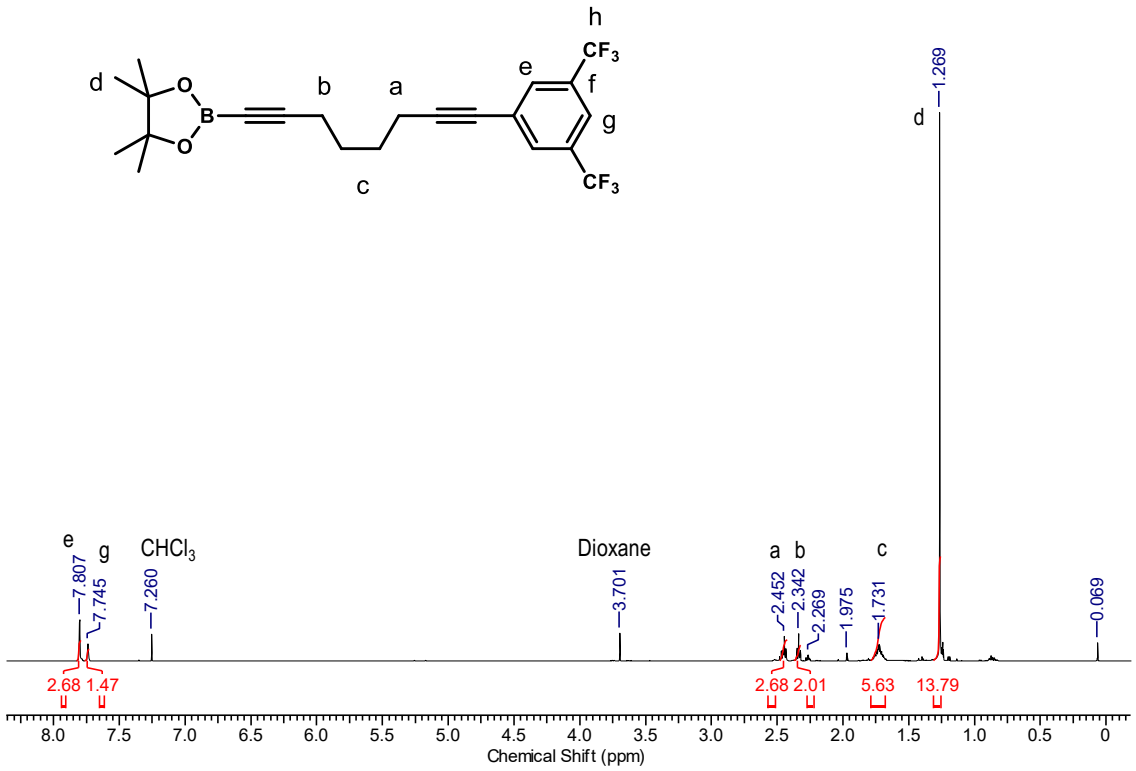

Figure 4.21. A) ^{1}H NMR spectrum of **B-C8-Ar^{F}** in $CDCl_3$.

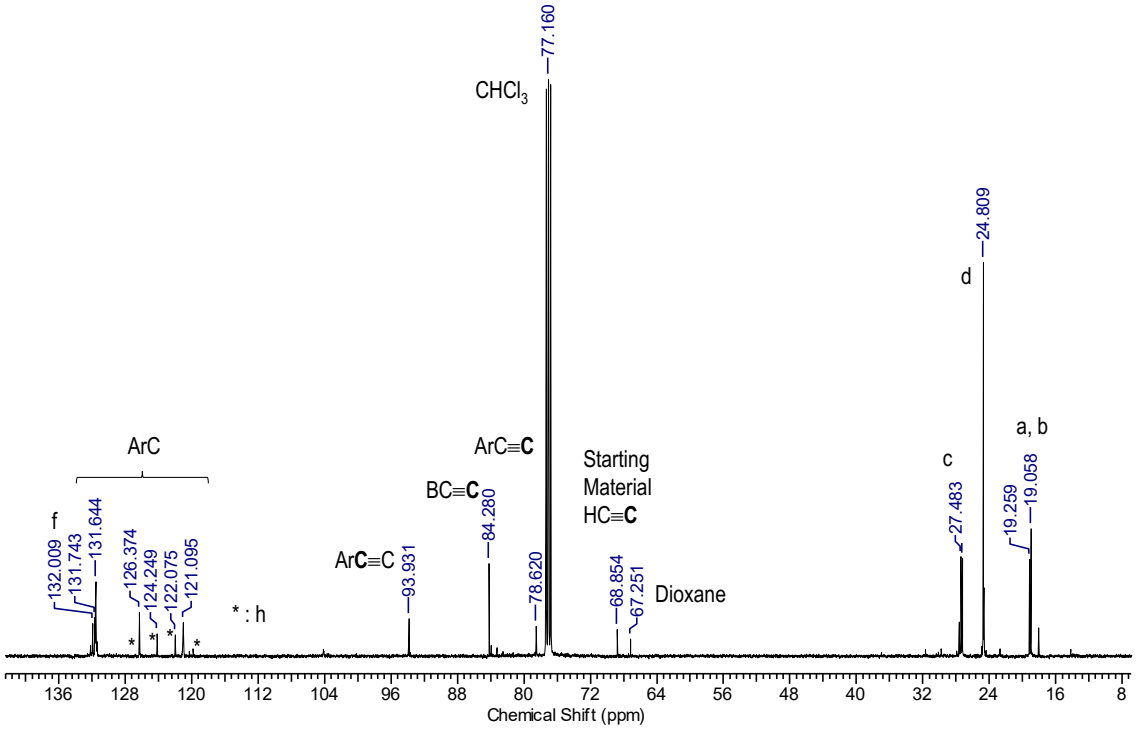

Figure 4.21. B) ^{13}C{^{1}H} NMR spectrum of **B-C8-Ar^{F}** in $CDCl_3$.

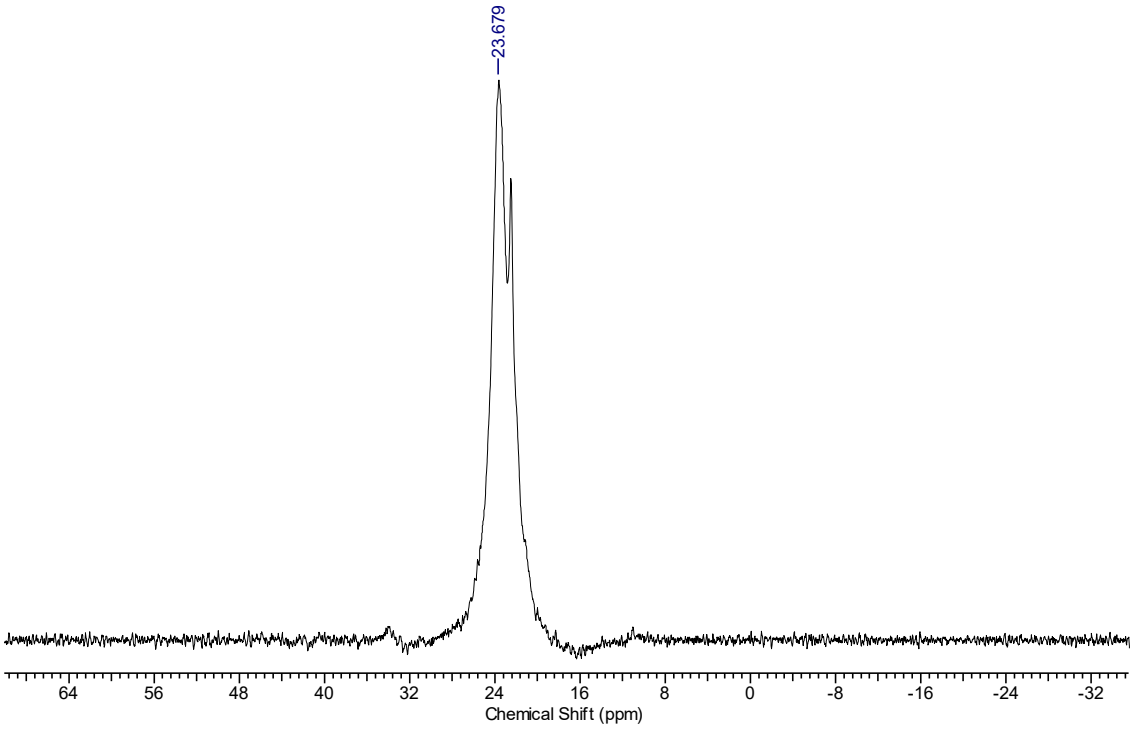

Figure 4.21. C) $^{11}B\{^{1}H\}$ NMR spectrum of **B-C8-Ar^{F}** in $CDCl_3$.

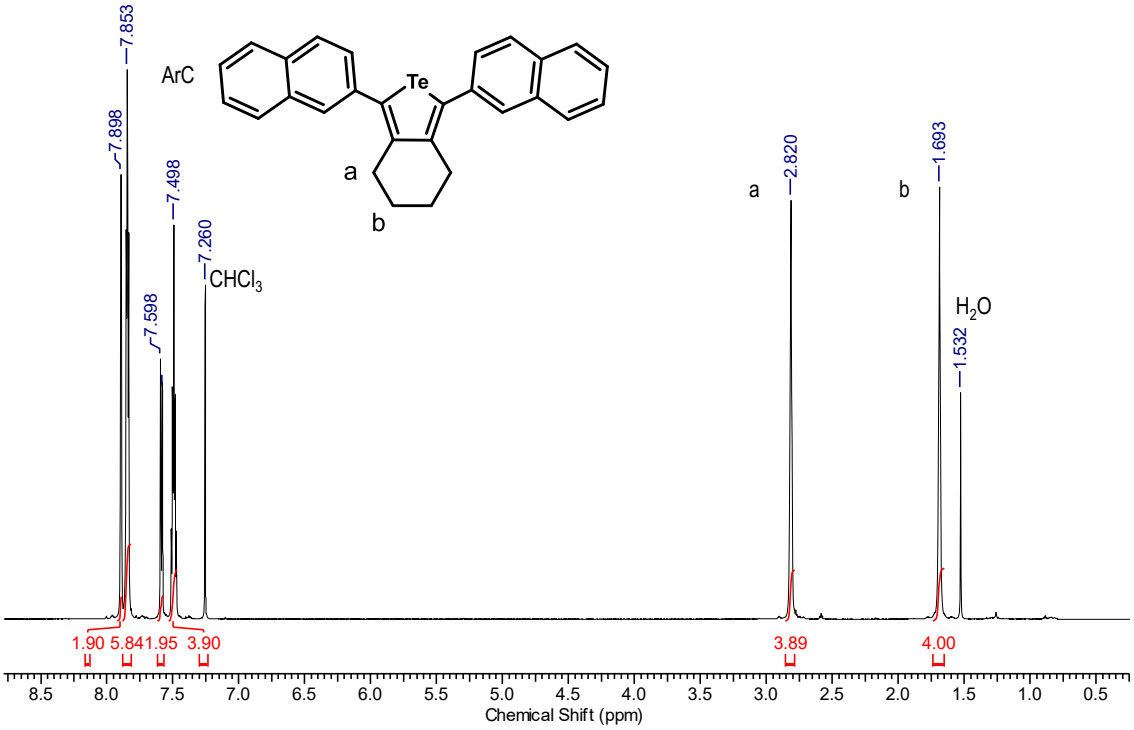

Figure 4.22. A) ^{1}H NMR spectrum of **Naph-Te-6-Naph** in $CDCl_3$.

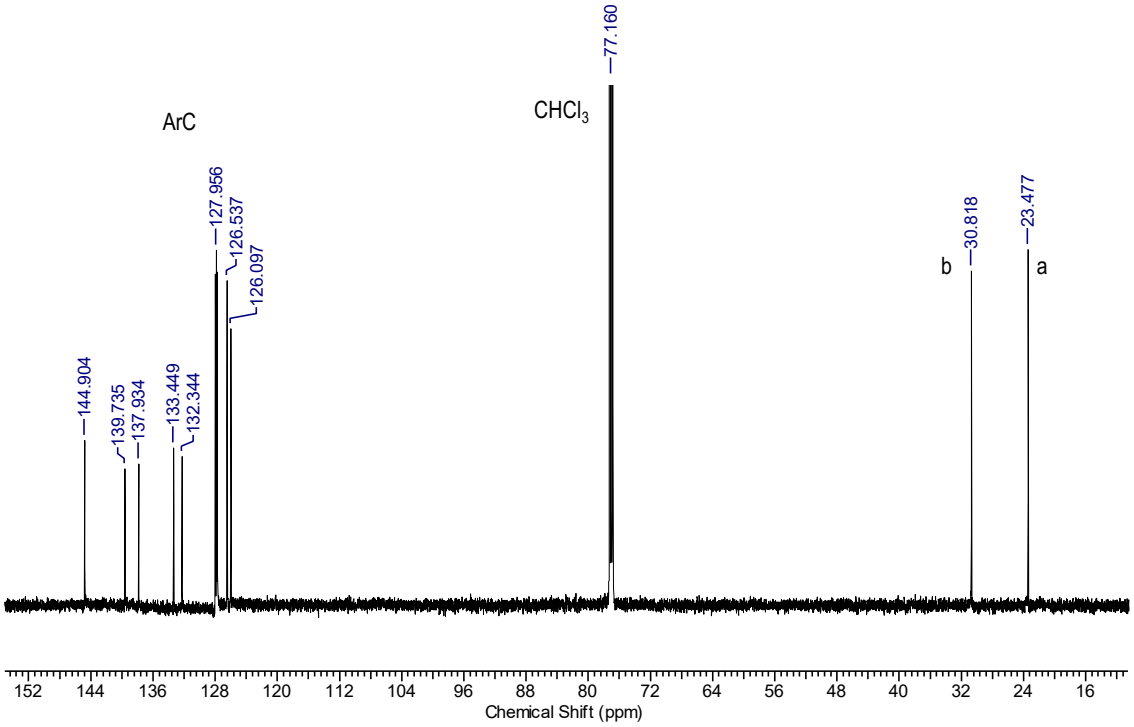

Figure 4.22. B) $^{13}C\{^{1}H\}$ NMR spectrum of **Naph-Te-6-Naph** in $CDCl_3$.

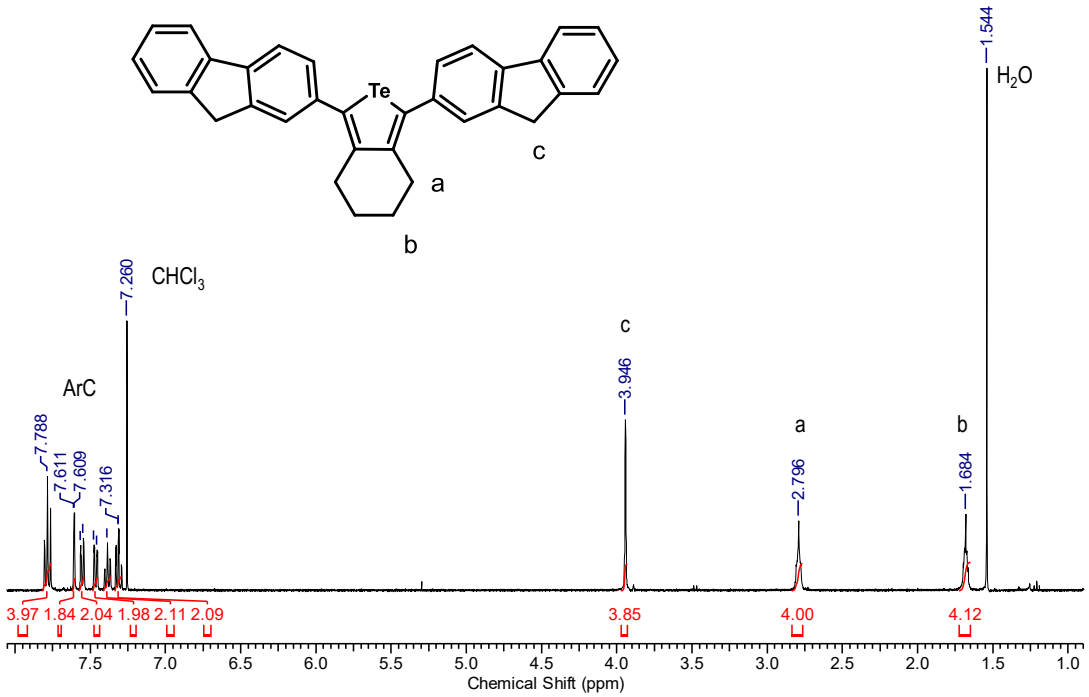

Figure 4.23. A) ^{1}H NMR spectrum of **Fl-Te-6-Fl** in $CDCl_3$.

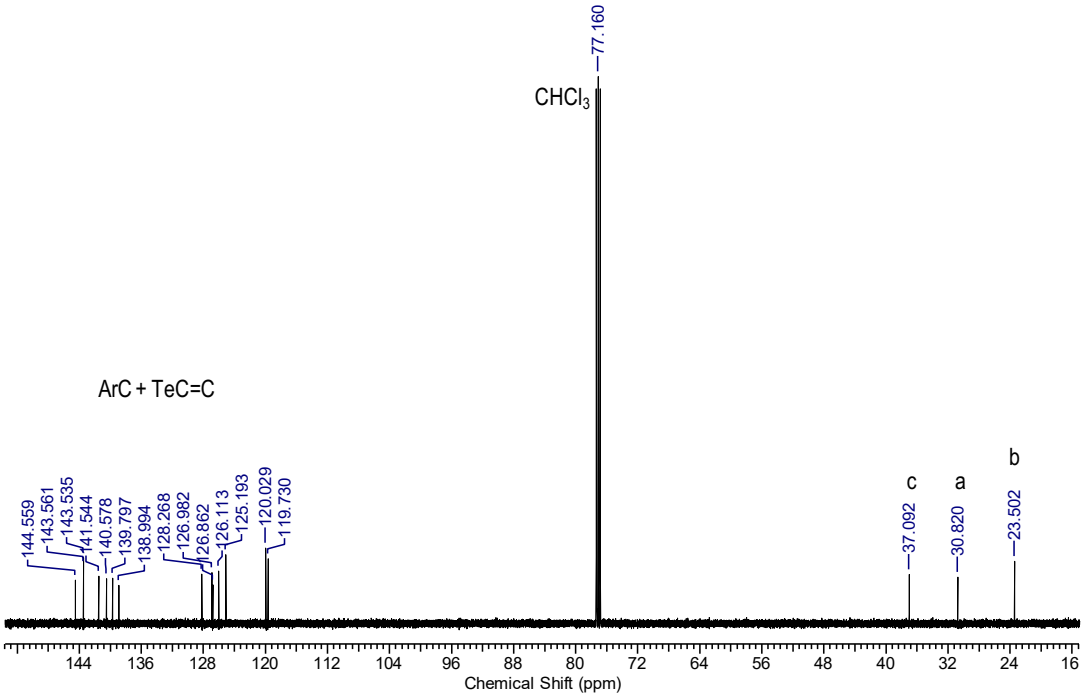

Figure 4.23. B) $^{13}C\{^{1}H\}$ NMR spectrum of **Fl-Te-6-Fl** in $CDCl_3$.

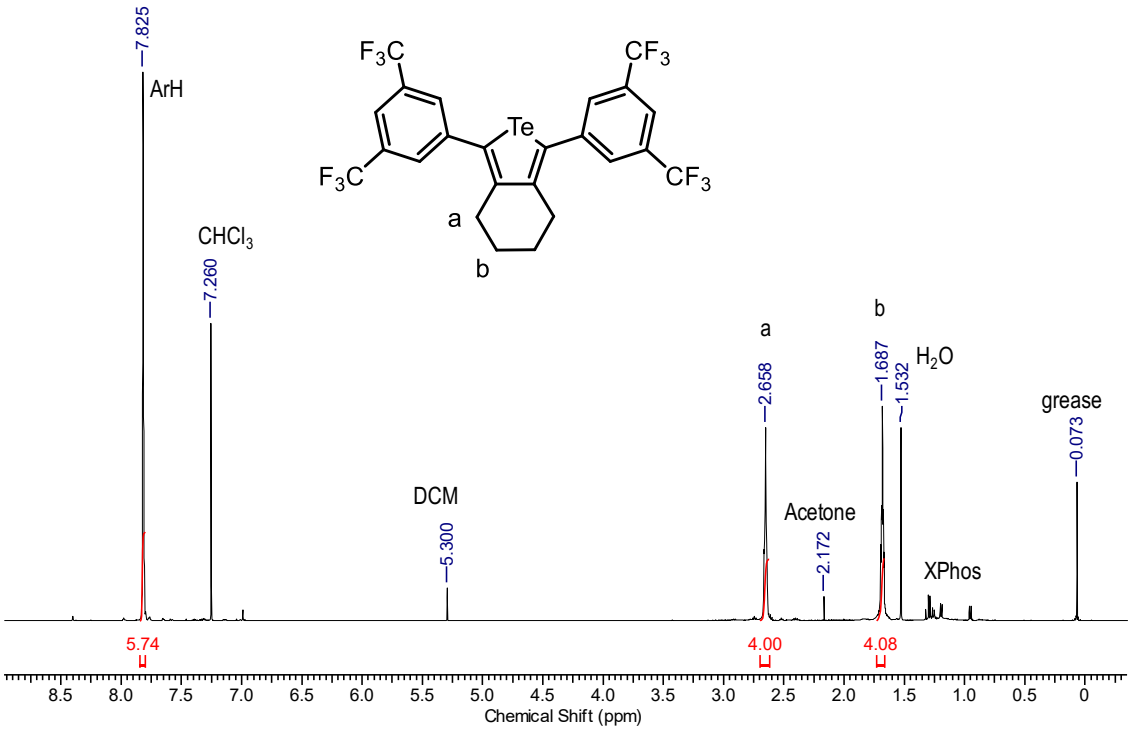

Figure 4.24. A) ^{1}H NMR spectrum of **Ar^F-Te-6-Ar^F** in $CDCl_3$.

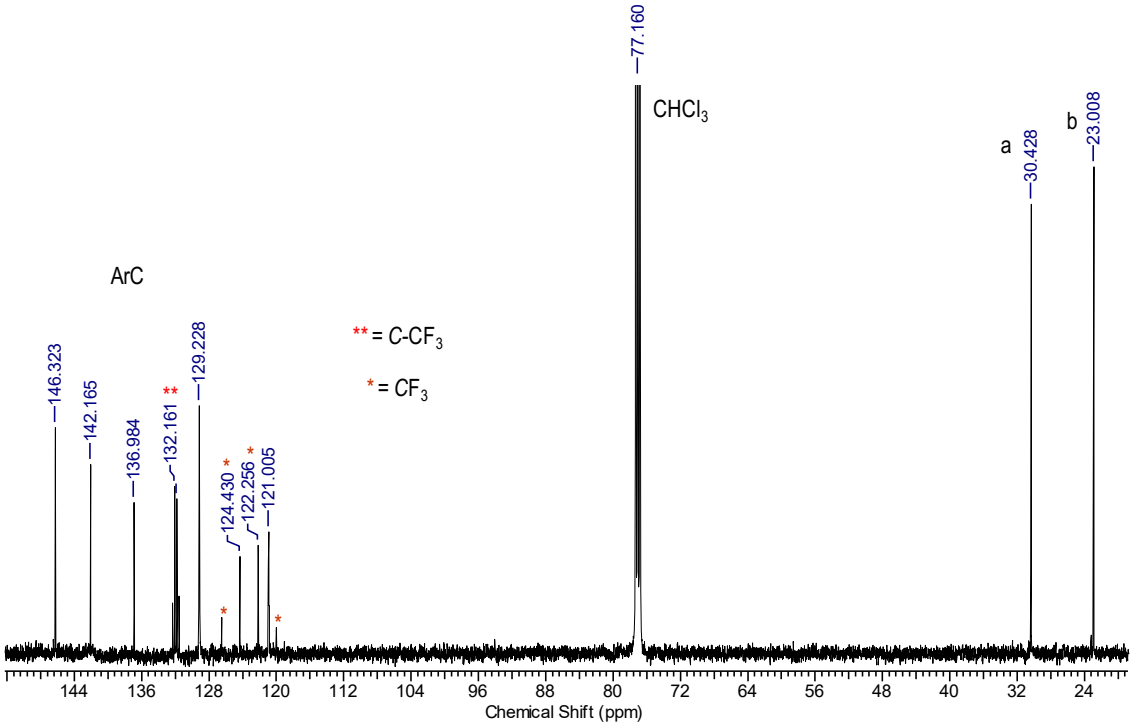

Figure 4.24. B) $^{13}C\{^{1}H\}$ NMR spectrum of **Ar^{F}-Te-6-Ar^{F}** in $CDCl_3$.

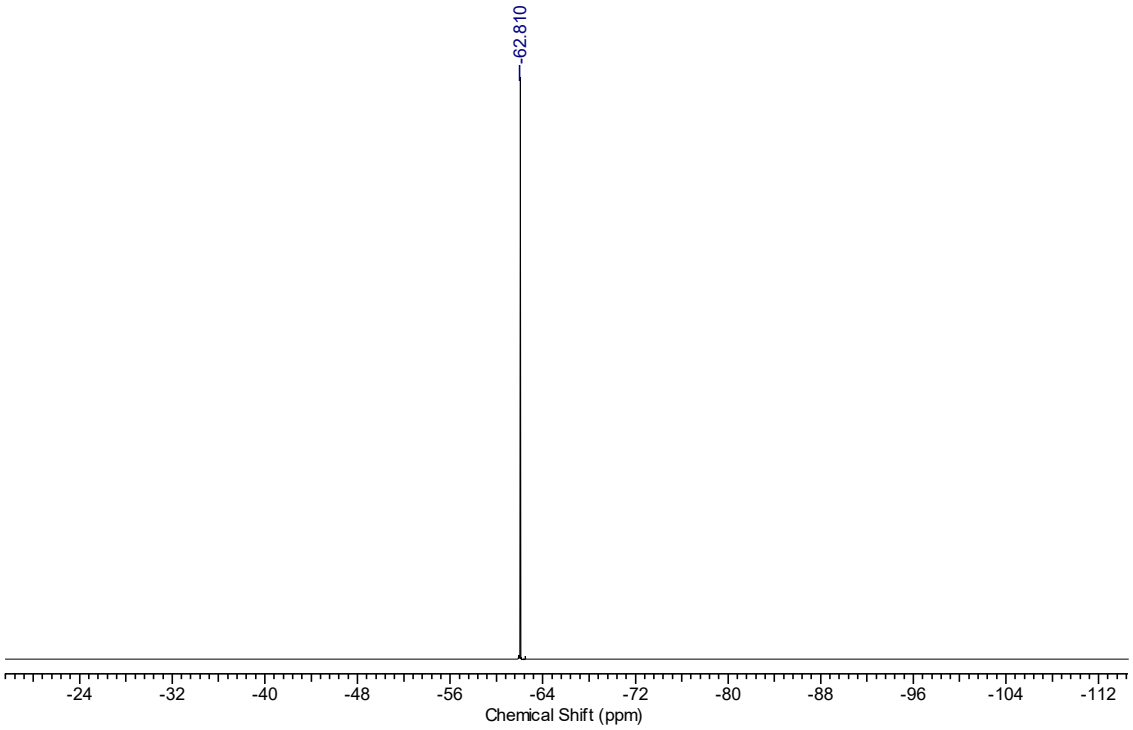

Figure 4.24. C) ^{19}F NMR spectrum of **Ar^{F}-Te-6-Ar^{F}** in $CDCl_3$.

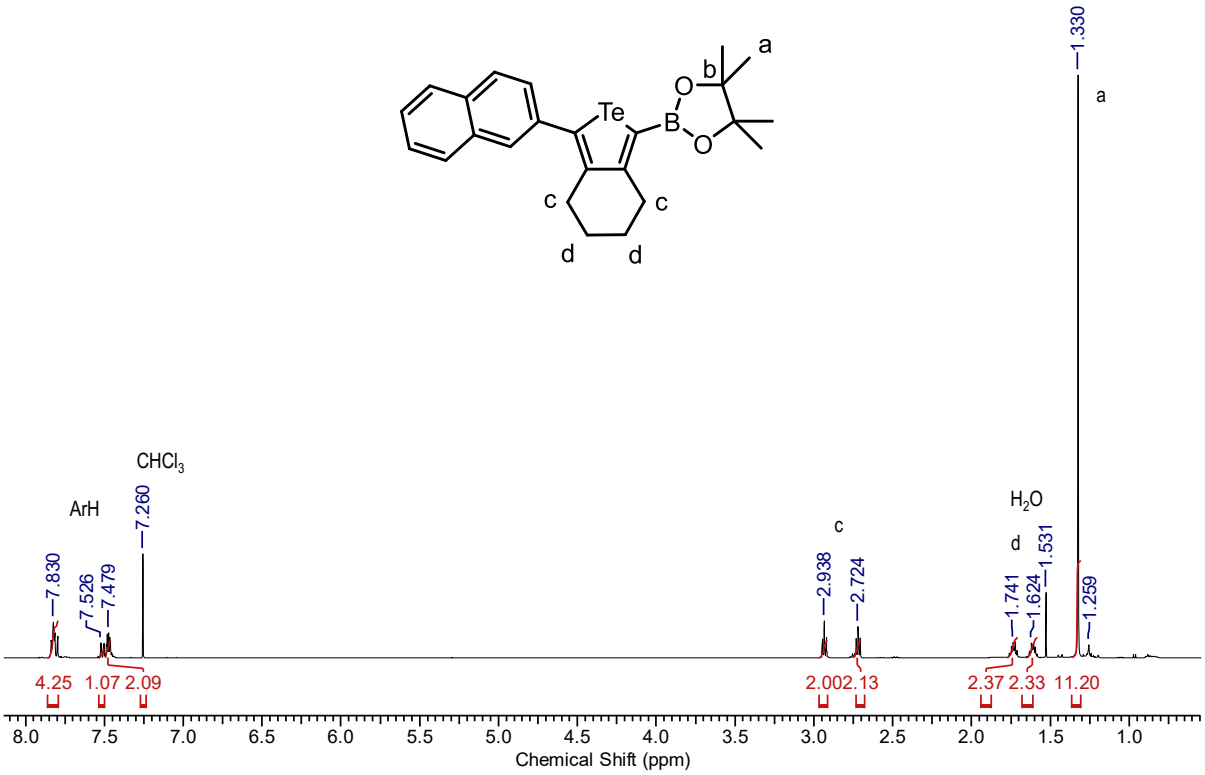

Figure 4.25. A) ^{1}H NMR spectrum of **B-Te-6-Naph** in $CDCl_3$.

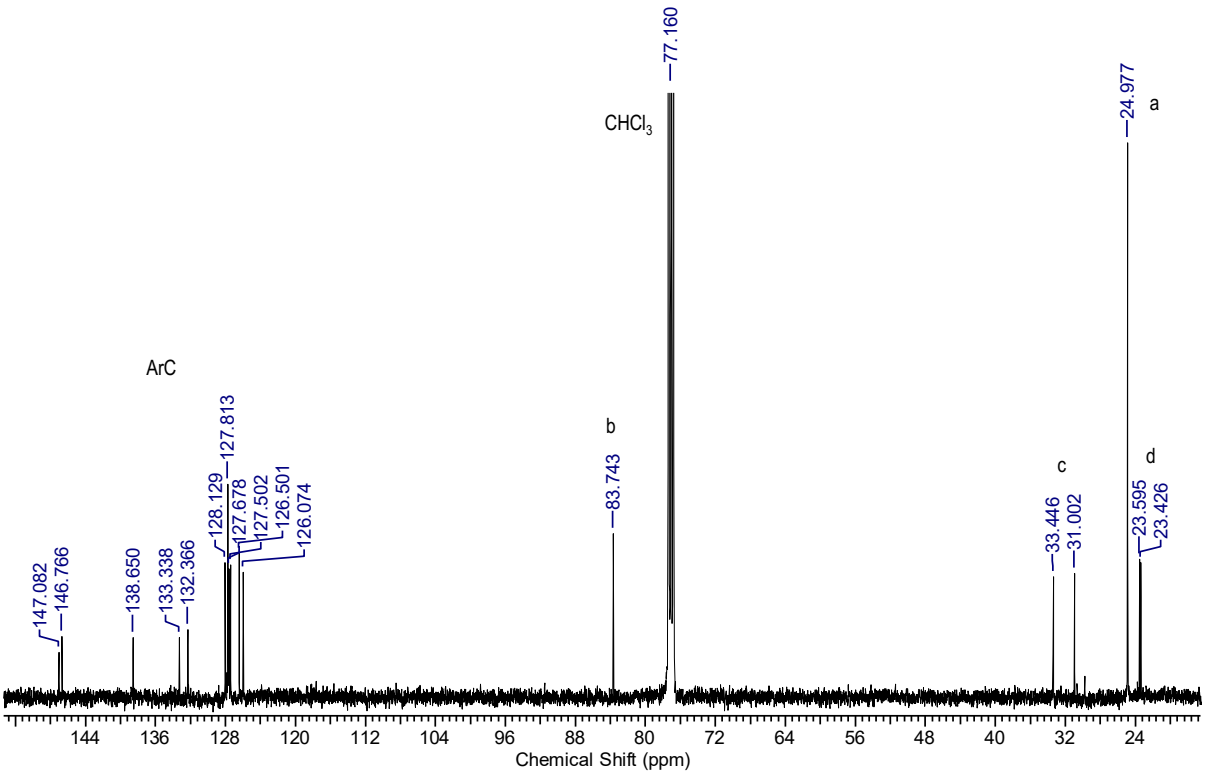

Figure 4.25. B) $^{13}C\{^{1}H\}$ NMR spectrum of **B-Te-6-Naph** in $CDCl_3$.

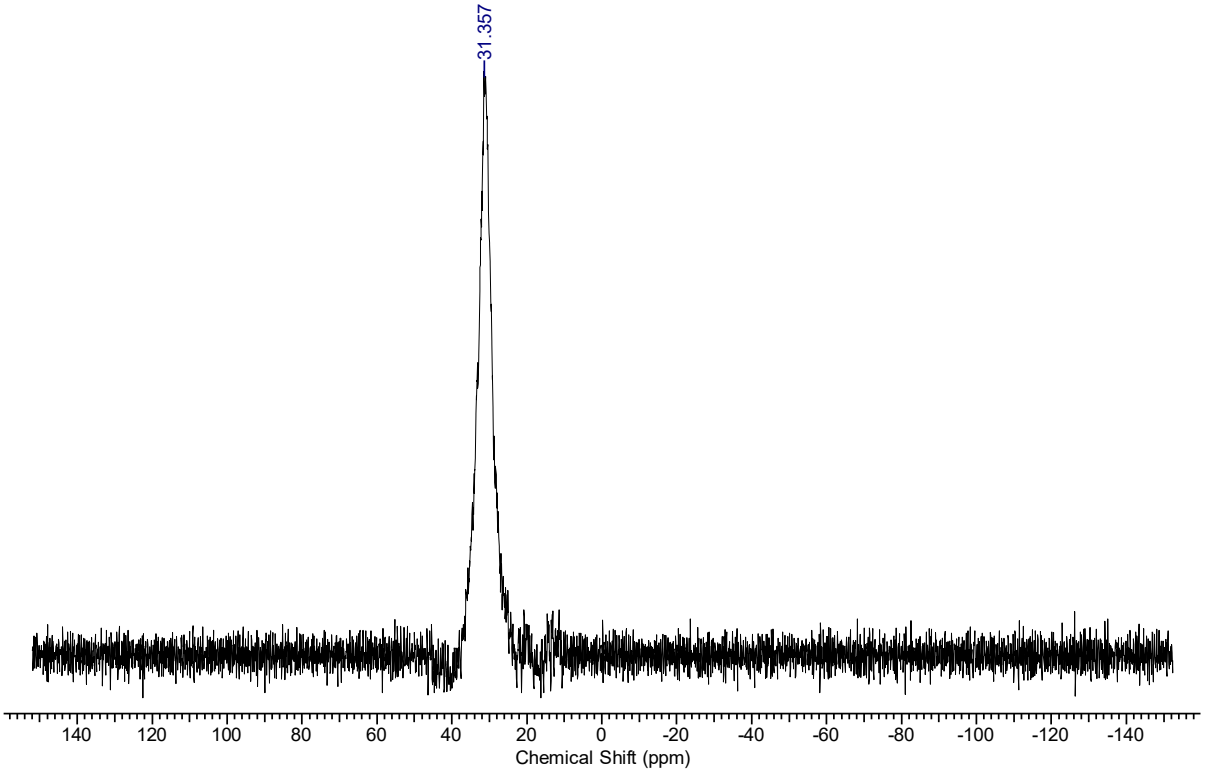

Figure 4.25. C) $^{11}B\{^{1}H\}$ NMR spectrum of **B-Te-6-Naph** in $CDCl_3$.

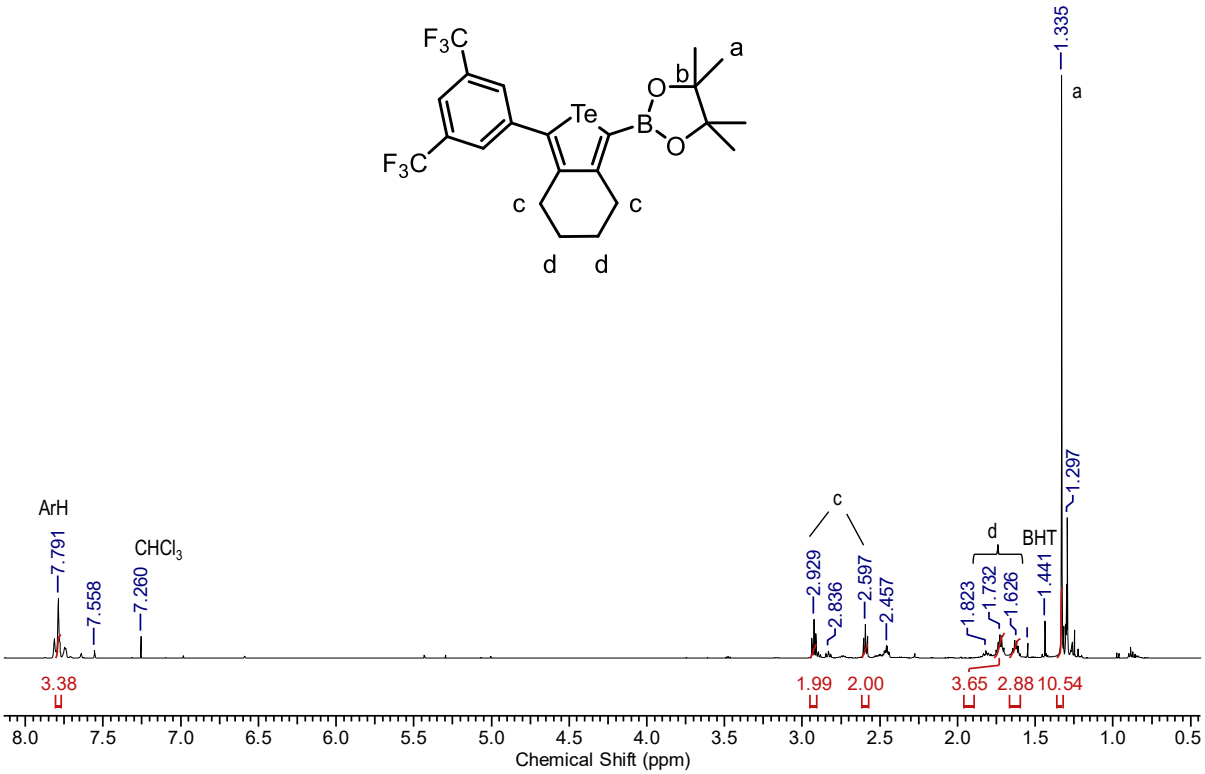

Figure 4.26. A) ^{1}H NMR spectrum of crude **B-Te-6-Ar^{F}** in $CDCl_3$.

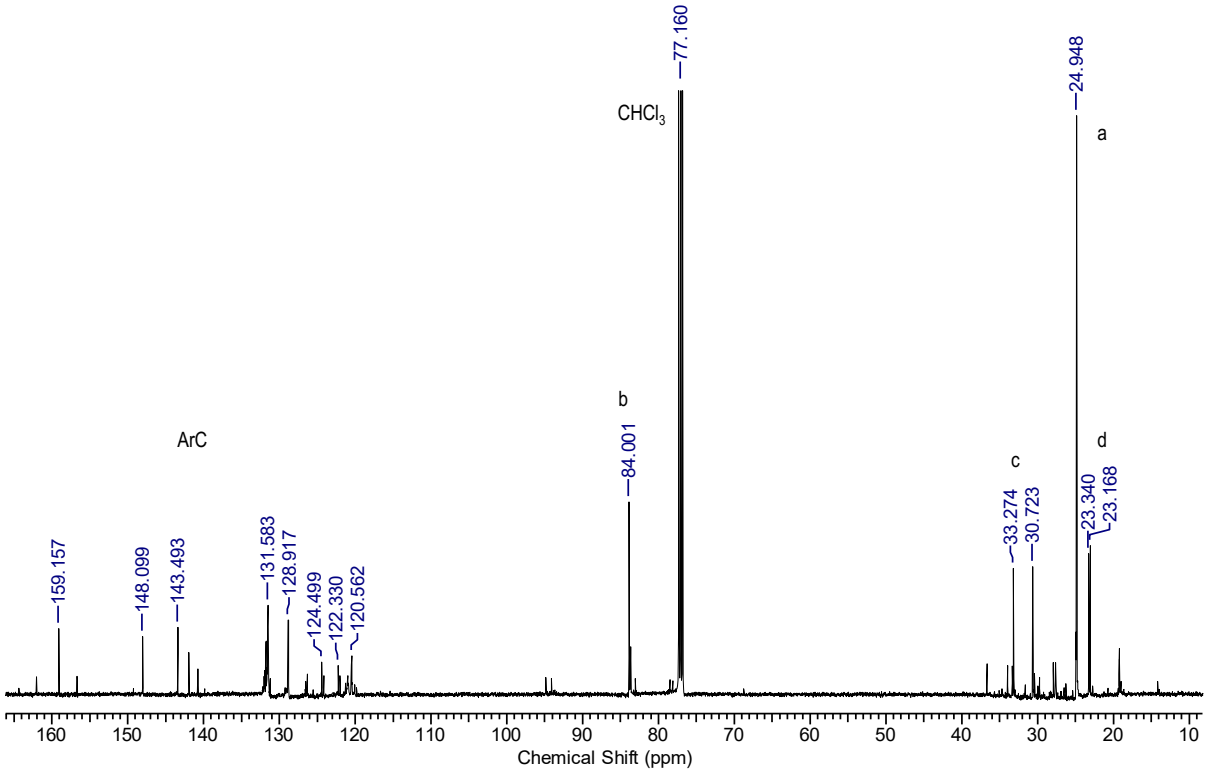

Figure 4.26. B) ^{13}C $\{^{1}H\}$ NMR spectrum of crude **B-Te-6-Ar^{F}** in $CDCl_3$.

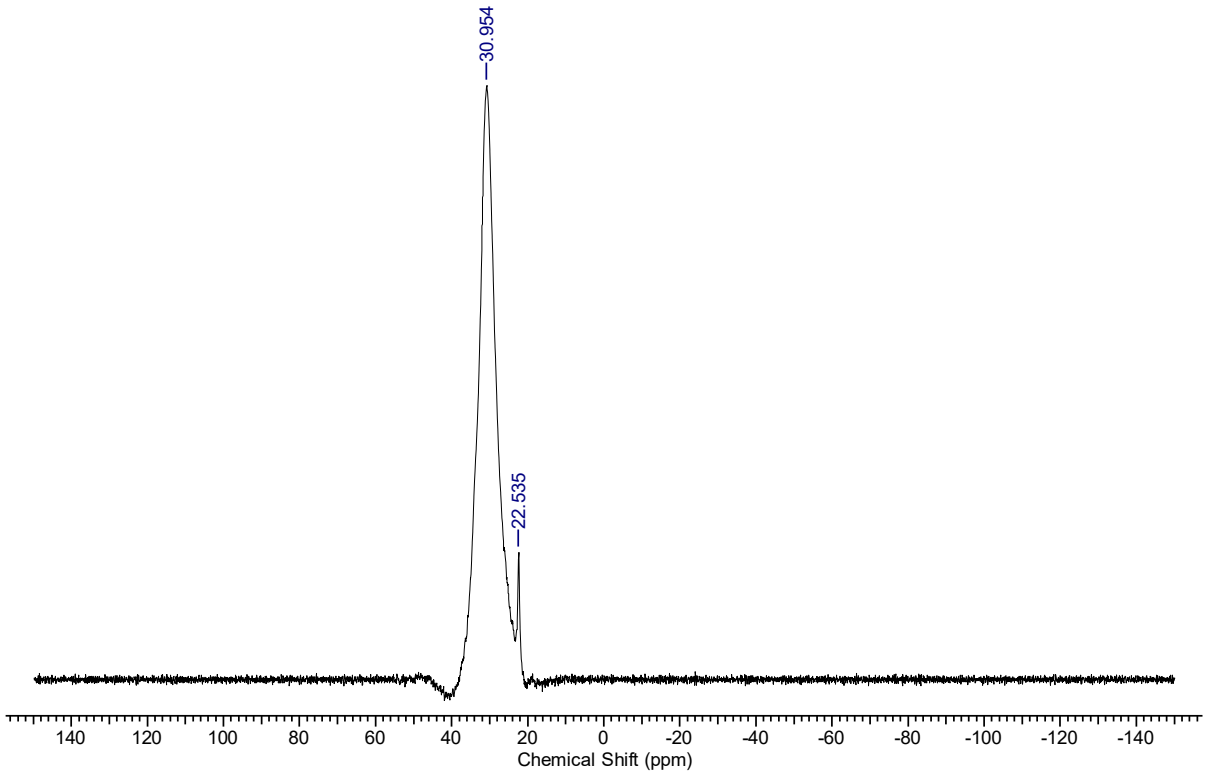

Figure 4.26. C) $^{11}B\{^{1}H\}$ NMR spectrum of **B-Te-6-Ar^{F}** in $CDCl_3$.

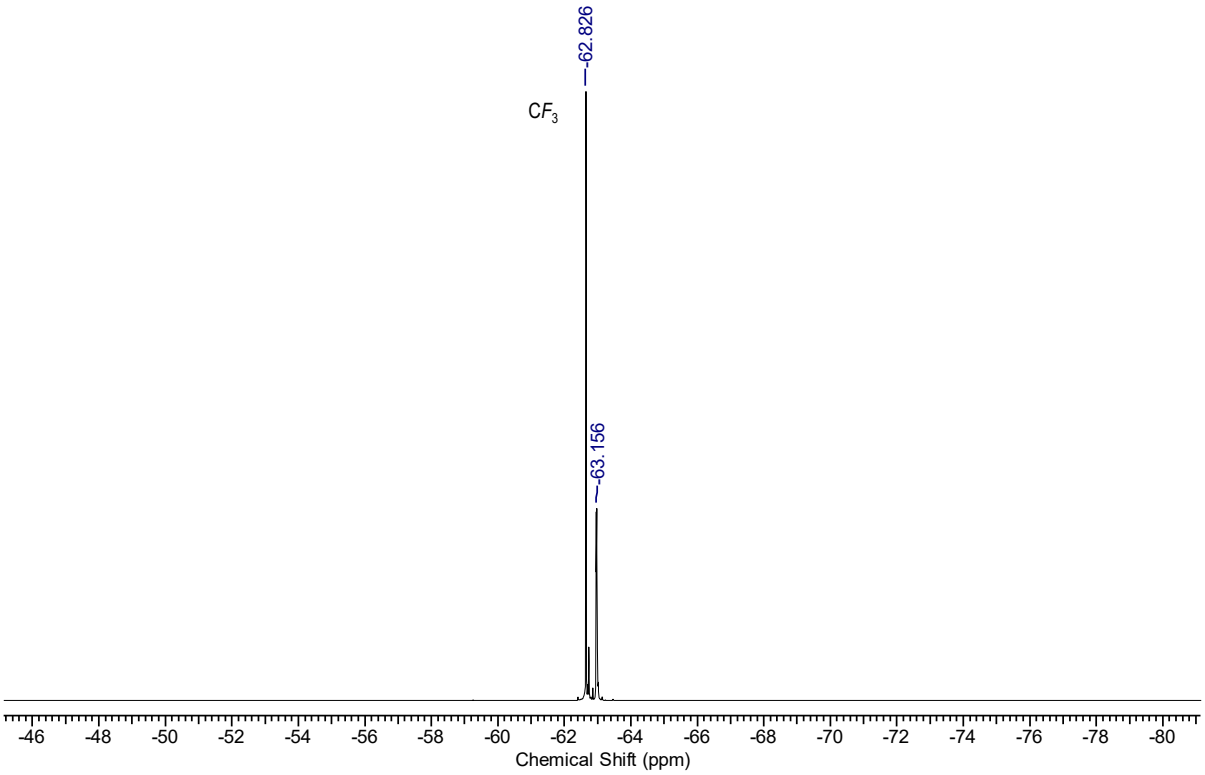

Figure 4.26. D) ^{19}F NMR spectrum of crude **B-Te-6-Ar^{F}** in $CDCl_3$.

4.6 REFERENCES

1. Zhao, Z.; Deng, C.; Chen, S.; Lam, J. W. Y.; Qin, W.; Lu, P.; Wang, Z.; Kwok, H. S.; Ma, Y.; Qiu, H.; Tang, B. Z. *Chem. Commun.* **2011**, *47*, 8847–8849.

2. Malytskyi, V.; Simon, J.-J.; Patrone, L.; Raimundo, J.-M. *RSC Adv.* **2014**, *5*, 354–397.

3. Kaur, N.; Singh, M.; Pathak, D.; Wagner, T.; Nunzi, J. M. *Synth. Met.* **2014**, *190*, 20–26.

4. Bull, S. D.; Davidson, M. G.; Van Den Elsen, J. M. H.; Fossey, J. S.; Jenkins, A. T. A.; Jiang, Y. B.; Kubo, Y.; Marken, F.; Sakurai, K.; Zhao, J.; James, T. D. *Acc. Chem. Res.* **2013**, *46*, 312–326.

5. Pron, A.; Gawrys, P.; Zagorska, M.; Djurado, D.; Demadrille, R. *Chem. Soc. Rev.* **2010**, *39*, 2577–2632.

6. Wakamiya, A.; Mori, K.; Yamaguchi, S. *Angew. Chem. Int. Ed.* **2007**, *46*, 4273–4276.

7. Bureš, F. *RSC Adv.* **2014**, *4*, 58826–58851.

8. Lin, S. L.; Chan, L. H.; Lee, R. H.; Yen, M. Y.; Kuo, W. J.; Chen, C. T.; Jeng, R. J. *Adv. Mater.* **2008**, *20*, 3947–3952.

9. Doi, H.; Kinoshita, M.; Okumoto, K.; Shirota, Y. *Chem. Mater.* **2003**, *15*, 1080–1089.

10. Schubert, C.; Wielopolski, M.; Mewes, L. H.; De Miguel Rojas, G.; Van Der Pol, C.; Moss, K. C.; Bryce, M. R.; Moser, J. E.; Clark, T.; Guldi, D. M. *Chem. Eur. J.* **2013**, *19*, 7575–7586.

11. Entwistle, C. D.; Marder, T. B. *Angew. Chem. Int. Ed.* **2002**, *41*, 2927–2931.

12. Zhao, C.; Wakamiya, A.; Inukai, Y.; Yamaguchi, S. *J. Am. Chem. Soc* **2006**, *128*, 15934–15935.

13. Sun, Z.-B.; Li, S.-Y.; Liu, Z.-Q.; Zhao, C.-H. *Chin. Chem. Lett.* **2016**, *27*, 1131–1138.

14. Fu, G. L.; Zhang, H. Y.; Yan, Y. Q.; Zhao, C. H. *J. Org. Chem.* **2012**, *77*, 1983–1990.

15. Schmidt, H. C.; Reuter, L. G.; Hamacek, J.; Wenger, O. S. *J. Org. Chem.* **2011**, *76*, 9081–9085.

16. Sudhakar, P.; Mukherjee, S.; Thilagar, P. *Organometallics* **2013**, *32*, 3129–3133.

17. Jia, W.-L.; Bai, D.-R.; McCormick, T.; Liu, Q.-D.; Motala, M.; Wang, R.-Y.; Seward, C.; Tao, Y.; Wang, S. *Chem. Eur. J.* **2004**, *10*, 994–1006.

18. Shirota, Y.; Kinoshita, M.; Noda, T.; Okumoto, K.; Ohara, T. *J. Am. Chem. Soc.* **2000**, *122*, 11021–11022.

19. Carrera, E. I.; Lanterna, A. E.; Lough, A. J.; Scaiano, J. C.; Seferos, D. S. *J. Am. Chem. Soc.* **2016**, *138*, 2678–2689.

20. Park, Y. S.; Kale, T. S.; Nam, C.-Y.; Choi, D.; Grubbs, R. B. *Chem. Commun.* **2014**, *50*, 7964–7967.

21. He, G.; Wiltshire, B. D.; Choi, P.; Savin, A.; Sun, S.; Mohammadpour, A.; Ferguson, M. J.; McDonald, R.; Farsinezhad, S.; Brown, A.; Shankar, K.; Rivard, E. *Chem. Commun.* **2015**, *51*, 5444–5447.

22. He, G.; Kang, L.; Torres Delgado, W.; Shynkaruk, O.; Ferguson, M. J.; McDonald, R.; Rivard, E. *J. Am. Chem. Soc.* **2013**, *135*, 5360–5363.

23. Shynkaruk, O. Ph.D. Dissertation, University of Alberta, **2016**.

24. Altenburger, K.; Arndt, P.; Spannenberg, A.; Baumann, W.; Rosenthal, U. *Eur. J. Inorg. Chem.* **2013**, 3200–3205.

25. Hydrio, J.; Gouygou, M.; Dallemer, F.; Daran, J.-C.; Balavoine, G. G. A. *J. Organomet. Chem.* **2000**, *595*, 261.

26. Gaal, M.; List, E. J. W.; Scherf, U. *Macromolecules* **2003**, *36*, 4236–4237.

27. Yan, W.; Wang, Q.; Lin, Q.; Li, M.; Petersen, J. L.; Shi, X. *Chem. Eur. J.* **2011**, *17*, 5011–5018.

28. Zhao, Z.; Su, H.; Zhang, P.; Cai, Y.; Kwok, R. T. K.; Chen, Y.; He, Z.; Gu, X.; He, X.; Sung, H. H.-Y.; Williams, I. D.; Lam, J. W. Y.; Zhang, Z.; Tang, B. Z. *J. Mater. Chem. B.* **2017**, *5*, 1650–1657.

29. Torres Delgado, W.; Shahin, F.; Ferguson, M. J.; McDonald, R.; He, G.; Rivard, E. *Organometallics* **2016**, *35*, 2140–2148.

30. Liégault, B.; Lapointe, D.; Caron, L.; Vlassova, A.; Fagnou, K. *J. Org. Chem.* **2009**, *74*, 1826–1834.

31. Desurmont, G.; Dalton, S.; Giolando, D. M.; Srebnik, M. *J. Org. Chem.* **1997**, *62*, 8907–8909.

32. Zheng, S. L.; Reid, S.; Lin, N.; Wang, B. *Tetrahedron Lett.* **2006**, *47*, 2331–2335.

33. Elangovan, A.; Wang, Y. H.; Ho, T. I. *Org. Lett.* **2003**, *5*, 1841–1844.

34. Liu, C.; Li, X.; Wu, Y.; Qiu, J. *RSC Adv.* **2014**, *4*, 54307–54311.

35. Chang, H. T.; Jeganmohan, M.; Cheng, C. H. *Org. Lett.* **2007**, *9*, 505–508.

36. Tian, H.; Shi, J.; He, B.; Hu, N.; Dong, S.; Yan, D.; Zhang, J.; Geng, Y.; Wang, F. *Adv. Funct. Mater.* **2007**, *17*, 1940–1951.

37. Liu, X.; Wallmann, I.; Boudinov, H.; Kjelstrup-Hansen, J.; Schiek, M.; Lützen, A.; Rubahn, H. G. *Org. Electron. Physics, Mater. Appl.* **2010**, *11*, 1096–1102.

38. McCormick, T. M.; Jahnke, A. A.; Lough, A. J.; Seferos, D. S. *J. Am. Chem. Soc.* **2012**, *134*, 3542–3548.

39. Suthan, T.; Rajesh, N. P.; Dhanaraj, P. V.; Mahadevan, C. K. *Spectrochim. Acta - Part A Mol. Biomol. Spectrosc.* **2010**, *75*, 69–73.

40. Ogawa, K.; Harada, J.; Fujiwara, T.; Takahashi, H. *Chem. Lett.* **2004**, *33*, 1446–1447.

41. Dumur, F.; Bui, T.-T.; Péralta, S.; Lepeltier, M.; Wantz, G.; Sini, G.; Goubard, F.; Gigmes, D. *RSC Adv.* **2016**, *6*, 60565–60577.

42. Bree, A.; Zwarich, R. *J. Chem. Phys.* **1969**, *51*, 903–912.

43. Correia, F. C.; Santos, T. C. F.; Garcia, J. R.; Peres, L. O.; Wang, S. H. *J. Braz. Chem. Soc.* **2015**, *26*, 84–91.

44. Berezin, M. Y.; Achilefu, S. *Chem. Rev.* **2010**, *110*, 2641–2684.

45. Zhao, Q.; Zhang, S.; Liu, Y.; Mei, J.; Chen, S.; Lu, P.; Qin, A.; Ma, Y.; Sun, J. Z.; Tang, B. Z. *J. Mater. Chem.* **2012**, *22*, 7387–7394.

46. Dutton, J. L.; Farrar, G. J.; Sgro, M. J.; Battista, T. L.; Ragogna, P. J. *Chem. Eur. J.* **2009**, *15*, 10263–10271.

Chapter 5

Summary and future work

In Chapter 2, I described the synthesis of the tetraborylated phosphorescent tellurophene, **4BTe**, and its sulfur and selenium analogues, **4BS** and **4BSe**.

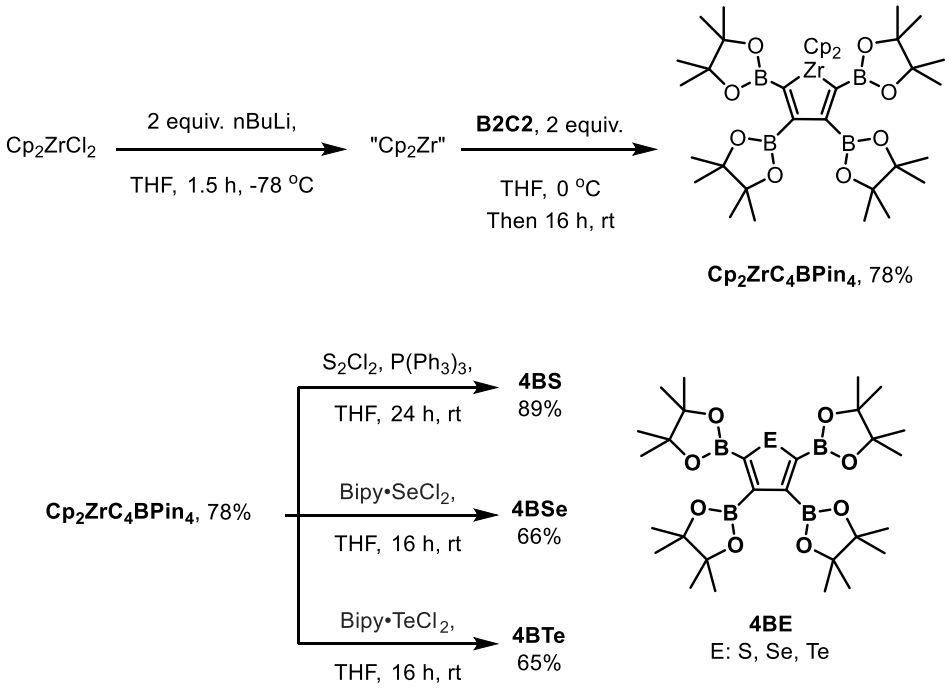

Scheme 5.1. Synthesis of the tetraboryl substituted chalcogenophenes.

The synthesis of these chalcogenophenes started with the formation of the zirconacycle complex $Cp_2ZrC_4BPin_4$ via ring closing using bis-pinacolato-diboronacetylene precursor PinBC≡CBPin and Negishi's reagent "Cp_2Zr". The moisture sensitive intermediate $Cp_2ZrC_4BPin_4$ can be isolated and characterized, or used *in situ* in the next step of metallacycle transfer with the corresponding chalcogen sources. The molecular structures of **4BSe** and **4BTe** were determined by X-ray crystallography and both presented similar propeller configurations of the peripheral BPin groups.

The absorption properties of **4BS**, **4BSe** and **4BTe** were measured in THF solution and **4BTe** in three different solvents (THF, toluene and CH_2Cl_2) to see the effect of substituting the heteroatom and the solvent on the optoelectronic properties. A red-shift in the absorption maximum (λ_{max}) was noted when moving to heavier chalcogenophenes (**4BS**: 262 nm; **4BSe**: 275 nm; **4BTe**: 291 and 338 nm and no noticeable solvatochromism of **4BTe** in different solvents. The optical band gaps were calculated from the onset of absorption and the values decreased when the heteroatom is changed from S to Se and Te (4.4, 4.1 and 3.4 eV, respectively). Based on calculations done in collaboration with Prof. Brown (University of Alberta), the lower energy absorption band at 338 nm was assigned as an electronic transition from the HOMO (mainly localized in a lone pair on the Te^{II} center) to the LUMO (B-C π-type orbitals involving the appended BPin groups). In accordance with cyclic voltammetry measurements, the reduction in the bandgap in **4BTe** is mainly driven by an increase in energy of the HOMO level (localized in a lone pair on the Te^{II} center).

In the solid state and in solution both, **4BS** and **4BSe** were not luminescent. However **4BTe** presented bright green phosphorescence (λ_{em} = 536 nm, τ = 156 μs and a quantum yield of ϕ = 20.3 %) in the solid state and faint luminescence in solutions of THF prepared under N_2 atmosphere; similar results occurred with **B-Te-6-B**. The faint emission in solution was completely quenched when solutions of both tellurophenes were exposed to air, suggesting that oxygen might be quenching their emission in solution (and partially in solid state) as confirmed by luminescence measurements. Notably enhanced quantum yields and increased lifetimes (quantum yield ϕ = 24.4 % and lifetime τ = 387 μs) were found for films of **4BTe** measured under argon. **4BTe** also showed AIE effects as it was evidenced by the formation of emissive aggregates in a mixture of THF/water (5:95). The nature of phosphorescence was explained based on theoretical calculations: the excited states S_1 and T_3 in **4BTe** were computed to be close in energy (~ 0.12 eV) and therefore intersystem crossing could occur, with assistance by the presence of the heavy atom tellurium.

Since **B-Te-6-B** and **4BTe** showed intense emission properties, it would be interesting to study the effect of different borane groups on the emission properties of tellurophenes by varying the Lewis acidity strength on the boron center. I proposed the future synthesis of new di-substituted boron/borole tellurophenes by a silicon boron exchange reaction and lithium

halogen exchange reactions as depicted in Scheme 5.2. New luminescent properties should be expected of these new tellurophenes **3** and **5**, since in the case of **3**, the electronic distribution around the tri-coordinated boron center could change from electron-donating Ar′ groups (anilines) to electron-accepting fluoroaryl groups.

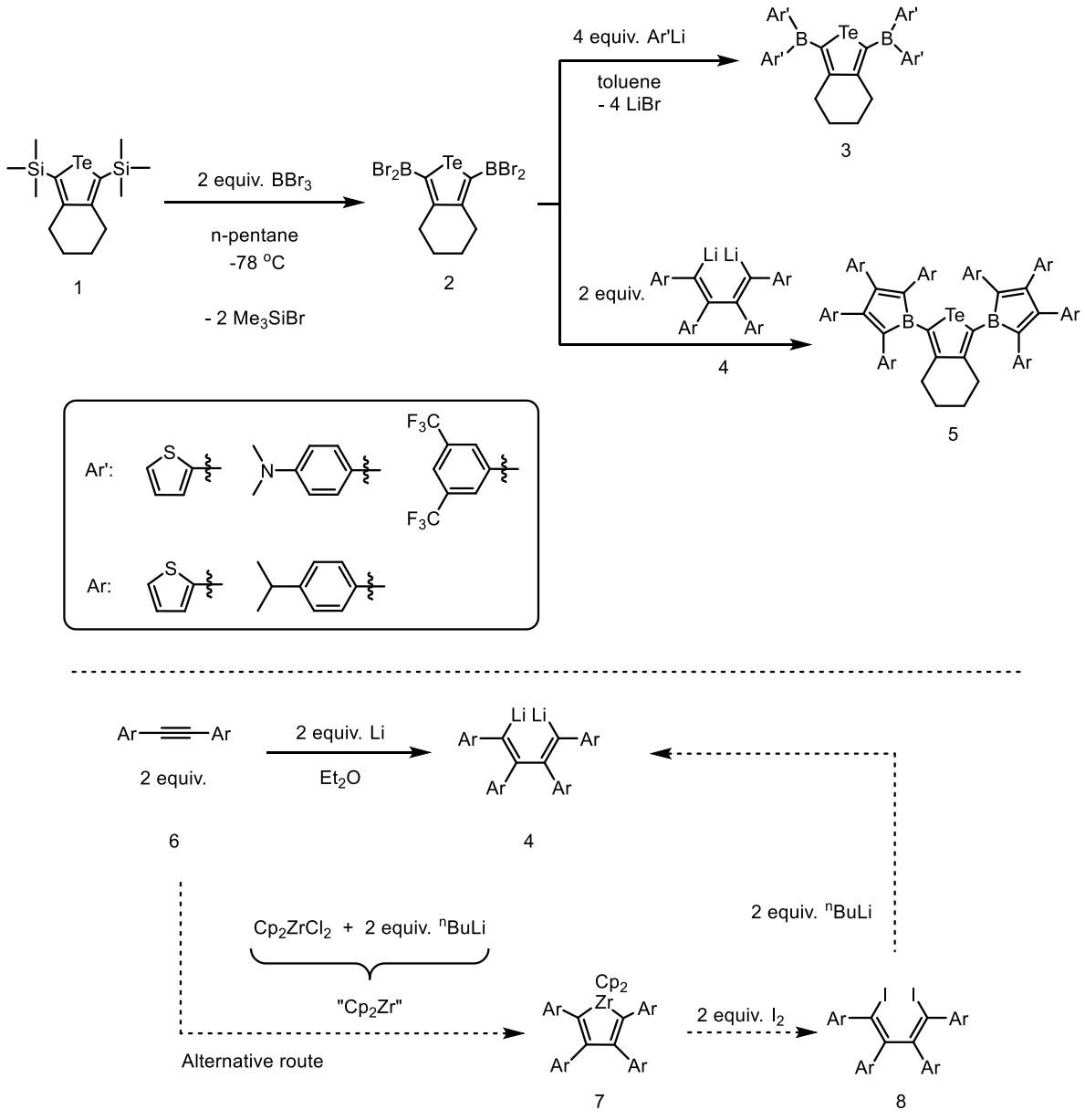

Scheme 5.2. Synthesis of organoboranes/organoboryl tellurophenes.

Compound **1**, **6** and **7**[1] have already been synthesized by the Rivard group. Borylation of **1** is accordance with literature procedures[2] to form bis-dibromoboranetellurophene **2**, which can be used later to form diarylboryl tellurophenes such as **3**.[2] In a similar fashion, compound **2** can react with the dilithiated diene **4** to form the respective the disubstituted boryltellurophene **5**.[3] Compound **4** could be synthesized according to literature procedures starting from known diarene acetylenes **6** (Scheme 5.2, bottom) or following the alternative procedure, via zirconacycle formation, described in the Scheme 5.2.[4]

In Chapter 3, I reported the synthetic routes to new BPin and bromide-functionalized tellurophenes. Protodeboronation of **4BTe** was carried out by K_2CO_3 aqueous under thermal conditions or using a microwave reactor to form **2BTe** or **BTe**, respectively. Bromination of **2BTe** or **BTe**, gave acceptable yields of the respective bromides **2BrTe** and **BrTe**, respectively (Scheme 5.3).

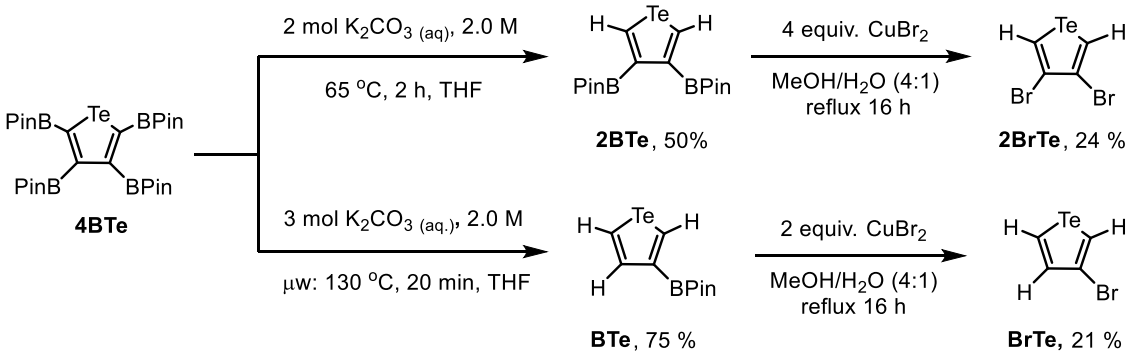

Scheme 5.3. Protodeboronation of **4BTe** followed by bromination with $CuBr_2$.

PDB of **B-Te-6-B** was performed with NaOH aqueous solution in THF. By varying the stoichiometry of base and time of reaction it was possible to control the outcome of the reaction towards one of the PDB products. PDB at both sides of **B-Te-6-B** proved to be difficult and the reaction needed longer reaction times (Scheme 5.4). Bromination of **B-Te-6-B** with $CuBr_2$ under mild conditions gave good results as evidenced by the good yield obtained of **Br-Te-6-Br** after purification by column chromatography.

The emission properties of **B-Te-6-H** were studied in film state and frozen glass in 2-Me-THF at low temperature (77 K). In film state, **B-Te-6-H** showed yellow luminescence, while in solution weak blue luminescence was found. The red-shift noted in the film state might be due to the formation of emissive excimers in the excited state.

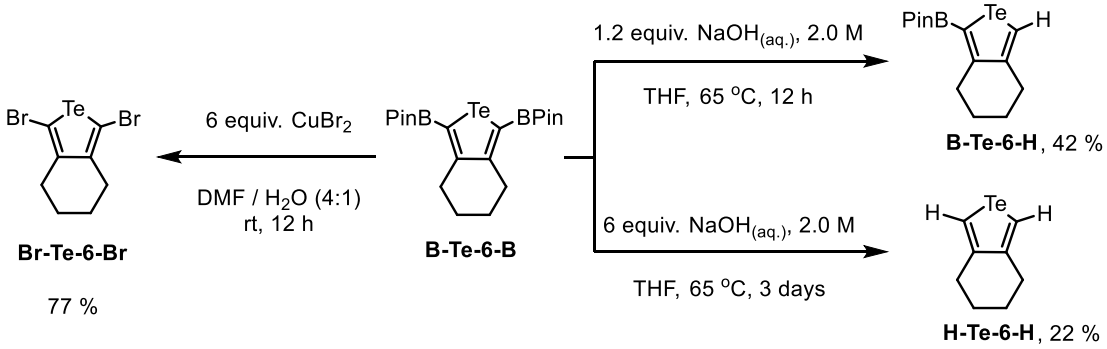

Scheme 5.4. Protodeboronation and bromination of **B-Te-6-B**.

There is a very interesting chemistry that can be developed around the PDB products of **4BTe**. Especially **BTe** shows great promise to be functionalized at 3-position by Suzuki-Miyaura cross-coupling. Currently known 3-functionalized tellurophenes generally limited to 3-alkyltellurophenes. Functionalization of **BTe** would allow an increase in the number of tellurophene precursors available for copolymerization reactions. In that sense, I propose the synthesis of arylated tellurophenes, **ArTe**, where the aromatic group holds strong electron withdrawing and donating groups in order to induce changes in the electronic properties of the tellurophene ring (Scheme 5.5). Then, halogenation of **ArTe** would possibly afford new valuable monomers for the synthesis of polytellurophenes as described in the Scheme 5.6.

Polymer 1 could be synthesized by Grignard metathesis (GRIM) method[5] to afford the respective homopolymer (Scheme 5.6). It would be interesting to study the optoelectronic properties of the homopolymer as a function of the appended aryl groups. Copolymerization of 3-aryltellurophene with acceptor units such as thiophene and benzothiadiazole (polymer 2 and 3, respectively. Scheme 5.6) and form donor-acceptor structures would be valuable in order to obtain polymers with small band gap for potential photovoltaic applications.

Reports[6] on polymers having benzothiadiazole as an acceptor group and other different donor groups, such as carbazoles, dithiophenes, siloles and fluorenes, have shown color tunable luminescence with potential applications in bio-imaging.

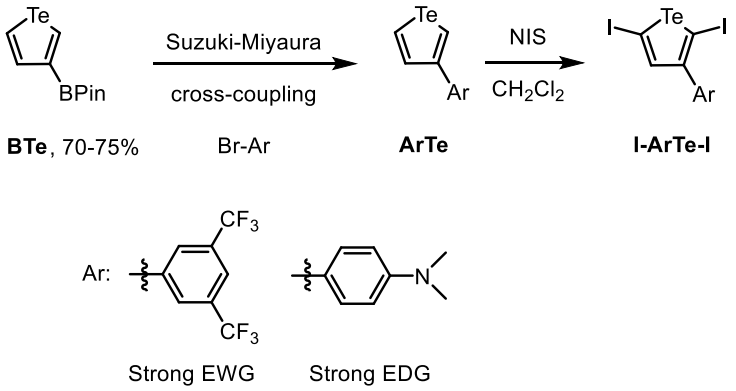

Scheme 5.5. Functionalization of **BTe** and halogenation to form diiodo-3-aryltellurophenes.

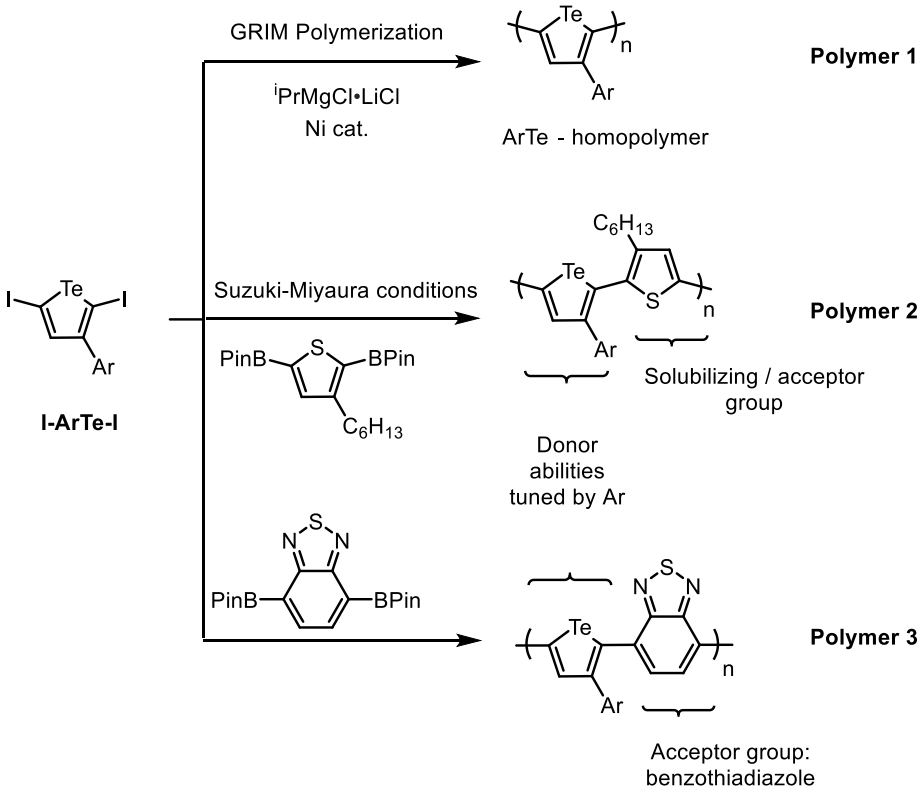

Scheme 5.6. Polymerization of **I-ArTe-I**.

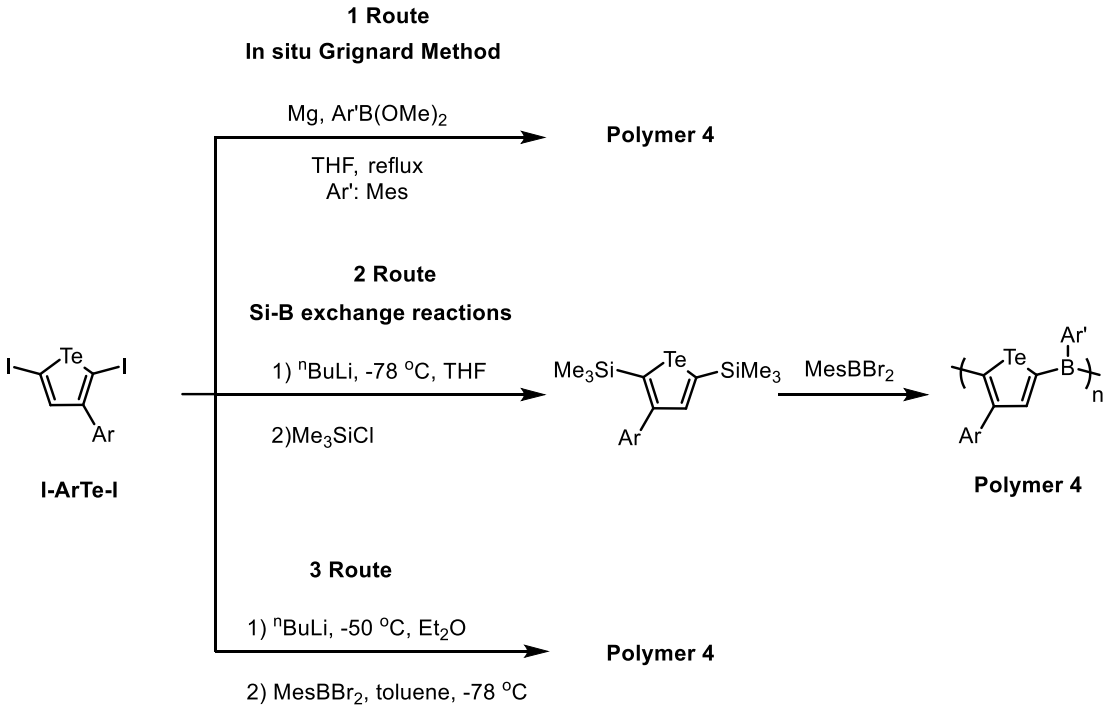

Scheme 5.7. Polymerization of **I-ArTe-I** to form polyboranetellurophenes.

The synthesis of boron-containing polytellurophenes (polymer 4, Scheme 5.7) could be very interesting. I proposed the synthesis of polymer 4 via three possible routes: the first is through Grignard substitution reactions[7] under reflux, the second is through a silicon-boron exchange reactions,[8,2] and the third via the formation of a lithium-aryl intermediate.[9] There are different characteristics of polymer 4 that make it attractive; the aryl group on tellurophene could tune the electron donating ability (and nature of luminescence) of the tellurophene backbone. By placing a bulky aryl group on boron, the resulting polymer could be moisture- and air-stable, while the presence of boron still allows conjugation along the main backbone. I consider polymer 4 the most interesting polymer of all to study, it is not only because of the expected emission properties but because of its design allows to tune different properties, such as solubility, stability and optical properties.

In Chapter 4, the synthesis of symmetric tellurophenes, **Naph-Te-6-Naph**, **Fl-Te-6-Fl** and **Ar^F-Te-6-Ar^F** was accomplished (Scheme 5.8) via Suzuki-Miyaura coupling reactions, as well as the formation of unsymmetrical tellurophenes **Naph-Te-6-B** and **Ar^F-Te-6-B**. A

general protocol for the synthesis of unsymmetric tellurophenes was developed, in which the synthesis of unsymmetric alkyne-functionalized octadiynes, **H-C8-Ar**, was addressed first via Sonogashira coupling (Scheme 5.9) before using this species to form the respective boronate esters **B-C8-Ar**. From this precursor, luminescent tellurophenes **B-Te-6-Ar** were formed via alkyne cyclization with Negishi's reagent "Cp_2Zr" followed by transmetallation with Bipy•$TeCl_2$.

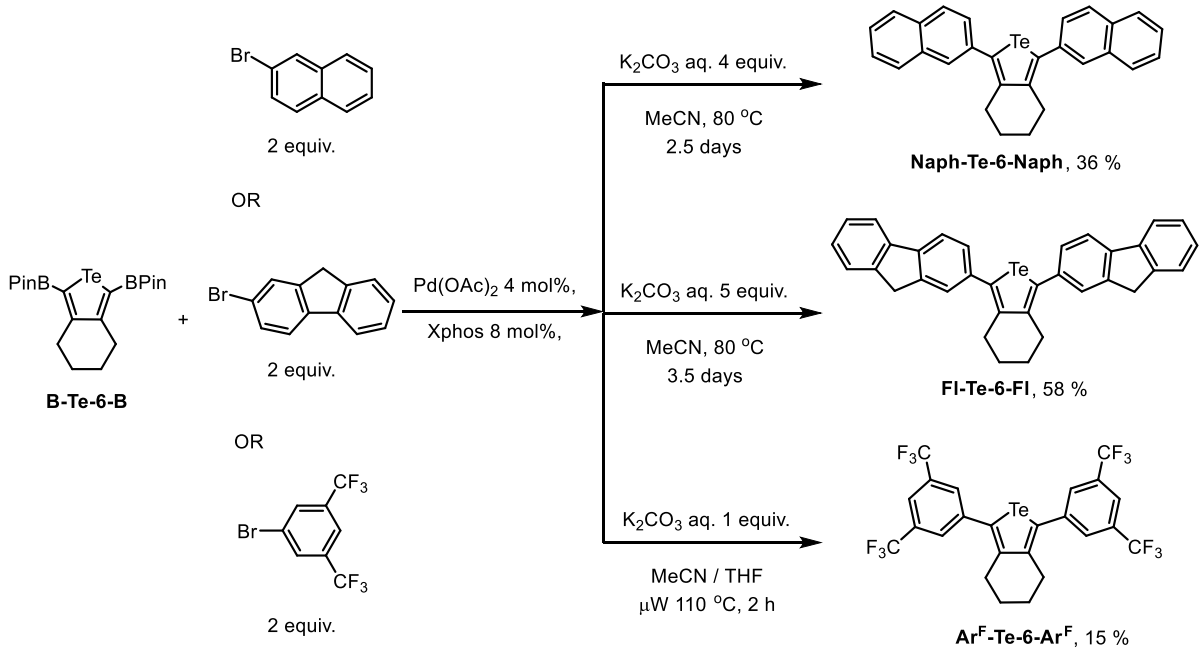

Scheme 5.8. Synthesis of symmetrical tellurophenes, **Naph-Te-6-Naph**, **Fl-Te-6-Fl** and **Ar^F-Te-6-Ar^F**, via Suzuki-Miyaura coupling reactions.

Suzuki-Miyaura coupling reaction on **B-Te-6-B** proved to be challenging, however, I managed to recover and purify the products by column chromatography. Unfortunately, the unsymmetric tellurophenes **Naph-Te-6-B** and **Ar^F-Te-6-B** partially decomposed during silica gel column chromatography. The molecular structures of **Naph-Te-6-Naph** and **Ar^F-Te-6-Ar^F** were also determined and show a non-coplanar configuration of the side-substituents in relation to the central tellurophene unit.

In the synthesis of the unsymmetrical octadiynes **H-C8-Naph** and **H-C8-Ar^F** (Scheme 5.9), an excess of 1,7-octadiyne was used with respect to the aryl halides in order to favor the

formation of the unsymmetrical compounds instead of the di-substituted by-products. Borylation was performed on **H-C8-Naph** and **H-C8-Ar^F** to form **B-C8-Naph** and **B-C8-Ar^F**, respectively (Scheme 5.10), and these alkynes were used in the crude form to obtain the respective unsymmetric tellurophenes **B-Te-6-Naph** and **B-Te-6-Ar^F** in 6-9 % yield (after prolonged purification protocols) by the standard method of cyclization via formation of the zirconacycle and transmetallation with Bipy•$TeCl_2$.

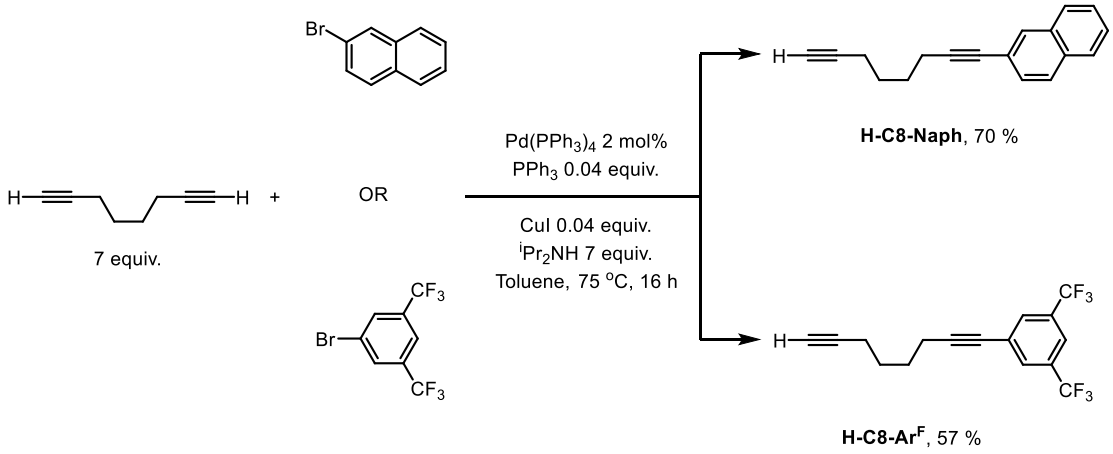

Scheme 5.9. Synthesis of the unsymmetrical octadiynes **H-C8-Naph** and **H-C8-Ar^F** via Sonogashira coupling reactions.

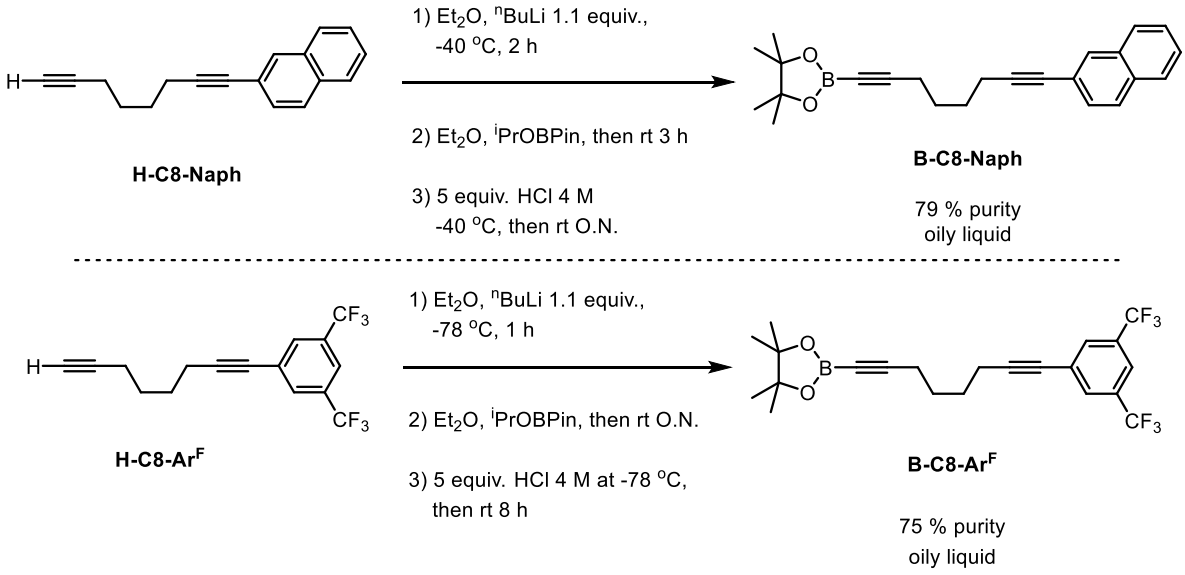

Scheme 5.10. Synthesis of the unsymmetrical octadiynes **B-C8-Naph** (top) and **B-C8-Ar^F** (bottom).

The absorption properties of **Naph-Te-6-Naph**, **Fl-Te-6-Fl**, **Ar^F-Te-6-Ar^F**, and **Naph-Te-6-B** were studied by UV-vis spectroscopy in solution of THF and the corresponding band gaps were calculated between 3.2-3.5 eV, with **Fl-Te-6-Fl** having the lower band gap and the broader absorption among these tellurophenes. In solution, none of these tellurophenes showed visible luminescence properties, not even under N_2. In the solid state (under UV-light) at room temperature and under aerated conditions, **Ar^F-Te-6-Ar^F** showed visible photoluminescence with intense yellow phosphorescence at 600 nm (τ = 29.3 μs) and an absolute quantum yield of ϕ of 9.4 %; **Naph-Te-6-B** gave faint red-orange emission in the solid state. When films of **Naph-Te-6-Naph** and **Fl-Te-6-Fl** were frozen in liquid N_2 and exposed immediately to UV light of 365 nm, faint orange-red and yellow-orange luminescence was detected in each solid sample, respectively. Luminescence measurements on these compounds suggest phosphorescence emission at low temperature given the large Stokes shift detected.

The yellow phosphorescence emission in the solid state observed in **Ar^F-Te-6-Ar^F** suggests that more examples of luminescent non-borylated tellurophenes could be made.

Since symmetric tellurophenes could still be phosphorescent in solid state at room temperature when strong electron-withdrawing Ar^F groups are appended onto a tellurophene, it would be interesting to prepare analogues Te heterocycles containing another electron-withdrawing groups such as (CHO)C_6H_4, (CN)C_6H_4 and (COOMe)C_6H_4, as side groups (Figure 5.1) and study their optoelectronic properties. For their synthesis, the protocol used to form the previous unsymmetric tellurophenes could be followed.

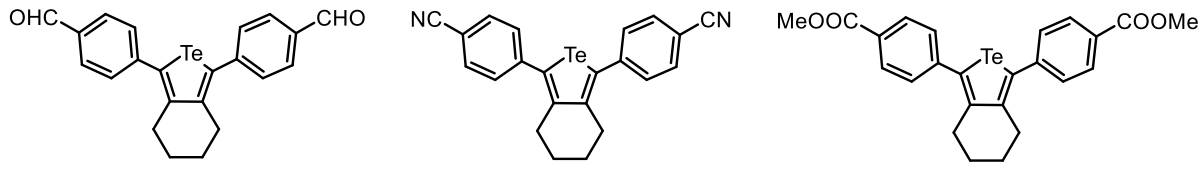

Figure 5.1. Symmetric tellurophenes with potential luminescent properties.

In Chapter 4, the unsymmetric octadiyne **B-C8-H** was formed in good yield, 87 %. This precursor and the recently diiodotellurophene (**I-Te-6-I**) developed by Rivard group could be used in the synthesis of tertellurophenes (**B-(Te-6)$_3$-B**) as proposed in the Scheme 5.11. The intermediate zirconacyclotellurophene structure is very versatile, since not only Te could be incorporated at both sides but also onto other chalcogenophenes such as those containing S and Se. The structure between BPin and the center tellurophene could be envisioned as a linker between the donor center (tellurophene) and the acceptor pinacolboronate ester placed at the end, forming Acceptor-Linker-Donor-Linker-Acceptor structures, which in turn it could lead to an increase in conjugation length, a decrease in the band gap and possible the enhancement of the luminescence intensity depending on the planarity of the structure.[10] Further chemistry on the final **B-(Te-6)$_3$-B** would allow to functionalize it with naphthalene units, which could form interesting and may be analogues nanowire structures as reported for **Naph-(Thiophene)$_3$-Naph**.[11,12]

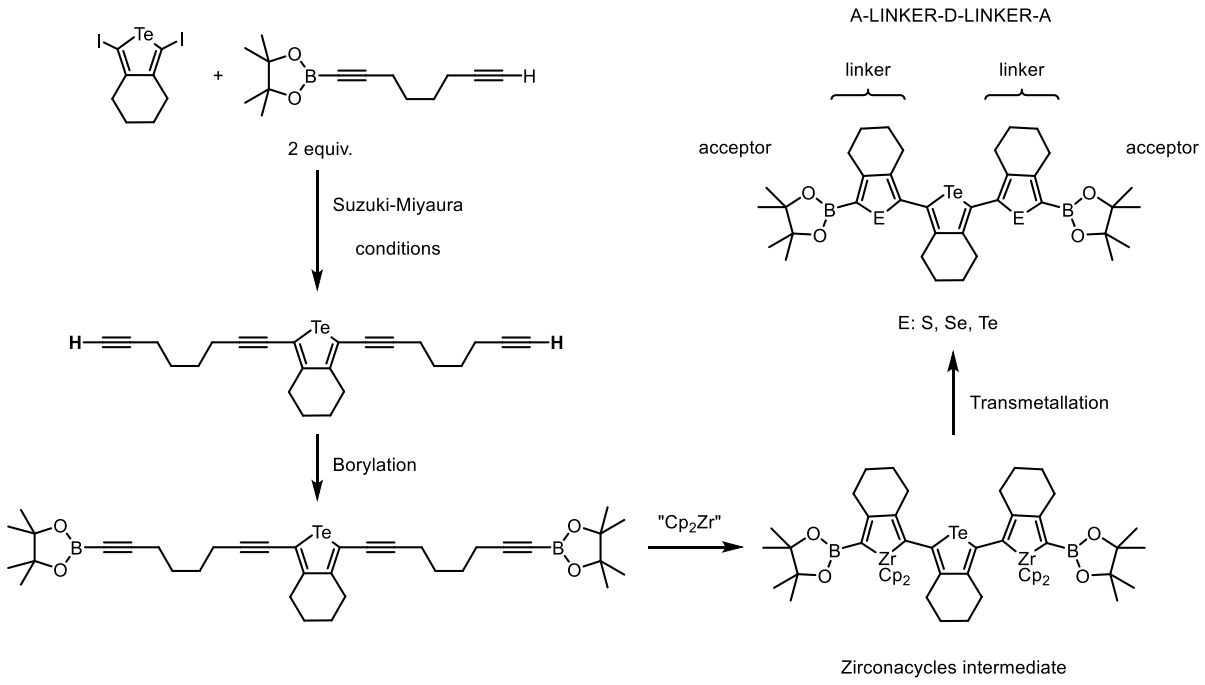

Scheme 5.11. Proposed synthesis of tertellurophenes (**B-(Te-6)$_3$-B**) or acceptor-linker-donor-linker-acceptor type chalcogenophene structures.

5.1. REFERENCES

1. Shynkaruk, O.; Qi, Y.; Cottrell-Callbeck, A.; Torres Delgado, W.; McDonald, R.; Ferguson, M. J.; He, G.; Rivard, E. *Organometallics* **2016**, *35*, 2232–2241.
2. Lik, A.; Fritze, L.; Müller, L.; Helten, H. *J. Am. Chem. Soc.* **2017**, *139*, 5692-5695.
3. Braunschweig, H.; Damme, A.; Jimenez-Halla, J. O. C.; Hörl, C.; Krummenacher, I.; Kupfer, T.; Mailänder, L.; Radacki, K. *J. Am. Chem. Soc.* **2012**, *134*, 20169–20177.
4. Eisch, J. J.; Galle, J. E.; Kozima, S. *J. Am. Chem. Soc.* **1986**, *108*, 379–385.
5. Jahnke, A. A.; Djukic, B.; McCormick, T. M.; Buchaca Domingo, E.; Hellmann, C.; Lee, Y.; Seferos, D. S. *J. Am. Chem. Soc.* **2013**, *135*, 951–954.
6. Liou, S. Y.; Ke, C. S.; Chen, J. H.; Luo, Y. W.; Kuo, S. Y.; Chen, Y. H.; Fang, C. C.; Wu, C. Y.; Chiang, C. M.; Chan, Y. H. *ACS Macro Lett.* **2016**, *5*, 154–157.
7. Matsumi, N.; Naka, K.; Chujo, Y. *J. Am. Chem. Soc.* **1998**, *120*, 10776–10777.
8. Qin, Y.; Cheng, G.; Sundararaman, A.; Jäkle, F. *J. Am. Chem. Soc.* **2002**, *124*, 12672–12673.
9. Devillard, M.; Brousses, R.; Miqueu, K.; Bouhadir, G.; Bourissou, D. *Angew. Chem. Int. Ed.* **2015**, *54*, 5722–5726.
10. Tigreros, A.; Ortiz, A.; Insuasty, B. *Dye. Pigment.* **2014**, *111*, 45–51.
11. Balzer, F.; Schiek, M.; Wallmann, I.; Schäfer, A.; Lützen, A.; Rubahn, H.-G. *Proc. SPIE* **2011**, *8094*, 809409-1-809409–7.
12. Balzer, F.; Schiek, M.; Osadnik, A.; Wallmann, I.; Parisi, J.; Rubahn, H.-G.; Lützen, A. *Phys. Chem. Chem. Phys.* **2014**, *16*, 5747.

BIBLIOGRAPHY

CHAPTER 1

1. Zhao, X.; Chaudhry, S. T.; Mei, J. In *Advances in Heterocyclic Chemistry*; Scriven, E. F. V.; Ramsden, C. A., Eds.; Elsevier Inc., **2016**; Vol. 121, pp. 133–171.

2. Fagan, P. J.; Nugent, W. A. *J. Am. Chem. Soc.* **1988**, *110*, 2310–2312.

3. Fagan, P. J.; Nugent, W. A.; Calabrese, J. C. *J. Am. Chem. Soc.* **1994**, *116*, 1880–1889.

4. O'Rourke, N. F.; Kier, M. J.; Micalizio, G. C. *Tetrahedron* **2016**, *72*, 7093–7123.

5. Gessner, V. H.; Tannaci, J. F.; Miller, A. D.; Tilley, T. D. *Acc. Chem. Res.* **2011**, *44*, 435–446.

6. Marek, I. *Titanium and Zirconium in Organic Synthesis*; Wiley-VCH Verlag GmbH & Co. KGaA, **2002**.

7. Reichard, H. A.; Rieger, J. C.; Micalizio, G. C. *Angew. Chem. Int. Ed.* **2008**, *47*, 7837–7840.

8. Braye, E. H.; Hübel, W.; Caplier, I. *J. Am. Chem. Soc.* **1961**, *83*, 4406–4413.

9. Dioumaev, V. K.; Harrod, J. F. *Organometallics* **1997**, *16*, 1452–1464.

10. Takahashi, T.; Kageyama, M.; Denisov, V.; Hara, R.; Negishi, E. *Tetrahedron Lett.* **1993**, *34*, 687–690.

11. Alt, H. G.; Denner, C. E. *J. Organomet. Chem.* **1990**, *390*, 53–60.

12. Rosenthal, U.; Ohff, A.; Baumann, W.; Tillack, A.; Görls, H.; Burlakov, V. V.; Shur, V. B. *Z. Anorg. Allg. Chem.* **1995**, *621*, 77–83.

13. Negishi, E.-I.; Cederbaum, F. E.; Takahashi, T. *Tetrahedron Lett.* **1986**, *27*, 2829–2832.

14. Rosenthal, U.; Ohff, A.; Michalik, M.; Görls, H.; Burlakov, V. V.; Shur, V. B. *Angew. Chem. Int. Ed.* **1993**, *32*, 1193–1195.

15. Denhez, C.; Médégan, S.; Hélion, F.; Namy, J.-L.; Vasse, J.-L.; Szymoniak, J. *Org. Lett.* **2006**, *8*, 2945–2947.

16. Ma, W.; Yu, C.; Chen, T.; Xu, L.; Zhang, W.-X.; Xi, Z. *Chem. Soc. Rev.* **2017**, *46*, 1160–1192.

17. Zirngast, M.; Marschner, C.; Baumgartner, J. *Organometallics* **2008**, *27*, 2570–2583.

18. Ren, S.; Seki, T.; Necas, D.; Shimizu, H.; Nakajima, K.; Kanno, K.; Song, Z.; Takahashi, T. *Chem. Lett.* **2011**, *40*, 1443–1444.

19. Johnson, S. A.; Liu, F. Q.; Suh, M. C.; Zürcher, S.; Haufe, M.; Mao, S. S. H.; Tilley, T. D. *J. Am. Chem. Soc.* **2003**, *125*, 4199–4211.

20. Negishi, E.; Holmes, S.; Tour, J. *J. Am. Chem. Soc.* **1989**, *111*, 3336–3346.

21. Nugent, W. A.; Thorn, D. L.; Harlow, R. L. *J. Am. Chem. Soc.* **1987**, *109*, 2788–2796.

22. Buchwald, S. L.; Nielsen, R. B. *J. Am. Chem. Soc.* **1989**, *111*, 2870–2874.

23. Hara, R.; Xi, Z.; Kotora, M.; Xi, C.; Takahashi, T. *Chem. Lett.* **1996**, *25*, 1003–1004.

24. Xi, Z.; Zhang, W.; Takahashi, T. *Tetrahedron Lett.* **2004**, *45*, 2427–2429.

25. Hamada, T.; Suzuki, D.; Urabe, H.; Sato, F. *J. Am. Chem. Soc.* **1999**, *121*, 7342–7344.

26. Perez, L. J.; Shimp, H. L.; Micalizio, G. C. *J. Org. Chem.* **2009**, *74*, 7211–7219.

27. Zhou, Y.; Yan, X.; Chen, C.; Xi, C. *Organometallics* **2013**, *32*, 6182–6185.

28. Bankwitz, U.; Sohn, H.; Powell, D. R.; West, R. *J. Organomet. Chem.* **1995**, *499*, C7–C9.

29. Xi, C.; Hou, S.; Afifi, T. H.; Hara, R.; Takahashi, T. *Tetrahedron Lett.* **1997**, *38*, 4099–4102.

30. Liao, Q.; Zhang, L.; Wang, F.; Li, S.; Xi, C. *Eur. J. Org. Chem.* **2010**, 5426–5431.

31. You, W.; Yan, X.; Liao, Q.; Xi, C. *Org. Lett.* **2010**, *12*, 3930–3933.

32. Gonzalez, J. L.; Stephens, C. E.; Wenzler, T.; Brun, R.; Tanious, F. A.; Wilson, W. D.; Barszcz, T.; Werbovetz, K. A.; Boykin, D. W. *Eur. J. Med. Chem.* **2007**, *42*, 552–557.

33. Wilhelm, E. A.; Gai, B. M.; Souza, A. C. G.; Bortolatto, C. F.; Roehrs, J. A.; Nogueira, C. W. *Mol. Cell. Biochem.* **2012**, *365*, 175–180.

34. Fleming, J.; Ghose, A.; Harrison, P. R. *Nutr. Cancer* **2001**, *40*, 42–49.

35. Gasparian, A. V; Yao, Y. J.; Lu, J.; Yemelyanov, A. Y.; Lyakh, L. A.; Slaga, T. J.; Budunova, I. V *Mol. Cancer Ther.* **2002**, *1*, 1079–1087.

36. Srivastava, P. C.; Robins, R. K. *J. Med. Chem.* **1983**, *26*, 445–448.

37. Jayaram, H. N.; Dion, R. L.; Glazer, R. I.; Johns, D. G.; Robins, R. K.; Srivastava, P. C.; Cooney, D. A. *Biochem. Pharmacol.* **1982**, *31*, 2371–2380.

38. Je, M.; Kobilka, B. M.; Hale, B. J. *Macromolecules* **2014**, *47*, 7253–7271.

39. Park, Y. S.; Kale, T. S.; Nam, C.-Y.; Choi, D.; Grubbs, R. B. *Chem. Commun.* **2014**, *50*, 7964–7967.

40. Yamaguchi, S.; Xu, C. H.; Okamoto, T. *Pure Appl. Chem.* **2006**, *78*, 721–730.

41. Manjare, S. T.; Kim, Y.; Churchill, D. G. *Acc. Chem. Res.* **2014**, *47*, 2985–2998.

42. Kryman, M. W.; Schamerhorn, G. A.; Hill, J. E.; Calitree, B. D.; Davies, K. S.; Linder, M. K.; Ohulchanskyy, T. Y.; Detty, M. R. *Organometallics* **2014**, *33*, 2628–2640.

43. Yamamoto, T.; Takimiya, K. *J. Am. Chem. Soc.* **2007**, *129*, 2224–2225.

44. Shinamura, S.; Osaka, I.; Miyazaki, E.; Takimiya, K. *Heterocycles* **2011**, *83*, 1187–1204.

45. Choi, T. L.; Han, K. M.; Park, J. I.; Kim, D. H.; Park, J. M.; Lee, S. *Macromolecules* **2010**, *43*, 6045–6049.

46. Tang, J.; Zhao, X. *RSC Adv.* **2012**, *2*, 5488–5490.

47. Curtis, R. F.; Hasnain, S. N.; Taylor, J. A. *J. Chem. Soc. Chem. Commun.* **1968**, 365.

48. Mack, W. *Angew. Chem. Int. Ed.* **1966**, *5*, 896.

49. Fringuelli, F.; Taticchi, A. *J. Chem. Soc. Perkin Trans. 1* **1972**, 199–203.

50. Sweat, D. P.; Stephens, C. E. *J. Organomet. Chem.* **2008**, *693*, 2463–2464.

51. Li, P.-F.; Carrera, E. I.; Seferos, D. S. *Chem Plus Chem* **2016**, *81*, 917–921.

52. He, G.; Kang, L.; Torres Delgado, W.; Shynkaruk, O.; Ferguson, M. J.; McDonald, R.; Rivard, E. *J. Am. Chem. Soc.* **2013**, *135*, 5360–5363.

53. Dutton, J. L.; Farrar, G. J.; Sgro, M. J.; Battista, T. L.; Ragogna, P. J. *Chem. Eur. J.* **2009**, *15*, 10263–10271.

54. Godoi, B.; Schumacher, R. F.; Zeni, G. *Chem. Rev.* **2011**, *111*, 2937–2980.

55. Larock, R. C.; Yue, D. *Tetrahedron Lett.* **2001**, *42*, 6011–6013.

56. Yue, D.; Larock, R. C. *J. Org. Chem.* **2002**, *67*, 1905–1909.

57. Roehrs, J. A.; Pistoia, R. P.; Back, D. F.; Zeni, G. *J. Org. Chem.* **2015**, *80*, 12470–12481.

58. Alves, D.; Luchese, C.; Nogueira, C. W.; Zeni, G. *J. Org. Chem.* **2007**, *72*, 6726–6734.

59. Dabdoub, M. J.; Dabdoub, B.; Pereira, M. A.; Zukerman-Schpector, J. *J. Org. Chem.* **1996**, *61*, 9503–9511.

60. Jung, E. H.; Bae, S.; Yoo, T. W.; Jo, W. H. *Polym. Chem.* **2014**, *5*, 6545–6550.

61. Chen, L.; Shen, P.; Zhang, Z.-G.; Li, Y. *J. Mater. Chem. A* **2015**, *3*, 12005–12015.

62. Westgate, T. D.; Skabara, P. J.; Cortizo-Lacalle, D. In *Handbook of Chalcogen Chemistry: New Perspectives in Sulfur, Selenium and Tellurium*; Devillanova, F. A.; Du Mont, W. W., Eds.; Royal Society of Chemistry, **2013**; Vol. 2, pp. 99–126.

63. Rivard, E. *Chem. Lett.* **2015**, *44*, 730–736.

64. Planells, M.; Schroeder, B. C.; McCulloch, I. *Macromolecules* **2014**, *47*, 5889–5894.

65. He, G.; Torres Delgado, W.; Schatz, D. J.; Merten, C.; Mohammadpour, A.; Mayr, L.; Ferguson, M. J.; McDonald, R.; Brown, A.; Shankar, K.; Rivard, E. *Angew. Chem. Int. Ed.* **2014**, *53*, 4587–4591.

66. He, G.; Wiltshire, B. D.; Choi, P.; Savin, A.; Sun, S.; Mohammadpour, A.; Ferguson, M. J.; McDonald, R.; Farsinezhad, S.; Brown, A.; Shankar, K.; Rivard, E. *Chem. Commun.* **2015**, *51*, 5444–5447.

67. Callis, P. R. *J. Mol. Struct.* **2014**, *1077*, 14–21.

68. Luo, J.; Xie, Z.; Lam, J. W. Y.; Cheng, L.; Tang, B. Z.; Chen, H.; Qiu, C.; Kwok, H. S.; Zhan, X.; Liu, Y.; Zhu, D. *Chem. Commun.* **2001**, *381*, 1740–1741.

69. Tang, B.; Zhan, X.; Yu, G.; Lee, P. *J. Mater. Chem.* **2001**, *11*, 2974–2978.

70. Hong, Y.; Lam, J. W. Y.; Tang, B. Z. *Chem. Soc. Rev.* **2011**, *40*, 5361–5388.

71. Mei, J.; Leung, N. L. C.; Kwok, R. T. K.; Lam, J. W. Y.; Tang, B. Z. *Chem. Rev.* **2015**, *115*, 11718–11940.

72. Kwok, R. T. K.; Leung, C. W. T.; Lam, J. W. Y.; Tang, B. Z. *Chem. Soc. Rev.* **2015**, *44*, 4228–4238.

73. Hu, R.; Kang, Y.; Tang, B. Z. *Polym. J.* **2016**, *48*, 359–370.

74. Hong, Y.; Lam, J. W. Y.; Tang, B. Z. *Chem. Commun.* **2009**, 4332–4353.

75. Ho, C. N.; Patonay, G.; Warner, I. M. *Trends Anal. Chem.* **1986**, *5*, 37–43.

76. Mátyus, L.; Szöllosi, J.; Jenei, A. *J. Photochem. Photobiol. B Biol.* **2006**, *83*, 223–236.

77. Van De Weert, M.; Stella, L. *J. Mol. Struct.* **2011**, *998*, 145–150.

78. Sasaki, S.; Drummen, G. P. C.; Konishi, G. *J. Mater. Chem. C* **2016**, *4*, 2731–2743.

79. Berezin, M. Y.; Achilefu, S. *Chem. Rev.* **2010**, *110*, 2641–2684.

80. Chai, J.; Wang, J.; Xu, Q.; Hao, F.; Liu, R. *Mol. Biosyst.* **2012**, *8*, 1902–1907.

81. Solovyov, K. N.; Borisevich, E. A. *Usp. Fiz. Nauk* **2005**, *48*, 231–253.

82. Koziar, J. C.; Cowan, D. O. *Acc. Chem. Res.* **1978**, *11*, 334–341.

83. Kuivila, H. G.; Keough, A. H.; Soboczenski, E. J. *J. Org. Chem.* **1953**, *19*, 780–783.

84. Liljebris, C.; Nilsson, B. M.; Resul, B.; Hacksell, U. *J. Org. Chem.* **1996**, *61*, 4028–4034.

85. Oshima, K.; Aoyama, Y. *J. Am. Chem. Soc.* **1999**, *121*, 2315–2316.

86. Oshima, K.; Kitazono, E. I.; Aoyama, Y. *Tetrahedron Lett.* **1997**, *38*, 5001–5004.

87. Duggan, P. J.; Tyndall, E. M. *J. Chem. Soc. Perkin Trans. 1* **2002**, 1325–1339.

88. Cho, J. Y.; Iverson, C. N.; Smith, M. R. *J. Am. Chem. Soc.* **2000**, *122*, 12868–12869.

89. Shimada, S.; Batsanov, A. S.; Howard, J. A. K.; Marder, T. B. *Angew. Chem. Int. Ed.* **2001**, *40*, 2168–2171.

90. Molander, G. A.; Trice, S. L. J.; Dreher, S. D. *J. Am. Chem. Soc.* **2010**, *132*, 17701–17703.

91. Bose, S. K.; Fucke, K.; Liu, L.; Steel, P. G.; Marder, T. B. *Angew. Chem. Int. Ed.* **2014**, *53*, 1799–1803.

92. Guo, L.; Rueping, M. *Chem. - A Eur. J.* **2016**, *22*, 16787–16790.

93. Warner, A. J.; Lawson, J. R.; Fasano, V.; Ingleson, M. J. *Angew. Chem. Int. Ed.* **2015**, *54*, 11245–11249.

94. Ahn, S. J.; Lee, C. Y.; Kim, N. K.; Cheon, C. H. *J. Org. Chem.* **2014**, *79*, 7277–7285.

95. Lozada, J.; Liu, Z.; Perrin, D. M. *J. Org. Chem.* **2014**, *79*, 5365–5368.

96. Liu, C.; Li, X.; Wu, Y.; Qiu, J. *RSC Adv.* **2014**, *4*, 54307–54311.

97. Liu, C.; Li, X.; Wu, Y. *RSC Adv.* **2015**, *5*, 15354–15358.

98. Thakur, A.; Zhang, K.; Louie, J. *Chem. Commun.* **2012**, *48*, 203.

99. Lee, C. Y.; Ahn, S. J.; Cheon, C. H. *J. Org. Chem.* **2013**, *78*, 12154–12160.

100. Lennox, A. J. J.; Lloyd-Jones, G. C. *Isr. J. Chem.* **2010**, *50*, 664–674.

101. Yamamoto, Y.; Takizawa, M.; Yu, X. Q.; Miyaura, N. *Angew. Chem. Int. Ed.* **2008**, *47*, 928–931.

102. Oberli, M. A.; Buchwald, S. L. *Org. Lett.* **2012**, *14*, 4606–4609.

103. Molander, G. A.; Biolatto, B. *J. Org. Chem.* **2003**, *68*, 4302–4314.

104. Molander, G. A.; Canturk, B.; Kennedy, L. E. *J. Org. Chem.* **2009**, *74*, 973–980.

105. Carrillo, J. A.; Ingleson, M. J.; Turner, M. L. *Macromolecules* **2015**, *48*, 979–986.

106. Billingsley, K. L.; Anderson, K. W.; Buchwald, S. L. *Angew. Chem. Int. Ed.* **2006**, *45*, 3484–3488.

107. Billingsley, K.; Buchwald, S. L. *J. Am. Chem. Soc.* **2007**, *129*, 3358–3366.

108. Martin, R.; Buchwald, S. L. *Acc. Chem. Res.* **2008**, *41*, 1461–1473.

109. Kinzel, T.; Zhang, Y.; Buchwald, S. L. *J. Am. Chem. Soc.* **2010**, *132*, 14073–14075.

110. Chivers, Tristram; Laitinen, R. S. *Chem. Soc. Rev.* **2015**, *44*, 1725–1739.

111. Carrera, E. I.; Seferos, D. S. *Macromolecules* **2015**, *48*, 297–308.

112. Barton, T. J.; Roth, R. W. *J. Organomet. Chem.* **1972**, *39*, 66–68.

113. Sweat, D.; Stephens, C. *Synthesis (Stuttg).* **2009**, 3214–3218.

114. Rhoden, C. R. B.; Zeni, G. *Org. Biomol. Chem.* **2011**, *9*, 1301–1313.

CHAPTER 2

1. Duhović, S.; Dincă, M. *Chem. Mater.* **2015**, *27*, 5487–5490.
2. Planells, M.; Schroeder, B. C.; McCulloch, I. *Macromolecules* **2014**, *47*, 5889–5894.
3. Park, Y. S.; Kale, T. S.; Nam, C.-Y.; Choi, D.; Grubbs, R. B. *Chem. Commun.* **2014**, *50*, 7964–7967.
4. Al-Hashimi, M.; Han, Y.; Smith, J.; Bazzi, H. S.; Alqaradawi, S. Y. A.; Watkins, S. E.; Anthopoulos, T. D.; Heeney, M. *Chem. Sci.* **2016**, *7*, 1093–1099.
5. Parke, S. M.; Boone, M. P.; Rivard, E. *Chem. Commun.* **2016**, *52*, 9485–9505.
6. Yamamoto, T.; Takimiya, K. *J. Am. Chem. Soc.* **2007**, *129*, 2224–2225.
7. Shinamura, S.; Osaka, I.; Miyazaki, E.; Takimiya, K. *Heterocycles* **2011**, *83*, 1187–1204.
8. Kremer, A.; Aurisicchio, C.; Deleo, F.; Ventura, B.; Wouters, J.; Armaroli, N.; Barbieri, A.; Bonifazi, D. *Chem. Eur. J.* **2015**, *21*, 15377–15387.
9. Manjare, S. T.; Kim, Y.; Churchill, D. G. *Acc. Chem. Res.* **2014**, *47*, 2985–2998.
10. Kaur, M.; Yang, D. S.; Choi, K.; Cho, M. J.; Choi, D. H. *Dye. Pigment.* **2014**, *100*, 118–126.
11. Kryman, M. W.; Schamerhorn, G. A.; Hill, J. E.; Calitree, B. D.; Davies, K. S.; Linder, M. K.; Ohulchanskyy, T. Y.; Detty, M. R. *Organometallics* **2014**, *33*, 2628–2640.
12. Godoi, B.; Schumacher, R. F.; Zeni, G. *Chem. Rev.* **2011**, *111*, 2937–2980.
13. Rhoden, C. R. B.; Zeni, G. *Org. Biomol. Chem.* **2011**, *9*, 1301–1313.
14. Primas, N.; Bouillon, A.; Rault, S. *Tetrahedron* **2010**, *66*, 8121–8136.

15. Borowska, E.; Durka, K.; Luliński, S.; Serwatowski, J.; Woźniak, K. *Eur. J. Org. Chem.* **2012**, 2208–2218.

16. He, G.; Kang, L.; Torres Delgado, W.; Shynkaruk, O.; Ferguson, M. J.; McDonald, R.; Rivard, E. *J. Am. Chem. Soc.* **2013**, *135*, 5360–5363.

17. He, G.; Torres Delgado, W.; Schatz, D. J.; Merten, C.; Mohammadpour, A.; Mayr, L.; Ferguson, M. J.; McDonald, R.; Brown, A.; Shankar, K.; Rivard, E. *Angew. Chem. Int. Ed.* **2014**, *53*, 4587–4591.

18. Erker, G.; Zwettler, R.; Krueger, C.; Hyla-Kryspin, I.; Gleiter, R. *Organometallics* **1990**, *9*, 524–530.

19. Negishi, E.-I.; Cederbaum, F. E.; Takahashi, T. *Tetrahedron Lett.* **1986**, *27*, 2829–2832.

20. Geng, W.; Wang, C.; Guang, J.; Hao, W.; Zhang, W. X.; Xi, Z. *Chem. Eur. J.* **2013**, *19*, 8657–8664.

21. Dutton, J. L.; Farrar, G. J.; Sgro, M. J.; Battista, T. L.; Ragogna, P. J. *Chem. Eur. J.* **2009**, *15*, 10263–10271.

22. Kang, Y. K.; Deria, P.; Carroll, P. J.; Therien, M. J. *Org. Lett.* **2008**, *10*, 1341–1344.

23. Takimiya, K.; Konda, Y.; Ebata, H.; Niihara, N.; Otsubo, T. *J. Org. Chem.* **2005**, *70*, 10569–10571.

24. Li, P.-F.; Carrera, E. I.; Seferos, D. S. *Chem Plus Chem* **2016**, *81*, 917–921.

25. Peral, F.; Gallego, E. *Spectrochim. Acta - Part A Mol. Biomol. Spectrosc.* **2000**, *56*, 2149–2155.

26. Tinoco, J. I. *J. Am. Chem. Soc.* **1960**, *82*, 4785–4790.

27. Misra, A.; Kumar, P.; Srivastava, R.; Dhawan, S. K.; Kamalasanan, M. N.; Chandra, S. *Indian J. Pure Appl. Phys.* **2005**, *43*, 921–925.

28. Je, M.; Kobilka, B. M.; Hale, B. J. *Macromolecules* **2014**, *47*, 7253–7271.

29. Planells, M.; Schroeder, B. C.; McCulloch, I. *Macromolecules* **2014**, *47*, 5889–5894.

30. Chai, J.; Wang, J.; Xu, Q.; Hao, F.; Liu, R. *Mol. Biosyst.* **2012**, *8*, 1902–1907.

31. He, G.; Wiltshire, B. D.; Choi, P.; Savin, A.; Sun, S.; Mohammadpour, A.; Ferguson, M. J.; McDonald, R.; Farsinezhad, S.; Brown, A.; Shankar, K.; Rivard, E. *Chem. Commun.* **2015**, *51*, 5444–5447.

32. Yersin, H.; Rausch, A. F.; Czerwieniec, R.; Hofbeck, T.; Fischer, T. *Coord. Chem. Rev.* **2011**, *255*, 2622–2652.

33. Ji, S.; Wu, W.; Wu, Y.; Zhao, T.; Zhou, F.; Yang, Y.; Zhang, X.; Liang, X.; Wu, W.; Chi, L.; Wang, Z.; Zhao, J. *Analyst* **2009**, *134*, 958–965.

34. Papkovsky, D. B.; Ponomarev, G. V; Trettnak, W.; Oleary, P. *Anal. Chem.* **1995**, *67*, 4112–4117.

35. Hong, Y.; Lam, J. W. Y.; Tang, B. Z. *Chem. Soc. Rev.* **2011**, *40*, 5361–5388.

36. Mei, J.; Hong, Y.; Lam, J. W. Y.; Qin, A.; Tang, Y.; Tang, B. Z. *Adv. Mater.* **2014**, *26*, 5429–5479.

37. Kwok, R. T. K.; Leung, C. W. T.; Lam, J. W. Y.; Tang, B. Z. *Chem. Soc. Rev.* **2015**, *44*, 4228–4238.

38. Dong, Y.; Lam, J. W. Y.; Qin, A.; Liu, J.; Li, Z.; Tang, B. Z.; Sun, J.; Kwok, H. S. *Appl. Phys. Lett.* **2007**, *91*, 1–4.

39. Samanta, S.; Goswami, S.; Hoque, M. N.; Ramesh, A.; Das, G. *Chem. Commun.* **2014**, *50*, 11833–11836.

40. Liu, X.; Liang, G. *Chem. Commun.* **2017**, *53*, 1037–1040.

41. Zhao, Z.; Su, H.; Zhang, P.; Cai, Y.; Kwok, R. T. K.; Chen, Y.; He, Z.; Gu, X.; He, X.; Sung, H. H.-Y.; Williams, I. D.; Lam, J. W. Y.; Zhang, Z.; Tang, B. Z. *J. Mater. Chem. B.* **2017**, *5*, 1650–1657.

42. Hong, Y.; Lam, J. W. Y.; Tang, B. Z. *Chem. Commun.* **2009**, 4332–4353.

43. Connelly, N. G.; Geiger, W. E. *Chem. Rev.* **1996**, *96*, 877–910.

44. Romero, N. A.; Nicewicz, D. A. *Chem. Rev.* **2016**, *116*, 10075–10166.

45. Roquet, S.; Cravino, A.; Leriche, P.; Aléveque, O.; Frère, P.; Roncali, J. *J. Am. Chem. Soc.* **2006**, *128*, 3459–3466.

46. Li, W.; Li, Q.; Duan, C.; Liu, S.; Ying, L.; Huang, F.; Cao, Y. *Dye. Pigment.* **2015**, *113*, 1–7.

47. Murphy, A. R.; Fréchet, J. M. J. *Chem. Rev.* **2007**, *107*, 1066–1096.

48. Pron, A.; Gawrys, P.; Zagorska, M.; Djurado, D.; Demadrille, R. *Chem. Soc. Rev.* **2010**, *39*, 2577–2632.

49. Ponomarenko, S. A.; Luponosov, Y. N.; Min, J.; Solodukhin, A. N.; Surin, N. M.; Shcherbina, M. A.; Chvalun, S. N.; Ameri, T.; Brabec, C. *Faraday Discuss.* **2014**, *174*, 313–339.

50. Ponomarenko, S. A.; Tatarinova, E. A.; Muzafarov, A. M.; Kirchmeyer, S.; Brassat, L.; Mourran, A.; Moeller, M.; Setayesh, S.; De Leeuw, D. *Chem. Mater.* **2006**, *18*, 4101–4108.

51. Dang, D.; Zhou, P.; Zhi, Y.; Bao, X.; Yang, R.; Meng, L.; Zhu, W. *J. Mater. Sci.* **2016**, *51*, 8018–8026.

52. Zhou, J. Y.; Zuo, Y.; Wan, X. J.; Long, G. K.; Zhang, Q.; Ni, W.; Liu, Y. S.; Li, Z.; He, G. R.; Li, C. X.; Kan, B.; Li, M. M.; Chen, Y. S. *J. Am. Chem. Soc.* **2013**, *135*, 8484–8487.

53. Kotwica, K.; Kostyuchenko, A. S.; Data, P.; Marszalek, T.; Skorka, L.; Jaroch, T.; Kacka, S.; Zagorska, M.; Nowakowski, R.; Monkman, A. P.; Fisyuk, A. S.; Pisula, W.; Pron, A. *Chem. Eur. J.* **2016**, *22*, 11795–11806.

54. Grana, E.; Katsigiannopoulos, D.; Avgeropoulos, A.; Goulas, V. *Int. J. Polym. Anal. Charact.* **2008**, *13*, 108–118.

55. Guzel, M.; Soganci, T.; Akgun, M.; Ak, M. *J. Electrochem. Soc.* **2015**, *162*, H527–H534.

56. Fan, Q.; Cui, J.; Liu, Y.; Su, W.; Wang, Y.; Tan, H.; Yu, D.; Gao, H.; Deng, X.; Zhu, W. *Synth. Met.* **2015**, *204*, 25–31.

57. Sun, Y.; Xiao, K.; Liu, Y.; Wang, J.; Pei, J.; Yu, G.; Zhu, D. *Adv. Funct. Mater.* **2005**, *15*, 818–822.

58. Ventura, B.; Barbieri, A.; Barigelletti, F.; Diring, S.; Ziessel, R. *Inorg. Chem.* **2010**, *49*, 8333–8346.

59. Shynkaruk, O.; He, G.; McDonald, R.; Ferguson, M. J.; Rivard, E. *Chem. Eur. J.* **2016**, *22*, 248–257.

60. Shynkaruk, O. Ph.D. Dissertation, University of Alberta, **2016**.

CHAPTER 3

1. Rivard, E. *Chem. Lett.* **2015**, *44*, 730-736.

2. Carrera, E. I.; Seferos, D. S. *Macromolecules* **2015**, *48*, 297-308.

3. He, G.; Shynkaruk, O.; Lui, M. W.; Rivard, E. *Chem. Rev.* **2014**, *114*, 7815-7880.

4. Jahnke, A. A.; Seferos, D. S. *Macrom. Rapid Commun.* **2011**, *32*, 943-951.

5. Chivers, T.; Laitinen, R. S. *Chem. Soc. Rev.* **2015**, *44*, 1725-1739.

6. He, G.; Torres Delgado, W.; Schatz, D. J.; Merten, C.; Mohammadpour, A.; Mayr, L.; Ferguson, M. J.; McDonald, R.; Brown, A.; Shankar, K.; Rivard, E. *Angew. Chem. Int. Ed.* **2014**, *53*, 4587-4591.

7. He, G.; Wiltshire, B. D.; Choi, P.; Savin, A.; Sun, S.; Mohammadpour, A.; Ferguson, M. J.; McDonald, R.; Farsinezhad, S.; Brown, A.; Shankar, K.; Rivard, E. *Chem. Commun.* **2015**, *51*, 5444-5447.

8. Kryman, M. W.; Schamerhorn, G. A.; Yung, K.; Sathyamoorthy, B.; Sukumaran, D. K.; Ohulchanskyy, T. Y.; Benedict, J. B.; Detty, M. R. *Organometallics* **2013**, *32*, 4321-4333.

9. Zander, M.; Kirsch, G. *Z. Naturforsch. A* **1989**, *44*, 205-209.

10. Lapkowski, M.; Motyka, R.; Suwinski, J.; Data, P. *Macromol. Chem. Phys.* **2012**, *213*, 29-35.

11. Kaur, M.; Yang, D. S.; Choi, K.; Cho, M. J.; Choi, D. H. *Dyes Pigments* **2014**, *100*, 118-126.

12. Annaka, T.; Nakata, N.; Ishii, A. *Organometallics* **2015**, *34*, 1272-1278.

13. Kremer, A.; Fermi, A.; Biot, N.; Wouters, J.; Bonifazi, D. *Chem. Eur. J.* **2016**, *22*, 5665-5675.

14. Carrera, E. I.; Lanterna, A. E.; Lough, A. J.; Scaiano, J. C.; Seferos, D. S. *J. Am. Chem. Soc*. **2016**, *138*, 2678-2689.

15. Inoue, S.; Jigami, T.; Nozoe, H.; Otsubo, T.; Ogura, F. *Tet. Lett.* **1994**, *35*, 8009-8012.

16. Planells, M.; Schroeder, B. C.; McCulloch, I. *Macromolecules* **2014**, *47*, 5889-5894.

17. Li, P. -F.; Schon, T. B.; Seferos, D. S. *Angew. Chem., Int. Ed.* **2015**, *54*, 9361-9366.

18. Mahrok, A. K.; Carrera, E. I.; Tilley, A. J.; Ye, S.; Seferos, D. S. *Chem. Commun.* **2015**, *51*, 5475-5478.

19. Park, Y. S.; Kale, T. S.; Nam, C. -Y.; Grubbs, R. B. *Chem. Commun.* **2014**, *50*, 7964 7967.

20. Jung, E. H.; Bee, S.; Yoo, T. W.; Jo, W. H. *Polym. Chem.* **2014**, *5*, 6545-6550.

21. Kaur, M.; Yang, D. S.; Shin, J.; Lee, T. W.; Choi, K.; Cho, M. J.; Choi, D. H. *Chem. Commun.* **2013**, *49*, 5495-5497.

22. Ashraf, R. S.; Meager, I.; Nikolka, M.; Kirkus, M.; Planells, M.; Schroeder, B. C.; Holliday, S.; Hurhangee, M.; Nielsen, C. B.; Sirringhaus, H.; McCulloch, I. *J. Am. Chem. Soc.* **2015**, *137*, 1314-1321.

23. Al-Hashimi, M.; Han, Y.; Smith, J.; Bazzi, H. S.; Alqaradawi, S. Y. A.; Watkins, S. E.; Anthopoulos, T. D.; Heeney, M. *Chem. Sci.* **2016**, *7*, 1093-1099.

24. Sweat, D. P.; Stephens, C. E. *Synthesis* **2009**, *19*, 3214-3218.

25. Sashida, H.; Kaname, M.; Ohyanagi, K. *Heterocycles* **2010**, *82*, 441-447.

26. He, G.; Kang, L.; Torres Delgado, W.; Shynkaruk, O.; Ferguson, M. J.; McDonald, R.; Rivard, E. *J. Am. Chem. Soc.* **2013**, *135*, 5360-5363.

27. Jahnke, A. A.; Djukic, B.; McCormick, T. M.; Domingo Buchaca, E.; Hellmann, C.; Lee, Y.; Seferos, D. S. *J. Am. Chem. Soc.* **2013**, *135*, 951-954.

28. Park, Y. S.; Wu, Q.; Nam, C. -Y.; Grubbs, R. B. *Angew. Chem., Int. Ed.* **2014**, *53*, 10691-10695.

29. Aprile, A.; Iversen, K. J.; Wilson, D. J. D.; Dutton, J. L. *Inorg. Chem.* **2015**, *54*, 4934-4939.

30. Osaka, I.; McCullough, R. D. *Acc. Chem. Res.* **2008**, *41*, 1202-1214.

31. Patra, A.; Bendikov, M. *J. Mater. Chem.* **2010**, *20*, 422-433.

32. Stefan, M. C.; Bhatt, M. P.; Sista, P.; Magurudeniya, H. D. *Polym. Chem.* **2012**, *7*, 1693-1701.

33. Higashihara, T.; Ueda, M. *Macromol. Res.* **2013**, *21*, 257-271.

34. Martin, M. L.; Trierweiler, M.; Galasso, V.; Fringuelli, F.; Taticchi, A. *J. Magn. Res.* **1981**, *42*, 155-158.

35. Bagherzadeh, S.; Mankad, N. P. *J. Am. Chem. Soc.* **2015**, *137*, 10898-10901.

36. Hawkeswood, S.; Stephan, D. W. *Dalton Trans.* **2005**, 2182-2187.

37. Shynkaruk, O.; He, G.; McDonald, R.; Ferguson, M. J.; Rivard, E. *Chem. Eur. J.* **2016**, *22*, 248-257.

38. Gandon, V.; Leca, D.; Aechtner, T.; Vollhardt, K. P. C.; Malacria, M.; Aubert, C. *Org. Lett.* **2014**, *6*, 3405-3407.

39. Dutton, J. L.; Farrar, G. J.; Sgro, M. J.; Battista, T. L.; Ragogna, P. J. *Chem. Eur. J.* **2009**, *15*, 10263-10271.

40. Kang, Y. K.; Deria, P.; Carroll, P. J.; Therein, M. J. *Org. Lett.* **2008**, *10*, 1341-1344.

41. Lozada, J.; Liu, Z.; Perrin, D. M. *J. Org. Chem.* **2014**, *79*, 5365-5368.

42. Ahn, S. -J.; Lee, C. -Y.; Kim, N. -K.; Cheon, C. -H. *J. Org. Chem.* **2014**, *79*, 7277-7285.

43. Liu, C.; Li, X.; Wu, Y.; Qiu, J. *RSC Adv.* **2014**, *4*, 54307-54311.

44. Liu, C.; Li, X.; Wu, Y. *RSC Adv.* **2015**, *5*, 15354-15358.

45. Li, G.; Shrotriya, V.; Huang, J. S.; Yao, Y.; Moriarty, T.; Emery, K.; Yang, Y. *Nature Mater.* **2005**, *4*, 864-868.

46. Jahnke, A. A.; Howe, G. W.; Seferos, D. S. *Angew. Chem., Int. Ed.* **2010**, *49*, 10140-10144.

47. Carrera, E. I.; McCormick, T. M.; Kapp, M. J.; Lough, A. J.; Seferos, D. S. *Inorg. Chem.* **2013**, *52*, 13779-13790.

48. Thompson, A. L.; Kabalka, G. W.; Akula, M. R.; Huffman, J. W. *Synthesis* **2005**, 547-550.

49. Shi, H.; Babinski, D. J.; Ritter, T. *J. Am. Chem. Soc.* **2015**, *137*, 3775-3778.

50. Jiang, Q.; Zhen, S.; Mo, D.; Lin, K.; Ming, S.; Wang, Z.; Liu, C.; Xu, J.; Yao, Y.; Duan, X.; Zhu, D.; Shi, H. *J. Polym. Sci. Part A Polym. Chem.* **2016**, *54*, 325–334.

51. Zhu, S. S.; Swager, T. M. *J. Am. Chem. Soc.* **1997**, *119*, 12568–12577.

CHAPTER 4

1. Zhao, Z.; Deng, C.; Chen, S.; Lam, J. W. Y.; Qin, W.; Lu, P.; Wang, Z.; Kwok, H. S.; Ma, Y.; Qiu, H.; Tang, B. Z. *Chem. Commun.* **2011**, *47*, 8847–8849.

2. Malytskyi, V.; Simon, J.-J.; Patrone, L.; Raimundo, J.-M. *RSC Adv.* **2014**, *5*, 354–397.

3. Kaur, N.; Singh, M.; Pathak, D.; Wagner, T.; Nunzi, J. M. *Synth. Met.* **2014**, *190*, 20–26.

4. Bull, S. D.; Davidson, M. G.; Van Den Elsen, J. M. H.; Fossey, J. S.; Jenkins, A. T. A.; Jiang, Y. B.; Kubo, Y.; Marken, F.; Sakurai, K.; Zhao, J.; James, T. D. *Acc. Chem. Res.* **2013**, *46*, 312–326.

5. Pron, A.; Gawrys, P.; Zagorska, M.; Djurado, D.; Demadrille, R. *Chem. Soc. Rev.* **2010**, *39*, 2577–2632.

6. Wakamiya, A.; Mori, K.; Yamaguchi, S. *Angew. Chem. Int. Ed.* **2007**, *46*, 4273–4276.

7. Bureš, F. *RSC Adv.* **2014**, *4*, 58826–58851.

8. Lin, S. L.; Chan, L. H.; Lee, R. H.; Yen, M. Y.; Kuo, W. J.; Chen, C. T.; Jeng, R. J. *Adv. Mater.* **2008**, *20*, 3947–3952.

9. Doi, H.; Kinoshita, M.; Okumoto, K.; Shirota, Y. *Chem. Mater.* **2003**, *15*, 1080–1089.

10. Schubert, C.; Wielopolski, M.; Mewes, L. H.; De Miguel Rojas, G.; Van Der Pol, C.; Moss, K. C.; Bryce, M. R.; Moser, J. E.; Clark, T.; Guldi, D. M. *Chem. Eur. J.* **2013**, *19*, 7575–7586.

11. Entwistle, C. D.; Marder, T. B. *Angew. Chem. Int. Ed.* **2002**, *41*, 2927–2931.

12. Zhao, C.; Wakamiya, A.; Inukai, Y.; Yamaguchi, S. *J. Am. Chem. Soc* **2006**, *128*, 15934–15935.

13. Sun, Z.-B.; Li, S.-Y.; Liu, Z.-Q.; Zhao, C.-H. *Chin. Chem. Lett.* **2016**, *27*, 1131–1138.

14. Fu, G. L.; Zhang, H. Y.; Yan, Y. Q.; Zhao, C. H. *J. Org. Chem.* **2012**, *77*, 1983–1990.

15. Schmidt, H. C.; Reuter, L. G.; Hamacek, J.; Wenger, O. S. *J. Org. Chem.* **2011**, *76*, 9081–9085.

16. Sudhakar, P.; Mukherjee, S.; Thilagar, P. *Organometallics* **2013**, *32*, 3129–3133.

17. Jia, W.-L.; Bai, D.-R.; McCormick, T.; Liu, Q.-D.; Motala, M.; Wang, R.-Y.; Seward, C.; Tao, Y.; Wang, S. *Chem. Eur. J.* **2004**, *10*, 994–1006.

18. Shirota, Y.; Kinoshita, M.; Noda, T.; Okumoto, K.; Ohara, T. *J. Am. Chem. Soc.* **2000**, *122*, 11021–11022.

19. Carrera, E. I.; Lanterna, A. E.; Lough, A. J.; Scaiano, J. C.; Seferos, D. S. *J. Am. Chem. Soc.* **2016**, *138*, 2678–2689.

20. Park, Y. S.; Kale, T. S.; Nam, C.-Y.; Choi, D.; Grubbs, R. B. *Chem. Commun.* **2014**, *50*, 7964–7967.

21. He, G.; Wiltshire, B. D.; Choi, P.; Savin, A.; Sun, S.; Mohammadpour, A.; Ferguson, M. J.; McDonald, R.; Farsinezhad, S.; Brown, A.; Shankar, K.; Rivard, E. *Chem. Commun.* **2015**, *51*, 5444–5447.

22. He, G.; Kang, L.; Torres Delgado, W.; Shynkaruk, O.; Ferguson, M. J.; McDonald, R.; Rivard, E. *J. Am. Chem. Soc.* **2013**, *135*, 5360–5363.

23. Shynkaruk, O. Ph.D. Dissertation, University of Alberta, **2016**.

24. Altenburger, K.; Arndt, P.; Spannenberg, A.; Baumann, W.; Rosenthal, U. *Eur. J. Inorg. Chem.* **2013**, 3200–3205.

25. Hydrio, J.; Gouygou, M.; Dallemer, F.; Daran, J.-C.; Balavoine, G. G. A. *J. Organomet. Chem.* **2000**, *595*, 261.

26. Gaal, M.; List, E. J. W.; Scherf, U. *Macromolecules* **2003**, *36*, 4236–4237.

27. Yan, W.; Wang, Q.; Lin, Q.; Li, M.; Petersen, J. L.; Shi, X. *Chem. Eur. J.* **2011**, *17*, 5011–5018.

28. Zhao, Z.; Su, H.; Zhang, P.; Cai, Y.; Kwok, R. T. K.; Chen, Y.; He, Z.; Gu, X.; He, X.; Sung, H. H.-Y.; Williams, I. D.; Lam, J. W. Y.; Zhang, Z.; Tang, B. Z. *J. Mater. Chem. B.* **2017**, *5*, 1650–1657.

29. Torres Delgado, W.; Shahin, F.; Ferguson, M. J.; McDonald, R.; He, G.; Rivard, E. *Organometallics* **2016**, *35*, 2140–2148.

30. Liégault, B.; Lapointe, D.; Caron, L.; Vlassova, A.; Fagnou, K. *J. Org. Chem.* **2009**, *74*, 1826–1834.

31. Desurmont, G.; Dalton, S.; Giolando, D. M.; Srebnik, M. *J. Org. Chem.* **1997**, *62*, 8907–8909.

32. Zheng, S. L.; Reid, S.; Lin, N.; Wang, B. *Tetrahedron Lett.* **2006**, *47*, 2331–2335.

33. Elangovan, A.; Wang, Y. H.; Ho, T. I. *Org. Lett.* **2003**, *5*, 1841–1844.

34. Liu, C.; Li, X.; Wu, Y.; Qiu, J. *RSC Adv.* **2014**, *4*, 54307–54311.

35. Chang, H. T.; Jeganmohan, M.; Cheng, C. H. *Org. Lett.* **2007**, *9*, 505–508.

36. Tian, H.; Shi, J.; He, B.; Hu, N.; Dong, S.; Yan, D.; Zhang, J.; Geng, Y.; Wang, F. *Adv. Funct. Mater.* **2007**, *17*, 1940–1951.

37. Liu, X.; Wallmann, I.; Boudinov, H.; Kjelstrup-Hansen, J.; Schiek, M.; Lützen, A.; Rubahn, H. G. *Org. Electron. Physics, Mater. Appl.* **2010**, *11*, 1096–1102.

38. McCormick, T. M.; Jahnke, A. A.; Lough, A. J.; Seferos, D. S. *J. Am. Chem. Soc.* **2012**, *134*, 3542–3548.

39. Suthan, T.; Rajesh, N. P.; Dhanaraj, P. V.; Mahadevan, C. K. *Spectrochim. Acta - Part A Mol. Biomol. Spectrosc.* **2010**, *75*, 69–73.

40. Ogawa, K.; Harada, J.; Fujiwara, T.; Takahashi, H. *Chem. Lett.* **2004**, *33*, 1446–1447.

41. Dumur, F.; Bui, T.-T.; Péralta, S.; Lepeltier, M.; Wantz, G.; Sini, G.; Goubard, F.; Gigmes, D. *RSC Adv.* **2016**, *6*, 60565–60577.

42. Bree, A.; Zwarich, R. *J. Chem. Phys.* **1969**, *51*, 903–912.

43. Correia, F. C.; Santos, T. C. F.; Garcia, J. R.; Peres, L. O.; Wang, S. H. *J. Braz. Chem. Soc.* **2015**, *26*, 84–91.

44. Berezin, M. Y.; Achilefu, S. *Chem. Rev.* **2010**, *110*, 2641–2684.

45. Zhao, Q.; Zhang, S.; Liu, Y.; Mei, J.; Chen, S.; Lu, P.; Qin, A.; Ma, Y.; Sun, J. Z.; Tang, B. Z. *J. Mater. Chem.* **2012**, *22*, 7387–7394.

46. Dutton, J. L.; Farrar, G. J.; Sgro, M. J.; Battista, T. L.; Ragogna, P. J. *Chem. Eur. J.* **2009**, *15*, 10263–10271.

CHAPTER 5

1. Shynkaruk, O.; Qi, Y.; Cottrell-Callbeck, A.; Torres Delgado, W.; McDonald, R.; Ferguson, M. J.; He, G.; Rivard, E. *Organometallics* **2016**, *35*, 2232–2241.
2. Lik, A.; Fritze, L.; Müller, L.; Helten, H. *J. Am. Chem. Soc.* **2017**, *139*, 5692-5695.
3. Braunschweig, H.; Damme, A.; Jimenez-Halla, J. O. C.; Hörl, C.; Krummenacher, I.; Kupfer, T.; Mailänder, L.; Radacki, K. *J. Am. Chem. Soc.* **2012**, *134*, 20169–20177.
4. Eisch, J. J.; Galle, J. E.; Kozima, S. *J. Am. Chem. Soc.* **1986**, *108*, 379–385.
5. Jahnke, A. A.; Djukic, B.; McCormick, T. M.; Buchaca Domingo, E.; Hellmann, C.; Lee, Y.; Seferos, D. S. *J. Am. Chem. Soc.* **2013**, *135*, 951–954.
6. Liou, S. Y.; Ke, C. S.; Chen, J. H.; Luo, Y. W.; Kuo, S. Y.; Chen, Y. H.; Fang, C. C.; Wu, C. Y.; Chiang, C. M.; Chan, Y. H. *ACS Macro Lett.* **2016**, *5*, 154–157.
7. Matsumi, N.; Naka, K.; Chujo, Y. *J. Am. Chem. Soc.* **1998**, *120*, 10776–10777.
8. Qin, Y.; Cheng, G.; Sundararaman, A.; Jäkle, F. *J. Am. Chem. Soc.* **2002**, *124*, 12672–12673.
9. Devillard, M.; Brousses, R.; Miqueu, K.; Bouhadir, G.; Bourissou, D. *Angew. Chem. Int. Ed.* **2015**, *54*, 5722–5726.
10. Tigreros, A.; Ortiz, A.; Insuasty, B. *Dye. Pigment.* **2014**, *111*, 45–51.
11. Balzer, F.; Schiek, M.; Wallmann, I.; Schäfer, A.; Lützen, A.; Rubahn, H.-G. *Proc. SPIE* **2011**, *8094*, 809409-1-809409–7.
12. Balzer, F.; Schiek, M.; Osadnik, A.; Wallmann, I.; Parisi, J.; Rubahn, H.-G.; Lützen, A. *Phys. Chem. Chem. Phys.* **2014**, *16*, 5747.